Direction of Arrival Estimation Using a Multiple-Input-Multiple-Output Radar with Applications to Automobiles

von der Fakultät Informatik, Elektrotechnik und Informationstechnik
der Universität Stuttgart
zur Erlangung der Würde eines Doktor-Ingenieurs (Dr.-Ing.)
genehmigte Abhandlung

vorgelegt von
Kilian Rambach
aus Schweinfurt

Hauptberichter:	Prof. Dr.-Ing. Bin Yang
Mitberichter:	Prof. Dr.-Ing. Johann F. Böhme
Tag der mündlichen Prüfung:	20.06.2016

Institut für Signalverarbeitung und Systemtheorie
der Universität Stuttgart

2017

Vorwort

Die vorliegende Arbeit entstand während meiner Forschungsarbeit am Institut für Signalverarbeiung und Systemtheorie (ISS) an der Universität Stuttgart. Ich bin froh darüber, Prof. Dr.-Ing. Bin Yang als meinen Doktorvater zu haben. Ich möchte mich recht herzlich bei ihm bedanken, für die Möglichkeit an seinem Institut zu promovieren, für die konstruktiven Diskussionen, die Freiheit eigene Ideen umzusetzen, sowie seine lockere und muntere Art. Das genaue Nachrechnen und Überprüfen meiner Berechnungen schätze ich sehr. Prof. Dr.-Ing. Johann Böhme danke ich für die Übernahme des Mitberichts.

Allen Kollegen am ISS danke ich für das gute Arbeitsklima, das freundliche Miteinander (inklusive Wasserschlachten) und den vielen fachlichen und auch nicht fachlichen Diskussionen. Mein besonderer Dank gilt Thomas Küstner, Dr. Benedikt Lösch und Lukas Mauch für das Korrekturlesen dieser Arbeit, auch in letzter Minute.

Ich bedanke mich bei Patrick Häcker, der mir insbesondere zu Beginn meiner Tätigkeit mit vielen fachlichen Gesprächen zur Seite gestanden hat. Danken möchte ich auch Dr. Christof Zeile für das Korrekturlesen und dass er dazu beigetragen hat, diesen Satz zu schreiben.

Weiterhin bedanke ich mich bei den Kollegen von Robert Bosch in Leonberg in der Abteilung ECR3, insbesondere Dr. Götz Kühnle, Dr. André Treptow, Volker Groß, Dr. Michael Schoor und Dr. Benedikt Lösch. Sie haben mit fruchtbaren Diskussionen und mit vielen Anregungen aus der Praxis zum Gelingen meiner Arbeit beigetragen. Ich bedanke mich bei Michael Schoor für das Korrekturlesen der Arbeit.

Mein besonderer Dank gilt meiner Partnerin Eva Schopf, die mich immer unterstützt und ermutigt hat. Ich bedanke mich auch für ihre Geduld insbesondere während des Zusammenschreibens der Arbeit.

Stuttgart, November 2015 Kilian Rambach

Contents

Notation and Abbreviations

Notation

x	scalar
$\underline{x}$	column vector
$\mathbf{X}$	matrix
$x^*, \underline{x}^*, \mathbf{X}^*$	complex conjugate of a scalar, vector or matrix
$\underline{x}^H, \mathbf{X}^H$	conjugate transpose of a vector or matrix
$\underline{x}^T, \mathbf{X}^T$	transpose of a vector or matrix
$\mathbf{X}^{-1}$	inverse of a matrix
$\mathbf{X}^+$	Moore–Penrose pseudo-inverse of a matrix
x_i or $[x]_i$	i-th element of vector $\underline{x}$
$[\mathbf{X}]_{i,j}$	element of matrix $\mathbf{X}$ at i-th row and j-th column
$\mathbf{0}_{K\times M}$	$\mathbf{0}_{K\times M} \in \mathbb{R}^{K\times M}$, matrix with all elements equal 0
$\mathbf{0}$	shortcut for $\mathbf{0}_{K\times M}$ with the dimension following from the context
$\underline{1}_K$	$\underline{1}_K \in \mathbb{R}^K$, vector of length K with all elements equal 1
$\underline{1}$	shortcut for $\underline{1}_K$ with the dimension following from the context
$\mathbf{1}_{K\times M}$	$\mathbf{1}_{K\times M} \in \mathbb{R}^{K\times M}$, matrix with all elements equal 1
$\mathbf{1}$	shortcut for $\mathbf{1}_{K\times M}$ with the dimension following from the context
$\mathbf{I}_{K\times K}$	$\mathbf{I}_{K\times K} \in \mathbb{R}^{K\times K}$, identity matrix
$\mathbf{I}$	identity matrix with the dimension following from the context
$\mathbb{Z}, \mathbb{R}, \mathbb{C}$	set of integer, real, and complex numbers

Mathematical Operations

$\neg A$	negation “not A”
$A \implies B$	implication, i. e. if A is true then B is true. Stated in other words, A is sufficient for B.
$A \iff B$	equivalence, i. e. A is true if and only if B is true. Stated in other words, A is necessary and sufficient for B.

$\|\|.\|\|$	Euclidean norm of a vector or matrix
$\odot$	entrywise Hadamard product, i. e. $\underline{x} = \underline{y} \odot \underline{z}$ means $x_i = y_i \cdot z_i \; \forall i$
$\otimes$	Kronecker tensor product
$\mathrm{Corr}^{\mathrm{S}}(.)$	sample cross-correlation, defined in Appendix A
$\mathrm{Corr}^{\mathrm{WS}}(.)$	weighted sample cross-correlation, defined in Appendix A
$\mathrm{Cov}^{\mathrm{S}}(.)$	sample cross-covariance, defined in Appendix A
$\mathrm{Cov}^{\mathrm{WS}}(.)$	weighted sample cross-covariance, defined in Appendix A
$\mathrm{diag}(\underline{x})$	diagonal matrix consisting of the elements of $\underline{x}$
$\mathrm{E}(.)$	expectation operator
$\mathrm{E}^{\mathrm{S}}(.)$	sample mean, defined in Appendix A
$\mathrm{E}^{\mathrm{WS}}(.)$	weighted sample mean, defined in Appendix A
$\exp(\underline{x})$ or $\mathrm{e}^{\underline{x}}$	exponential function of each element of vector $\underline{x}$, i. e. $\underline{y} = \exp(\underline{x})$ means $y_i = \exp(x_i) \; \forall i$
$\max(\underline{x})$	the element with the maximal value of the real vector $\underline{x}$
$\min(\underline{x})$	the element with the minimal value of the real vector $\underline{x}$
r_x	autocorrelation of x
$\mathrm{Re}(.)$	real part of a complex number or matrix
$\sqrt{\underline{x}}$	square root of each element of vector $\underline{x}$, i. e. $\underline{y} = \sqrt{\underline{x}}$ means $y_i = \sqrt{x_i} \; \forall i$
$\mathrm{Tr}(\mathbf{X})$	trace of a matrix

Symbols

Latin Symbols

$\propto$	proportional to
$\hat{.}$	estimated value of a parameter, e. g. $\hat{\Theta}$ is the estimated value of Θ
$\underline{a}^{\mathrm{Rx}}$, $\underline{a}^{\mathrm{Tx}}$, $\underline{a}^{\mathrm{Pulse}}$, $\underline{a}^{\mathrm{Virt}}$	steering vector of the Rx and Tx array, the array defined by $\underline{d}^{\mathrm{Pulse}}$, and virtual array, respectively
$\mathbf{A}^{\mathrm{Rx}}$, $\mathbf{A}^{\mathrm{Tx}}$	steering matrix of the Rx and Tx array, respectively
$\underline{b}(u, \omega)$	steering vector of a TDM MIMO radar as a function of the electrical angle u and Doppler frequency ω
$\mathbf{B}(\underline{U}, \underline{\omega})$	steering matrix of a TDM MIMO radar as a function of the electrical angles $\underline{U}$ and Doppler frequencies $\underline{\omega}$ of several targets
$b_{\hat{\Theta}}$, $\underline{b}_{\underline{\hat{\Theta}}}$	bias of $\hat{\Theta}$ and $\underline{\hat{\Theta}}$, respectively
B	transmit beampattern
c	speed of light
$\mathbf{C}_{\underline{n}}$	noise covariance matrix

$C_{\hat{\Theta}}$, $\mathbf{C}_{\underline{\hat{\Theta}}}$	variance of $\hat{\Theta}$ and covariance matrix of $\underline{\hat{\Theta}}$, respectively
CRB_{Θ}	CRB of a scalar parameter Θ
$\mathbf{CRB}_{\underline{\Theta}}$	CRB of a parameter vector $\underline{\Theta}$
d	distance of the target
d_0, d_M	distance of the target at the beginning and at the middle of the transmission of a chirp, respectively
$\underline{d}^{\mathrm{Pulse}}$, $\mathbf{D}^{\mathrm{Pulse}}$	positions of the Tx antennas in the sequence in which they transmit, divided by $\frac{\lambda}{2\pi}$, for a linear and planar array, respectively
$\underline{d}^{\mathrm{Rx}}$, $\mathbf{D}^{\mathrm{Rx}}$	positions of the Rx antennas, divided by $\frac{\lambda}{2\pi}$, for a linear and planar array, respectively
$\underline{d}^{\mathrm{Tx}}$, $\mathbf{D}^{\mathrm{Tx}}$	positions of the Tx antennas, divided by $\frac{\lambda}{2\pi}$, for a linear and planar array, respectively
$\underline{d}^{\mathrm{Virt}}$, $\mathbf{D}^{\mathrm{Virt}}$	positions of the virtual antennas, divided by $\frac{\lambda}{2\pi}$, for a linear and planar array, respectively
Δd^{Rx}, Δd^{Tx}	geometrical size of the Rx and Tx array, respectively
f_0	carrier frequency
f_{d}	Doppler frequency
f_{diff}	difference frequency for a chirp or FMCW radar
f_s	sampling frequency
f_{Rx}, f_{Tx}	received and transmitted frequency of a chirp, respectively
F, F_ω	bandwidth of a chirp in terms of frequency or angular frequency
j	imaginary unit $j = \sqrt{-1}$
$\mathbf{J}$	Fisher Information Matrix
L	number of measurement cycles
$M_{\hat{\Theta}}$, $\mathbf{M}_{\underline{\hat{\Theta}}}$	mean square error of $\hat{\Theta}$ and $\underline{\hat{\Theta}}$, respectively
n	dependent on the context: scalar noise or discrete sampling point in time
$\underline{n}$, $\mathbf{N}$	noise
N_{Pulse}	number of transmitted chirps or pulses
N_{Rx}	number of Rx antennas
N_{samples}	number of samples per chirp
N_{Tx}	number of Tx antennas
N_{Virt}	number of virtual antenna elements. Depending on the context $N_{\mathrm{Virt}} = N_{\mathrm{Rx}}N_{\mathrm{Tx}}$ or $N_{\mathrm{Virt}} = N_{\mathrm{Rx}}N_{\mathrm{Pulse}}$
N_{Targets}	number of targets
p, $\underline{p}$	transmission power of one Tx antenna or of several pulses
$p^{\max}$	maximal transmission power
P_{D}, P_{FA}	probability of detection and false alarm, respectively

$\mathbf{R}_{\mathbf{\Phi}}$	correlation matrix of the transmitted codes
$\mathrm{RMSE}_{\hat{\Theta}}$	root mean square error of $\hat{\Theta}$
s, $\underline{s}$	complex signal strength of one and several targets, respectively
$\mathbf{S}$	matrix containing the complex signal strengths of several targets
$s_{\mathrm{Tx}}(t)$	transmitted signal
S	total SNR
t	continuous time
t_{start}	start time of the transmission of a chirp
t_{M}	time in the middle of a chirp
$\Delta t_{\mathrm{M},1k}$	difference between the time in the middle of chirp k and chirp 1
Δt	depending no the context: sampling time $\Delta t = 1/f_s$, difference between the transmission time of two successive pulses, or the duration of one pulse
$\underline{\Delta t} \in \mathbb{R}^{N_{\mathrm{Pulse}}}$	durations of the transmitted pulses
$\underline{t} \in \mathbb{R}^{N_{\mathrm{Pulse}}}$	transmission times of the transmitted pulses
$\underline{t}^{(k)}$	transmission times of the pulses transmitted by the k-th Tx antenna
T	chirp duration
T_{cycle}	time of one measurement cycle, i. e. one coherent processing interval
T_{total}	total measurement time
u	electrical angle of a target
$\underline{u}$	electrical angles of one target, when estimating two DOAs using a planar array
$\underline{U} \in \mathbb{R}^{N_{\mathrm{Targets}}}$	electrical angles of N_{Targets} targets
ΔU	difference of the electrical angles of two targets
U_{SIMO}, U_{MIMO}	sample variance of the Rx antenna positions in a SIMO array and the virtual antenna positions in a MIMO array, respectively
v	relative radial velocity of the target
$\underline{x}$	depending on the context: signal after range processing, used for the DOA estimation, or the baseband signal
$\mathbf{X}$	signal after range compression for code division multiplexing

Greek Symbols

β	radial velocity over speed of light $\beta = \frac{v}{c}$
$\delta_{l,m}$	Kronecker delta, i. e. $\delta_{l,m} = 1$ if $l = m$ and $\delta_{l,m} = 0$ otherwise
δ_{RL}, δ_{ARL}	resolution and angular resolution, respectively
λ	carrier wavelength
φ	dependent on the context: Elevation angle in the case of a planar antenna array or phase of the baseband signal

$\varphi_{\mathrm{Rx}}(t)$, $\varphi_{\mathrm{Tx}}(t)$	time dependent phase of the received and transmitted signal, respectively
$\Delta\varphi_{1k}$	phase difference between the first and k-th pulse
$\varphi_{\mathrm{base}}(t)$	time dependent phase of the baseband signal
$\mathbf{\Phi}$	transmitted codes in CDM MIMO radar
ψ^{TDM}	parameters which characterize a TDM scheme
ρ_{s}	energy per sample
$\underline{\rho}$	energy of the transmitted pulses
$\underline{\rho}^{(k)}$	energy of the pulses transmitted by the k-th Tx antenna
$\sigma_{\hat{\Theta}}$	standard deviation of $\hat{\Theta}$
σ^2, σ_n^2	variance of the noise
σ_s^2	signal strength
ϑ	direction of arrival, the azimuth
Θ	unknown scalar parameter
$\underline{\Theta}$	unknown parameter vector
$\hat{\Theta}$, $\underline{\hat{\Theta}}$	estimated parameter or parameter estimator for a scalar and vector parameter, respectively
τ	time delay between transmitted and received signal (round trip time). Precise definition depends on the context.
τ_0, τ_M	time delay (round trip time) at the beginning and at the middle of the transmission of a chirp, respectively
χ_f, χ	chirp rate of the frequency and angular frequency, respectively
ω_0	angular carrier frequency
$\omega_{0\mathrm{M}}$	angular carrier frequency in the middle of a chirp
$\omega_{\mathrm{Doppler}}$	angular Doppler frequency
ω	dependent on the context: general angular frequency or short notation for the angular Doppler frequency of a target
$\underline{\omega}$	angular Doppler frequency of several targets
$\Delta\omega$	difference of the angular Doppler frequencies of two targets
$\omega(t)$	time dependent angular frequency of a frequency modulated chirp
ω_{diff}	angular difference frequency for a chirp or FMCW radar

Abbreviations

ADC	analog to digital converter
CDM	code division multiplexing
CPI	coherent processing interval

CRB	Cramer-Rao bound
DFT	discrete Fourier transform
DML	deterministic maximum likelihood
DOA	direction of arrival
DTFT	discrete time Fourier transform
FDM	frequency division multiplexing
FFT	fast Fourier transform
FIM	Fisher Information Matrix
FMCW	frequency modulated continuous wave
GLRT	generalized likelihood ratio test
GMTI	ground moving target indication
iff	if and only if
MC	Monte-Carlo
MIMO	multiple input multiple output
ML	maximum likelihood
MSE	mean squared error
pdf	probability density function
RCS	radar cross section
RMSE	root-mean-square error
R-TDMA	randomized time division multiple access
Rx	receiver or receiving
SIMO	single input multiple output
SNR	signal-to-noise ratio
SINR	signal-to-noise-and-interference ratio
STAP	space time adaptive processing
SCR	signal-to-clutter ratio
TDM	time division multiplex
TDMA	time division multiple access
Tx	transmitter or transmitting
ULA	uniform linear array
w. l. o. g.	without loss of generality
w. r. t.	with respect to

Abstract

The thesis at hand investigates the direction of arrival (DOA) estimation using a Multiple-Input-Multiple-Output (MIMO) radar system. The application of MIMO radars in automobiles is studied. A MIMO radar consists of several transmitting (Tx) and receiving (Rx) antennas. We focus on a time division multiplexed (TDM) MIMO radar with colocated Tx and Rx antennas. The motivation is the use of a radar as a security system in automotive applications, e. g. to identify a dangerous situation and react automatically. Security systems must be very reliable. Hence, besides a good estimation of the distance and velocity, a high performance in DOA estimation is necessary. This is a demanding task, since only a small number of antennas is used and the radar is limited to a small geometrical size. Compared to the corresponding Single-Input-Multiple-Output (SIMO) radar, a MIMO radar with colocated antennas can achieve a higher accuracy in DOA estimation due to its larger virtual aperture. Therefore it is a promising technique for the use in automobiles. The obtained results of this thesis enable us to find optimal TDM schemes which yield a very high DOA accuracy for targets which are stationary as well as for targets which are moving relative to the radar system. The results are not confined to MIMO radars in automobiles, but can be used in other applications as well.

In Chapter 2 we introduce the basics of radar systems, which are important for this thesis. First we present three different kinds of radars, the pulse Doppler radar, the frequency modulated continuous wave (FMCW) radar, and the chirp sequence radar. After that, the performance measures of a radar system, which are used in the following chapters, are introduced. For that purpose, the concept of parameter estimators are presented. Thereafter, the accuracy is defined and a definition for the resolution is given.

Chapter 3 gives an overview on the two types of MIMO radars: The MIMO radar with widely separated antennas and the colocated MIMO radar. A survey on the research already done on MIMO radars is presented. Thereafter, the different multiplexing techniques are discussed, which can be used in a MIMO radar to separate the signals of the different Tx antennas. The last part of Chapter 3 focuses on the application of MIMO radars in automobiles. It shows why TDM MIMO radars are suitable for the use in automotive applications.

In Chapter 4 we study the DOA estimation for stationary targets, i. e. the targets are not moving relative to the radar. We investigate SIMO and MIMO radars and compute the deterministic Cramer-Rao Bound (CRB) of the DOA for both types of systems. With these results we can determine the maximal achievable DOA accuracy. We compare both CRBs and show under which conditions

the MIMO radar achieves a lower CRB. Furthermore, we analyze the DOA performance of a code division multiplexed (CDM) MIMO radar. If the total transmission power of the radar is limited by the maximal transmission power of one Tx antenna, then the TDM and CDM MIMO radar yield the same CRB for the DOA. If certain properties of the noise covariance matrix are satisfied, we can show with the concept of sufficient statistics that both radars even yield the same amount of information on the DOA. Hence, not only the CRB but all statistical properties like the ambiguities, sidelobe levels, and resolution are the same for the TDM and CDM MIMO radar.

Chapter 5 contains the main contribution of the thesis. In this chapter targets which are moving relative to the radar are studied. To estimate the DOA using a SIMO radar, the phases of the received baseband signals are analyzed. In a MIMO radar the phase relation between the Tx antennas is processed as well. A target which is moving relative to the radar induces an additional phase shift in the baseband signal due to the Doppler effect. In general, this decreases the DOA estimation accuracy, since the Doppler frequency has to be estimated in addition. We study this scenario. After a precise derivation of the signal model, the deterministic CRB is computed for a general TDM scheme for one moving target. This enables to investigate the maximal achievable accuracy of the DOA estimation of a TDM MIMO radar. Different TDM MIMO radars are compared. Moreover we derive TDM schemes which result in a decoupling of the DOA and Doppler frequency in the CRB. Hence, using those TDM schemes, the CRB for the DOA is as small as for a stationary target. Under different practical boundary conditions, optimal TDM schemes are derived, which achieve the highest possible DOA accuracy. Thereafter, we investigate the DOA estimation of two and more targets. Conditions on the TDM schemes are derived which guarantee the decoupling of the DOAs from the Doppler frequencies for certain scenarios. Besides the DOA accuracy, the resolution is investigated for different TDM schemes.

Chapter 6 summarizes the thesis and gives an outlook on possible future work.

Kurzfassung

In der vorliegenden Arbeit wird die Winkelschätzung (auch Einfallsrichtung genannt, engl. Direction of Arrival (DOA)) mit Hilfe eines Multiple-Input-Multiple-Output (MIMO) Radars untersucht. Darüber hinaus wird die Verwendung eines MIMO Radars in automobilien Anwendungen betrachtet. Ein MIMO Radar besteht aus mehreren Sende- (Tx) und Empfangsantennen (Rx). Wir betrachten insbesondere MIMO Radare die im Zeitmultiplexverfahren (engl. time division multiplex (TDM)) betrieben werden und geometrisch nahe beieinander liegende Antennen (engl. colocated) besitzen. Die Motivation dieser Untersuchungen ist die Verwendung von Radarsystemen als Sicherheitssysteme in Fahrzeugen, z.B. um eine gefährliche Situation zu detektieren und darauf automatisch zu reagieren. Sicherheitssysteme müssen sehr zuverlässig sein. Daher ist neben einer genauen Abstands- und Geschwindigkeitsschätzung auch eine hohe Performance in der Winkelschätzung nötig. Dies ist eine anspruchsvolle Aufgabe, da nur eine geringe Anzahl an Antennen zur Verfügung steht und das Radarsystem nur eine kleine geometrische Größe aufweisen darf. Im Vergleich zu einem entsprechenden Single-Input-Multiple-Output (SIMO) Radar kann ein colocated MIMO Radar aufgrund seiner größeren virtuellen Apertur eine höhere Winkelgenauigkeit erreichen. Daher ist es eine vielversprechende Technik für die Anwendung in Fahrzeugen. Die Ergebnisse dieser Arbeit ermöglichen uns optimale Zeitmultiplexverfahren zu finden, welche sowohl für stationäre Objekte als auch für Objekte die sich relativ zum Radar bewegen, eine hohe Winkelgenauigkeit erreichen. Die Ergebnisse beschränken sich nicht nur auf Radare in Fahrzeugen, sondern können auch in anderen Anwendungen verwendet werden.

In Kapitel 2 führen wir die Grundlagen der Radarsysteme ein, welche für die vorliegende Arbeit wichtig sind. Zuerst stellen wir drei verschiedene Typen von Radaren vor: Das Puls-Doppler-Radar, das frequenzmodulierte Dauerstichradar (engl. frequency modulated continuous wave (FMCW) radar) und das Radar mit einer langen Folge von chirps (engl. chirp sequence radar). Daraufhin werden die Performancemaße eines Radars eingeführt, die in den folgenden Kapiteln benutzt werden. Für diesen Zweck wird das Konzept der Parameterschätzung vorgestellt. Danach definieren wir die Genauigkeit und Trennfähigkeit (auch Auflösung genannt).

In Kapitel 3 geben wir einen Überblick über die zwei Typen von MIMO Radaren: MIMO Radare mit räumlich weit getrennten Antennen (engl. widely separated antennas) und colocated MIMO Radare. Wir stellen den Stand der Technik zu MIMO Radaren vor. Daraufhin diskutieren wir verschiedene Multiplexverfahren die in einem MIMO Radar verwendet werden können, um die Signale der verschiedenen Sender zu unterscheiden. Der letzte Teil von Kapitel 3 behandelt die Anwendung von

MIMO Radaren in Fahrzeugen. Es wird gezeigt warum TDM MIMO Radare für die Anwendung in Automobilen geeignet sind.

In Kapitel 4 untersuchen wir die Winkelschätzung stationärer Ziele, d.h. das Ziel bewegt sich nicht relativ zum Radar. Wir betrachten SIMO und MIMO Radare und berechnen die deterministische Cramer-Rao Schranke des Winkels für beide Systeme (engl. Cramer-Rao Bound (CRB)). Mit dem Ergebnis können wir die maximal mögliche Winkelgenauigkeit bestimmen. Wir vergleichen beide CRBs und zeigen unter welchen Bedingungen das MIMO Radar eine kleinere CRB erreicht. Darüber hinaus analysieren wir die Winkelperformance eines MIMO Radars welches mit code division multiplex (CDM) betrieben wird. Wenn die gesamte Sendeleistung des Radars durch die maximale Sendeleistung einer Antenne beschränkt ist, dann besitzen das TDM und CDM MIMO Radar die gleiche CRB des Winkels. Erfüllt die Kovarianzmatrix des Rauschens bestimmte Voraussetzungen, dann können wir mit Hilfe der sufficient statistics zeigen, dass beide Radarsysteme sogar die gleiche Information über den Winkel liefern. Daher ist dann nicht nur die CRB gleich, sondern alle statistischen Eigenschaften, wie z.B. die Mehrdeutigkeiten, die Höhe der Nebenkeulen und die Auflösung, sind für das TDM und CDM MIMO Radar identisch.

Kapitel 5 entählt den Hauptbeitrag der vorliegenden Arbeit. In diesem Kapitel werden Ziele untersucht, welche sich relativ zum Radar bewegen. Um den Winkel mit einem SIMO Radar zu schätzen werden die Phasen des empfangenen Basisbandsignals analysiert. In einem MIMO Radar wird die Phasenbeziehung zwischen den Sendeantennen ebenfalls verarbeitet. Ein Ziel, das sich relative zum Radar bewegt, bewirkt einen zusätzliche Phasenverschiebung aufgrund des Dopplereffekts. Im Allgemeinen wird dadurch die Winkelgenauigkeit schlechter, da die Dopplerfrequenz zusätzlich geschätzt werden muss. Wir untersuchen dieses Szenario. Nach einer genauen Herleitung des Signalmodells berechnen wir die deterministische CRB für ein allgemeines Zeitmultiplexschema für ein bewegtes Ziel. Dadurch können wir die maximal erreichbare Winkelgenauigkeit eines TDM MIMO Radars untersuchen. Verschiedene TDM MIMO Radare werden miteinander verglichen. Außerdem leiten wir Zeitmultiplexschemata her, welche zu einem Entkoppeln des Winkels und der Dopplerfrequenz in der CRB führen. Wenn man also solche Zeitmultiplexschemata benutzt, dann ist die CRB des Winkels genauso groß wie für ein stationäres Ziel. Für verschiedene praktische Randbedingungen werden optimale Zeitmultiplexschemata hergeleitet, welche die höchst mögliche Winkelgenauigkeit erreichen. Weiterhin untersuchen wir die Winkelschätzung für zwei und mehr Ziele. Wir leiten Bedingungen an die Zeitmultiplexschemata her, welche für bestimmte Szenarien ein Entkoppeln der Winkel von der Dopplerfrequenz garantieren. Neben der Genauigkeit wird auch die Trennfähigkeit für verschiedene Zeitmultiplexschemata untersucht.

In Kapitel 6 fassen wir die vorliegende Arbeit zusammen und geben einen Ausblick auf weitere mögliche Arbeiten.

1. Introduction

The history of radar started with the invention of Christian Hulsmeyer in 1904, who developed the first form of a radar. In 1935 Sir Robert Watson-Watt demonstrated a working radar system and in world war II the research and development of radars increased further [Li and Stoica, 2009, Ch. 2]. Nowadays radar systems are not only used for air surveillance or military applications, but also in completely different topics. They are used e.g. in breast cancer imaging [Klemm et al., 2010] or in automobiles, in order to offer different security and comfort functions [Winner, 2012].

With the availability of more and more computer capabilities, more complex systems like Multiple-Input-Multiple-Output (MIMO) radars are built. MIMO systems consist of several transmitting (Tx) and receiving (Rx) antennas. In general, every transmitter can transmit an arbitrary and independent waveform. In communications, MIMO systems gained much attention in the 1990s [Li and Stoica, 2009, Ch. 3]. One goal is the optimization of these systems to achieve a high transfer rate [Sayeed and Raghavan, 2007]. There are several similarities between MIMO communication systems and MIMO radar systems, but the radar systems are designed to achieve a different goal. They are used to detect and track targets and estimate target parameters, e.g. the distance, the direction of arrival (DOA), the speed or the radar cross section. To the best of our knowledge, the first colocated MIMO radar was invented at the end of the 80s [Lesturgie, 2011], under the name “Synthetic Antenna and Impulse Radar” (RIAS) [Dorey et al., 1989; Luce et al., 1992]. A similar radar, called “Sparse-array Synthetic Impulse and Aperture Radar” (SIAR) was developed later [Baixiao et al., 2001]. By using digital beamforming, this radar system is able to track several targets at the same time. Many additional interesting aspects are investigated nowadays, e.g. the performance gain of a MIMO radar compared to the Single-Input-Multiple-Output (SIMO) counterpart [Friedlander, 2009], the design of the transmitted waveforms [Li et al., 2008], and the development of new estimation techniques [Chen, 2009].

The motivation for our work is the use of MIMO radars in automotive applications. Radars in automobiles offer comfort functions, e. g. adaptive cruise control, and even more important, security functions [Winner, 2012]. If a radar identifies a possible accident, e. g. two cars are moving too fast in the direction of each other, it can warn the driver or react automatically. In many situations, automatic systems can react faster than human beings. Hence, radar systems can help to prevent injuries or even deaths of humans. In order to be used as a security system, the radar has to be reliable and offer good estimation performance of the target’s parameters. The DOA estimation is a difficult task and still has to be improved. Consider a car at a large distance. To decide if it

is on the left or right driving lane, an accurate DOA estimation is required. Usually only a small number of antennas can be used in an automotive radar and their positions are constrained to a small geometrical size. A MIMO radar is a promising approach to improve the DOA estimation under these conditions since it offers a larger virtual aperture than the corresponding SIMO radar [Chen, 2009].

We are especially interested in the DOA accuracy. The Cramer-Rao bound (CRB) is a lower bound on the covariance matrix of any unbiased estimator [Kay, 1993]. Therefore we can use it to examine the maximum DOA accuracy of a radar system, independent of the used estimation algorithm. The CRB has been derived for different settings and radar systems. The CRB for a SIMO radar is computed in [Stoica and Nehorai, 1989]. In [Ward, 1995; Dogandzic and Nehorai, 2001], the CRB for non-stationary targets is studied. The DOA estimation for a SIMO radar with only one Rx channel is investigated in [Lee et al., 2004]. The authors of [Bekkerman and Tabrikian, 2006; Forsythe and Bliss, 2005] derived the CRB for the DOA estimation of a stationary target using a MIMO radar with a general transmit signal. A MIMO radar with simultaneously transmitting antennas is considered in [Boyer, 2011; Chong et al., 2011] and the CRB for the DOA and Doppler estimation is computed.

A MIMO radar can be realized by different multiplexing techniques like frequency, code, or time division multiplexing (TDM). All multiplexing techniques come with different advantages and drawbacks. In this thesis, we focus on TDM MIMO radars. In general, they have lower hardware requirements than other multiplexing techniques. Furthermore, the transmit signal can be kept as in a SIMO radar, since the antennas do not transmit simultaneously. Hence, waveforms which have been already optimized for distance and velocity estimation can still be used, e. g. linear frequency modulated continuous waves (LFMCW). TDM MIMO radars have been investigated experimentally [Feger et al., 2009; Jahn et al., 2012; Schmid et al., 2012; Guetlein et al., 2012, 2013a], but quantitative comparisons with different radar systems, especially for the DOA estimation of moving targets, are still missing.

We fill this gap by studying the DOA estimation of stationary and non-stationary targets using SIMO and TDM MIMO radars. Note that the Tx antennas in a TDM MIMO radar transmit successively and not simultaneously. Therefore the signal model has a different structure than that in [Boyer, 2011; Chong et al., 2011], where simultaneously transmitting Tx antennas are assumed.

We introduce the basics of radar systems in Chapter 2 and give an overview of the working principle of MIMO radars and the current state of the art in Chapter 3. The DOA estimation of stationary targets is studied in Chapter 4 and a comparison between SIMO and MIMO radars is made with respect to the achievable DOA accuracy. Moreover, we compare TDM and CDM MIMO radars. We extend the studies to moving targets in Chapter 5. In DOA estimation, the phases of the baseband signals are processed. A MIMO radar analyzes the phase relation between the Tx channels as well. A moving target induces an additional phase shift in the baseband signals due to the Doppler effect. Thus, the Doppler frequency has to be estimated in addition to the DOA. In general, this decreases the DOA accuracy. We investigate this scenario and derive the CRB for the DOA for linear and

planar antenna arrays and study different TDM schemes. Optimal TDM schemes are presented, which lead to a decoupling of the DOAs from the Doppler frequency. Thus, a DOA accuracy can be achieved which is as high as for a stationary target, despite the unknown Doppler frequency. Chapter 6 concludes the thesis and gives an outlook on possible future work.

Chapter 4 and 5 contain the contributions to the research on MIMO radars. Chapter 5 contains the main results of the thesis for TDM MIMO radars.

2. Radar Basics

In this chapter, we give a brief overview of the working principle of different radar systems which are considered in the context of the MIMO radar in later chapters. Moreover, we present some important performance measures. For more details see e. g. [Skolnik, 2001].

2.1. Working Principle of a Radar

A radar transmits an electromagnetic wave. The wave propagates, is reflected at different objects, and a part of it travels back to the radar. This is the signal which the radar receives. This signal can be analyzed to determine different parameters of the objects. The parameters which can be measured and are important for automotive applications are the distance d of a target to the radar, its relative radial velocity v and the angle ϑ under which the target appears, see Fig. 2.1. The angle ϑ is also called direction of arrival (DOA). The distance can be determined by the time delay between the transmitted and received signal. Due to the Doppler frequency, the velocity can be estimated. One possibility to measure the DOA is the use of an array of receiving (Rx) antennas, i. e. several antennas at different positions. In Fig. 2.2 an antenna array and the propagation direction of the reflected signal are depicted for a target which is far away compared to the geometrical size of the antenna array. Hence, the reflected wave can be approximated by a plane wave. For $\vartheta \neq 0$, the time at which the signal is received is different for each Rx antenna. The time differences depend on ϑ and can therefore be used to estimate ϑ.

In the following, we briefly present three different radar types.

2.1.1. Pulse Doppler Radar

A pulse Doppler radar transmits several short pulses repetitively. The pulses have a constant transmission frequency f_0. The time delay τ between the transmitted and received echo pulse is measured to determine the distance d. The relation between τ and d is

$$\tau = \frac{2\,d}{c}, \tag{2.1}$$

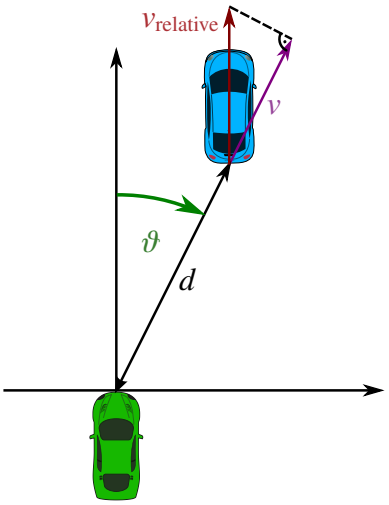

Figure 2.1.: The target's parameters d, v, and ϑ. v_{relative} is the total relative velocity and v the radial part of it. [Openclipart, 2014, graphical parts used and adapted]

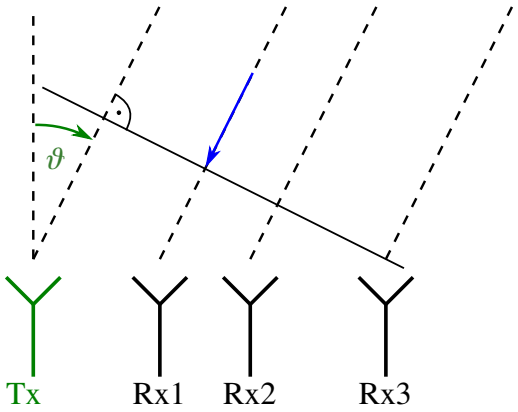

Figure 2.2.: Antenna array with several Rx antennas. The blue arrow indicates the propagation direction of the reflected plane wave.

where c is the speed of light. The factor 2 arises from the fact that the pulse has to travel forth and back. Compared to the transmitted signal, the received signal is shifted in frequency by the Doppler frequency f_{d} with [Skolnik, 2001]

$$f_{\text{d}} \approx 2\,\frac{v}{c}\,f_0. \tag{2.2}$$

Here, the velocity v is defined to be positive, if the target moves away from the radar. The approximation is valid for $|v| \ll c$. The relation between the received frequency f_{Rx}, the transmitted one f_0 and the Doppler frequency is

$$f_{\text{d}} = f_0 - f_{\text{Rx}}. \tag{2.3}$$

This radar type is described in more detail in [Skolnik, 2001; Bühren, 2008].

2.1.2. Linear Frequency Modulated Continuous Wave Radar

A linear frequency modulated continuous wave (LFMCW, often just FMCW) radar transmits pulses with a linearly changing frequency. These pulses are also called chirps. The transmitted (Tx) time dependent frequency $f_{\mathrm{Tx}}(t)$ of one pulse, depicted in Fig. 2.3, can be written as

$$f_{\mathrm{Tx}}(t) = f_0 + \chi_f\,(t - t_{\mathrm{M}}), \quad t \in [t_{\mathrm{start}}, t_{\mathrm{start}} + T] \tag{2.4}$$

where t is the time, f_0 the frequency at time $t_{\mathrm{M}} = t_{\mathrm{start}} + \frac{T}{2}$ in the middle of the chirp and χ_f the chirp rate. t_{start} is the start of the transmission time and T the duration of the transmission. The received signal is mixed with the transmitted signal with an IQ-mixer. Afterwards a low pass filter is applied. This is depicted in Fig. 2.4. Hence, the baseband signal contains the difference frequency f_{diff}, which is the difference between the transmitted frequency $f_{\mathrm{Tx}}(t)$ and received frequency $f_{\mathrm{Rx}}(t)$. The received frequency differs from the transmitted frequency because of the round trip delay τ and the Doppler effect, cf. Fig. 2.5. f_{diff} is constant and given by [Stove, 1992; Reiher, 2012]

$$f_{\mathrm{diff}} = f_{\mathrm{Tx}}(t) - f_{\mathrm{Rx}}(t) \approx f_{\mathrm{d}} + \chi_f\,\tau. \tag{2.5}$$

Thus, the baseband signal is a complex oscillation $\exp\left(j\,(2\pi\,f_{\mathrm{diff}}\,t + \varphi)\right)$ with constant frequency f_{diff} and phase offset φ. In an FMCW radar, f_{diff} is usually determined by a fast Fourier transform (FFT). Due to (2.1) and (2.2) we can write

$$f_{\mathrm{diff}} \approx 2\,\frac{v}{c}\,f_0 + \chi_f\,\frac{2\,d}{c}. \tag{2.6}$$

Thus, f_{diff} depends both on the unknown velocity v and the unknown distance d. Hence we have one equation but two unknowns. Because of this, at least two measurements are necessary using chirps with different chirp rates χ_f, which can also be negative. For several targets, more chirps have to be transmitted and processed. Then, in general, each received baseband signal contains several difference frequencies. The difference frequencies in each baseband signal, which correspond to the same target, have to be matched in order to estimate d and v of the target. This process is called frequency matching which is investigated in detail in [Reiher, 2012]. As an example for the different

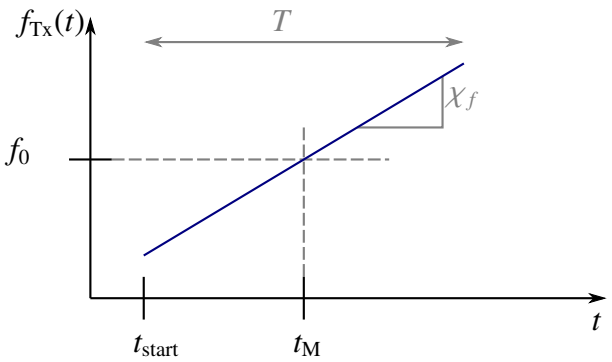

Figure 2.3.: Linear modulated frequency

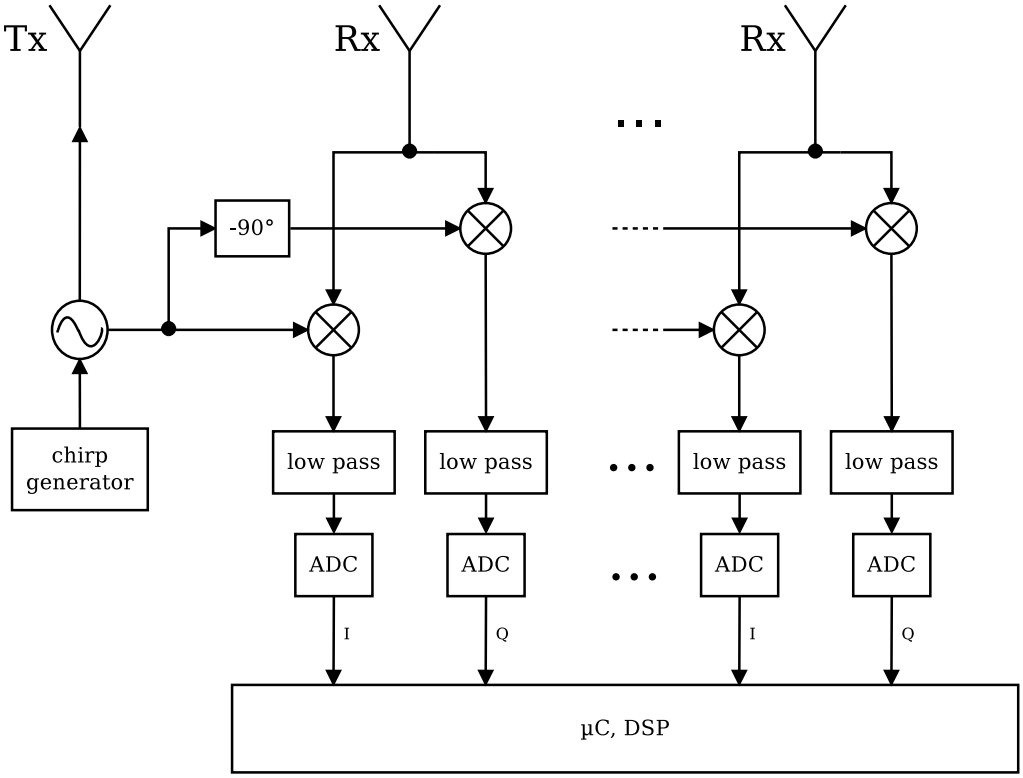

Figure 2.4.: Structure of an FMCW or chirp sequence radar system with an IQ mixer

radar parameters, we consider a typical FMCW radar which is used in automotive applications. It transmits 4 chirps which have a duration T of 2 to 10 ms and a bandwidth F of a few hundred MHz. The chirps have all different chirp rates χ_f, some of them positive and some of them negative.

A detailed derivation of the received baseband signal is presented in Section 5.1.1.

The Fourier transformed baseband signal is also called the compressed pulse, because the energy of the signal is not distributed in all time domain samples, but only in a few frequency bins. Mixing down the received signal with the transmitted one and taking the Fourier transform of it is similar to the correlation of the received signal with the transmitted one. This technique is called pulse compression [Skolnik, 2001]. For an array with N_{Rx} Rx antennas, we have N_{Rx} received baseband signals. For each received baseband signal, the complex value of the Fourier transform at the difference frequency f_{diff} of the target is taken. These values, denoted by $\underline{x} \in \mathbb{C}^{N_{\mathrm{Rx}}}$, are used to estimate the target's DOA [Van Trees, 2002; Schoor, 2010]. Thus, $\underline{x}$ is the signal after pulse compression. The principle of DOA estimation is explained in more detail in the context of colocated MIMO radars in Section 3.1.2.

A thorough treatment of the FMCW radar is presented in [Reiher, 2012; Lübbert, 2005].

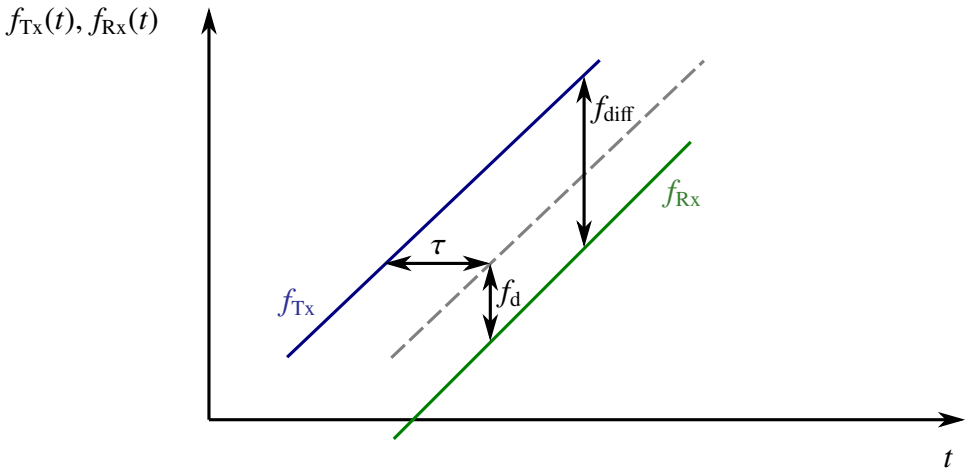

Figure 2.5.: Relation between Tx and Rx chirp

2.1.3. Chirp Sequence Radar

Another type of radar transmits many equal chirps of short duration. Such a radar is called a chirp sequence radar [Winner, 2012]. The structure is the same as the FMCW radar, cf. Fig. 2.4. Exemplary values are 512 chirps of a duration of 10 to 100 μs and a bandwidth of approximately 1 GHz. Thus, the chirp rate χ_f is much higher than that in an FMCW radar. As a consequence, the term $\chi_f \tau$ in (2.5) is usually much larger than the Doppler frequency f_d. Hence the difference frequency f_diff depends approximately only on the distance [Winner, 2012]

$$f_\mathrm{diff} \approx \chi_f \tau = \chi_f \frac{2d}{c}. \tag{2.7}$$

Therefore, the distance d can be determined from f_diff. Compared to the FMCW radar, in the case of several targets no matching algorithm, which relates several difference frequencies to one target, is necessary. This is a big advantage. As in the FMCW radar, f_diff is usually determined by a FFT. The Doppler effect becomes perceivable by a phase shift between the successive received chirps. Hence the velocity v can be determined by analyzing the phase change from chirp to chirp. This is usually done by another FFT. For each bin of the first FFT, the second FFT is computed. This corresponds to a two dimensional FFT. For a SIMO radar with an array of N_Rx Rx antennas, the values of the two dimensional Fourier transform at the estimated values $\hat{d}$, $\hat{v}$ for each Rx antenna are used as the signal $\underline{x} \in \mathbb{C}^{N_\mathrm{Rx}}$ for the DOA estimation. Hence, $\underline{x}$ is gained by pulse compressing the baseband signal two times. For a detailed derivation of the baseband signal of a chirp sequence radar, see Section 5.1.1.

2.2. Parameter Estimation and Performance Measures

In a radar system, different unknown parameters of a target, e. g. its distance, velocity, and DOA, have to be estimated from the measured data. First we introduce the notation of a general parameter

estimator. After that we take a look at the performance measures to characterize a radar system. There are many different ones, e. g. the accuracy and resolution of certain parameters, ambiguities and sidelobe levels, the robustness of the radar against different perturbations, the number of detectable targets, and the clutter rejection ability. In this thesis, we focus on the accuracy and the resolution of the DOA.

2.2.1. Parameter Estimation

We want to determine the unknown, deterministic parameter vector $\underline{\Theta} \in \mathbb{R}^M$ from a measurement $\underline{x} \in \mathbb{R}^K$. The statistical signal model is defined by a random vector $\underline{X}$ with its probability density function $f_{\underline{X}}$. The measurement $\underline{x}$ is an observed value, i. e. a realization of $\underline{X}$. The estimation function $\underline{g}$ is used to estimate the unknown parameter $\underline{\Theta}$ from the measurement $\underline{x}$

$$\begin{aligned} \underline{g}: \quad & \mathbb{R}^K \to \mathbb{R}^M, \\ & \underline{x} \quad \mapsto \underline{g}(\underline{x}). \end{aligned} \tag{2.8}$$

For one measurement $\underline{x}$, the estimate of $\underline{\Theta}$ is the value $\hat{\underline{\vartheta}} = \underline{g}(\underline{x})$. With the random vector $\underline{X}$, we can define the new random vector $\hat{\underline{\Theta}} = \underline{g} \circ \underline{X}$. $\hat{\underline{\Theta}}$ is called the estimator. Often the estimation function is also denoted by $\hat{\underline{\Theta}}$. It is clear from the context what $\hat{\underline{\Theta}}$ denotes.

In some applications, the measurements are complex values $\underline{x} \in \mathbb{C}^K$. This is for example the case, if a radar system with an IQ-mixer is investigated, which results in a complex baseband signal. This can be mapped to the real case by considering the real and imaginary part separately.

2.2.2. Accuracy and Lower Bounds

To define the accuracy, we first define the bias, the covariance, and the mean square error (MSE) of an estimator.

Bias, Covariance and MSE The estimator's bias $\underline{b}_{\hat{\underline{\Theta}}}$, covariance matrix $\mathbf{C}_{\hat{\underline{\Theta}}}$ and mean square error (MSE) matrix $\mathbf{M}_{\hat{\underline{\Theta}}}$ are defined as

$$\underline{b}_{\hat{\underline{\Theta}}} = \mathrm{E}\left(\hat{\underline{\Theta}} - \underline{\Theta}\right), \tag{2.9}$$

$$\mathbf{C}_{\hat{\underline{\Theta}}} = \mathrm{E}\left(\left[\hat{\underline{\Theta}} - \mathrm{E}\left(\hat{\underline{\Theta}}\right)\right]\left[\hat{\underline{\Theta}} - \mathrm{E}\left(\hat{\underline{\Theta}}\right)\right]^T\right), \tag{2.10}$$

$$\mathbf{M}_{\hat{\underline{\Theta}}} = \mathrm{E}\left(\left[\hat{\underline{\Theta}} - \underline{\Theta}\right]\left[\hat{\underline{\Theta}} - \underline{\Theta}\right]^T\right), \tag{2.11}$$

respectively. Here, E(.) denotes the expectation operator. It can easily be shown that

$$\mathbf{M}_{\underline{\hat{\Theta}}} = \underline{b}_{\underline{\hat{\Theta}}}\,\underline{b}_{\underline{\hat{\Theta}}}^{T} + \mathbf{C}_{\underline{\hat{\Theta}}}. \tag{2.12}$$

An estimator is called unbiased if $\underline{b}_{\underline{\hat{\Theta}}} = \underline{0}$. For a scalar parameter Θ, the standard deviation $\sigma_{\hat{\Theta}}$ and root mean square error (RMSE) of the estimator $\hat{\Theta}$ are defined as the square root of the variance $C_{\hat{\Theta}}$ and MSE $M_{\hat{\Theta}}$, respectively:

$$\sigma_{\hat{\Theta}} = \sqrt{C_{\hat{\Theta}}}, \tag{2.13}$$

$$\mathrm{RMSE}_{\hat{\Theta}} = \sqrt{M_{\hat{\Theta}}}. \tag{2.14}$$

Accuracy For a scalar unknown parameter $\Theta \in \mathbb{R}$, the accuracy of an estimator is defined as the root mean square error (RMSE) of the estimator [Skolnik, 2001]. Sometimes the accuracy is defined to be proportional to the RMSE, where the proportional constant depends on the definition. For an unknown parameter vector $\underline{\Theta} \in \mathbb{R}^K$, the MSE matrix $\mathbf{M}_{\underline{\hat{\Theta}}}$ can be used in order to specify how accurate the parameter vector is estimated.

If an estimator is unbiased, or the bias is negligible compared to the covariance, then $\mathbf{M}_{\underline{\hat{\Theta}}} \approx \mathbf{C}_{\underline{\hat{\Theta}}}$. In that case the covariance matrix can be used to specify the accuracy.

Given a signal model of the radar and the target, there exist different lower bounds on the MSE or the covariance matrix. These bounds depend only on the signal model and are independent of the used estimator. They are usually valid for all estimators which satisfy certain conditions. Hence they can be used to determine the maximal achievable accuracy of a radar system. This is a big advantage compared to the investigation of the accuracy of a specific estimator. Moreover, for certain bounds an analytical expression can be derived. This enables to optimize different parameters of the radar system, e. g. the positions of the Tx and Rx antennas or the transmission times of the pulses. It is important that the bound under investigation is tight, i. e. a certain estimator actually achieves the bound. This can be verified by numerical simulations. If the bound is not tight, the optimization could be useless. Some well known lower bounds are the Cramer-Rao bound (CRB) [Cramer, 1945; Rao, 1945] and the Weiss Weinstein bound [Weiss and Weinstein, 1985]. A brief overview of different lower bounds is presented in [Uhlich, 2012]. We focus on the CRB, since it is easier to compute than many other bounds and analytical results are feasible in many cases. For an introduction to the CRB, see [Kay, 1993].

The CRB has the following property: Under some regularity conditions on the likelihood function, the CRB matrix $\mathbf{CRB}_{\underline{\Theta}}$ is a lower bound for the covariance matrix of any unbiased estimator [Kay, 1993]

$$\mathbf{C}_{\underline{\hat{\Theta}}} \geq \mathbf{CRB}_{\underline{\Theta}}, \tag{2.15}$$

where $\geq$ means that the difference $\mathbf{C}_{\underline{\hat{\Theta}}} - \mathbf{CRB}_{\underline{\Theta}}$ is a positive semidefinite matrix.

2.2.3. Resolution

The resolution describes the ability of a system to distinguish between two or more targets. Roughly speaking, the resolution is the smallest possible distance between two objects such that they can be distinguished, i. e. the system detects two and not only one target. Here the distance is the difference of one or more physical quantities, depending on the considered system, e. g. the frequency, the DOA or the geometrical position. Resolution is an important performance criterion, not only in radar systems. In astronomy, the resolution of a telescope describes how far two point like objects (e. g. stars) have to be separated in the angle in order to be resolved. There are many different definitions for the resolution, see a survey in [den Dekker and van den Bos, 1997]. Some of them cannot be justified thoroughly. One classical, often used definition for angular resolution or the resolution in frequency is the Rayleigh criterion: Two targets can be resolved if they are separated such that the first minimum of the main lobe of the first target is at the position of the maximum of the main lobe of the second target [den Dekker and van den Bos, 1997]. This definition does not depend on the signal-to-noise-ratio (SNR). But it is obvious that the ability to distinguish between two targets clearly depends on the SNR of both targets, and therefore a meaningful definition of resolution should incorporate this. In [Clark, 1995], the resolution is defined using ellipsoidal confidence regions. But in this approach the cross correlation between the parameter estimates of different targets is neglected.

We are interested in the angular resolution. A promising definition of the angular resolution is presented in [Liu and Nehorai, 2007]. They study a signal model of two closely spaced sources. To decide, if one or two targets are present, a binary hypothesis test is considered. They use the generalized likelihood ratio test (GLRT). Since its distribution is difficult to obtain in general, its asymptotic distribution is computed. The dependence of the GLRT on the separation distance of the targets is used to define the resolution. The authors of [El Korso et al., 2011] extend this resolution definition to multiple parameters. Below we present the definition for one parameter of interest φ_i per target, $i = 1, 2$. The parameter of interest could be the DOA for example. Then, the resolution δ_{RL} is defined implicitly as the solution of the following equation [El Korso et al., 2011]

$$\delta_{\mathrm{RL}} = \eta \sqrt{\mathrm{CRB}_{\delta}(\delta_{\mathrm{RL}})}. \tag{2.16}$$

Here, η is a factor which depends on the probability of false alarm P_{FA} and probability of detection P_{D}

$$\eta = \eta(P_{\mathrm{FA}}, P_{\mathrm{D}}) \tag{2.17}$$

and CRB_{δ} is the CRB of the parameter $\delta = |\Delta\varphi|$ where $\Delta\varphi = \varphi_2 - \varphi_1$ is the difference of the parameters of interest of the two targets. In general, CRB_{δ} is a function of δ, i. e. $\mathrm{CRB}_{\delta} = \mathrm{CRB}_{\delta}(\delta)$. Assuming $\eta = 1$, then the resolution δ_{RL} is the distance between the two targets at which the estimation uncertainty $\sqrt{\mathrm{CRB}_{\delta}}$ is as large as the distance δ_{RL}, as depicted in Fig. 2.6. The factor η includes

the fact that the detection process depends on P_{FA} and P_{D}. Fig. 2.7 shows the dependence of η on P_{FA} and P_{D}: For increasing P_{D} and/or decreasing P_{FA}, η increases. Fig. 2.6 shows that a larger η leads to a larger δ_{RL}. We can interpret this in the following way: For a higher detection probability P_{D} with the same P_{FA}, the targets must have a larger separation. This makes sense, since targets with a larger separation can be detected easier. Also, for a smaller P_{FA} the separation has to be larger, such that fewer false detections happen. It is interesting to note that this resolution definition relates detection to estimation theory: CRB_δ is a result of estimation theory and equation (2.16) is derived by means of detection theory using the asymptotic distribution of the GLRT.

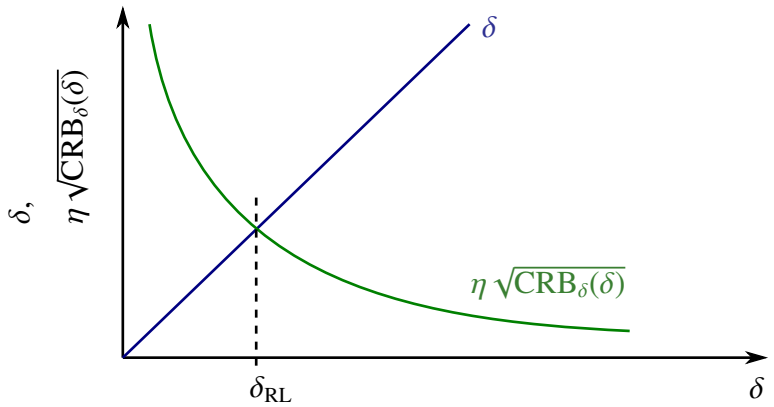

Figure 2.6.: Implicit definition of the resolution δ_{RL}

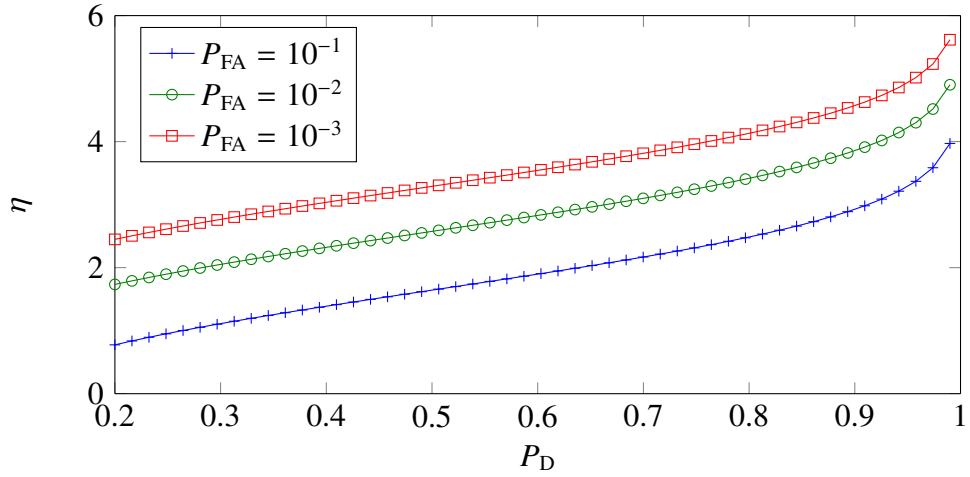

Figure 2.7.: η as a function of $P_{\mathrm{FA}}, P_{\mathrm{D}}$. For increasing P_{D} and decreasing P_{FA}, η increases. The computation of η is described in [Liu and Nehorai, 2007; El Korso et al., 2011].

3. MIMO Radar Concepts and State of the Art

In this chapter, we give an overview of the different aspects of a MIMO radar and their current state of the art.

MIMO radars have several Tx and Rx antenna elements which can be used independently. Hence every Tx antenna can transmit an arbitrary waveform and the signal received by a Rx antenna can be recorded independently of the other Rx antennas. We denote the number of Tx antennas by N_{Tx} and the number of Rx antennas by N_{Rx}. Thus there are $N_{\mathrm{Tx}} \cdot N_{\mathrm{Rx}}$ different antenna combinations which are used in the signal processing. In general, each combination receives a different signal. As a rough rule of thumb, the hardware complexity grows as $N_{\mathrm{Tx}} + N_{\mathrm{Rx}}$ and the number of different signals as $N_{\mathrm{Tx}} \cdot N_{\mathrm{Rx}}$, which is a promising property of a MIMO radar. We present different types of MIMO radars and their properties in Section 3.1. Different multiplexing techniques which can be used in a MIMO radar are discussed in Section 3.2. The application of MIMO radars in automobiles and the relation to our research is described in Section 3.3.

3.1. Types and Properties of MIMO Radars

MIMO radars can be divided into two different regimes: MIMO radars with widely separated antennas [Haimovich et al., 2008] and MIMO radars with colocated antennas [Li and Stoica, 2007; Boyer, 2011]. The term *widely separated antennas* means that the geometrical distance between some or all of the antennas is comparable or larger than the distance between an antenna and the target. An example is depicted in Fig. 3.1a. Here we can see that in general the angle under which the target appears is different for the different antennas. On the other hand, if the distance between all antennas is much smaller than the target's distance, the radar is called colocated MIMO radar. In such a radar system, the target's DOA is approximately the same for all antennas, cf. Fig. 3.1b. We give some important aspects on MIMO radars with widely separated antennas and then focus on MIMO radars with colocated antennas.

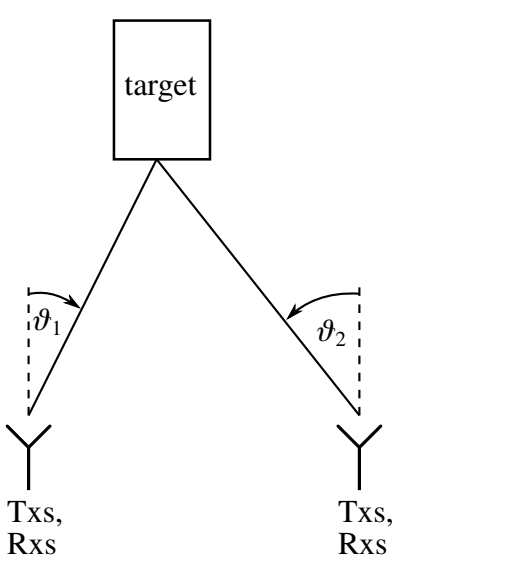

(a) MIMO radar with widely separated antennas, $\vartheta_1 \neq \vartheta_2$

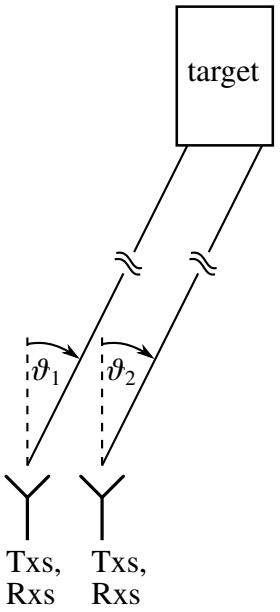

(b) colocated MIMO radar, $\vartheta_1 = \vartheta_2$

Figure 3.1.: Example of two different types of MIMO radars

3.1.1. MIMO Radar with Widely Separated Antennas

The Tx and/or Rx array elements are widely separated such that each Tx-Rx combination gives an independent scattering response of the target [Li and Stoica, 2009, Ch. 2]. Therefore, this kind of radar is also called *statistical MIMO radar* or, due to the different geometrical positions, *multistatic MIMO radar*. A survey of this radar type is presented in [Haimovich et al., 2008]. In [Lehmann et al., 2007] and [Fishler et al., 2004], a model is derived which states the conditions under which independent scattering responses are observed. Statistical MIMO radars offer several advantages, which we present briefly in the following.

Usually the radar cross section (RCS) of a target is strongly angle dependent [Skolnik, 2001]. Hence it is possible that from a particular direction a target's signal is weak, whereas from another direction at the same distance to the target, it is much stronger. A MIMO radar with widely separated antennas can mitigate these angle-dependent fluctuations of the radar cross section and thus offer a higher resolution in target localization [Haimovich et al., 2008]. Moreover, this can also lead to a higher accuracy in estimating the DOA [Lehmann et al., 2007; Fishler et al., 2004], and slowly moving targets can be handled better by using Doppler estimates from different directions [Haimovich et al., 2008]. The larger number of degrees of freedom of a MIMO radar compared to a SIMO radar can result in a larger number of parameters which can be estimated uniquely [Haimovich et al., 2008].

The benefits of a such a MIMO radar come at the cost of a more complex hardware since the Tx antennas have to be controlled independently. Moreover, one can use a system consisting of widely separated Tx antennas and colocated Rx antennas. This allows coherent signal processing for DOA estimation, but requires the phase of all Tx antenna elements to be kept synchronized despite the

Table 3.1.: Advantages and disadvantages of MIMO radars with widely separated antennas compared to SIMO radars

advantages	mitigation of RCS fluctuations high resolution in target localization better detection of slowly moving targets estimation of a larger number of parameters
disadvantages	phase synchronization over large distances more complex hardware more demanding signal processing algorithms higher computational burden

large distance, or it has to be estimated as well [Fletcher and Robey, 2003]. Moreover, the signal processing algorithms become more complex and in general the computational effort is higher.

The mentioned advantages and disadvantages of a MIMO radar with widely separated antennas compared to a SIMO radar are summarized in Tab. 3.1.

3.1.2. Colocated MIMO Radar

In this kind of MIMO radar all antenna elements are colocated, i.e. their geometrical distance is small compared to the distance to the target. Therefore, the target's RCS is the same for every Tx-Rx combination and the target appears under the same angle for every antenna. The signals can be processed coherently. This is the reason why this kind of radar is sometimes also called *coherent MIMO radar*. An overview on these radars can be found in [Li and Stoica, 2007] and in the introduction part of [Boyer, 2011]. Several different aspects of colocated MIMO radars are investigated in [Bekkerman and Tabrikian, 2006]. The properties of colocated MIMO radars and important investigations, already done by different authors, are presented in the following.

Virtual Array First we present the signal model for DOA estimation of a SIMO radar. Afterwards we introduce the signal model for a MIMO radar from which the concept of the virtual array follows.

We consider a SIMO radar with one Tx antenna and a linear array of N_{Rx} receiving antennas. All antennas are assumed to have isotropic transmitting and receiving characteristics. The target is in the far field, i. e. the antenna array receives a plane wave. This is depicted in Fig. 3.2. The target's DOA ϑ is measured perpendicular to the antenna array. The sign of ϑ is defined such that $\vartheta > 0$ in Fig. 3.2. The time delay between the receiving of the signal at the different Rx antennas results in phase changes of the baseband signal. The DOA can be estimated by analyzing the phase relation of the N_{Rx} receiving antennas. The positions of the Rx antennas normalized by $\frac{\lambda}{2\pi}$ are given in

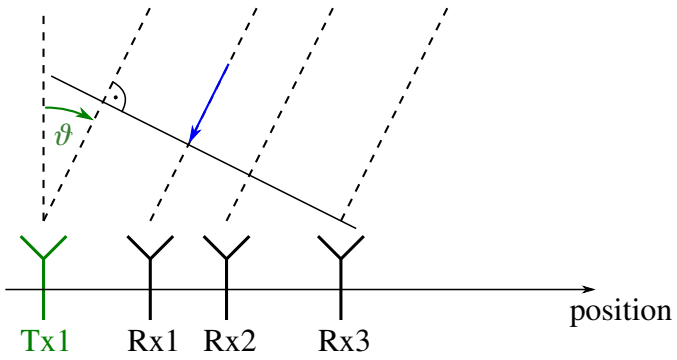

Figure 3.2.: Antenna array of a SIMO radar. The blue arrow indicates the propagation direction of the wave front.

$\underline{d}^{\mathrm{Rx}} \in \mathbb{R}^{N_{\mathrm{Rx}}}$. Here, λ denotes the carrier wavelength. We divide by $\frac{\lambda}{2\pi}$ because it allows a convenient notation in the following. As an example, $d_i^{\mathrm{Rx}} = \pi$ means that the i-th Rx antenna is at position $\pi \cdot \frac{\lambda}{2\pi} = \frac{\lambda}{2}$. Hence, $\underline{d}^{\mathrm{Rx}}$ has the unit $\frac{\lambda}{2\pi}$. The complex signal $\underline{x}_{\mathrm{SIMO}}$ after pulse compression, i. e. after Fourier transform and range and velocity estimation, can be modeled as [Krim and Viberg, 1996; Schoor, 2010; Van Trees, 2002]

$$\underline{x}_{\mathrm{SIMO}} = \underline{a}^{\mathrm{Rx}}(u)\, s + \underline{n} \in \mathbb{C}^{N_{\mathrm{Rx}}}. \tag{3.1}$$

Here, $s \in \mathbb{C}$ is the complex signal strength of the target. It includes several quantities, e. g. the radar cross section (RCS) of the target as well as the damping of the electromagnetic wave during propagation. $\underline{n} \in \mathbb{C}^{N_{\mathrm{Rx}}}$ denotes the measurement noise and $\underline{a}^{\mathrm{Rx}}(u)$ is the so called steering vector defined as

$$\underline{a}^{\mathrm{Rx}}(u) = \exp(j\, \underline{d}^{\mathrm{Rx}} u) \in \mathbb{C}^{N_{\mathrm{Rx}}}. \tag{3.2}$$

We use j as the symbol for the imaginary unit, i. e. $j^2 = -1$. For any vector $\underline{x} \in \mathbb{C}^K$, the expression $\exp(\underline{x})$ is to be understood as an element-by-element operation, i. e. $\underline{y} = \exp(\underline{x})$ means $y_i = \exp(x_i)\, \forall i = 1, \ldots, K$. The electrical angle u is defined as

$$u = \sin(\vartheta). \tag{3.3}$$

The steering vector $\underline{a}^{\mathrm{Rx}}(u)$ describes the phase change of the Rx antennas due to their different positions. The signal model (3.1) requires that the narrow band assumption for an array is fulfilled [Krim and Viberg, 1996]: The geometrical size of the Rx array Δd^{Rx}, the bandwidth F of the signal and the propagation speed c have to satisfy $\Delta d^{\mathrm{Rx}} F \ll c$. For an automotive radar, $\Delta d^{\mathrm{Rx}} \leq 50\,\mathrm{mm}$ and $c = 3 \cdot 10^8 \frac{\mathrm{m}}{\mathrm{s}}$ is the speed of light. Hence F has to satisfy $F \ll 6\,\mathrm{GHz}$. This condition is fulfilled for usual automotive radars.

Now we present the signal model for a MIMO radar with N_{Tx} Tx and N_{Rx} Rx antennas and a stationary target. An example of the MIMO radar is depicted in Fig. 3.3. Let every Tx antenna transmit once. Similar to the SIMO radar we denote the complex signal after pulse compression gained by

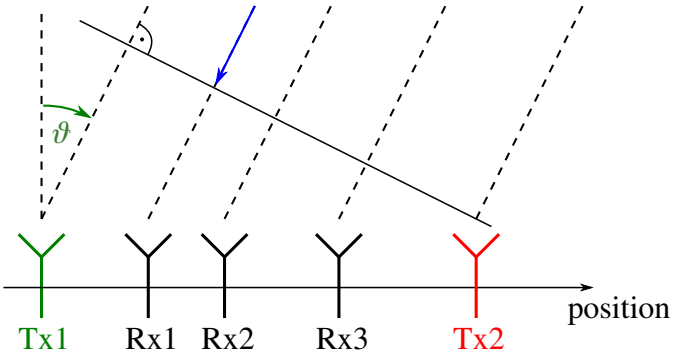

Figure 3.3.: Antenna array of a MIMO radar. The blue arrow indicates the propagation direction of the wave front.

the transmitted signal of the i-th Tx antenna by $\underline{x}_{\text{SIMO}}^{\text{Tx}\,i} \in \mathbb{C}^{N_{\text{Rx}}}$. Since every Tx antenna transmits once, we have N_{Tx} complex signals $\underline{x}_{\text{SIMO}}^{\text{Tx}\,i}$, $i = 1, \ldots, N_{\text{Tx}}$. We stack these vectors to define the new vector

$$\underline{x}_{\text{MIMO}} = \begin{bmatrix} \underline{x}_{\text{SIMO}}^{\text{Tx}1} \\ \vdots \\ \underline{x}_{\text{SIMO}}^{\text{Tx}N_{\text{Tx}}} \end{bmatrix} \in \mathbb{C}^{N_{\text{Tx}} \cdot N_{\text{Rx}}}. \tag{3.4}$$

In addition to the phase change due to the different Rx antenna positions, we get a phase change due to the different Tx antenna positions as well. Therefore, we introduce the steering vector of the Tx array

$$\underline{a}^{\text{Tx}}(u) = \exp(j\,\underline{d}^{\text{Tx}}\,u) \in \mathbb{C}^{N_{\text{Tx}}}, \tag{3.5}$$

where $\underline{d}^{\text{Tx}} \in \mathbb{R}^{N_{\text{Tx}}}$ contains the positions of the Tx antennas in unit of $\frac{\lambda}{2\pi}$. Then, the complex signal $\underline{x}_{\text{MIMO}}$ after pulse compression is given as [Chen, 2009] [Li and Stoica, 2009, Ch. 2]

$$\underline{x}_{\text{MIMO}} = \underline{a}^{\text{Tx}}(u) \otimes \underline{a}^{\text{Rx}}(u)\, s + \underline{n} \in \mathbb{C}^{N_{\text{Tx}} \cdot N_{\text{Rx}}}. \tag{3.6}$$

Here, $\otimes$ is the Kronecker tensor product or outer vector product. For vectors $\underline{y} \in \mathbb{C}^K, \underline{z} \in \mathbb{C}^M$ it is defined as

$$\underline{x} = \underline{y} \otimes \underline{z} = \begin{bmatrix} y_1 \cdot \underline{z} \\ \vdots \\ y_K \cdot \underline{z} \end{bmatrix} \in \mathbb{C}^{K \cdot M}. \tag{3.7}$$

We define the new steering vector $\underline{a}^{\text{Virt}}(u) = \underline{a}^{\text{Tx}}(u) \otimes \underline{a}^{\text{Rx}}(u)$ which contains all Tx-Rx combinations.

It can be written as

$$\begin{aligned} \underline{a}^{\text{Virt}}(u) &= \underline{a}^{\text{Tx}}(u) \otimes \underline{a}^{\text{Rx}}(u) \\ &= \exp(j\,\underline{d}^{\text{Tx}}\,u) \otimes \exp(j\,\underline{d}^{\text{Rx}}\,u) \\ &= \exp(j\,\underline{d}^{\text{Virt}}\,u) \in \mathbb{C}^{N_{\text{Virt}}}, \end{aligned} \tag{3.8}$$

$$N_{\text{Virt}} = N_{\text{Tx}} \cdot N_{\text{Rx}}, \tag{3.9}$$

with

$$\underline{d}^{\text{Virt}} = \underline{d}^{\text{Tx}} \otimes \underline{1}_{N_{\text{Rx}}} + \underline{1}_{N_{\text{Tx}}} \otimes \underline{d}^{\text{Rx}} \in \mathbb{R}^{N_{\text{Virt}}}. \tag{3.10}$$

Here, $\underline{1}_K \in \mathbb{R}^K$ denotes a vector with all elements equal 1. $\underline{d}^{\text{Virt}}$ are the positions of a new array, called virtual array, and $\underline{a}^{\text{Virt}}(u)$ is the corresponding steering vector. Using (3.8) we can write

$$\underline{x}_{\text{MIMO}} = \underline{a}^{\text{Virt}}(u)\, s + \underline{n} \in \mathbb{C}^{N_{\text{Virt}}}. \tag{3.11}$$

Let us interpret this: The signal of the MIMO radar $\underline{x}_{\text{MIMO}}$ (3.11) can be written in the same way as that of the SIMO radar $\underline{x}_{\text{SIMO}}$ (3.1) with the Rx array replaced by the virtual array. Thus the MIMO radar with N_{Tx} Tx and N_{Rx} Rx antennas is mathematical equivalent to a SIMO radar with 1 Tx and $N_{\text{Virt}} = N_{\text{Tx}} \cdot N_{\text{Rx}}$ Rx antennas. An example of a virtual array is depicted in Fig. 3.4. Descriptively speaking, the virtual array can be constructed by taking the Rx array and putting it at the position of the first Tx antenna, at the position of the second Tx antenna and so on. Mathematically, this is the convolution between the Tx and Rx array. The concept of the virtual array can be easily generalized to two-dimensional arrays, i. e. planar arrays [Chen, 2009]. An example is depicted in Fig. 3.5.

The virtual array of the MIMO radar has a larger aperture than the receiving or transmitting array alone. This yields a narrower beam for DOA estimation which results in a higher angular accuracy and a higher angular resolution. That is one important benefit of a colocated MIMO radar. The geometric positions of the Tx and Rx antenna elements can be optimized in several ways. For

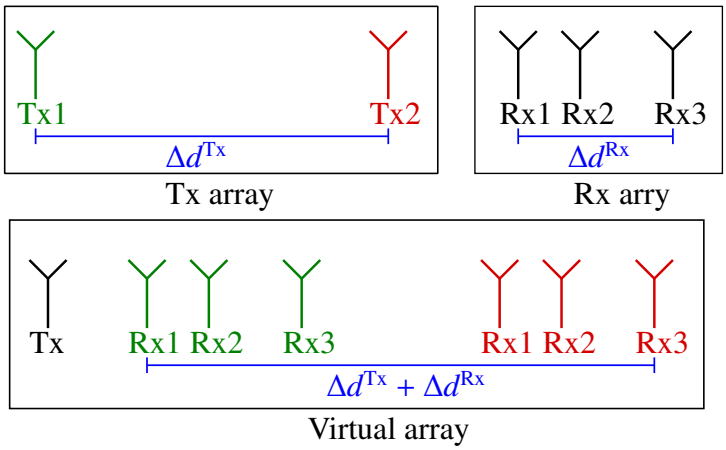

Figure 3.4.: Example of the construction of a linear virtual array

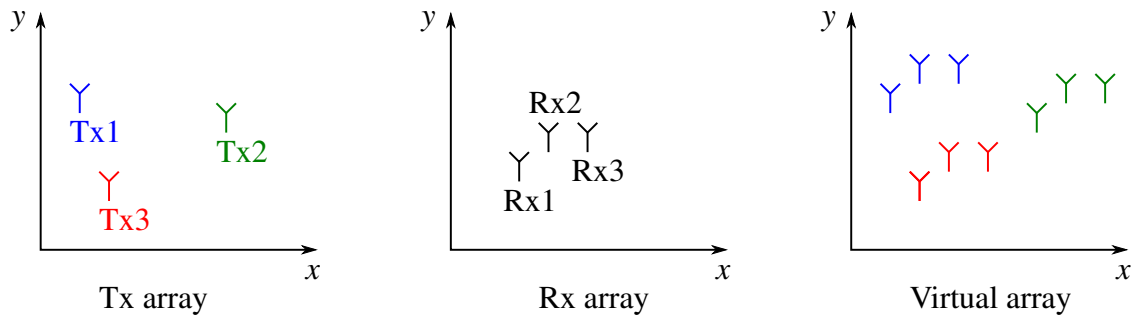

Figure 3.5.: Example of the construction of a planar virtual array

example, they can be optimized to result in a virtual array with a) a large aperture and b) low sidelobe levels. Some considerations and examples for such optimizations are given in [Li and Stoica, 2009, Ch. 2]. Moreover, it is possible to construct a virtual array, in which the spacing between two antenna elements is smaller than the real geometrical spacing. Hence sparse Tx or Rx arrays can be used to decrease the mutual coupling between antenna elements, and therefore increase the performance of the radar system [Feger et al., 2009]. Moreover, the antenna gain can be increased by using larger antenna patches, without violating the sampling theorem, which would result in ambiguities in angle estimation (grating lobes) [Feger et al., 2008, 2009].

In addition, a MIMO radar has a larger number of received signals compared to a SIMO array, $N_{\mathrm{Tx}} \cdot N_{\mathrm{Rx}}$ for a MIMO and N_{Rx} for a SIMO array. This leads to a larger number of targets that can be detected uniquely [Bekkerman and Tabrikian, 2006; Li and Stoica, 2007].

General Comparison of SIMO and MIMO Radars In order to compare the performance of a SIMO and MIMO radar, it is important to know under which conditions the radars receive the same signals or the information in the signals is exactly the same. The author of [Friedlander, 2009] shows which requirements have to be fulfilled such that a MIMO radar and an appropriate SIMO radar receive the same information. In these cases, the theoretical knowledge, e.g. performance bounds and algorithms, can be easily transferred from a SIMO to a MIMO radar. In [Vaidyanathan and Pal, 2009], the signal-to-noise (SNR), signal-to-clutter (SCR), and signal-to-interference ratios (SIR) are compared for SIMO and MIMO radars and a third radar system, called interpolated finite impulse response (IFIR) radar.

DOA Estimation Accuracy and Design of Transmit Beampatterns To investigate the achievable DOA accuracy, the Cramer Rao Bound (CRB) has been computed for different settings as presented in Chapter 1.

The Weiss-Weinstein bound is a lower bound on the MSE in parameter estimation [Weiss and Weinstein, 1985]. It requires no bias assumption, like the CRB, and can be used to analyze the threshold point of estimators. It is tighter than the CRB and the Bobrovsky-Zakai bound, but more complicated to compute. In [Tran et al., 2012], the Weiss-Weinstein bound is applied to colocated MIMO radars

to predict the SNR threshold point. Since the computation is difficult, an analytical approximation is derived. This bound can be used to help the design of the array geometry.

In a MIMO radar, Tx antennas can be used which transmit an isotropic or a very broad beam, because the beam forming of the Tx antennas is done digitally in the signal processing. Hence the coverage, i. e. the area in which targets can be detected, is larger compared to a SIMO radar [Bekkerman and Tabrikian, 2006]. Moreover, the spatial transmitted peak power density can be smaller, which is important in radar systems which should not be detected, e. g. in military applications. On the other hand, the larger number of transmit antennas of a MIMO radar offers a larger number of degrees of freedom to realize a given transmit beampattern [Li and Stoica, 2007]. This property can be used for adaptive transmit beampattern design: First, the target's DOA is estimated roughly. Then a transmit beampattern is formed which steers a certain beam in the direction of the target. Thus the target's DOA can be estimated more precisely. The disadvantage of such a beam is a smaller coverage area. In [Forsythe and Bliss, 2005; Li et al., 2008], the CRB for DOA estimation of several stationary targets is computed as a function of the covariance matrix of the transmitted signals. Then the transmitted signals are optimized in order to achieve a small CRB in a certain sense under the constraint of a constant total transmitting power. The optimal signals depend on the number and positions of the Tx and Rx antenna elements as well as on the optimization criterion. For the one target case, the solutions are a sum beam which steers the transmit power in the direction of the target, a difference beam which places a null in the direction of the target, or orthogonal signals. There is a trade-off between the sum beam and orthogonal signals, since the sum beam provides a higher SNR and the orthogonal signals lead to a larger virtual aperture. It depends on the geometrical arrangement of the antenna positions which beam is better. For the two target case, the optimization is even more complicated, but the results suggest that the waveform diversity of a MIMO radar is even more important in the two target case than in the one target case. In [Li and Stoica, 2009, Ch. 2], the one target case is examined further. The authors show that mixing a difference beam with orthogonal signals leads to a good performance in DOA estimation.

Friedlander shows in [Friedlander, 2012] the effects of a mismatch between the signal model and the reality in MIMO radar. The numerical studies suggest that, especially for null steering, i.e. placing a null at the target's DOA, model mismatch can be crucial. Beamforming seems not to be so sensitive to model errors.

The authors of [Hassanien and Vorobyov, 2010a,b] study the DOA estimation performance of a so called phased MIMO radar. The MIMO radar has the benefit of a large virtual aperture, but a lower SNR than the SIMO radar, since the latter uses transmit beamforming to focus more transmitted power on the target. The phased MIMO radar is a mix of a SIMO and MIMO radar. The transmit array is partitioned into several subarrays. The transmitters belonging to the same subarray transmit the same waveform coherently as in a SIMO radar. This results in a transmit beam gain. The waveforms of the subarrays are orthogonal to each other, a typical property of a MIMO radar. Since a transmitting antenna can belong to several subarrays, the transmitted waveforms become more

complex. This idea corresponds to transforming the transmit element space to the transmit beam space [Hassanien and Vorobyov, 2010b]. For the comparison of these different radar systems, the authors investigate especially the different beampatterns and SNRs. If the target's DOA is known approximately a priori, a coherent processing gain can be achieved by steering the transmit beam in this direction. In automotive applications, the location of several targets is estimated with one measurement. In general, they have different DOAs. Hence, in these applications it is not possible to steer the transmit beam in one certain direction in order to achieve a processing gain for the whole estimation process.

If we want to transmit a given spatial beampattern using a MIMO radar, we must be able to compute the signals to transmit which yield the desired beampattern. For that purpose, the authors of [Fuhrmann and San Antonio, 2004] derive an algorithm to compute the cross-correlation matrix of the transmitted signals such that the true beampattern achieves a given spatial beampattern. Moreover, they present in [Fuhrmann and San Antonio, 2008] an algorithm to compute the code sequences of coded binary phase shift keyed (BPSK) waveforms which yield the desired cross-correlation matrix.

Ambiguity Function With the help of the CRB, local properties of estimators like the DOA accuracy can be investigated. In order to examine not only local but also global properties of a radar system, the ambiguity function was invented, which is contributed to Ville and Woodward [Li and Stoica, 2009, Ch. 3]. It enables to examine the accuracy, resolution as well as ambiguities of a radar system. A new ambiguity function for more general parameter estimation problems was derived by the authors of [Rendas and Moura, 1998]. Woodward's ambiguity function is a special case of this one for narrowband radar systems. An ambiguity function specially for MIMO radar systems is derived in [Li and Stoica, 2009, Ch. 3] and [San Antonio et al., 2007]. The authors show how the ambiguity function depends on the covariance matrix of the transmitted waveforms. Hence it can be used as a tool to optimize the transmitted signals to achieve a high accuracy, a good resolution and few ambiguities.

Space Time Adaptive Processing and Ground Moving Target Indication Space Time Adaptive Processing (STAP) tries to maximize the signal-to-interference-and-noise ratio (SINR) by linearly combining the received signals [Brennan and Reed, 1973; Melvin, 2004]. It can be used to suppress clutter and interference and is applied e.g. in airborne radar systems for ground moving target indication (GMTI). The application of STAP in MIMO radars is an interesting topic and active research area due to the large number of degrees of freedom [Chen, 2009]. The CRB for STAP is derived by the authors of [Chong et al., 2011], and multipath clutter mitigation is investigated in [Mecca et al., 2006]. Different multiplexing schemes in slow-time for moving targets are compared in the context of GMTI in [Xue et al., 2009, 2010], where both the angle and Doppler frequency

Table 3.2.: Advantages and disadvantages of colocated MIMO radars compared to SIMO radars

advantages	larger virtual array
	higher angular accuracy
	higher angular resolution
	lower sidelobe levels in DOA estimation
	larger coverage area
	smaller spatial transmitted peak power density
	use of sparse real arrays which result in a non-sparse virtual array
	larger number of detectable targets
	flexible transmit beampattern design
	larger degrees of freedom especially for STAP
disadvantages	more complex hardware
	SNR loss compared to a focused transmit beam
	more demanding signal processing algorithms
	higher computational burden
	more complicated calibration of the Tx antennas

are estimated. Furthermore, [Li and Stoica, 2007] reports a higher detection rate for slowly moving targets.

General Disadvantages of MIMO Radars Many advantages and disadvantages depend on the precise implementation and application of the MIMO radar. But in general, MIMO radars need a more demanding and complicated hardware compared to SIMO radars [Bekkerman and Tabrikian, 2006]. Moreover, the signal models are more involved which also leads to more demanding signal processing algorithms. This results in a higher computational burden. The use of several colocated Tx antennas can lead to electromagnetic coupling problems [Feger et al., 2009]. This also reduces the power efficiency and impacts the decoding and signal processing. Moreover, it makes the calibration of the Tx antennas more complicated.

The mentioned advantages and drawbacks of colocated MIMO radars compared to conventional SIMO radars are summarized in Tab. 3.2. The relation of the presented state of the art of MIMO radars to our work is discussed in Section 3.3.

3.2. Multiplexing Techniques

In order to use all Tx-Rx combinations in the signal processing, one has to distinguish which part of the received signal corresponds to which Tx antenna. There are several multiplexing techniques which can be used for that purpose. If the transmitted signals are mutually orthogonal, then in

principle every portion of the received signal can be assigned perfectly to one Tx antenna. But it is also possible that some transmitters send the same signal, but phase shifted, which can be used for beamforming. We discuss several different multiplexing techniques in the following.

3.2.1. Time Division Multiplexing

To distinguish the transmitted signals at the receiver side, we can just activate only one transmitter at one time instant. The next transmitter starts sending just after the one before has stopped, or more precisely, after a delay of the maximum round trip time of the signal. This is called time division multiplexing (TDM) or time division multiple access (TDMA). The sequence of the transmitters can be chosen deterministic or randomly, the latter named randomized time division multiple access (R-TDMA) [Xue et al., 2009]. TDM has low hardware requirements, because always only one antenna transmits.

TDM allows to use conventional radar waveforms, e. g. chirps, which have already been optimized for range and Doppler estimation. Since only one transmitter is active at one time instant, the maximum transmission power is limited by the maximum power of one antenna. One drawback of this multiplexing technique arises, if the observed targets are non-stationary: Due to the motion of the target, the received baseband signal is shifted by the corresponding Doppler frequency. This results in a phase change between successive pulses which has to be estimated or compensated in the following signal processing, see Section 5.1 for more details. This is especially important in direction of arrival (DOA) estimation, which relies on the phase relation of the signals. In other words, every received signal originated from a slightly different environment. If all signals shall be processed coherently, this has to be accounted for. We will discuss and investigate this in detail in this thesis.

3.2.2. Frequency Division Multiplexing

In frequency division multiplexing (FDM), different carrier frequencies are used for every transmitter while the transmitted baseband signal stays the same for all transmitters. Each received signal is mixed down with all used carrier frequencies, which results in N_{Tx} baseband signals. Obviously, opposed to the TDM approach, all transmitters can send at the same time and the overall power is not limited by the maximum power of one transmitter. In exchange, the hardware requirements are higher. Moreover, for a fixed total bandwidth, the bandwidth for each Tx antenna is reduced. Another disadvantage is the different phase of the received baseband signals: Due to the distinctive carrier frequencies, the carrier wavelengths are not the same. Given a fixed distance to the target, the ratio of the distance to the wavelength differs, resulting in a different phase of the received baseband signal. Hence this phase has to be estimated or compensated in the following processing steps, which is especially important in DOA estimation. The coupling of the range and angle can also be visualized by the range-angle ambiguity function, cf. [Sun et al., 2014]. Doppler division

multiple access is another approach which can be considered as a special kind of FDM. In that case, the center frequencies of the different Tx antennas are only slightly different, such that they can be distinguished in the Doppler domain [Xue et al., 2009; Sun et al., 2014].

3.2.3. Code Division Multiplexing

Code Division Multiplexing (CDM) is another approach. The transmitted signals are modulated by a unique code for every transmitter such that they can be distinguished on receiving. There are two types of CDM, called CDM in fast time and CDM in slow time.

Consider a MIMO radar in which every transmitter sends several pulses with a unique shape of the baseband signal. The number of pulses per transmitter is denoted by N_{Pulse}. If the baseband signals of all pulses, sent at the same time instance, are orthogonal to each other, then we can distinguish the signals at the receiver side in every pulse separately. This is called multiplexing in fast time [Li and Stoica, 2009, Ch. 7], [Xue et al., 2009], since the modulation happens within one pulse. On the other hand, modulations which extend over all $N_{\text{Tx}} \cdot N_{\text{Pulse}}$ pulses are called CDM in slow time.

3.2.3.1. CDM in Fast Time

Using orthogonal pulses in fast time has the advantage of distinguishing the transmitters in every received pulse by using a matched filter [Haimovich et al., 2008], and the subsequent signal processing is easier. For good separation of the signals, the pulses of the different transmitters have to have a low cross correlation. On the other hand, a high autocorrelation with low range sidelobe levels is required for a good range estimation and range compression. Hence a trade-off between both properties has to be achieved [Xue et al., 2009]. High range sidelobes lead to a coupling of the range and DOA. An example of a simulated range angle ambiguity function is given in [Sun et al., 2014]. MIMO radars using modulation in fast time have been investigated e.g. in [Fletcher and Robey, 2003; Robey et al., 2004]. In general, the hardware is much more demanding than in a SIMO radar due to the generation of N_{Tx} orthogonal waveforms at the same time.

3.2.3.2. CDM in Slow Time

For each Tx antenna, the sequence of N_{Pulse} pulses is modulated by a unique code. Typically this is achieved by a change of the phase of every pulse. Usually, these phase codes are orthogonal. After receiving all $N_{\text{Tx}} \cdot N_{\text{Pulse}}$ pulses from all transmitters, the parts originating from a certain transmitter can be reconstructed. Often the relative velocity of the target is estimated by the phase change of successive pulses, e.g. by using a chirp sequence radar. Moreover, the DOA estimation also uses the phase information of the baseband signals. Hence, when encoding of the signals, the Doppler as well as the DOA estimation have to be done at once. This results in a high computational load. A typical

example is the application of a MIMO radar for ground moving target indication (GMTI), where an angle Doppler map is constructed [Xue et al., 2009, 2010]. Code multiplexing can be combined with transmit beamforming to focus the transmitted energy into a certain angular region. This is investigated for the DOA estimation of multiple stationary targets in [Li et al., 2008]. Compared to CDM in fast time, the signals of the pulses, which are transmitted at the same time instance, do not have to have a low cross correlation. Therefore, they can achieve better autocorrelation properties. In addition, the bandwidth requirements are lower and, opposed to TDM, the transmission power is not limited by the transmission power of one antenna, since all antenna transmit at the same time.

3.2.4. Summary

Table 3.3.: Comparison of different multiplexing techniques. The symbol ✓means 'yes' and ↯ means 'no'.

	TDM	FDM	CDM fast time	CDM slow time
low hardware requirements	✓	↯	↯	↯
total transmission power limited by transmission power of one antenna	✓	↯	↯	↯
coupling of Doppler frequency and DOA	✓	↯	↯	✓
coupling of distance and DOA	↯	✓	✓	↯
larger bandwidth requirements	↯	✓	✓	↯
distinguishing of the Txs in every pulse	↯	✓	✓	↯
good autocorrelation properties of Tx signals	✓	✓	↯	✓
low computational load for encoding	✓	✓	✓	↯

The advantages and drawbacks of the different multiplexing techniques are summarized in Tab. 3.3.

3.3. MIMO Radars for Automotive Applications and Relation to our Work

Radar systems in automotive applications have to be produced at low cost. The hardware requirements for a TDM MIMO radar are less complex than for other multiplexing techniques. Therefore, TDM is a promising approach. For radars in automobiles, the total transmission power is limited by law. Usually this power limit is already achieved by only one Tx antenna. Hence, the disadvantage of TDM that the total transmission power is limited by the transmission power of one antenna is not crucial for automotive applications. Moreover, the transmission signals which are already optimized for the distance and velocity estimation in SIMO radars can still be used in a TDM MIMO radar. Due to these reasons, we investigate TDM MIMO radars in this thesis.

Proposed Implementations of MIMO Radars and Experimental Investigations The authors of [Zwanetski and Rohling, 2012] suggest a MIMO radar using TDM with signals optimized for automotive radars. The distance, relative velocity and DOA are estimated by evaluating the received signals by a three dimensional discrete Fourier transform (DFT). In [Wintermantel, 2010], a radar system is proposed in which the Tx antennas transmit chirp sequences with many chirps of short duration, e.g. 512 chirps with a duration of 10 microseconds. The Tx antennas transmit sequentially or all at the same time, but with a different phase modulation. The distance, velocity and DOA are estimated by a three dimensional DFT. Due to special phase modulation, the transmitters can be distinguished by using the DFT. The proposed system works using a chirp sequence of many chirps. It cannot be used with a few linear frequency modulated continuous wave (FMCW) chirps. Moreover, the hardware is more complex when using a phase modulation instead of TDM.

In [Feger et al., 2009; Jahn et al., 2012; Schmid et al., 2012; Guetlein et al., 2012, 2013a], experimental investigations of TDM MIMO radars are reported. In a TDM MIMO radar with non-stationary targets, the phase shift of the baseband signal due to the Doppler effect has to be accounted for in the DOA estimation as well, cf. Section 3.2.1. The authors of [Feger et al., 2009; Schmid et al., 2012] propose to use a MIMO radar with receiving and transmitting antenna positions such that at least two antenna elements of the virtual array have the same geometrical position (redundant position). Then, for a non-stationary target, the unknown Doppler phase of the baseband signal can be estimated by computing the phase difference of the antenna elements at the redundant positions. This Doppler phase estimation is then used in the angle estimation algorithm. Since only the antenna elements at the redundant positions are used to estimate the unknown Doppler phase, the noise at these antenna elements has a larger influence on the DOA estimation than the noise at the other antenna elements, which is a drawback of this approach. In [Guetlein et al., 2012] and [Guetlein et al., 2013a], two different switching sequences are proposed in order to estimate the Doppler phase of the baseband signal and experimental results are presented. In [Guetlein et al., 2013b], it is shown that one of the switching sequences might be difficult to realize exactly in practice. In the mentioned experiments, quantitative comparisons to different radar systems in the non-stationary case, especially in DOA estimation, are still missing.

We fill this gap by investigating the DOA estimation using SIMO and TDM MIMO radars in the following chapters. First we consider stationary targets and after that we extend the studies to non-stationary targets. In doing so, we compare different radar types quantitatively.

4. DOA Estimation of Stationary Targets

We study the DOA performance of different radar systems. There are different performance measures of a radar system, e. g. the accuracy, the resolution and sidelobe levels, and the robustness, cf. Section 2.2. A high accuracy of the DOA estimation is important in many applications. Consider an automotive radar system: In order to decide if an object is on the right or the left lane of the street, the DOA has to be more accurate, the larger the distance to the object. We investigate the maximum achievable DOA accuracy in terms of the CRB. Since the CRB is a lower bound on the covariance matrix of any unbiased estimator, the investigations based on the CRB are independent of the used estimation algorithm. It enables to compare the maximum accuracy of different radar systems.

We give an overview of the considered radar system in Section 4.1. In Section 4.2, we introduce the signal model for the SIMO radar and compute the CRB of the DOA. In Section 4.3, we consider the TDM MIMO radar for a stationary target, i.e. the target is not moving relative to the radar. We present the signal model, compute the CRB and finally compare it to the CRB of a SIMO radar in Section 4.4. In Section 4.5, we compare the performance of a MIMO radar using code division multiplexing (CDM) with orthogonal codes and TDM. We compare the CRBs of both systems and show, using the concept of sufficient statistics, under which conditions the received signals of both systems contain the same information. Section 4.5 is based on [Rambach and Yang, 2016b].[1] The results are summarized in Section 4.6.

4.1. Radar System

We consider a radar system consisting of a linear array with N_{Rx} receiving (Rx) and N_{Tx} transmitting (Tx) colocated, isotropic antennas. An example of such a radar system is depicted in Fig. 4.1. The positions of the N_{Rx} Rx antennas and N_{Tx} Tx antennas are given in $\underline{d}^{\mathrm{Rx}} \in \mathbb{R}^{N_{\mathrm{Rx}}}$ and $\underline{d}^{\mathrm{Tx}} \in \mathbb{R}^{N_{\mathrm{Tx}}}$, respectively, in the unit of $\frac{\lambda}{2\pi}$ where λ is the carrier wavelength. For example $d_i^{\mathrm{Rx}} = \pi$ means that the position of the i-th Rx antenna is $\pi \cdot \frac{\lambda}{2\pi} = \frac{\lambda}{2}$. The target is modeled as a point source and the transmitted signal is narrowband. The target is in the far field. The DOA of the target, measured perpendicular to the linear array, is denoted by ϑ, as depicted in Fig. 3.3 on page 37. The parameters of the SIMO and MIMO radar under consideration are shown in Tab. 4.1. In the SIMO case, only one Tx antenna transmits (Fig. 4.2a) or the Tx antennas transmit the same signal up to a complex scaling

[1] This chapter contains quotations of our own work [Rambach and Yang, 2016b] which are not marked additionally.

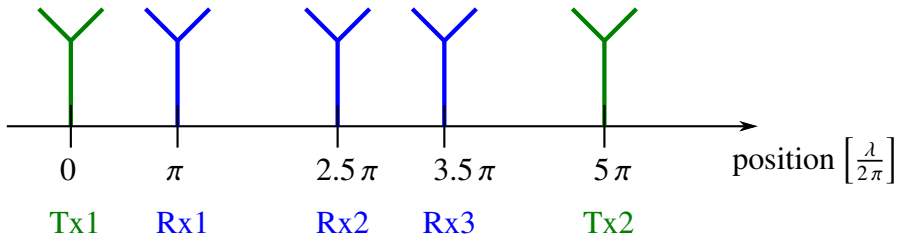

Figure 4.1.: A radar system with $N_{\mathrm{Tx}} = 2$ Tx and $N_{\mathrm{Rx}} = 3$ Rx antennas at positions $\underline{d}^{\mathrm{Tx}} = \pi\,[0, 5]^T$, $\underline{d}^{\mathrm{Rx}} = \pi\,[1, 2.5, 3.5]^T$

Table 4.1.: Overview of the parameters of the SIMO and MIMO radar

	SIMO	TDM MIMO
Rx antennas	N_{Rx}	N_{Rx}
Tx antennas	N_{Tx}, transmitting the same waveform up to a phase shift	N_{Tx}
total Tx power of the whole radar system	p	p
time of one measurement cycle	T_{cycle}	T_{cycle}
number of FMCW chirps per cycle	1	N_{Pulse}
chirp duration	T_{cycle}	$T_{\mathrm{cycle}}/N_{\mathrm{Pulse}}$
number of samples per chirp	N_{samples}	$N_{\mathrm{samples}}/N_{\mathrm{Pulse}}$
number of measurement cycles	L	L
total measurement time T_{total}	$L\,T_{\mathrm{cycle}}$	$L\,T_{\mathrm{cycle}}$

factor, i. e. with a different amplitude and phase shift, in order to focus the transmitted energy to a certain angular region (Fig. 4.2b). The total transmission power of the whole radar is p. Hence, if only one Tx antenna transmits, its transmission power is p. If several Tx antennas transmit, the total transmission power p has to be distributed among them. In the TDM MIMO system, the antennas transmit one at a time, each with transmission power p (Fig. 4.2c). Thus, the SIMO and MIMO radar use the same total transmission power. A measurement cycle consists of one or several chirps and the signals during one cycle are processed coherently, i. e. one measurement cycle is a coherent processing interval (CPI). The SIMO radar transmits one chirp per cycle and the MIMO radar N_{Pulse} chirps of equal duration per cycle. We assume that the time gap between adjacent chirps is negligible. The duration of one cycle is given by T_{cycle}, hence the duration of one chirp of the MIMO radar equals $T_{\mathrm{cycle}}/N_{\mathrm{Pulse}}$. This ensures that both radar systems transmit the same total energy, which is crucial for a fair comparison. One measurement cycle for the SIMO and MIMO radar is depicted in Fig. 4.3. The radar systems transmits L measurement cycles. Hence the total transmission time T_{total} is

$$T_{\mathrm{total}} = L\,T_{\mathrm{cycle}}. \tag{4.1}$$

We assume that the sampling rate is the same for both radar systems. The SIMO system takes N_{samples} of one chirp, and the MIMO radar $N_{\mathrm{samples}}/N_{\mathrm{Pulse}}$ samples per chirp for all N_{Pulse} chirps.

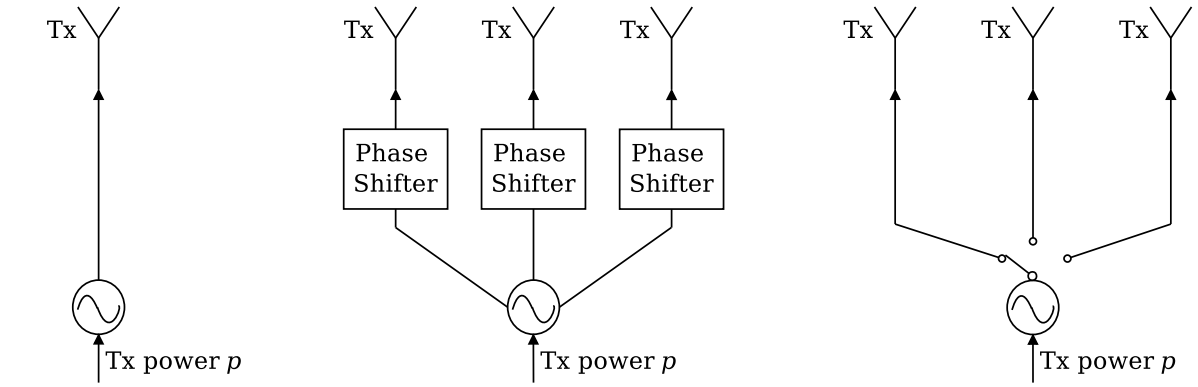

(a) SIMO radar with one Tx antenna

(b) SIMO radar with several Tx antennas

(c) TDM MIMO radar with successively transmitting antennas

Figure 4.2.: Different configurations of the SIMO and MIMO radars. The total Tx power p is the same for all configurations.

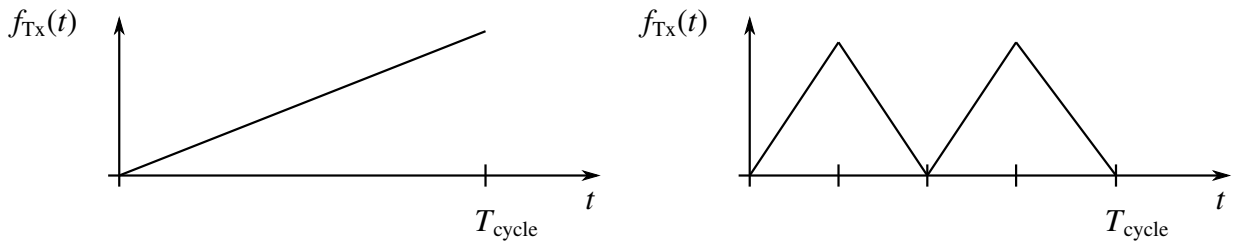

(a) SIMO radar

(b) MIMO radar with $N_{\mathrm{Pulse}} = 4$

Figure 4.3.: Example of the transmitted chirps of a SIMO and MIMO radar

4.2. SIMO Radar

We investigate the accuracy of the DOA estimation using a SIMO radar. We first present the signal model and then derive the CRB.

4.2.1. Signal Model

The signal model of the SIMO radar is similar to the model (3.1) introduced in Section 3.1.2 in the context of the virtual array. It is given by

$$\underline{x}(l) = B(u)\,\underline{a}^{\mathrm{Rx}}(u)\,s_{\mathrm{SIMO}}(l) + \underline{n}(l),\ l = 1, \ldots L \tag{4.2}$$

where $\underline{x}(l)$ is the signal after range processing. l denotes the cycle. Here

$$u = \sin(\vartheta) \tag{4.3}$$

is the electrical angle with ϑ being the DOA of the target. $B(u)$ is the transmit beampattern. For a SIMO radar with one isotropic Tx antenna, depicted in Fig. 4.2a, $B(u) = 1\ \forall u$. If several Tx antennas

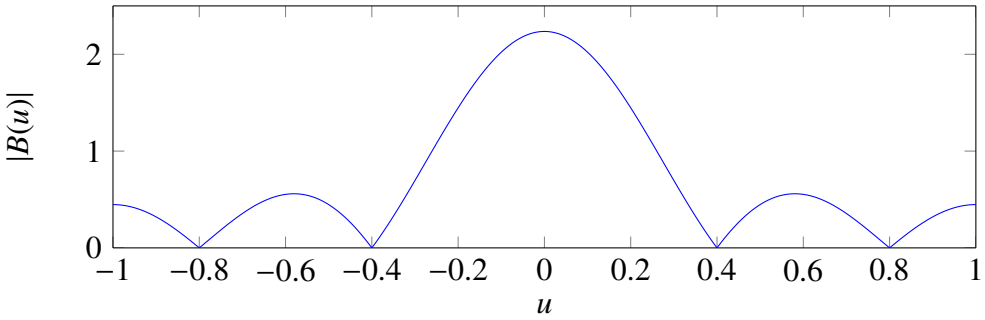

Figure 4.4.: Beampattern of an ULA of 5 isotropic Tx antennas with $\lambda/2$ spacing. All Tx antennas transmit the same signal without a phase shift. The main beam is directed to $u = 0$.

transmit the same signal up to a phase shift, cf. Fig. 4.2b, $B(u)$ changes depending on the position and the phase shifts of the Tx antennas. The phase shifts can be chosen such that the transmitted energy of the Tx antennas is directed to a certain DOA. An example of a transmit beampattern is depicted in Fig. 4.4. Note that $B(u)$ is normalized such that the total transmission power p remains constant. $\underline{a}^{\mathrm{Rx}}(u)$ is the steering vector with

$$\underline{a}^{\mathrm{Rx}}(u) = \exp(j\,\underline{d}^{\mathrm{Rx}}u). \tag{4.4}$$

$s_{\mathrm{SIMO}}(l)$ is the complex signal strength and $\underline{n}(l)$ the additional noise. Defining

$$\underline{g}(u) = B(u)\,\underline{a}^{\mathrm{Rx}}(u), \tag{4.5}$$

the model reads

$$\underline{x}(l) = \underline{g}(u)\,s_{\mathrm{SIMO}}(l) + \underline{n}(l). \tag{4.6}$$

We make the following assumptions:

- $\underline{n}(l)$ is circular complex Gaussian with zero mean, spatially and temporally uncorrelated with $\mathrm{E}\left(\underline{n}(l)\,\underline{n}^{H}(m)\right) = \delta_{l,m}\,\sigma^2\,\mathbf{I}$. Here, $\mathbf{I}$ is the identity matrix and σ^2 the variance of the noise. This assumption can be justified in the following way: Usually, the baseband signal in the time domain is processed by a fast Fourier transform (FFT). The FFT transformed signal is used for the further signal processing steps. If the number of samples in the time domain baseband signal is large enough, under some weak assumptions, the FFT transformed signal of the noise has the following properties [Böhme, 1998]
  - the real and imaginary part of the FFT signal are uncorrelated,
  - both parts are Gaussian distributed with the same variance,
  - the FFT signals at different frequencies are uncorrelated.
- Let τ_{prop} be the propagation time of the signal across the array and BW the bandwidth of the

signal. We assume that $\tau_{\text{prop}} \ll \frac{1}{\text{BW}}$, known as the narrowband array assumption [Dogandzic and Nehorai, 2001].

- The target's distance to the MIMO radar is much larger than the aperture of the radar such that we have a far field situation. Hence the radar receives a plane wave and the radar cross section as well as the DOA ϑ of the target and therefore also the electrical angle u are the same for all antennas.

The unknown deterministic quantities to be estimated from $\underline{x}(l)$, $1 \leq l \leq L$, are denoted by

$$\underline{\Theta} = \left[u,\ s_{\text{SIMO}}(1),\ \ldots,\ s_{\text{SIMO}}(L),\ \sigma^2\right]^T. \tag{4.7}$$

Note that if the SIMO radar transmits with a higher transmission power p, the signal strengths $|s_{\text{SIMO}}(l)|$ are larger.

4.2.2. Cramer-Rao Bound

In the following, we derive the deterministic CRB for the electrical angle and discuss the result.

4.2.2.1. Derivation

In our model, the unknown parameter vector is given in (4.7). We want to derive that part of the deterministic CRB of $\underline{\Theta}$ which corresponds to the electrical angle u. Hence we have to compute the Fisher information matrix (FIM) $\mathbf{J}$ of the whole parameter vector $\underline{\Theta}$ and then its inverse $\mathbf{J}^{-1}$. After that we take the entry of $\mathbf{J}^{-1}$ corresponding to u. This part is denoted by $\text{CRB}_{u,\text{SIMO}}$. Following [Yau and Bresler, 1992]

$$\text{CRB}^{-1}_{u,\text{SIMO}} = 2\,L\,\frac{\sigma^2_{s,\text{SIMO}}}{\sigma^2}\,\text{Re}(C) \tag{4.8}$$

where

$$\sigma^2_{s,\text{SIMO}} = \frac{1}{L}\sum_{l=1}^{L} |s_{\text{SIMO}}(l)|^2, \tag{4.9}$$

$$C = \underline{D}^H \mathbf{P}^{\perp}_{\underline{g}}\,\underline{D}, \tag{4.10}$$

$$\underline{D} = \frac{\partial \underline{g}(u)}{\partial u}, \tag{4.11}$$

$$\mathbf{P}^{\perp}_{\underline{g}} = \mathbf{I} - \underline{g}\left(\underline{g}^H \underline{g}\right)^{-1} \underline{g}^H. \tag{4.12}$$

$\mathbf{P}_{\underline{g}}^{\perp}$ is the projection matrix on the subspace which is orthogonal to the subspace spanned by $\underline{g}$. After some computations, this results in (cf. Appendix B)

$$\mathrm{CRB}_{u,\mathrm{SIMO}} = \frac{1}{2\,L}\frac{1}{S_{\mathrm{SIMO}}}\frac{1}{U_{\mathrm{SIMO}}} \tag{4.13}$$

with

$$S_{\mathrm{SIMO}} = \mathrm{SNR}_{\mathrm{SIMO}} \cdot N_{\mathrm{Rx}} \cdot |B(u)|^2, \tag{4.14}$$

$$\mathrm{SNR}_{\mathrm{SIMO}} = \frac{\sigma_{s,\mathrm{SIMO}}^2}{\sigma^2}, \tag{4.15}$$

$$U_{\mathrm{SIMO}} = \mathrm{Var}^{\mathrm{S}}(\underline{d}^{\mathrm{Rx}}). \tag{4.16}$$

Here, $\mathrm{Var}^{\mathrm{S}}(\underline{d}^{\mathrm{Rx}})$ is the sample variance of $\underline{d}^{\mathrm{Rx}}$. It is defined in (A.10) in Appendix A. There, some important properties are derived as well. It can be written as

$$\mathrm{Var}^{\mathrm{S}}(\underline{d}^{\mathrm{Rx}}) = \frac{1}{N_{\mathrm{Rx}}}\sum_{i=1}^{N_{\mathrm{Rx}}}\left(d_i^{\mathrm{Rx}} - \mathrm{E}^{\mathrm{S}}(\underline{d}^{\mathrm{Rx}})\right)^2, \tag{4.17}$$

$$\text{with } \mathrm{E}^{\mathrm{S}}(\underline{d}^{\mathrm{Rx}}) = \frac{1}{N_{\mathrm{Rx}}}\underline{1}^T\underline{d}^{\mathrm{Rx}}. \tag{4.18}$$

Roughly speaking, $\mathrm{Var}^{\mathrm{S}}(\underline{d}^{\mathrm{Rx}})$ quantifies how far the Rx antenna positions are distributed around the mean value $\mathrm{E}^{\mathrm{S}}(\underline{d}^{\mathrm{Rx}})$. $\mathrm{SNR}_{\mathrm{SIMO}}$ denotes the SNR at each Rx antenna. S_{SIMO} is the total SNR of the radar including the Rx antenna gain N_{Rx} and the Tx beam characteristics $|B(u)|^2$. The term U_{SIMO} is the sample variance of the Rx antenna positions.

The CRB $\mathrm{CRB}_{\vartheta,\mathrm{SIMO}}$ for the DOA ϑ can be easily derived from (4.13) by the rules of transformation of parameters [Kay, 1993]. Since

$$\frac{\partial u(\vartheta)}{\partial \vartheta} = \cos(\vartheta) \tag{4.19}$$

$\mathrm{CRB}_{\vartheta,\mathrm{SIMO}}$ is given by

$$\begin{aligned}\mathrm{CRB}_{\vartheta,\mathrm{SIMO}} &= \frac{1}{\cos(\vartheta)^2}\,\mathrm{CRB}_{u,\mathrm{SIMO}} \\ &= \frac{1}{2\,L\,\cos(\vartheta)^2}\frac{1}{S_{\mathrm{SIMO}}}\frac{1}{U_{\mathrm{SIMO}}}.\end{aligned} \tag{4.20}$$

4.2.2.2. Discussion

The smaller the CRB, the more accurate the electrical angle can be estimated. According to (4.13) and (4.14), the larger the SNR $\frac{\sigma_{s,\mathrm{SIMO}}^2}{\sigma^2}$, the smaller $\mathrm{CRB}_{u,\mathrm{SIMO}}$.

Moreover, (4.14) shows that the transmit beampattern B is equivalent to an SNR gain. Only the

magnitude of $B(u)$ at the target's electrical angle u is important, not the shape or derivative of $B(u)$. In a SIMO radar, all Tx antennas transmit the same waveform up to a phase shift. Hence, the maximal gain can be achieved, if the Tx beam is steered at the target's true angle. This is known as the beamforming gain. To be able to do that, the true angle has to be known approximately a priori. The maximum value of $|B|$ in the case of N_{Tx} isotropic Tx antennas and a constant total transmit power is $B_{\max} = \sqrt{N_{\mathrm{Tx}}}$, cf. Appendix C. Thus, the maximal achievable SNR gain in (4.14) is $B_{\max}^2 = N_{\mathrm{Tx}}$. If one Tx antenna is used, i. e. $B(u) = 1$, (4.13) simplifies to the expression derived in [Stoica and Nehorai, 1989] and given in a more compact form in [Athley, 2005].

The influence of the position of the Rx antennas on the CRB is expressed by $U_{\mathrm{SIMO}} = \mathrm{Var}^{\mathrm{S}}(\underline{d}^{\mathrm{Rx}})$. The larger $\mathrm{Var}^{\mathrm{S}}(\underline{d}^{\mathrm{Rx}})$, the smaller $\mathrm{CRB}_{u,\mathrm{SIMO}}$. This can be interpreted easily: Consider a radar with 2 Rx antennas. The larger the distance between both antennas, the larger the phase change of the baseband signal due to a change of the electrical angle. Hence, the radar is more sensitive to a change of the electrical angle, which results in a higher accuracy. This is reflected in (4.13) and (4.16): The larger the distance between both antennas, the larger $\mathrm{Var}^{\mathrm{S}}(\underline{d}^{\mathrm{Rx}})$ and the smaller $\mathrm{CRB}_{u,\mathrm{SIMO}}$.

4.3. MIMO Radar

Now we investigate the DOA estimation using a TDM MIMO radar. We present the signal model and derive the CRB for the electrical angle.

4.3.1. Signal Model

The MIMO radar consists of a linear array of N_{Tx} Tx and N_{Rx} Rx isotropic, colocated antennas. The positions of the Tx antennas in the sequence in which they transmit are given by $\underline{d}^{\mathrm{Pulse}} \in \mathbb{R}^{N_{\mathrm{Pulse}}}$ in the unit of $\frac{\lambda}{2\pi}$. $\underline{d}^{\mathrm{Pulse}} = [d_1^{\mathrm{Tx}}, d_2^{\mathrm{Tx}}, d_1^{\mathrm{Tx}}]^T$ means, for example, that the first antenna transmits, then the second one, and again the first one, see Fig. 4.5. Thus, if an antenna transmits more than once, its position occurs several times in $\underline{d}^{\mathrm{Pulse}}$. Similar to Section 3.1.2, the signal model for the MIMO radar is given by

$$\underline{x}(l) = \underline{a}^{\mathrm{Pulse}}(u) \otimes \underline{a}^{\mathrm{Rx}}(u)\, s_{\mathrm{MIMO}}(l) + \underline{n}(l),\ l = 1, \ldots L, \tag{4.21}$$

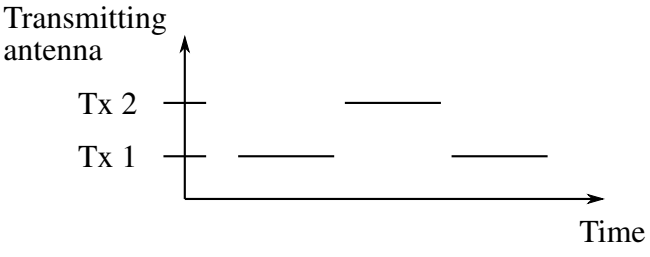

Figure 4.5.: Example of a TDM sequence with $\underline{d}^{\mathrm{Pulse}} = [d_1^{\mathrm{Tx}}, d_2^{\mathrm{Tx}}, d_1^{\mathrm{Tx}}]^T$

where $\underline{x}(l)$ is the measured signal of cycle l after pulse compression.

$$\underline{a}^{\text{Pulse}}(u) = \exp(j\,\underline{d}^{\text{Pulse}} u) \tag{4.22}$$

is the steering vector of the transmitting antennas given by $\underline{d}^{\text{Pulse}}$. $\underline{a}^{\text{Rx}}(u)$ is defined in (4.4). $s_{\text{MIMO}}(l)$ is the complex signal of the target and $\underline{n}(l)$ the additional noise. Note that $\underline{x}(l), \underline{n}(l) \in \mathbb{C}^{N_{\text{Virt}}}$, where

$$N_{\text{Virt}} = N_{\text{Pulse}} \cdot N_{\text{Rx}}. \tag{4.23}$$

Thus, the measured signal $\underline{x}(l)$ has N_{Virt} components due to the different transmitting antennas in contrast to the SIMO case with N_{Rx} components. Because of the shorter chirp duration, the modulus of s_{MIMO} is in general smaller than the modulus of s_{SIMO}, cf. Section 2.1.2. We define the steering vector of the virtual array

$$\underline{a}^{\text{Virt}}(u) = \underline{a}^{\text{Pulse}}(u) \otimes \underline{a}^{\text{Rx}}(u) \in \mathbb{C}^{N_{\text{Virt}}}. \tag{4.24}$$

$\underline{a}^{\text{Virt}}(u)$ incorporates all transmitter-receiver combinations. It can be written as

$$\begin{aligned} \underline{a}^{\text{Virt}}(u) &= \exp(j\,\underline{d}^{\text{Pulse}} u) \otimes \exp(j\,\underline{d}^{\text{Rx}} u) \\ &= \exp(j\,\underline{d}^{\text{Virt}} u) \end{aligned} \tag{4.25}$$

with the antenna positions of the virtual TDM MIMO array

$$\underline{d}^{\text{Virt}} = \underline{1}_{N_{\text{Pulse}}} \otimes \underline{d}^{\text{Rx}} + \underline{d}^{\text{Pulse}} \otimes \underline{1}_{N_{\text{Rx}}} \in \mathbb{R}^{N_{\text{Virt}}}. \tag{4.26}$$

Note that $\underline{d}^{\text{Virt}}$ already contains the transmitting sequence in $\underline{d}^{\text{Pulse}}$. Hence the dimension of $\underline{d}^{\text{Virt}}$ is $N_{\text{Rx}}\,N_{\text{Pulse}}$ and not $N_{\text{Rx}}\,N_{\text{Tx}}$. With these notations, we can write the signal model for the MIMO radar as

$$\underline{x}(l) = \underline{a}^{\text{Virt}}(u)\, s_{\text{MIMO}}(l) + \underline{n}(l),\ l = 1, \ldots L. \tag{4.27}$$

We make the same assumptions as in Section 4.2.1.

Similar to (4.7), the unknown deterministic parameters to be estimated from $\underline{x}(l),\ 1 \le l \le L$, are denoted by

$$\underline{\Theta} = \left[u,\ s_{\text{MIMO}}(1),\ \ldots,\ s_{\text{MIMO}}(L),\ \sigma^2\right]^T. \tag{4.28}$$

Note that in general $|s_{\text{MIMO}}(l)| < |s_{\text{SIMO}}(l)|$, since the MIMO radar transmits chirps with a shorter chirp duration than the SIMO radar, but uses the same transmission power p as the SIMO radar. Thus the transmitted energy per chirp is smaller, resulting in a smaller signal strength $|s_{\text{MIMO}}(l)|$. We investigate this in detail in Section 4.4.

4.3.2. Cramer-Rao Bound

The unknown parameter vector is given in (4.28). Again we are interested in that part of the CRB of $\underline{\Theta}$ which corresponds to the electrical angle u. We denote this part by $\mathrm{CRB}_{u,\mathrm{MIMO}}$. The MIMO signal model (4.27) has the same form as the SIMO model (4.6) if we set $B(u) = 1$. Hence we can use the result for the SIMO radar (4.13) if we replace the variables accordingly. This gives

$$\mathrm{CRB}_{u,\mathrm{MIMO}} = \frac{1}{2L}\frac{1}{S_{\mathrm{MIMO}}}\frac{1}{U_{\mathrm{MIMO}}} \tag{4.29}$$

with

$$S_{\mathrm{MIMO}} = \mathrm{SNR}_{\mathrm{MIMO}} \cdot N_{\mathrm{Virt}}, \tag{4.30}$$

$$\mathrm{SNR}_{\mathrm{MIMO}} = \frac{\sigma^2_{s,\mathrm{MIMO}}}{\sigma^2}, \tag{4.31}$$

$$\sigma^2_{s,\mathrm{MIMO}} = \frac{1}{L}\sum_{l=1}^{L} |s_{\mathrm{MIMO}}(l)|^2, \tag{4.32}$$

$$U_{\mathrm{MIMO}} = \mathrm{Var}^{\mathrm{S}}(\underline{d}^{\mathrm{Virt}}). \tag{4.33}$$

S_{MIMO} is the total SNR of the MIMO radar system, similar to the SIMO radar. U_{MIMO} depends on the Rx and Tx antenna positions. Using the properties of $\mathrm{Var}^{\mathrm{S}}$, cf. Appendix A.2.1 and A.2.4, the sample variance of the virtual array positions can be expressed as

$$\begin{aligned}
\mathrm{Var}^{\mathrm{S}}(\underline{d}^{\mathrm{Virt}}) &= \mathrm{Cov}^{\mathrm{S}}(\underline{1}_{N_{\mathrm{Pulse}}} \otimes \underline{d}^{\mathrm{Rx}} + \underline{d}^{\mathrm{Pulse}} \otimes \underline{1}_{N_{\mathrm{Rx}}}, \underline{1}_{N_{\mathrm{Pulse}}} \otimes \underline{d}^{\mathrm{Rx}} + \underline{d}^{\mathrm{Pulse}} \otimes \underline{1}_{N_{\mathrm{Rx}}}) \\
&= \mathrm{Cov}^{\mathrm{S}}(\underline{1}_{N_{\mathrm{Pulse}}} \otimes \underline{d}^{\mathrm{Rx}}, \underline{1}_{N_{\mathrm{Pulse}}} \otimes \underline{d}^{\mathrm{Rx}}) + \mathrm{Cov}^{\mathrm{S}}(\underline{1}_{N_{\mathrm{Pulse}}} \otimes \underline{d}^{\mathrm{Rx}}, \underline{d}^{\mathrm{Pulse}} \otimes \underline{1}_{N_{\mathrm{Rx}}}) \\
&+ \mathrm{Cov}^{\mathrm{S}}(\underline{d}^{\mathrm{Pulse}} \otimes \underline{1}_{N_{\mathrm{Rx}}}, \underline{1}_{N_{\mathrm{Pulse}}} \otimes \underline{d}^{\mathrm{Rx}}) + \mathrm{Cov}^{\mathrm{S}}(\underline{d}^{\mathrm{Pulse}} \otimes \underline{1}_{N_{\mathrm{Rx}}}, \underline{d}^{\mathrm{Pulse}} \otimes \underline{1}_{N_{\mathrm{Rx}}}) \\
&= \mathrm{Var}^{\mathrm{S}}(\underline{d}^{\mathrm{Rx}}) + \mathrm{Var}^{\mathrm{S}}(\underline{d}^{\mathrm{Pulse}}).
\end{aligned} \tag{4.34}$$

Thus

$$U_{\mathrm{MIMO}} = \mathrm{Var}^{\mathrm{S}}(\underline{d}^{\mathrm{Rx}}) + \mathrm{Var}^{\mathrm{S}}(\underline{d}^{\mathrm{Pulse}}). \tag{4.35}$$

Hence the positions of the Rx as well as the positions of the Tx antennas influence the CRB of the electrical angle.

4.4. Comparison of the SIMO and MIMO Radar

In order to see which radar system can achieve a higher accuracy, we compare $\mathrm{CRB}_{u,\mathrm{SIMO}}$ in (4.13) and $\mathrm{CRB}_{u,\mathrm{MIMO}}$ in (4.29). Different comparisons of the CRBs for MIMO radars to other radars have already been investigated, e. g. in [Li et al., 2008], but the comparisons depend on the precise type

of the MIMO radar and its application. Here we compare the TDM MIMO radar using an FMCW or chirp sequence modulation to the SIMO radar. We discuss the result w. r. t. the application in automobiles.

$\mathrm{CRB}_{u,\mathrm{SIMO}}$ and $\mathrm{CRB}_{u,\mathrm{MIMO}}$ have the same form but the formulas for the total SNR and the sample variance of the antenna positions differ. Since the chirp durations of the SIMO and MIMO radar differ the SNRs $\mathrm{SNR}_{\mathrm{SIMO}}$ and $\mathrm{SNR}_{\mathrm{MIMO}}$ are not equal. Hence, we have to compute the SNRs first. This is done in the next section. Then, we compare the SNRs, the CRBs and discuss the results. Numerical simulations are presented afterwards.

4.4.1. SNR Computation

In an FMCW and chirp sequence radar, the signal used for DOA estimation is gained by a discrete Fourier transform (DFT) of the complex baseband signal of one chirp and taking the complex amplitude of the highest peak in the spectrum. We consider the complex baseband signal of one target, i. e. a complex oscillation, and derive the SNR after doing the DFT. The measured, sampled signal $x(n)$ at one Rx antenna is

$$x(n) = \sqrt{\rho_\mathrm{s}}\, s(n) + n(n),\ n \in \mathbb{Z} \tag{4.36}$$

where n is the time index and ρ_s is the transmitted energy per sample. $s(n)$ is the complex signal strength. It includes the RCS, damping effects due to the distance to the target, and the antenna gain of the Rx and Tx antennas. $n(n)$ denotes additional noise. Note that the phase shift due to the position of the Rx antenna, which is described by $\underline{a}^{\mathrm{Rx}}(u)$, and the transmit beampattern $B(u)$ is not incorporated here. The transmitted energy per sample ρ_s can be written as

$$\rho_\mathrm{s} = p\,\Delta t. \tag{4.37}$$

where p is the transmitted power and Δt the sampling time interval of the ADC for one sample. Hence $\Delta t = 1/f_s$ with the sampling frequency f_s. Let

$$s(n) = s_0\, \mathrm{e}^{\,j\,(\omega_\mathrm{diff}\, n + \varphi)} \tag{4.38}$$

with the real and positive amplitude $s_0 \geq 0$. ω_diff is the angular difference frequency of the target and φ the additional phase, cf. Section 2.1.2. Let the noise be stationary, zero mean, and white Gaussian with variance σ_n^2 and autocorrelation function

$$r_n(n) = \sigma_n^2\, \delta(n) = \begin{cases} \sigma_n^2 & \text{if } n = 0, \\ 0 & \text{if } n \neq 0. \end{cases} \tag{4.39}$$

The SNR before the Fourier transform, defined as the ratio of the received signal energy to the variance of the noise, is

$$\mathrm{SNR}_{\mathrm{before}} = \frac{\left|\sqrt{\rho_\mathrm{s}}\, s(n)\right|^2}{\mathrm{Var}\,(n(n))} = \frac{\rho_\mathrm{s}\, s_0^2}{\sigma_n^2}. \tag{4.40}$$

There is only a finite number of samples per chirp available, which we denote by N. We incorporate this by multiplying $x(n)$ with a real window function $w(n)$ which is nonzero only for $0 \leq n \leq N-1$. Hence the discrete-time Fourier transform (DTFT) $X_w(\omega)$ of the windowed signal at angular frequency ω is given by

$$\begin{aligned} X_w(\omega) &= \sum_{n=-\infty}^{\infty} w(n)\, x(n)\, \mathrm{e}^{-j\omega n} \\ &= \sum_{n=0}^{N-1} w(n)\, x(n)\, \mathrm{e}^{-j\omega n}\,. \end{aligned} \tag{4.41}$$

Plugging in (4.36) yields

$$\begin{aligned} X_w(\omega) &= \sqrt{\rho_\mathrm{s}} \sum_{n=0}^{N-1} w(n)\, s(n)\ \mathrm{e}^{-j\omega n} + \sum_{n=0}^{N-1} w(n)\, n(n)\ \mathrm{e}^{-j\omega n} \\ &= \sqrt{\rho_\mathrm{s}}\, S_w(\omega) + N_w(\omega) \end{aligned} \tag{4.42}$$

with

$$S_w(\omega) = \sum_{n=0}^{N-1} w(n)\, s(n)\ \mathrm{e}^{-j\omega n}, \tag{4.43}$$

$$N_w(\omega) = \sum_{n=0}^{N-1} w(n)\, n(n)\ \mathrm{e}^{-j\omega n}\,. \tag{4.44}$$

The complex value that is used for the DOA estimation is $X_w(\omega_{\max})$, where $\omega_{\max}$ is the angular frequency at which $|X_w(\omega)|$ is maximal, i. e.

$$\omega_{\max} = \arg\max_{\omega}\ |X_w(\omega)|\,. \tag{4.45}$$

For simplicity, we assume that the SNR is large enough such that the difference between $\omega_{\max}$ and the true angular frequency ω_{diff} is negligible, hence $\omega_{\max} = \omega_{\mathrm{diff}}$. Since we are doing a DFT, the samples of $X_w(\omega)$ are only available at discrete frequencies ω_k, $k = 0, 1, \ldots$. We assume that, by frequency interpolation or zero-padding, the exact value of $\omega_{\max}$ is found. Then

$$\begin{aligned} X_w(\omega_{\max}) &= \sqrt{\rho_\mathrm{s}}\, S_w(\omega_{\max}) + N_w(\omega_{\max}) \\ &= \sqrt{\rho_\mathrm{s}}\, S_w(\omega_{\mathrm{diff}}) + N_w(\omega_{\mathrm{diff}}). \end{aligned} \tag{4.46}$$

The SNR after the DFT is defined as

$$\mathrm{SNR}_{\mathrm{after}} = \frac{\left|\sqrt{\rho_s}\, S_w(\omega_{\max})\right|^2}{\mathrm{Var}\left(N_w(\omega_{\max})\right)}. \tag{4.47}$$

In Appendix D, it is shown that

$$\mathrm{SNR}_{\mathrm{after}} = \mathrm{SNR}_{\mathrm{before}} \cdot \mathrm{SNR}_{\mathrm{gain}} \tag{4.48}$$

with the SNR gain

$$\mathrm{SNR}_{\mathrm{gain}} = \frac{\left(\sum_{n=0}^{N-1} w(n)\right)^2}{\sum_{n=0}^{N-1} w^2(n)}. \tag{4.49}$$

$\mathrm{SNR}_{\mathrm{gain}}$ depends on the window used. For the rectangular window, $w(n) = 1$ for $0 \le n \le N-1$ and thus $\mathrm{SNR}_{\mathrm{gain}} = N\ \forall N$. For other windows, $\mathrm{SNR}_{\mathrm{gain}} \le N$, which follows from the Cauchy-Schwartz inequality. In Fig. 4.6, $\frac{\mathrm{SNR}_{\mathrm{gain}}}{N}$ is plotted for some typical windows as a function of N. We see that

$$\frac{\mathrm{SNR}_{\mathrm{gain}}}{N} \approx \mathrm{const} = w_{\mathrm{gain}}, \quad \text{for } N > N_0 = 100, \tag{4.50}$$

where we have defined the window dependent gain $w_{\mathrm{gain}} \le 1$. Thus if the DFT length is larger than N_0, we can write

$$\mathrm{SNR}_{\mathrm{gain}} \approx w_{\mathrm{gain}} \cdot N. \tag{4.51}$$

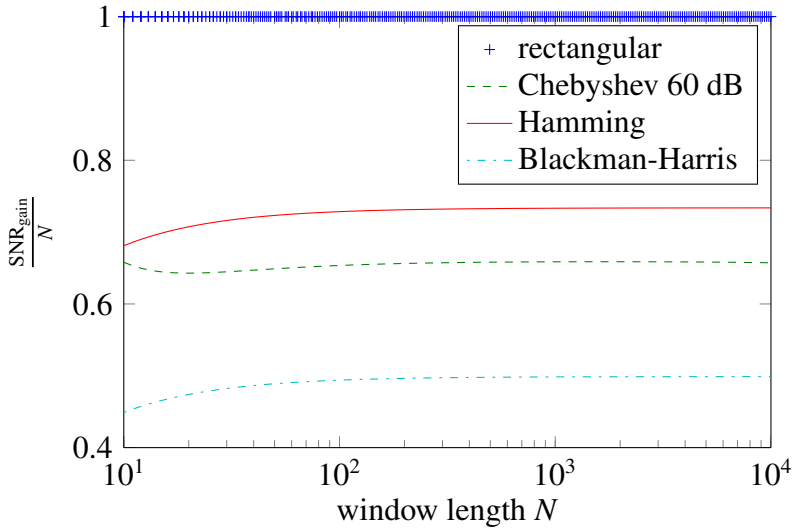

Figure 4.6.: SNR gain for different windows. Note, for the rectangular window $\frac{\mathrm{SNR}_{\mathrm{gain}}}{N} = 1$.

4.4.2. Comparison of the SNRs for SIMO and MIMO Radar

With the gained, results we determine

$$\mathrm{SNR}_{\mathrm{SIMO}} = \frac{1}{L}\sum_{l=1}^{L}\frac{|s_{\mathrm{SIMO}}(l)|^2}{\sigma^2} \tag{4.52}$$

in (4.15). We consider the l-th cycle and the k-th Rx antenna. Then $\sigma^2 = \mathrm{E}(|n_k(l)|^2) = \mathrm{Var}(n_k(l))$. The signal and noise, without the Tx beampattern $B(u)$ and $a_k^{\mathrm{Rx}}(u)$, is given by (4.46):

$$s_{\mathrm{SIMO}}(l) + n_k(l) = \sqrt{\rho_{\mathrm{s}}}\, S_w(\omega_{\max}) + N_w(\omega_{\max}). \tag{4.53}$$

Hence

$$\begin{aligned}\frac{|s_{\mathrm{SIMO}}(l)|^2}{\sigma^2} &= \frac{|s_{\mathrm{SIMO}}(l)|^2}{\mathrm{Var}(n_k(l))}\\ &= \frac{\left|\sqrt{\rho_{\mathrm{s}}}\, S_w(\omega_{\max})\right|^2}{\mathrm{Var}\left(N_w(\omega_{\max})\right)}\\ &= \mathrm{SNR}_{\mathrm{after}}.\end{aligned} \tag{4.54}$$

This is valid for all l. Thus

$$\mathrm{SNR}_{\mathrm{SIMO}} = \mathrm{SNR}_{\mathrm{after}}. \tag{4.55}$$

The number of samples per chirp are N_{samples}, cf. Tab. 4.1. Hence, for $N_{\mathrm{samples}} > N_0$ and with (4.48) to (4.51) follows

$$\mathrm{SNR}_{\mathrm{SIMO}} = \mathrm{SNR}_{\mathrm{before}} \cdot w_{\mathrm{gain}} \cdot N_{\mathrm{samples}}. \tag{4.56}$$

This results in the total SNR in (4.14)

$$S_{\mathrm{SIMO}} = \mathrm{SNR}_{\mathrm{before}} \cdot w_{\mathrm{gain}} \cdot N_{\mathrm{samples}} \cdot N_{\mathrm{Rx}} \cdot |B(u)|^2\,. \tag{4.57}$$

Analogously, we obtain for the MIMO radar

$$\mathrm{SNR}_{\mathrm{MIMO}} = \mathrm{SNR}_{\mathrm{before}} \cdot w_{\mathrm{gain}} \cdot \frac{N_{\mathrm{samples}}}{N_{\mathrm{Pulse}}} \tag{4.58}$$

and with (4.30) and (4.23)

$$\begin{aligned}S_{\mathrm{MIMO}} &= \mathrm{SNR}_{\mathrm{before}} \cdot w_{\mathrm{gain}} \cdot \frac{N_{\mathrm{samples}}}{N_{\mathrm{Pulse}}} \cdot N_{\mathrm{Rx}} \cdot N_{\mathrm{Pulse}}\\ &= \mathrm{SNR}_{\mathrm{before}} \cdot w_{\mathrm{gain}} \cdot N_{\mathrm{samples}} \cdot N_{\mathrm{Rx}}.\end{aligned} \tag{4.59}$$

Comparing (4.57) and (4.59) yields

$$S_{\mathrm{SIMO}} = |B(u)|^2 \cdot S_{\mathrm{MIMO}}. \tag{4.60}$$

Let us discuss this result. First we consider the case without a Tx beampattern, i. e. $B(u) = 1$. The SNR of one chirp $\mathrm{SNR}_{\mathrm{MIMO}}$ is by the factor of N_{Pulse} smaller than $\mathrm{SNR}_{\mathrm{SIMO}}$, since the chirp duration is shorter. The total SNRs S_{MIMO} and S_{SIMO} are equal, since the MIMO radar uses N_{Pulse} chirps. Now let us consider the influence of the Tx beampattern. $B(u)$ increases S_{SIMO}, if it is steered in the direction of the target, or decreases S_{SIMO}, if it is steered at another direction.

4.4.3. Comparison of the CRBs and Discussion

With the results gained in Section 4.4.2, we can compare the CRBs of the SIMO and MIMO radar $\mathrm{CRB}_{u,\mathrm{SIMO}}$ (4.13) and $\mathrm{CRB}_{u,\mathrm{MIMO}}$ (4.29), respectively.

$$\begin{aligned}\frac{\mathrm{CRB}_{u,\mathrm{SIMO}}}{\mathrm{CRB}_{u,\mathrm{MIMO}}} &= \frac{S_{\mathrm{MIMO}}\, U_{\mathrm{MIMO}}}{S_{\mathrm{SIMO}}\, U_{\mathrm{SIMO}}} \\ &= \frac{\mathrm{Var}^{\mathrm{S}}(\underline{d}^{\mathrm{Virt}})}{|B(u)|^2\ \mathrm{Var}^{\mathrm{S}}(\underline{d}^{\mathrm{Rx}})}\end{aligned} \tag{4.61}$$

where we have used (4.57) and (4.59). First we discuss the case without a Tx beampattern of the SIMO radar, i. e. $B(u) = 1$, and afterwards with a Tx beampattern.

4.4.3.1. Without Tx Beampattern, $B(u) = 1$

If there is no Tx beampattern, i. e. the SIMO radar uses one omnidirectional Tx antenna, cf. Fig. 4.2a on page 49, then $B(u) = 1$. Hence, the ratio of the CRBs is given by the ratio of the sample variance of the virtual and Rx array. Using (4.34) we get

$$\begin{aligned}\frac{\mathrm{CRB}_{u,\mathrm{SIMO}}}{\mathrm{CRB}_{u,\mathrm{MIMO}}} &= \frac{\mathrm{Var}^{\mathrm{S}}(\underline{d}^{\mathrm{Virt}})}{\mathrm{Var}^{\mathrm{S}}(\underline{d}^{\mathrm{Rx}})} \\ &= 1 + \frac{\mathrm{Var}^{\mathrm{S}}(\underline{d}^{\mathrm{Pulse}})}{\mathrm{Var}^{\mathrm{S}}(\underline{d}^{\mathrm{Rx}})}.\end{aligned} \tag{4.62}$$

Hence the virtual array of the MIMO radar has two effects. a) Due to the larger number of virtual antennas, it compensates the SNR loss of one chirp: in the CRB only the total SNR S_{MIMO} is relevant, which is given by $\mathrm{SNR}_{\mathrm{MIMO}} \cdot N_{\mathrm{Virt}}$. Due to the factor N_{Virt}, it stays as large as $\mathrm{SNR}_{\mathrm{SIMO}}$. b) In general, the virtual aperture of the radar is larger then the one of the SIMO radar. This is reflected by the sample variance $\mathrm{Var}^{\mathrm{S}}(\underline{d}^{\mathrm{Virt}})$. It contains not only the variance of the Rx antennas, $\mathrm{Var}^{\mathrm{S}}(\underline{d}^{\mathrm{Rx}})$, but also of the transmitting antennas, $\mathrm{Var}^{\mathrm{S}}(\underline{d}^{\mathrm{Pulse}})$. Thus $\mathrm{CRB}_{u,\mathrm{MIMO}}$ becomes smaller. Illustrative spoken,

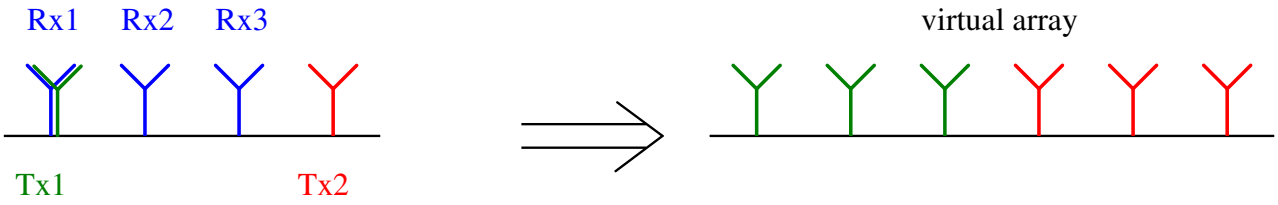

Figure 4.7.: Example of an ULA of Rx antennas. The Tx antennas are positioned, such that the virtual array is an ULA as well. Antenna Rx 1 and Tx 1 are at the same position, they are depicted slightly shifted just for illustrative purposes.

due to the larger virtual array, the digitally formed beam is sharper than that of the SIMO radar. As an example, we consider a uniform linear array (ULA) of Rx antennas with a distance between the antennas of Δ^{Rx}. We place the Tx antennas of the MIMO radar such that the virtual array is also an ULA, cf. Fig. 4.7. The sample variances are given by

$$\mathrm{Var}^{\mathrm{S}}(\underline{d}^{\mathrm{Rx}}) = \frac{1}{12}\left(N_{\mathrm{Rx}}^2 - 1\right) \approx \frac{1}{12} N_{\mathrm{Rx}}^2 \text{ for } N_{\mathrm{Rx}}^2 \gg 1 \tag{4.63}$$

$$\mathrm{Var}^{\mathrm{S}}(\underline{d}^{\mathrm{Virt}}) = \frac{1}{12}\left(N_{\mathrm{Virt}}^2 - 1\right) \approx \frac{1}{12} N_{\mathrm{Rx}}^2 N_{\mathrm{Pulse}}^2 \text{ for } N_{\mathrm{Virt}}^2 \gg 1. \tag{4.64}$$

Hence

$$\frac{\mathrm{Var}^{\mathrm{S}}(\underline{d}^{\mathrm{Virt}})}{\mathrm{Var}^{\mathrm{S}}(\underline{d}^{\mathrm{Rx}})} \approx N_{\mathrm{Pulse}}^2. \tag{4.65}$$

Thus the ratio of the CRBs increases as N_{Pulse}^2.

4.4.3.2. With Tx Beampattern

Up to now, we have considered the SIMO array without a Tx beampattern, i. e. one omnidirectional Tx antenna. If the target's DOA is known approximately a priori, the Tx antennas can transmit a signal such that the DOA can be estimated more precisely. We consider the case, where the same signal is transmitted from every Tx antenna, but phase shifted such that the transmitted energy is focused on the a priori known DOA. This is called a sum beam, cf. Fig. 4.8 for an example. The configuration of such a SIMO radar is depicted in Fig. 4.2b on page 49. To make a fair comparison, the total transmit power p is fixed. It is shown in Appendix C that the maximal achievable beamforming gain at the angle u_0, at which the beam is steered, subject to a constant transmit power p, is given by

$$B_{\max} = |B(u_0)| = \sqrt{N_{\mathrm{Tx}}}. \tag{4.66}$$

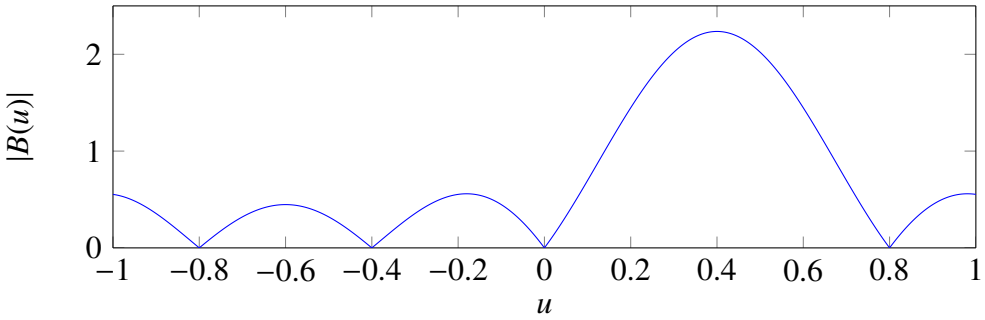

Figure 4.8.: Example of a sum beam steered to $u_0 = 0.4$ for an ULA of 5 isotropic Tx antennas with $\lambda/2$ spacing. Here, $|B(u_0)| = \sqrt{N_{\mathrm{Tx}}} = \sqrt{5}$.

It is achieved when every Tx antenna transmits with the same power $\frac{p}{N_{\mathrm{Tx}}}$. Thus, from (4.61) follows

$$\frac{\mathrm{CRB}_{u,\mathrm{SIMO}}}{\mathrm{CRB}_{u,\mathrm{MIMO}}} \geq \frac{\mathrm{Var}^{\mathrm{S}}(\underline{d}^{\mathrm{Virt}})}{N_{\mathrm{Tx}}\,\mathrm{Var}^{\mathrm{S}}(\underline{d}^{\mathrm{Rx}})}. \tag{4.67}$$

Let us compare the SIMO radar with the maximal achievable beamforming gain to the TDM MIMO radar. $\mathrm{CRB}_{u,\mathrm{SIMO}}$ at u_0 is smaller than $\mathrm{CRB}_{u,\mathrm{MIMO}}$ if

$$|B(u_0)|^2 = N_{\mathrm{Tx}} > \frac{\mathrm{Var}^{\mathrm{S}}(\underline{d}^{\mathrm{Virt}})}{\mathrm{Var}^{\mathrm{S}}(\underline{d}^{\mathrm{Rx}})}. \tag{4.68}$$

Consider an antenna array, where $\mathrm{Var}^{\mathrm{S}}(\underline{d}^{\mathrm{Pulse}}) = \mathrm{Var}^{\mathrm{S}}(\underline{d}^{\mathrm{Rx}})$. Then (4.68) is fulfilled for $N_{\mathrm{Tx}} > 3$, i. e. the beamforming gain is more important than the gain due to the virtual array. An example of such an array is given in Fig. 4.9 a). On the other hand, the array depicted in Fig. 4.9 b) fulfills $\mathrm{Var}^{\mathrm{S}}(\underline{d}^{\mathrm{Pulse}}) > \mathrm{Var}^{\mathrm{S}}(\underline{d}^{\mathrm{Rx}})$, since the distance between the Tx antennas is as large as the maximal distance between the Rx antennas. Here, the gain due to the virtual array has a larger impact than the beamforming gain, and $\mathrm{CRB}_{u,\mathrm{MIMO}} < \mathrm{CRB}_{u,\mathrm{SIMO}}$. The disadvantage of the sum beam is the necessary a priori information. Moreover, e. g. in automotive applications, different DOAs of several targets are estimated in one measurement. Focusing the beam with the maximum beamforming gain on all targets at once is not possible. On the contrary, the MIMO radar transmits an omni-directional pattern, such that all DOAs can be estimated. This is an important advantage. A disadvantage of the MIMO radar are the lower number of samples per chirp, due to the shorter chirp duration. Therefore the accuracy and resolution of the frequency estimation becomes worse. The combination of

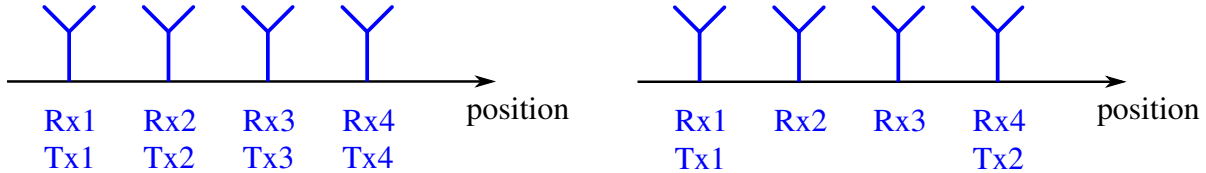

(a) Here, $\mathrm{Var}^{\mathrm{S}}(\underline{d}^{\mathrm{Pulse}}) = \mathrm{Var}^{\mathrm{S}}(\underline{d}^{\mathrm{Rx}})$

(b) Here, $\mathrm{Var}^{\mathrm{S}}(\underline{d}^{\mathrm{Pulse}}) > \mathrm{Var}^{\mathrm{S}}(\underline{d}^{\mathrm{Rx}})$

Figure 4.9.: Comparison of $\mathrm{Var}^{\mathrm{S}}(\underline{d}^{\mathrm{Pulse}})$ with $\mathrm{Var}^{\mathrm{S}}(\underline{d}^{\mathrm{Rx}})$. In both examples (a) and (b) $\underline{d}^{\mathrm{Pulse}} = \underline{d}^{\mathrm{Tx}}$, i. e. every Tx antenna transmits once.

several chirps, with the same frequency modulation, could overcome this problem. Due to the advantages, we focus on the MIMO radar in the following and neglect the possible beamforming gain for convenience.

4.4.4. Notes on $\mathrm{CRB}_{u,\mathrm{SIMO}}$

We show that $\mathrm{CRB}_{u,\mathrm{SIMO}}$ only depends on the overall transmission time T_{total} (4.1) and not on the number of transmitted chirps, as long as every chirp has got a certain minimum duration.

The total SNR is given by (4.57)

$$S_{\mathrm{SIMO}} = \mathrm{SNR}_{\mathrm{before}}\, w_{\mathrm{gain}}\, N_{\mathrm{samples}}\, N_{\mathrm{Rx}}\, |B(u)|^2\,, \quad \text{for } N_{\mathrm{samples}} \geq N_0. \tag{4.69}$$

Plugging in (4.40) and using (4.37) yields

$$\begin{aligned} S_{\mathrm{SIMO}} &= p\,\Delta t\,\frac{s_0^2}{\sigma_n^2}\, w_{\mathrm{gain}}\, N_{\mathrm{samples}}\, N_{\mathrm{Rx}}\, |B(u)|^2 \\ &\propto \Delta t\, N_{\mathrm{samples}} \end{aligned} \tag{4.70}$$

Since the SIMO radar transmits one chirp per cycle, the duration of one cycle is

$$T_{\mathrm{cycle}} = \Delta t\, N_{\mathrm{samples}} \tag{4.71}$$

and thus

$$S_{\mathrm{SIMO}} \propto T_{\mathrm{cycle}}. \tag{4.72}$$

With (4.13) follows for $\mathrm{CRB}_{u,\mathrm{SIMO}}$

$$\begin{aligned} \mathrm{CRB}_{u,\mathrm{SIMO}} &= \frac{1}{2L}\frac{1}{U_{\mathrm{SIMO}}}\frac{1}{S_{\mathrm{SIMO}}} \\ &\propto \frac{1}{L\,T_{\mathrm{cycle}}} = \frac{1}{T_{\mathrm{total}}}. \end{aligned} \tag{4.73}$$

with T_{total} defined in (4.1). Since the radar transmits one chirp per cycle and L is the number of cycles, L equals also the number of transmitted chirps. Hence, $\mathrm{CRB}_{u,\mathrm{SIMO}}$ stays the same, independent of the number of transmitted chirps as long as T_{total} stays constant and the chirp duration is larger than $\Delta t\, N_0$.

4.4.5. Numerical Example

The CRB is a lower bound on the variance of any unbiased estimator. It is important to verify that the computed CRB is a tight bound, i. e. it is actually achieved by an estimator. Otherwise the conclusions, drawn from the CRB, could be misleading. We do this by numerical simulations. We compute the bias $b_{\hat{u}}$, standard deviation $\sigma_{\hat{u}}$, and root mean square error $\mathrm{RMSE}_{\hat{u}}$ of the deterministic Maximum Likelihood (ML) estimate $\hat{u}$ of u by doing Monte-Carlo simulations. After that, we compare the result to the CRB. We consider a radar system which consists of a linear array with 4 Rx and Tx antennas. The Rx and Tx antennas are uniformly spaced with an antenna distance of $\lambda/2$, i. e. $\underline{d}^{\mathrm{Rx}} = \underline{d}^{\mathrm{Tx}} = \pi \cdot [0, 1, 2, 3]^T$. The DOA of the target is $u = \sin(10°)$ and we consider $L = 1$ cycle. We assume that the DOA of the target is not known approximately a priori and therefore the SIMO radar uses 1 isotropic Tx antenna. Thus, the beamforming gain is $B(u) = 1$ and the signal model (4.6) simplifies to

$$\underline{x}(l) = \underline{a}^{\mathrm{Rx}}(u)\, s_{\mathrm{SIMO}}(l) + \underline{n}(l). \tag{4.74}$$

Note that the unknown parameter vector to be estimated is $\underline{\Theta}$ in (4.7) and not u alone. According to (E.23) in Appendix E, the ML estimate of u can be computed by

$$\hat{u} = \arg\max_{u} \sum_{l=1}^{L} \left| \left(\underline{a}^{\mathrm{Rx}}(u)\right)^H \underline{x}(l) \right|^2, \tag{4.75}$$

where we have dropped the normalization $1/\|\underline{a}^{\mathrm{Rx}}(u)\|^2$, since $\|\underline{a}^{\mathrm{Rx}}(u)\| = \text{const.}$ $\hat{u}$ is computed by a grid search, followed by a local interpolation. The MIMO array under consideration transmits $N_{\mathrm{Pulse}} = 4$ pulses with transmission sequence $\underline{d}^{\mathrm{Pulse}} = \underline{d}^{\mathrm{Tx}}$. The signal model is given in (4.27). It has exactly the same structure as (4.74) and the ML estimate $\hat{u}$ can be computed analogously. We consider different values of the total SNR S. For each value, 5000 Monte-Carlo simulations are carried out to determine $b_{\hat{u}}$, $\sigma_{\hat{u}}$, and $\mathrm{RMSE}_{\hat{u}}$. Since $B(u) = 1$, according to (4.60), the total SNR S of the SIMO and MIMO radar are equal. First we compare the bias $b_{\hat{u}}$ to the standard deviation $\sigma_{\hat{u}}$. The results for the SIMO radar are depicted in Fig. 4.10. It shows that $|b_{\hat{u}}|$ is much smaller than $\sigma_{\hat{u}}$ for all SNR values. The same is true for the MIMO radar (not depicted here). Thus, the bias can be neglected and $\sigma_{\hat{u}} \approx \mathrm{RMSE}_{\hat{u}}$. Hence, we can compare $\mathrm{RMSE}_{\hat{u}}$ to CRB_u in the following. The results are depicted in Fig. 4.11. It shows that both ML estimators reach the corresponding CRB above a threshold of approximately 14 dB. If the SNR is too low, ambiguities arise in the estimation process. This leads to a higher RMSE. The CRB is a bound which incorporates only the local properties of the likelihood function and therefore does not include ambiguities. Because of this, the ML estimators deviate from the CRBs below the threshold value. As expected, the MIMO radar achieves a lower RMSE than the SIMO radar, due to its larger virtual aperture. Since the ML estimators indeed achieve the CRBs, we can conclude that the CRB is a useful tool to study the DOA accuracy in our applications. Here, we have investigated the behavior of the ML estimator for increasing SNR. For

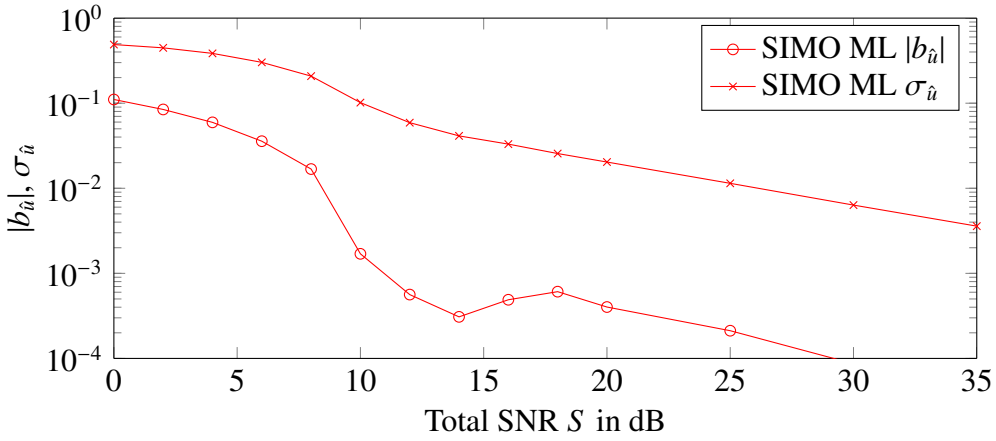

Figure 4.10.: Absolute value of bias $|b_{\hat{u}}|$ and standard deviation $\sigma_{\hat{u}}$ of the estimated electrical angle for the SIMO radar. $|b_{\hat{u}}|$ is negligible compared to $\sigma_{\hat{u}}$.

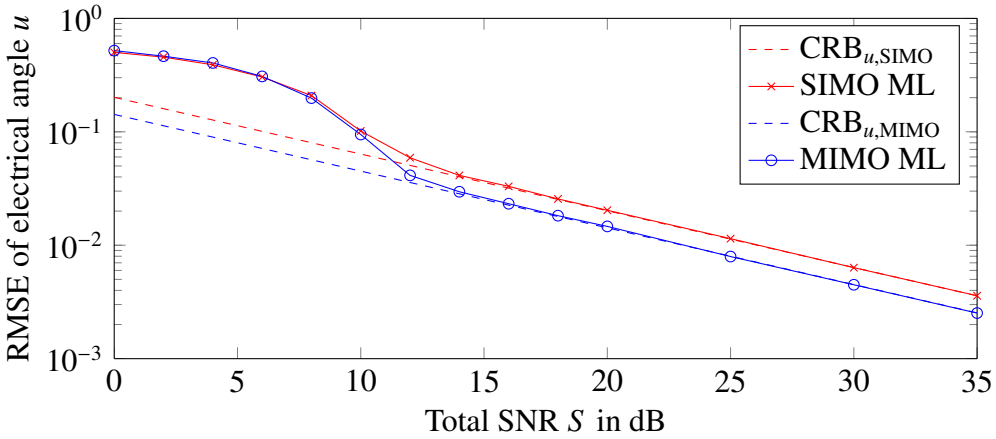

Figure 4.11.: RMSE of the electrical angle of a stationary target for a SIMO and MIMO radar

an increasing number of observations, asymptotic properties of the ML estimator can be shown, see Appendix F for details. Nevertheless these asymptotic properties cannot be used in our automotive radar application because the number of observations, which correspond here to the number of cycles L, is small.

4.5. Comparison of Code and Time Division Multiplexing

In the following, we compare a MIMO radar using code division multiplexing (CDM) in slow time with a MIMO radar using TDM. Both radars use the same Tx and Rx antenna array, only the multiplexing techniques are different. We consider several stationary targets. We investigate under which circumstances both radar systems yield the same performance for DOA estimation. In order to do that, we use the concept of sufficient statistics: The received signal $\mathbf{X}$ is transformed to a compressed signal $\mathbf{Y}$, which contains the same amount of information on the targets' DOAs as the original received signal $\mathbf{X}$. Hence $\mathbf{Y}$ contains sufficient information for the DOA estimation. In general, the

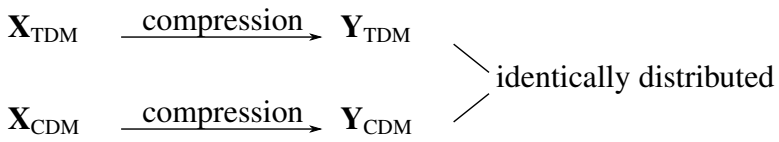

Figure 4.12.: Relation between the received signals $\mathbf{X}_{\mathrm{TDM}}$, $\mathbf{X}_{\mathrm{CDM}}$ and the compressed signals $\mathbf{Y}_{\mathrm{TDM}}$, $\mathbf{Y}_{\mathrm{CDM}}$

received signal $\mathbf{X}_{\mathrm{CDM}}$ of the CDM MIMO radar is different from the received signal $\mathbf{X}_{\mathrm{TDM}}$ of the TDM MIMO radar. We show under which conditions the compressed signal of the CDM radar $\mathbf{Y}_{\mathrm{CDM}}$ and the compressed signal of the TDM radar $\mathbf{Y}_{\mathrm{TDM}}$ are identically distributed and therefore the received signals $\mathbf{X}_{\mathrm{CDM}}$ and $\mathbf{X}_{\mathrm{TDM}}$ contain the same information on the DOAs, cf. Fig. 4.12. From this follows that their performance in DOA estimation is the same.

We consider the signal model of [Li et al., 2008], adapted to our notation,

$$\mathbf{X} = \sum_{k=1}^{N_{\mathrm{Targets}}} \underline{a}^{\mathrm{Rx}}(U_k)\, s_k\, \underline{a}^{\mathrm{Tx}\,T}(U_k)\, \mathbf{\Phi} + \mathbf{N} \quad \in \mathbb{C}^{N_{\mathrm{Rx}} \times N_{\mathrm{Pulse}}} \tag{4.76}$$

with $\mathbf{X}$ being the received data and N_{Pulse} the number of chirps. N_{Targets} is the number of targets. U_k and $s_k, 1 \leq k \leq N_{\mathrm{Targets}}$ are the DOAs and complex signals of the targets, respectively. $\underline{a}^{\mathrm{Rx}}(U) \in \mathbb{C}^{N_{\mathrm{Rx}} \times 1}$ and $\underline{a}^{\mathrm{Tx}}(U) \in \mathbb{C}^{N_{\mathrm{Tx}} \times 1}$ are the steering vectors of the Rx and Tx array, respectively. This model describes both the TDM and CDM MIMO radar. In the case of the CDM radar, $\mathbf{\Phi} \in \mathbb{C}^{N_{\mathrm{Tx}} \times N_{\mathrm{Pulse}}}$ contains the known and deterministic transmitted codes, where row i of $\mathbf{\Phi}$ is the code of Tx i. For the TDM MIMO radar, $\mathbf{\Phi}$ has to be chosen such that only one Tx transmits at a time, i. e. only one entry of each column in $\mathbf{\Phi}$ is unequal 0. Hence the TDM and CDM radar differ only in $\mathbf{\Phi}$. $\mathbf{N} \in \mathbb{C}^{N_{\mathrm{Rx}} \times N_{\mathrm{Pulse}}}$ is the noise. It is assumed that the columns of $\mathbf{N}$ are independent and identically distributed circularly symmetric complex Gaussian random vectors with mean zero and unknown covariance $\mathbf{C}_{\underline{n}}$.

$$\mathbf{N} = \left[\underline{n}_1, \ldots, \underline{n}_{N_{\mathrm{Pulse}}}\right], \tag{4.77}$$

$$\mathrm{E}\left(\underline{n}_i\, \underline{n}_j^H\right) = \delta_{ij}\, \mathbf{C}_{\underline{n}} \in \mathbb{C}^{N_{\mathrm{Rx}} \times N_{\mathrm{Rx}}}. \tag{4.78}$$

Note that in the case of one target and covariance matrix $\mathbf{C}_{\underline{n}} = \sigma^2 \mathbf{I}$, for a TDM MIMO radar this model is the same as the model presented in Section 4.3.1 for one cycle $L = 1$, using a different notation. The model can be rewritten as

$$\mathbf{X} = \mathbf{A}^{\mathrm{Rx}}(\underline{U})\, \mathbf{S}\, \mathbf{A}^{\mathrm{Tx}\,T}(\underline{U})\, \mathbf{\Phi} + \mathbf{N} \tag{4.79}$$

with

$$\mathbf{A}^{\mathrm{Rx}}(\underline{U}) = [\underline{a}^{\mathrm{Rx}}(U_1), \ldots, \underline{a}^{\mathrm{Rx}}(U_{N_{\mathrm{Targets}}})] \in \mathbb{C}^{N_{\mathrm{Rx}} \times N_{\mathrm{Targets}}}, \tag{4.80}$$

$$\mathbf{A}^{\mathrm{Tx}}(\underline{U}) = [\underline{a}^{\mathrm{Tx}}(U_1), \ldots, \underline{a}^{\mathrm{Tx}}(U_{N_{\mathrm{Targets}}})] \in \mathbb{C}^{N_{\mathrm{Tx}} \times N_{\mathrm{Targets}}}, \tag{4.81}$$

$$\underline{U} = [U_1, \ldots, U_{N_{\text{Targets}}}]^T, \tag{4.82}$$

$$\underline{s} = [s_1, \ldots, s_{N_{\text{Targets}}}]^T, \tag{4.83}$$

$$\mathbf{S} = \text{diag}(\underline{s}) \in \mathbb{C}^{N_{\text{Targets}} \times N_{\text{Targets}}}. \tag{4.84}$$

The unknown parameters to be estimated are $\underline{U}, \underline{s}, \mathbf{C}_{\underline{n}}$. In [Li et al., 2008], the part of the deterministic CRB corresponding to $\underline{U}$ and $\underline{s}$ is computed. It is shown that it only depends on $\mathbf{M}_{\mathbf{\Phi}}$

$$\mathbf{CRB}_{\underline{U},\underline{s}} = \mathbf{CRB}_{\underline{U},\underline{s}}(\mathbf{M}_{\mathbf{\Phi}}) \tag{4.85}$$

with the correlation matrix of the transmitted codes

$$\mathbf{M}_{\mathbf{\Phi}} = \mathbf{\Phi}\mathbf{\Phi}^H \in \mathbb{C}^{N_{\text{Tx}} \times N_{\text{Tx}}}. \tag{4.86}$$

We consider transmitted codes $\mathbf{\Phi}$ such that $\mathbf{\Phi}\mathbf{\Phi}^H$ is invertible. A necessary condition for that is $N_{\text{Pulse}} \geq N_{\text{Tx}}$. Then, the received signal $\mathbf{X}$ can be compressed by multiplying it with $\mathbf{\Phi}^H(\mathbf{\Phi}\mathbf{\Phi}^H)^{-1/2}$, where $(.)^{-1/2}$ denotes the inverse of the Hermitian square root of a matrix. The compressed signal is

$$\begin{aligned} \mathbf{Y} &= \mathbf{X}\,\mathbf{\Phi}^H\,(\mathbf{\Phi}\mathbf{\Phi}^H)^{-1/2} \\ &= \mathbf{A}^{\text{Rx}}(\underline{U})\,\mathbf{S}\,\mathbf{A}^{\text{Tx}^T}(\underline{U})\,(\mathbf{\Phi}\mathbf{\Phi}^H)^{1/2} + \tilde{\mathbf{N}} \quad \in \mathbb{C}^{N_{\text{Rx}} \times N_{\text{Tx}}} \end{aligned} \tag{4.87}$$

with

$$\tilde{\mathbf{N}} = \left[\tilde{\underline{n}}_1, \ldots, \tilde{\underline{n}}_{N_{\text{Tx}}}\right] = \mathbf{N}\,\mathbf{\Phi}^H\,(\mathbf{\Phi}\mathbf{\Phi}^H)^{-1/2} \quad \in \mathbb{C}^{N_{\text{Rx}} \times N_{\text{Tx}}}. \tag{4.88}$$

It can be shown that choosing $\mathbf{\Phi}^H(\mathbf{\Phi}\mathbf{\Phi}^H)^{-1/2}$ to compress the signal guarantees that the noise term stays temporally white [Li et al., 2008]. Moreover, $\tilde{\mathbf{N}}$ and $\mathbf{N}$ have the same statistical properties [Li et al., 2008], i. e. the columns of $\tilde{\mathbf{N}}$ are independent and identically distributed circularly symmetric complex Gaussian random vectors with mean zero and unknown covariance $\mathbf{C}_{\underline{n}}$

$$\text{E}\left(\tilde{\underline{n}}_i\,\tilde{\underline{n}}_j^H\right) = \delta_{ij}\,\mathbf{C}_{\underline{n}} \in \mathbb{C}^{N_{\text{Rx}} \times N_{\text{Rx}}}, \tag{4.89}$$

where $\mathbf{C}_{\underline{n}}$ is the same matrix as in (4.78). Thus, the pdf of $\tilde{\mathbf{N}}$ is independent of $\mathbf{\Phi}$. If the covariance matrix $\mathbf{C}_{\underline{n}}$ is known to be a scaled identity matrix

$$\mathbf{C}_{\underline{n}} = \sigma^2\mathbf{I}, \tag{4.90}$$

then $\mathbf{Y}$ is a sufficient statistic for $\underline{U}, \underline{s}$ [Li et al., 2008]. That means, $\mathbf{Y}$ contains the same amount of information as $\mathbf{X}$ to estimate $\underline{U}, \underline{s}$. Note that $\mathbf{Y}$ in (4.87) only depends on $\mathbf{M}_{\mathbf{\Phi}} = \mathbf{\Phi}\mathbf{\Phi}^H$ and not on $\mathbf{\Phi}$ alone.

In the following, we compute how $\mathbf{M}_{\mathbf{\Phi}}$ looks like for CDM using orthogonal codes and show how to choose a TDM sequence which yields the same correlation matrix $\mathbf{M}_{\mathbf{\Phi}}$. If the CDM and TDM radar

system have the same correlation matrix $\mathbf{M}_{\mathbf{\Phi}}$, $\mathbf{CRB}_{\underline{U},\underline{s}}$ is the same for both systems. Moreover, the compressed signals of the systems $\mathbf{Y}_{\mathrm{CDM}}$ and $\mathbf{Y}_{\mathrm{TDM}}$ are identically distributed, cf. Fig. 4.12, since $\mathbf{Y}_{\mathrm{CDM}}$ and $\mathbf{Y}_{\mathrm{TDM}}$ depend only on $\mathbf{M}_{\mathbf{\Phi}}$ and not on $\mathbf{\Phi}$ alone and the pdf of $\tilde{\mathbf{N}}$ is independent of $\mathbf{\Phi}$.

4.5.1. Code Division Multiplexing using Orthogonal Codes

We compute how $\mathbf{M}_{\mathbf{\Phi}}$ looks like when using CDM in slow time with orthogonal codes. The total transmitting time is denoted by T_{total}. The maximum transmission power over all Tx antennas is given by $p^{\max}$. We divide T_{total} into N_{Pulse} periods of equal length

$$\Delta t = \frac{T_{\mathrm{total}}}{N_{\mathrm{Pulse}}}. \tag{4.91}$$

Since we consider CDM in slow time, one period corresponds to one compressed radar pulse. We write

$$\mathbf{\Phi} = \begin{bmatrix} \underline{c}_1^T \\ \vdots \\ \underline{c}_{N_{\mathrm{Tx}}}^T \end{bmatrix} \tag{4.92}$$

where $\underline{c}_i$ is the transmitted code of the ith Tx. The power constraint can be written as

$$\sum_{n=1}^{N_{\mathrm{Tx}}} |[\mathbf{\Phi}]_{nl}|^2 \leq p^{\max} \Delta t, \quad 1 \leq l \leq N_{\mathrm{Pulse}}. \tag{4.93}$$

We consider the case where we transmit with the maximal available power, hence

$$\sum_{n=1}^{N_{\mathrm{Tx}}} |[\mathbf{\Phi}]_{nl}|^2 = p^{\max} \Delta t. \tag{4.94}$$

The orthogonality of the codes results in

$$\underline{c}_i^H \underline{c}_j = \delta_{ij}\, T_{\mathrm{total}}\, p_i^{\mathrm{mean}} \tag{4.95}$$

where p_i^{mean} is the mean power of the i-th Tx over all pulses. Thus

$$\mathbf{M}_{\mathbf{\Phi}} = \mathbf{\Phi}\mathbf{\Phi}^H = T_{\mathrm{total}} \begin{bmatrix} p_1^{\mathrm{mean}} & & 0 \\ & \ddots & \\ 0 & & p_{N_{\mathrm{Tx}}}^{\mathrm{mean}} \end{bmatrix}. \tag{4.96}$$

The transmitted energy W^{Tx} of all Tx antennas can be computed by

$$W^{\mathrm{Tx}} = \mathrm{Tr}\left(\mathbf{\Phi}\mathbf{\Phi}^H\right) = \sum_{l=1}^{N_{\mathrm{Pulse}}} \sum_{n=1}^{N_{\mathrm{Tx}}} |[\mathbf{\Phi}]_{nl}|^2 = \sum_{l=1}^{N_{\mathrm{Pulse}}} p^{\max} \Delta t = p^{\max} N_{\mathrm{Pulse}} \Delta t$$
$$= p^{\max} T_{\mathrm{total}}. \tag{4.97}$$

4.5.2. Time Division Multiplexing

Given the same total transmitting time T_{total} and the same maximum transmission power $p^{\max}$ as in the CDM case, we show how to construct a TDM scheme which yields the same correlation matrix $\mathbf{M}_{\mathbf{\Phi}}$ in (4.96).

Choose N_{Tx} pulses of length Δt_i such that

$$\Delta t_i \, p^{\max} = T_{\mathrm{total}} \, p_i^{\mathrm{mean}}, \quad 1 \le i \le N_{\mathrm{Tx}}. \tag{4.98}$$

Hence

$$\Delta t_i = T_{\mathrm{total}} \frac{p_i^{\mathrm{mean}}}{p^{\max}}. \tag{4.99}$$

We write $\mathbf{\Phi}$ as in (4.92). Since now we transmit N_{Tx} pulses, $\mathbf{\Phi} \in \mathbb{C}^{N_{\mathrm{Tx}} \times N_{\mathrm{Tx}}}$. We set

$$\underline{c}_i = [0, \ldots, \sqrt{\Delta t_i p^{\max}}, \ldots, 0]^T \tag{4.100}$$

where all elements of $\underline{c}_i$ are 0 except the i-th element. This ensures that only one Tx antenna is transmitting at a time. $\mathbf{M}_{\mathbf{\Phi}}$ can be computed with the help of

$$\underline{c}_i^H \underline{c}_j = \delta_{ij} \, p^{\max} \, \Delta t_i$$
$$= \delta_{ij} \, T_{\mathrm{total}} \, p_i^{\mathrm{mean}} \tag{4.101}$$

which gives

$$\mathbf{M}_{\mathbf{\Phi}} = \mathbf{\Phi}\mathbf{\Phi}^H = T_{\mathrm{total}} \begin{bmatrix} p_1^{\mathrm{mean}} & & 0 \\ & \ddots & \\ 0 & & p_{N_{\mathrm{Tx}}}^{\mathrm{mean}} \end{bmatrix}. \tag{4.102}$$

Hence such a TDM scheme results in the same correlation matrix $\mathbf{M}_{\mathbf{\Phi}}$ as using CDM with orthogonal codes (4.96). Moreover, the total transmitted energy W^{Tx} in (4.97) is the same.

4.5.3. Discussion

For a fixed total transmission time T_{total} and maximal transmission power $p^{\max}$, we have derived the correlation matrix $\mathbf{M}_{\mathbf{\Phi}}$ for orthogonal CDM. We have shown that the same correlation matrix is achieved for a TDM MIMO radar, if the TDM sequence is chosen appropriately. Since the CRB of the DOAs (4.85) only depends on $\mathbf{M}_{\mathbf{\Phi}}$, the CRB is the same for both multiplexing schemes. Hence, the CDM and TDM MIMO radar can achieve the same accuracy of the DOAs.

The compressed signal $\mathbf{Y}$ in (4.87) depends on $\mathbf{M}_{\mathbf{\Phi}}$. Moreover, the noise $\tilde{\mathbf{N}}$ has the same statistical properties as $\mathbf{N}$ with the same covariance matrix, cf. (4.89), independent of $\mathbf{\Phi}$. Thus, $\tilde{\mathbf{N}}$ has the same pdf for the TDM and CDM MIMO radar. Therefore, for a CDM and TDM radar with the same $\mathbf{M}_{\mathbf{\Phi}}$, the compressed signal of the CDM radar $\mathbf{Y}_{\text{CDM}}$ and of the TDM radar $\mathbf{Y}_{\text{TDM}}$ are identically distributed and have the same likelihood function. If the noise covariance matrix is a scaled identity matrix (4.90), the compressed signals are sufficient statistics for the DOA estimation [Li et al., 2008], i. e. $\mathbf{Y}_{\text{CDM}}$ contains the same information on the DOAs as the received signal $\mathbf{X}_{\text{CDM}}$ and $\mathbf{Y}_{\text{TDM}}$ contains the same information on the DOAs as the received signal $\mathbf{X}_{\text{TDM}}$. Since $\mathbf{Y}_{\text{CDM}}$ and $\mathbf{Y}_{\text{TDM}}$ are identically distributed, $\mathbf{X}_{\text{CDM}}$ and $\mathbf{X}_{\text{TDM}}$ contain the same information on the DOAs as well. In that case, the CDM and TDM radars do not only have the same CRBs, but all other properties, like the ambiguity and resolution, are equal since the likelihood functions of the compressed signals are the same. Thus, by choosing the transmission matrix $\mathbf{\Phi}$ of the TDM MIMO radar appropriately, it achieves the same DOA performance as the CDM radar.

Obviously, if the power is not constrained by the overall power but by the transmission power per Tx antenna, in general we cannot find a TDM scheme which results in the same CRB as the CDM, since the CDM can transmit with a higher overall power. As discussed in Section 3.3, this is not a concern for MIMO radars in automotive applications since the total transmission power is limited by law and usually this power limit is already achieved by one Tx antenna.

4.6. Summary

We have investigated the DOA estimation of a stationary target. The CRBs of the DOA for a SIMO and MIMO radar have been derived to compare the maximal achievable accuracy. Dependent on the application, the SIMO radar can have a beamforming gain, if the target's DOA is known approximately a priori. The MIMO radar has the advantage of a larger virtual aperture. Whether the possible beamforming gain or the gain due to the virtual array dominates, depends on the positions and number of the Rx and Tx antennas.

Moreover, a MIMO radar using CDM with orthogonal codes has been considered and compared to a TDM MIMO radar. Under the constraint that the overall transmit power is limited, we have shown that a TDM scheme can be constructed such that the CRB of the DOAs is the same for the TDM and

CDM radar. Moreover, if the noise covariance matrix has a certain structure, the received signals of both radar systems contain the same information for DOA estimation. Then the CDM and TDM radar do not only have the same CRBs of the DOAs, but all other properties which depend on the likelihood function, e. g. the ambiguity, are the same.

5. DOA Estimation of Moving Targets

In a SIMO radar, the DOA can be estimated by analyzing the phase relation of the baseband signal of the Rx channels. In a MIMO system, the phase relation between the transmitting channels is used as well which makes it possible to construct a virtual array with a larger aperture than the receiving or transmitting array alone. Therefore, it can achieve a more accurate DOA estimation. We consider a TDM MIMO radar. However, a non-stationary target, i. e. a target which is moving relative to the radar, results in an additional phase change of the baseband signal due to the Doppler effect. This phase change distorts the phase change caused by the target's DOA. For an accurate DOA estimation it has to be considered as well, i. e. jointly estimated or canceled. In general, this leads to a decrease in the DOA estimation accuracy which we want to avoid.

We analyze this situation in this chapter. We present the signal model in Section 5.1. We consider both an one-dimensional antenna array for azimuth estimation and a two-dimensional antenna array for azimuth and elevation estimation. In Section 5.2, the one target case is considered. In order to analyze the maximal achievable DOA accuracy, we derive the CRB of DOA estimation for a non-stationary target for a general TDM scheme. This allows a quantitative comparison of different MIMO and SIMO radars. We use the results to find optimal TDM schemes which minimize the CRB. The DOA estimation of two moving targets is investigated in Section 5.3. The CRB is derived and the implications on the accuracy and resolution are investigated. In Section 5.4, the DOA estimation of more than two targets is studied briefly. The results are summarized in Section 5.5.

This chapter is based on [Rambach and Yang, 2013, 2014; Rambach et al., 2014; Rambach and Yang, 2016a].[1]

5.1. Signal Model

We derive the signal model for DOA estimation for a TDM MIMO radar and a non-stationary target. Non-stationary means that the target is moving relative to the radar. Since we are using a TDM MIMO radar and the target is moving relative to the radar, the received signal of different transmitted pulses changes. The signal used for DOA estimation is gained by a Fourier transform of the time domain baseband signal, cf. Section 2.1.2. In order to see how the signal for the DOA estimation

[1] This chapter contains quotations of our own published works [Rambach and Yang, 2013, 2014; Rambach et al., 2014; Rambach and Yang, 2016a] which are not marked additionally.

changes from pulse to pulse, we derive the baseband signal in the time domain for a moving target and compute the phase change between different pulses in Section 5.1.1. After that, we present the signal model for the DOA estimation using a TDM MIMO radar in Section 5.1.2.

5.1.1. Baseband Signal Model in the Time Domain

In a TDM MIMO radar, several Tx antennas transmit a signal, one after the other, cf. Fig. 5.1 for an example. The data gained by the different Tx antennas is combined. To estimate the target's DOA, the phases of the complex baseband signals are processed. Since the target is moving relative to the radar, the Doppler effect causes a phase shift of the baseband signal, which depends on the transmission time. We compute this phase shift for different kinds of radars. The result is used to establish an appropriate signal model for the DOA estimation of a moving target using a TDM MIMO radar.

5.1.1.1. Baseband Signal of a Pulse Doppler Radar

For a pulse Doppler radar, the received baseband signal $s_{\text{pulseDoppler}}(n)$ of pulse n has already been computed in [Bühren, 2008]. It is given by

$$s_{\text{pulseDoppler}}(n) \propto \sin(\omega_{\text{Doppler}}\, n\, \Delta t + \varphi_0), \tag{5.1}$$

where ω_{Doppler} is the Doppler frequency, Δt the difference between the transmission times of two successive pulses and φ_0 a constant, absolute phase. ω_{Doppler} is given as

$$\omega_{\text{Doppler}} \approx 2\,\frac{v}{c}\,\omega \tag{5.2}$$

for $|v| \ll c$, with the angular carrier frequency ω, the relative velocity of the target v and the speed of light c. v is defined to be positive if the target moves away from the radar. This is the well known Doppler frequency in radar applications. Hence, for a pulse Doppler radar, the phase shift $\Delta\varphi_{1k}$

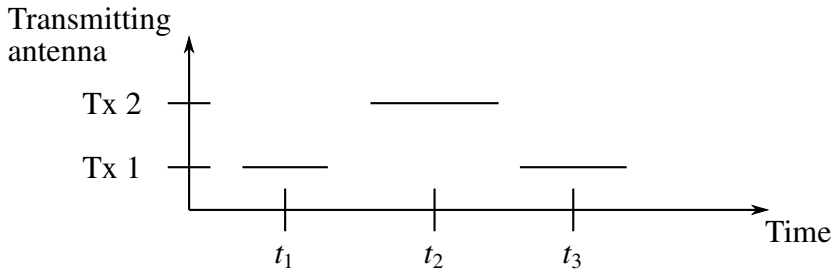

Figure 5.1.: Example of two Tx antennas transmitting at different times. First Tx antenna 1 transmits, then antenna 2 and after that antenna 1 again.

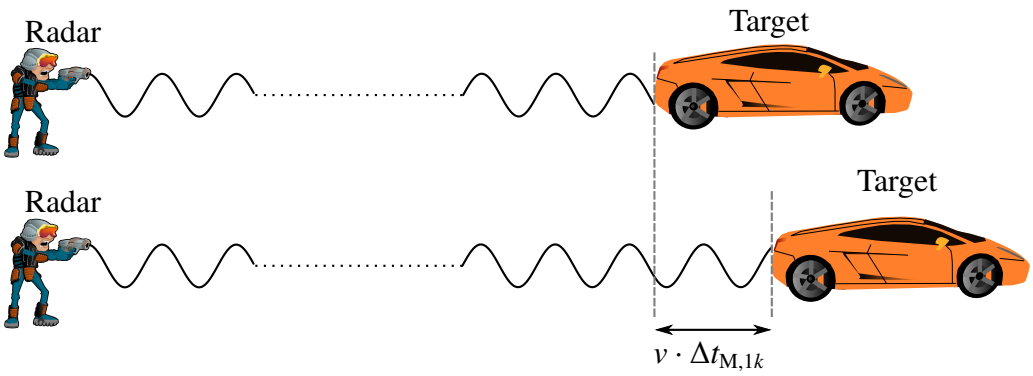

Figure 5.2.: Illustrative explanation of the Doppler phase shift. [Openclipart, 2014, graphical parts used and adapted]

between pulse 1 and k is

$$\Delta\varphi_{1k} = \omega_{\mathrm{Doppler}}\, \Delta t_{\mathrm{M},1k}, \tag{5.3}$$

where $\Delta t_{\mathrm{M},1k}$ is the difference between the transmission times of pulse 1 and k

$$\Delta t_{\mathrm{M},1k} = t_{\mathrm{M},k} - t_{\mathrm{M},1}. \tag{5.4}$$

Here, $t_{\mathrm{M},i}$, $i = 1, k$, is the middle of the transmission time of the i-th pulse. Note that since all transmitted pulses are equal, i. e. they have the same shape and duration, it does not matter if we define $t_{\mathrm{M},i}$ to be the start time or the middle of the transmission time of the i-th pulse. The Doppler phase shift $\omega_{\mathrm{Doppler}}\, \Delta t_{\mathrm{M},1k}$ can be interpreted in the following way, cf. Fig. 5.2: in the time $\Delta t_{\mathrm{M},1k}$ the target moves a distance of $v \cdot \Delta t_{\mathrm{M},1k}$. With λ being the carrier wavelength, this corresponds to a phase change of $2\pi \frac{v\, \Delta t_{\mathrm{M},1k}}{\lambda} = \omega \frac{v}{c} \Delta t_{\mathrm{M},1k}$. The radar wave has to travel forth and back, which results in the additional factor 2, i. e. the phase shift is $\omega\, 2 \frac{v}{c} \Delta t_{\mathrm{M},1k} = \omega_{\mathrm{Doppler}}\, \Delta t_{\mathrm{M},1k}$.

(5.1) can easily be generalized to a complex baseband signal, which is obtained by using an IQ-mixer.

5.1.1.2. Baseband Signal of an FMCW and Chirp Sequence Radar

We are interested in an FMCW and a chirp sequence radar. Both radar systems transmit linear frequency modulated chirps. They differ in the chirp duration and the number of transmitted chirps. A chirp sequence radar transmits many pulses of short durations, e. g. 1000 chirps with a chirp duration of $T = 10\,\mu$s. In an FMCW radar, few chirps of longer durations are transmitted, e. g. 4 chirps with durations of the order of ms. In these cases, the phase change of the received baseband signal between two pulses is more complicated than (5.3) and will be investigated below. First we consider one transmitted chirp and compute the received baseband signal. Having this result, we compute the difference of the phases of the baseband signals of two chirps transmitted at different transmission times. After that we discuss and summarize the result.

Baseband Signal of One Chirp Without loss of generality (w. l. o. g.) the Tx antenna starts to transmit at $t = 0$. The transmitted signal at time t is given by

$$s_{\mathrm{Tx}}(t) = A_{\mathrm{Tx}} \cos\left(\varphi_{\mathrm{Tx}}(t) + \varphi_0\right), \quad t \in [0, T], \tag{5.5}$$

where A_{Tx} is the amplitude, $\varphi_{\mathrm{Tx}}(t)$ the time dependent phase and φ_0 the phase at $t = 0$. T is the duration of the chirp. $\varphi_{\mathrm{Tx}}(t)$ can be computed by

$$\varphi_{\mathrm{Tx}}(t) = \int_0^t \omega(\tilde{t})\, \mathrm{d}\tilde{t} \tag{5.6}$$

with the linear changing angular frequency

$$\omega(t) = \omega_0 + \chi\, t, \quad t \in [0, T], \tag{5.7}$$

where ω_0 is the angular frequency at the beginning of the chirp and χ is the chirp rate, cf. Fig. 5.3. Hence

$$\varphi_{\mathrm{Tx}}(t) = \omega_0\, t + \tilde{\varphi}(t), \tag{5.8}$$

$$\tilde{\varphi}(t) = \frac{1}{2}\chi\, t^2. \tag{5.9}$$

The transmitted signal travels to the target, is reflected at the target and travels back to the radar. The target is moving relative to the radar. Therefore, due to the Doppler effect, the signal is modified. To compute the signal which is received by the radar, we express the transmitted signal by its inverse Fourier transform

$$s_{\mathrm{Tx}}(t) = \int_{-\infty}^{\infty} S_{\mathrm{Tx}}(\omega)\, \mathrm{e}^{j\omega t}\, \frac{1}{2\pi} \mathrm{d}\omega, \tag{5.10}$$

where $S_{\mathrm{Tx}}(\omega)$ is the Fourier transform of $s_{\mathrm{Tx}}(t)$. ω is the angular frequency. Since the Maxwell equations are linear, we can derive the change in frequency due to the Doppler effect for $\exp(j\,\omega t)$ and transform back to the time domain afterwards. In the computations in Appendix G.1, it is shown that the angular frequency of the received signal changes by $\omega_{\mathrm{Doppler}}$ defined in (5.2).

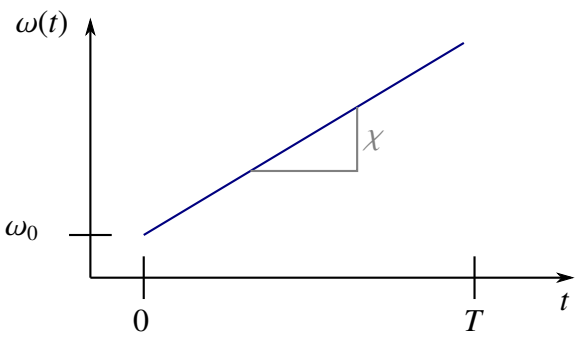

Figure 5.3.: Linear frequency modulated chirp

The received signal $s_{\mathrm{Rx}}(t)$ can be computed from the transmitted one, modified by the Doppler effect and time-delayed by the time which the electromagnetic wave needs to travel to the target and back to the radar. $s_{\mathrm{Rx}}(t)$ is derived in detail in Appendix G.1 and and can be written as

$$s_{\mathrm{Rx}}(t) = A_{\mathrm{Rx}} \cos\left(\varphi_{\mathrm{Rx}}(t)\right), \tag{5.11}$$

where A_{Rx} is the amplitude of the received signal and $\varphi_{\mathrm{Rx}}(t)$ its time dependent phase given in (G.26). A_{Rx} also includes the damping due to reflection at the target and the propagation of the signal.

The received signal $s_{\mathrm{Rx}}(t)$ is mixed in an IQ-mixer with the transmitted one, i. e. it is mixed with $A_{\mathrm{Tx}} \cos\left(\varphi_{\mathrm{Tx}}(t) + \varphi_0\right)$ and $A_{\mathrm{Tx}} \sin\left(\varphi_{\mathrm{Tx}}(t) + \varphi_0\right)$. Afterwards a band pass filter is applied and the I- and Q-signal are combined to a complex baseband signal. We assume the signal to be narrowband, i. e. the bandwidth is much smaller than the carrier frequency. Thus the phase of the complex baseband signal is given as the difference of the Tx phase $\varphi_{\mathrm{Tx}}(t) + \varphi_0$ and the Rx phase $\varphi_{\mathrm{Rx}}(t)$ in (G.26). In Appendix G.2, the complex baseband signal $s(t)$ is computed. It is given by

$$s(t) = A \exp\left(\, j\, \varphi_{\mathrm{base}}(t)\,\right), \tag{5.12}$$

with

$$\varphi_{\mathrm{base}}(t) = \varphi_{\mathrm{base},a} + \varphi_{\mathrm{base},b}(t) + \varphi_{\mathrm{base},c}(t), \tag{5.13}$$

$$\varphi_{\mathrm{base},a} = \omega_0\, \tau_0\, (1 - \beta) - \frac{1}{2} \chi\, \tau_0^2, \tag{5.14}$$

$$\varphi_{\mathrm{base},b}(t) = t\, [\omega_0\, 2\beta + \chi\, \tau_0\, (1 - 3\beta)], \tag{5.15}$$

$$\varphi_{\mathrm{base},c}(t) = t^2 2 \chi\, \beta. \tag{5.16}$$

Here, A is the complex amplitude of the baseband signal. It incorporates also the phase jump at the reflection of the signal at the target. β is defined as

$$\beta = \frac{v}{c}. \tag{5.17}$$

It is the ratio of the target's velocity v and the speed of light c. τ_0 is given by

$$\tau_0 = 2\, \frac{d_0}{c}. \tag{5.18}$$

It is the time the signal needs to travel to the target at distance d_0 and back to the radar. d_0 is the distance of the target at $t = 0$. τ_0 is also called the round trip time. For a moving target, the distance between target and radar changes during the measurement.

Let us interpret the terms in (5.13). $\varphi_{\mathrm{base},a}$ is a time independent phase shift which depends on the

Table 5.1.: Maximal values of the parameters used to compute the order of magnitude of different terms

Radar parameters		
	FMCW	chirp sequence
carrier frequency $f_0 = \frac{1}{2\pi}\omega_0$	76.5 GHz	76.5 GHz
chirp bandwidth $F = \frac{1}{2\pi}F_\omega$	1 GHz	1 GHz
chirp duration T	10 ms	100 μs
chirp rate $\frac{\mathrm{d}f}{\mathrm{d}t} = \frac{1}{2\pi}\chi$	$\frac{1\,\mathrm{GHz}}{5\,\mathrm{ms}} = 2 \cdot 10^{11}\,\frac{1}{\mathrm{s}^2}$	$\frac{1\,\mathrm{GHz}}{100\,\mu\mathrm{s}} = 10^{13}\,\frac{1}{\mathrm{s}^2}$
time difference Δt_M between last and first chirp	40 ms	20 ms
Target parameters		
distance d	250 m	
velocity v	$80\,\frac{\mathrm{m}}{\mathrm{s}}$ $\left(= 288\,\frac{\mathrm{km}}{\mathrm{h}}\right)$	

time delay τ_0 of the target. $\varphi_{\mathrm{base},b}$ can be written as

$$\varphi_{\mathrm{base},b}(t) = \omega_\mathrm{diff}\, t, \tag{5.19}$$

$$\omega_\mathrm{diff} = \omega_0\, 2\beta + \chi\, \tau_0\, (1 - 3\beta) \approx \omega_0\, 2\beta + \chi\, \tau_0. \tag{5.20}$$

ω_diff is the angular frequency difference between the transmitted and received signal due to the Doppler effect $\omega_0\, 2\beta$ and the propagation time τ_0, i. e. the distance of the target. The difference frequency is depicted in Fig. 2.5 on page 27. It is used to estimate the distance and relative velocity of the target. For a chirp sequence radar with high chirp rate χ, the joint distance and velocity estimation can be decoupled to a sequential distance and velocity estimation. For example, we consider a chirp sequence radar with a chirp rate $\chi = 2\pi \cdot 10^{13}\,\frac{1}{\mathrm{s}^2}$ and carrier frequency $f_0 = 76.5\,\mathrm{GHz}$. Then, for a target with a large velocity $v = 80\,\frac{\mathrm{m}}{\mathrm{s}}$ ($288\,\frac{\mathrm{km}}{\mathrm{h}}$) at a small distance $d_0 = 10\,\mathrm{m}$, the second term in (5.20) is still about 10 times larger than the first one and therefore $\omega_\mathrm{diff} \approx \chi\, \tau_0$. Thus only the distance information is included in ω_diff. This is an advantage of the chirp sequence radar compared to the FMCW radar, since in that case no matching algorithms are necessary.

Now we take a closer look at $\varphi_{\mathrm{base},c}(t)$. It can be seen as a distortion to the complex wave $A \cdot \exp\{j\,(\,\varphi_{\mathrm{base},a} + \varphi_{\mathrm{base},b}(t)\,)\}$ since it is a quadratic function in t. We estimate the maximum value of $\varphi_{\mathrm{base},c}(t)$. The bandwidth F_ω of the angular frequency of the chirp can be computed by

$$F_\omega = T\,\chi. \tag{5.21}$$

Then $|\varphi_{\mathrm{base},c}(t)| \leq |\varphi_{\mathrm{base},c}(T)| = 2\,T F_\omega \beta$. We use the values given in Tab. 5.1 as maximum values for the different parameters to compute the maximum value of $|\varphi_{\mathrm{base},c}(T)|$. For a chirp sequence radar $|\varphi_{\mathrm{base},c}(T)| \approx 0.3$ follows. For the angle estimation, the phase $\varphi_{\mathrm{base},a}$ is used. It has to be estimated modulo 2π. For the estimation of $\varphi_{\mathrm{base},a}$, in general $\varphi_{\mathrm{base},c}(t)$ is negligible, since

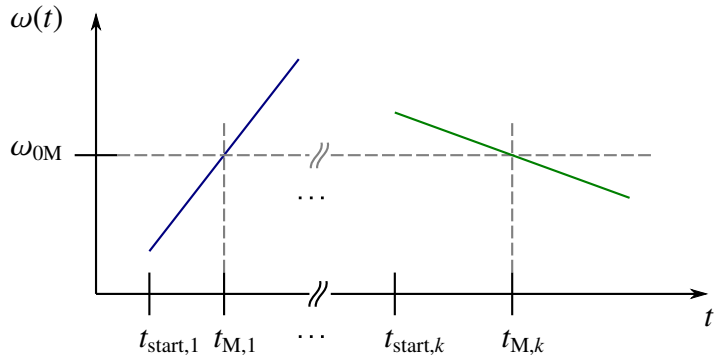

Figure 5.4.: Several chirps transmitted at different start times $t_{\text{start},i}$, with different chirp rates χ_i but with the same middle frequencies $\omega_i(t_{\text{M},i}) = \text{const} = \omega_{0\text{M}}\ \forall i$

$|\varphi_{\text{base},c}(t)| \leq |\varphi_{\text{base},c}(T)| \ll 2\pi\ \forall\, t \in [0, T]$. In the case of an FMCW radar, depending on the used chirp parameters, $\varphi_{\text{base},c}(T)$ could be of the order of magnitude 10, i. e. it has to be considered. Otherwise, the estimation of $\varphi_{\text{base},a}$ could be wrong. In [Kulpa et al., 2000] a simple algorithm for the estimation of nonlinear frequency distortions, like $\varphi_{\text{base},c}(t)$, is investigated.

Phase Difference Between Two Chirps Now we compute the phase difference of the baseband signal of the first transmitted chirp and the k-th chirp, $k \neq 1$. The chirps are transmitted at different transmission times. In the following, the subscript i denotes that the corresponding variable belongs to the i-th chirp. We study chirps which have the same carrier frequency $\omega_{0\text{M}}$ in the middle of the chirp [2]

$$\omega_1(t_{\text{M},1}) = \omega_k(t_{\text{M},k}) = \omega_{0\text{M}}. \tag{5.22}$$

$t_{\text{M},i}$ is the time at the middle of chirp i

$$t_{\text{M},i} = t_{\text{start},i} + \frac{1}{2}\, T_i, \tag{5.23}$$

and $t_{\text{start},i}$ is the start time of the transmission of chirp i and T_i its duration, cf. Fig. G.1 on page 165. An example of such chirps is depicted in Fig. 5.4. We compute the difference $\Delta\varphi_{1k}$ of the phases of the baseband signals at the time in the middle of the chirps. In Appendix G.4 it is shown that $\Delta\varphi_{1k}$ can be written as

$$\Delta\varphi_{1k} = \varphi_{\text{base},k}(t_{\text{M},k}) - \varphi_{\text{base},1}(t_{\text{M},1}). \tag{5.24}$$

Here

$$\varphi_{\text{base},i}(t) = \varphi^{(i)}_{\text{base}}(t - t_{\text{start},i}), \tag{5.25}$$

[2] Considering chirps which have the same frequency at the beginning of the chirps, $\omega_{0,1}(t_{\text{start},1}) = \omega_{0,k}(t_{\text{start},k}) = \omega_0$, leads to analogous results as (5.31) and (5.35). In that case, $\omega_{0\text{M}}$ has to be replaced by ω_0, $\tau_{M,1}$ by $\tau_{0,1}$, and $\Delta t_{\text{M},1k}$ by $\Delta t_{\text{start},1k} = t_{\text{start},k} - t_{\text{start},1}$.

where $\varphi^{(i)}_{\text{base}}(t)$ is the same as $\varphi_{\text{base}}(t)$ defined in (5.13), but the chirp dependent parameters ω_0, τ_0, χ in (5.14) to (5.16) are replaced by $\omega_{0,i}, \tau_{0,i}, \chi_i$, respectively. Computations in Appendix G.4 yield

$$\Delta\varphi_{1k} = \omega_{\text{Doppler}}\, \Delta t_{\text{M},1k} - \left(\frac{1}{2} \chi_k\, \tau^2_{M,k} - \frac{1}{2} \chi_1\, \tau^2_{M,1} \right) \tag{5.26}$$

with

$$\omega_{\text{Doppler}} = \omega_{0\text{M}}\, 2\, \frac{v}{c}, \tag{5.27}$$

$$\Delta t_{\text{M},1k} = t_{\text{M},k} - t_{\text{M},1}. \tag{5.28}$$

$\tau_{M,i}$ is the round trip time at the middle of chirp i, i. e. the distance of the target equals

$$d_{M,i} = d_{0,i} + v \frac{1}{2} T_i, \tag{5.29}$$

with the chirp duration T_i and $d_{0,i}$ being the distance of the target at the start of the transmission of chirp i. Hence

$$\tau_{M,i} = 2\, \frac{d_{M,i}}{c}. \tag{5.30}$$

Let us interpret the result: (5.26) shows that the phase difference $\Delta\varphi_{1k}$ contains a phase shift $\omega_{\text{Doppler}}\, \Delta t_{\text{M},1k}$ due to the Doppler effect. This is the same phase shift as for the pulse Doppler radar (5.3). But here $\Delta\varphi_{1k}$ contains additional contributions due to the chirp rates χ_i and the distance of the target, contained in $\tau_{M,i}$. If $\chi_i = 0\, \forall i$, i. e. pulses with constant frequency are transmitted as in the case of a pulse Doppler radar, (5.26) simplifies to the phase shift of a pulse Doppler radar (5.3).

We analyze and simplify (5.26) further. First we consider a chirp sequence radar, then an FMCW radar.

Chirp Sequence Radar A chirp sequence radar transmits many equal chirps. Hence, all chirp rates are equal with $\chi_1 = \chi_k = \chi$. In that case, (5.26) can be simplified further, cf. Appendix G.5, and $\Delta\varphi_{1k}$ has the simple form

$$\Delta\varphi_{1k} = \omega_{\text{pseudoDoppler}}\, \Delta t_{\text{M},1k} \tag{5.31}$$

with the pseudo Doppler frequency

$$\omega_{\text{pseudoDoppler}} = 2\, \frac{v}{c} \left(\omega_{0\text{M}} - \chi\, \tau_{M,1} \right). \tag{5.32}$$

We call it pseudo Doppler frequency, since it contains not only the Doppler frequency ω_{Doppler} but also a correction due to the round trip time $\tau_{M,1}$. Let us interpret it: $(\omega_{0\text{M}} - \chi\, \tau_{M,1})$ is the Tx frequency transmitted at time $t_{\text{M},1} - \tau_{M,1}$. If there was not a Doppler effect this would be the frequency received

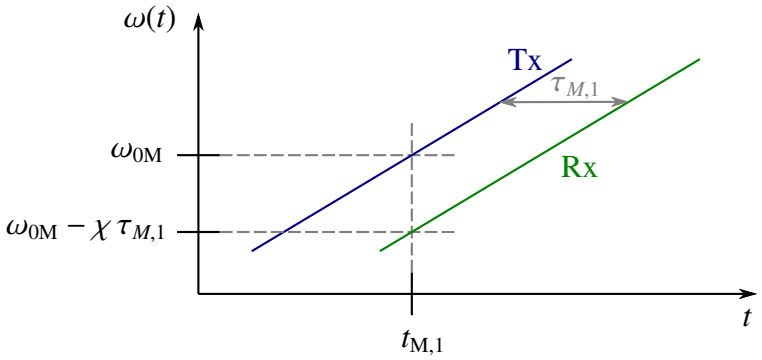

Figure 5.5.: Tx and Rx angular frequencies, neglecting the Doppler frequency, for the interpretation of (5.32)

at the radar at time $t_{\mathrm{M},1}$, cf. Fig. 5.5. $\omega_{\mathrm{pseudoDoppler}}$ is the Doppler frequency associated with this frequency.

FMCW Radar In general, the chirp rates χ_i of the different chirps are not equal and we cannot simplify $\Delta\varphi_{1k}$ as in the case of a chirp sequence radar. In the typical signal processing chain of an FMCW radar, the distance and velocity of the target are already estimated before the DOA estimation. Using the estimated velocity, the distance of the target $d_{M,i}$ at the middle of chirp i can be estimated as well for every chirp. Therefore we can use the estimated distances $\hat{d}_{M,1}, \hat{d}_{M,k}$ to compute a corrected phase difference $\Delta\varphi_{\mathrm{corrected},1k}$. We plug (5.30) in (5.26) to write

$$\Delta\varphi_{1k} = \omega_{\mathrm{Doppler}}\,\Delta t_{\mathrm{M},1k} - \frac{2}{c^2}\left(\chi_k\, d_{M,k}^2 - \chi_1\, d_{M,1}^2\right). \tag{5.33}$$

We define $\Delta\varphi_{\mathrm{corrected},1k}$ as

$$\Delta\varphi_{\mathrm{corrected},1k} = \Delta\varphi_{1k} + \frac{2}{c^2}\left(\chi_k\, \hat{d}_{M,k}^2 - \chi_1\, \hat{d}_{M,1}^2\right). \tag{5.34}$$

Then

$$\Delta\varphi_{\mathrm{corrected},1k} \approx \omega_{\mathrm{Doppler}}\,\Delta t_{\mathrm{M},1k}, \tag{5.35}$$

where $\omega_{\mathrm{Doppler}}$ is given in (5.27). There is no exact equal sign in (5.35), since in general $\hat{d}_{M,1}, \hat{d}_{M,k}$ have an estimation error. Usually this error is negligible, as shown in Appendix G.6.

5.1.1.3. Summary and Discussion

We have presented the baseband signal in the time domain for a pulse Doppler, an FMCW and a chirp sequence radar. We have computed the phase change between the first and the k-th pulse for these different radar systems. For convenience, we repeat the results here. For a pulse Doppler radar

the phase change is given by (5.3)

$$\Delta\varphi_{1k} = \omega_{\text{Doppler}}\, \Delta t_{\text{M},1k}. \tag{5.36}$$

For an FMCW radar, the phase change after distance and velocity estimation as well as a phase correction is (5.35)

$$\Delta\varphi_{\text{corrected},1k} \approx \omega_{\text{Doppler}}\, \Delta t_{\text{M},1k}, \tag{5.37}$$

and for the chirp sequence radar it is (5.31)

$$\Delta\varphi_{1k} = \omega_{\text{pseudoDoppler}}\, \Delta t_{\text{M},1k}, \tag{5.38}$$

where $\omega_{\text{pseudoDoppler}}$ is given in (5.32). Thus, for all of these radar types, the phase change has the same structure. In the following, we abbreviate these three cases by

$$\Delta\varphi_{1k} = \omega\, \Delta t_{1k}, \tag{5.39}$$

where ω is defined appropriately, depending on the considered radar system, and Δt_{1k} is a shortcut for $\Delta t_{\text{M},1k}$. These phase shifts have to be incorporated in the signal model for the DOA estimation of a moving target. W. l. o. g. we set the phase of the first chirp, due to the Doppler effect, to ωt_1, where t_1 is the time in the middle of the first chirp. Then the phase shift φ_k of the k-th transmitted pulse is

$$\begin{aligned} \varphi_k &= \omega\,(t_1 + \Delta t_{1k}) \\ &= \omega\, t_k, \end{aligned} \tag{5.40}$$

with t_k being the transmission time in the middle of the k-th chirp. In the TDM MIMO radar φ_k are the phase shifts caused by the different pulses of different Tx antennas transmitted at different times. We incorporate these phase shifts in the signal model for the virtual array of the TDM MIMO radar in the next sections. Since the structure of the phase shifts are the same for the pulse Doppler, FMCW, and chirp sequence radar, the DOA estimation model presented in the following section works for all kinds of these radars.

5.1.2. Signal Model of a TDM MIMO Radar for DOA estimation

We present the signal model for the DOA estimation of a non-stationary target for a TDM MIMO radar. We consider a radar system with a planar, i. e. two-dimensional antenna array in Section 5.1.2.1. In Section 5.1.2.3, we present the signal model for a linear antenna array as a special case of the planar one.

5.1.2.1. Planar Array

We investigate a TDM MIMO radar with a planar antenna array. We consider one non-stationary target. Hence we extend the model given in Section 4.3.1 from a linear to a planar array and from a stationary to a non-stationary target. Moreover, we include different transmission powers and chirp lengths, which result in different energies transmitted by the Tx antennas.

The MIMO radar consists of N_{Tx} Tx and N_{Rx} Rx colocated, isotropic antennas. The transmitted signal is narrowband. The moving target is modeled as a point target reflecting the transmitted signals. The target is in the far field. The positions of the Rx antennas are given by

$$\underline{d}^{\mathrm{Rx},1}, \ldots, \underline{d}^{\mathrm{Rx},N_{\mathrm{Rx}}} \in \mathbb{R}^2 \tag{5.41}$$

and the positions of the Tx antennas by

$$\underline{d}^{\mathrm{Tx},1}, \ldots, \underline{d}^{\mathrm{Tx},N_{\mathrm{Tx}}} \in \mathbb{R}^2. \tag{5.42}$$

All positions are in the unit of $\frac{\lambda}{2\pi}$, where λ is the carrier wavelength corresponding to the middle frequency of the chirps. The Tx antennas transmit a sequence of N_{Pulse} pulses at the time instances given by $\underline{t} \in \mathbb{R}^{N_{\mathrm{Pulse}}}$. Here t_i is the time in the middle of the i-th transmitted pulse as depicted in Fig. 5.6. In the following, we call $\underline{t}$ just transmission times. The pulse durations are $\underline{\Delta t} \in \mathbb{R}^{N_{\mathrm{Pulse}}}$ and the pulses are transmitted with transmission powers $\underline{p} \in \mathbb{R}^{N_{\mathrm{Pulse}}}$. The positions of the Tx antennas in the sequence in which they transmit are denoted by

$$\underline{d}^{\mathrm{Pulse},1}, \ldots, \underline{d}^{\mathrm{Pulse},N_{\mathrm{Pulse}}} \in \mathbb{R}^2, \tag{5.43}$$

also in the unit of $\frac{\lambda}{2\pi}$. We put the position vectors in matrices

$$\mathbf{D}^{\mathrm{Rx}} = \left[\underline{d}^{\mathrm{Rx},1}, \ldots, \underline{d}^{\mathrm{Rx},N_{\mathrm{Rx}}}\right]^T \in \mathbb{R}^{N_{\mathrm{Rx}} \times 2}, \tag{5.44}$$

$$\mathbf{D}^{\mathrm{Tx}} = \left[\underline{d}^{\mathrm{Tx},1}, \ldots, \underline{d}^{\mathrm{Tx},N_{\mathrm{Tx}}}\right]^T \in \mathbb{R}^{N_{\mathrm{Tx}} \times 2}, \tag{5.45}$$

$$\mathbf{D}^{\mathrm{Pulse}} = \left[\underline{d}^{\mathrm{Pulse},1}, \ldots, \underline{d}^{\mathrm{Pulse},N_{\mathrm{Pulse}}}\right]^T \in \mathbb{R}^{N_{\mathrm{Pulse}} \times 2}. \tag{5.46}$$

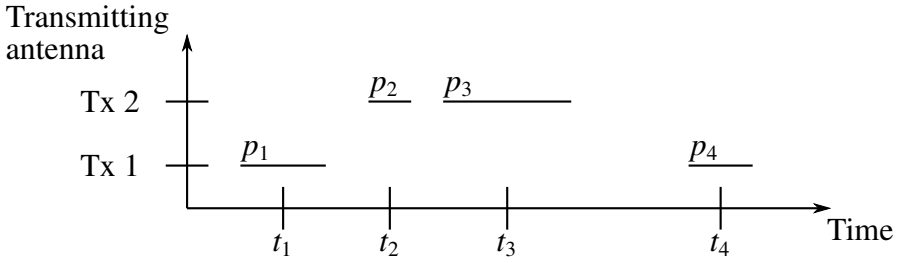

Figure 5.6.: Example of a TDM scheme: 2 transmitters transmitting at times $\underline{t} = [t_1, t_2, t_3, t_4]^T$ with power $\underline{p} = [p_1, p_2, p_3, p_4]^T$. Here, $\mathbf{D}^{\mathrm{Pulse}} = \left[\underline{d}^{\mathrm{Tx},1}, \underline{d}^{\mathrm{Tx},2}, \underline{d}^{\mathrm{Tx},2}, \underline{d}^{\mathrm{Tx},1}\right]^T$.

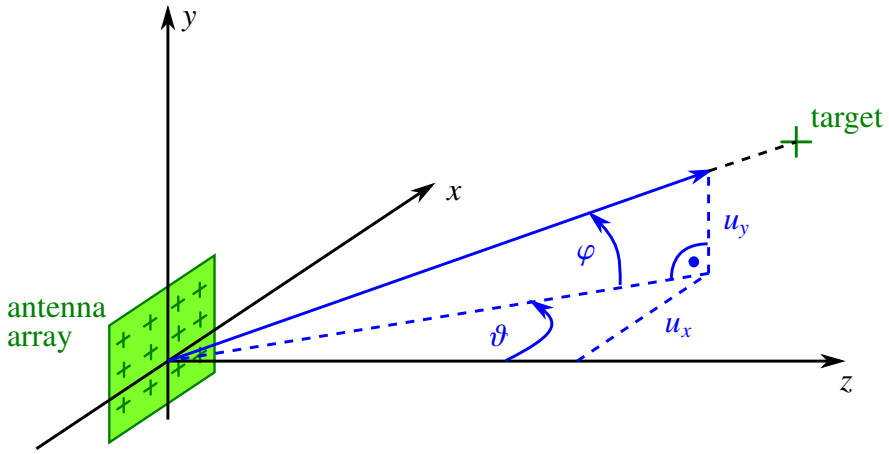

Figure 5.7.: Azimuth ϑ and elevation φ of a target and its electrical angles u_x, u_y

If an antenna transmits more than once, its position occurs several times in $\mathbf{D}^{\text{Pulse}}$, see Fig. 5.6 for an example. Note that $\mathbf{D}^{\text{Tx}}$ contains only the possible Tx antenna positions, whereas $\mathbf{D}^{\text{Pulse}}$ contains really the positions of the used Tx antennas. $\mathbf{D}^{\text{Pulse}}$ and $\underline{t}$ can be chosen independently. The planar antenna array is located in the x, y-plane and the two unknown DOAs of the target are the azimuth ϑ and elevation φ, cf. Fig. 5.7. The unit vector in the direction of the target in the Cartesian coordinate system is

$$\underline{u}_{\text{unit}} = \begin{bmatrix} u_x \\ u_y \\ u_z \end{bmatrix} = \begin{bmatrix} \cos\varphi \sin\vartheta \\ \sin\varphi \\ \cos\varphi \cos\vartheta \end{bmatrix} \in \mathbb{R}^3. \tag{5.47}$$

For convenience, we did not choose the usual spherical coordinate system but we chose the coordinate system such that ϑ and φ denote the azimuth and elevation, respectively. Since the array is located in the x, y-plane, we need only the two electrical angles

$$\underline{u} = \begin{bmatrix} u_x \\ u_y \end{bmatrix} = \begin{bmatrix} \cos\varphi \sin\vartheta \\ \sin\varphi \end{bmatrix} \in \mathbb{R}^2 \tag{5.48}$$

in the following. The steering vector of the Rx array is

$$\underline{a}^{\text{Rx}}(\underline{u}) = \exp(j\,\mathbf{D}^{\text{Rx}}\underline{u}) \in \mathbb{C}^{N_{\text{Rx}}}. \tag{5.49}$$

The steering vector of the Tx array with the transmitting sequence $\mathbf{D}^{\text{Pulse}}$ is given by

$$\underline{a}^{\text{Pulse}}(\underline{u}) = \exp(j\,\mathbf{D}^{\text{Pulse}}\underline{u}) \in \mathbb{C}^{N_{\text{Pulse}}}. \tag{5.50}$$

Our model consists of L measurement cycles, where each cycle is made up of N_{Pulse} pulses as explained in Section 4.1. One cycle is one coherent processing interval (CPI). The transmission se-

quence of one cycle is given in $\mathbf{D}^{\text{Pulse}}$ and remains the same for all L measurement cycles. The received baseband signal of the virtual array for cycle l is

$$\underline{x}(l) = \left\{ \sqrt{\underline{\rho}} \odot \exp(j\,\underline{t}\omega) \odot \underline{a}^{\text{Pulse}}(\underline{u}) \right\} \otimes \underline{a}^{\text{Rx}}(\underline{u})\, s(l) + \underline{n}(l) \in \mathbb{C}^{N_{\text{Pulse}} \cdot N_{\text{Rx}}}, \quad l = 1, \ldots, L, \tag{5.51}$$

where $s(l) \in \mathbb{C}$ is the unknown, deterministic complex target signal and $\underline{n}(l)$ the noise. $\underline{\rho} \in \mathbb{R}^{N_{\text{Pulse}}}$ contains the transmission energies of the pulses, i. e. ρ_i is the energy of pulse i. The square root is to be understood as an element by element operation, i. e. for any vector $\underline{y} \in \mathbb{R}^K$, the expression $\underline{z} = \sqrt{\underline{y}}$ means that $z_i = \sqrt{y_i}\, \forall i = 1, \ldots, K$. $\odot$ denotes the entrywise Hadamard product. The pulse energies are given by the Hadamard product of the transmission powers and pulse durations

$$\underline{\rho} = \underline{p} \odot \underline{\Delta t}. \tag{5.52}$$

ω is the target's angular Doppler frequency. The term $\exp(j\,\underline{t}\omega)$ describes the phase change in the received signal $\underline{x}(l)$ due to the Doppler effect caused by the movement of the target, cf. (5.40). This phase change has been derived in detail in Section 5.1.1. Note that in the model (5.51), the transmission time t_i is coupled to the position of the transmitting antenna $\underline{d}^{\text{Pulse},i}$, which is contained in $\underline{a}^{\text{Pulse}}(\underline{u})$. Hence the time domain is coupled to the spacial domain and because of this, the model has a different structure than many models in the literature which are space-time separable, e. g. the SIMO radar model in [Dogandzic and Nehorai, 2001], and it does not satisfy the sufficient conditions of space-time separability in [Pasupathy and Venetsanopoulos, 1974].

We define the new steering vector

$$\underline{b}(\underline{u}, \omega) = \left\{ \sqrt{\underline{\rho}} \odot \exp(j\,\underline{t}\omega) \odot \underline{a}^{\text{Pulse}}(\underline{u}) \right\} \otimes \underline{a}^{\text{Rx}}(\underline{u}) \in \mathbb{C}^{N_{\text{Virt}}}, \tag{5.53}$$

$$N_{\text{Virt}} = N_{\text{Pulse}} \cdot N_{\text{Rx}}, \tag{5.54}$$

to write the signal as

$$\underline{x}(l) = \underline{b}(\underline{u}, \omega)\, s(l) + \underline{n}(l) \in \mathbb{C}^{N_{\text{Virt}}}, \quad l = 1, \ldots, L. \tag{5.55}$$

For convenience, we write $\underline{b}(\underline{u}, \omega)$ in another way

$$\underline{b}(\underline{u}, \omega) = \sqrt{\underline{\rho}^{\text{Virt}}} \odot \exp(j\,\underline{t}^{\text{Virt}}\omega) \odot \underline{a}^{\text{Virt}}(\underline{u}) \in \mathbb{C}^{N_{\text{Virt}}}, \tag{5.56}$$

where we have defined

$$\underline{\rho}^{\text{Virt}} = \underline{\rho} \otimes \underline{1}_{N_{\text{Rx}}} \in \mathbb{R}^{N_{\text{Virt}}}, \tag{5.57}$$

$$\underline{t}^{\text{Virt}} = \underline{t} \otimes \underline{1}_{N_{\text{Rx}}} \in \mathbb{R}^{N_{\text{Virt}}}, \tag{5.58}$$

$$\underline{a}^{\text{Virt}}(\underline{u}) = \underline{a}^{\text{Pulse}}(\underline{u}) \otimes \underline{a}^{\text{Rx}}(\underline{u}) \in \mathbb{C}^{N_{\text{Virt}}}. \tag{5.59}$$

$\underline{a}^{\text{Virt}}(\underline{u})$ is the steering vector of the virtual array which includes all Rx-Tx combinations of all transmitted pulses. It can also be written as

$$\underline{a}^{\text{Virt}}(\underline{u}) = \exp(j\,\mathbf{D}^{\text{Virt}}\underline{u}) \tag{5.60}$$

where the matrix with the positions of the virtual array is given by

$$\mathbf{D}^{\text{Virt}} = \underline{1}_{N_{\text{Pulse}}} \otimes \mathbf{D}^{\text{Rx}} + \mathbf{D}^{\text{Pulse}} \otimes \underline{1}_{N_{\text{Rx}}} \in \mathbb{R}^{N_{\text{Virt}} \times 2}. \tag{5.61}$$

Note that the transmission sequence is already incorporated in $\mathbf{D}^{\text{Pulse}}$ and thus in $\mathbf{D}^{\text{Virt}}$.

We make the following assumptions:

- $\underline{n}(l)$ is circular complex Gaussian with zero mean, spatially and temporally uncorrelated with $\mathrm{E}\left(\underline{n}(l)\,\underline{n}^H(m)\right) = \delta_{l,m}\,\sigma^2\,\mathbf{I}$. An explanation for this assumption is given in Section 4.2.1.
- Let τ_{prop} be the propagation time of the signal across the array and BW the bandwidth of the signal. We assume that $\tau_{\text{prop}} \ll \frac{1}{\text{BW}}$, known as the narrowband array assumption [Dogandzic and Nehorai, 2001].
- The target's distance to the MIMO radar is much larger than the aperture of the radar such that we have a far field situation. Hence the radar receives a plane wave and the radar cross section as well as the target's DOAs ϑ, φ, and therefore also the electrical angles $\underline{u}$ are the same for all antennas.
- The DOAs do not change significantly during the L measurement cycles, i.e. the change is much smaller than the DOA accuracy of the radar and can thus be ignored.
- The target moves with constant relative radial velocity during the L measurement cycles. Hence the Doppler frequency ω is constant.

Thus the unknown quantities $\underline{\Theta}$ to be estimated from $\underline{x}(l)$, $1 \le l \le L$, are

$$\underline{\Theta} = \left[u_x,\, u_y,\, \omega,\, s(1),\, \ldots,\, s(L),\, \sigma^2\right]^T. \tag{5.62}$$

Compared to a stationary target, we have to estimate the Doppler frequency ω additionally.

As an example, consider a radar with a carrier frequency of 76.5 GHz in an automotive application. This corresponds to a carrier wavelength $\lambda \approx 4\,\text{mm}$. The antenna array is a rectangular array with 4×4 antennas spaced with half wavelength spacing. Thus the geometrical size of the antenna array is approximately $6\,\text{mm} \times 6\,\text{mm}$. Let the cycle time of the radar be 15 ms and consider a measurement with $L = 1$ cycle. The target, another car, is located on the neighboring driving lane with a lateral distance of 4 m and a radial distance of 30 m. It is moving ahead with a relative velocity of $15\,\frac{\text{m}}{\text{s}}$. The radar scattering center is located at the same height as the radar. This corresponds to the DOAs $\varphi = 0°$ and $\vartheta = 7.7°$. Obviously, the far field condition is fulfilled. The change of ϑ during the

measurement is 0.06°, which is much smaller than the typical DOA accuracy of such a radar system. On the other hand, the phase change during the measurement due to the Doppler effect is $113.8 \cdot 2\pi$, which is significant. The radial relative velocity changes by 10^{-2} %, therefore it can be neglected.

5.1.2.2. Notes and Discussion of the Model

In the model (5.55), the electrical angles $\underline{u}$ and the Doppler frequency ω have to be estimated jointly, in addition to the other parameters in (5.62).

In a usual pulse Doppler and chirp sequence radar, the Doppler frequency ω, and therefore the velocity v, is estimated from the phase shift from pulse to pulse, which is given by $\exp(j\,\underline{t}\omega)$ in (5.53). This is called the slow time domain. The successive estimation of ω and $\underline{u}$, i. e. first ω is estimated and using this result $\underline{u}$ is estimated, is worse or at most equally good as the joint estimation of ω and $\underline{u}$. Due to that, we investigate the estimation of both at once. In general, this introduces a higher computational burden. As we will see in Section 5.2.3.2, by exploiting certain properties of the signal model, the computational burden can be diminished.

In an FMCW radar, the velocity v of the target, and therefore its Doppler frequency, is estimated before the DOA estimation. In general, the estimation error of v is too large to be used for the DOA estimation. We show this in the following example: Consider a radar with carrier frequency $f_0 = 76.5\,\mathrm{GHz}$. An automotive radar can typically achieve an estimation accuracy of the velocity $\sigma_v = 0.1\,\frac{\mathrm{m}}{\mathrm{s}}$. Using (5.39), the phase change between the first and second pulse is $\Delta\varphi_{12} = \omega\,\Delta t_{12}$. Plugging in the Doppler frequency (5.27) leads to $\Delta\varphi_{12} = 2\,\frac{v}{c}\,2\pi\,f_0\,\Delta t_{12}$. A typical chirp duration is about 5 ms. Hence we set $\Delta t_{12} = 5\,\mathrm{ms}$. Then the error in the phase change is $\sigma_{\Delta\varphi_{12}} = 2\,\frac{\sigma_v}{c}\,2\pi\,f_0\,\Delta t_{12} \approx 1.6 \approx \pi/2$. This is much too large to be used in the DOA estimation. The error in the phase shift between the first and k-th pulse, $k = 3, 4, \ldots$, is even larger. Thus the Doppler frequency and the electrical angles have to be estimated jointly, together with the other parameters given in (5.62). The result of the estimation of the Doppler frequency in the DOA estimation process could be used to refine the first velocity estimation of the FMCW radar, which is done before the DOA estimation.

5.1.2.3. Linear Array

Now we consider a TDM MIMO radar where the Tx and Rx antennas are arranged in a linear array. W. l. o. g. let the linear array be situated on the x-axes of the Cartesian coordinate system. The signal model is a special case of the signal model introduced in Section 5.1.2.1. The positions of the Rx and Tx antennas are just real numbers

$$d^{\mathrm{Rx},1}, \ldots, d^{\mathrm{Rx},N_{\mathrm{Rx}}} \in \mathbb{R}, \tag{5.63}$$

$$d^{\mathrm{Tx},1}, \ldots, d^{\mathrm{Tx},N_{\mathrm{Tx}}} \in \mathbb{R}, \tag{5.64}$$

respectively. The same is valid for the positions of the Tx antennas in the sequence in which they transmit

$$d^{\text{Pulse},1}, \ldots, d^{\text{Pulse},N_{\text{Pulse}}} \in \mathbb{R}. \tag{5.65}$$

The matrices $\mathbf{D}^{\text{Rx}}$ in (5.44) and $\mathbf{D}^{\text{Pulse}}$ in (5.46) simplify to vectors, which we denote by $\underline{d}^{\text{Rx}}$ and $\underline{d}^{\text{Pulse}}$, respectively.

$$\underline{d}^{\text{Rx}} = \begin{bmatrix} d^{\text{Rx},1} & \ldots & d^{\text{Rx},N_{\text{Rx}}} \end{bmatrix}^T \in \mathbb{R}^{N_{\text{Rx}}}, \tag{5.66}$$

$$\underline{d}^{\text{Pulse}} = \begin{bmatrix} d^{\text{Pulse},1} & \ldots & d^{\text{Pulse},N_{\text{Pulse}}} \end{bmatrix}^T \in \mathbb{R}^{N_{\text{Pulse}}}. \tag{5.67}$$

For convenience, we also define

$$\underline{d}^{\text{Tx}} = \begin{bmatrix} d^{\text{Tx},1} & \ldots & d^{\text{Tx},N_{\text{Tx}}} \end{bmatrix}^T \in \mathbb{R}^{N_{\text{Tx}}}. \tag{5.68}$$

Since we consider a linear antenna array, we can only estimate one DOA. W. l. o. g. let the target be located in the x,z-plane, i. e. $\varphi = 0°$, cf. Fig. 5.7. Then the unknown DOA ϑ, the azimuth, is measured perpendicular to the linear array as depicted in Fig. 5.8. For convenience, we denote the x-component of the target's electrical angle by u. It is given in (5.48) and here simplifies to

$$u = u_x = \sin(\vartheta) \in \mathbb{R}. \tag{5.69}$$

We make the same assumptions as in Section 5.1.2.1. Hence we can write the signal model as a special case of (5.55)

$$\underline{x}(l) = \underline{b}(u, \omega)\, s(l) + \underline{n}(l), \quad l = 1, \ldots, L, \tag{5.70}$$

with

$$\underline{b}(u, \omega) = \left\{ \sqrt{\underline{\rho}} \odot \exp(j\, \underline{t}\omega) \odot \underline{a}^{\text{Pulse}}(u) \right\} \otimes \underline{a}^{\text{Rx}}(u) \in \mathbb{C}^{N_{\text{Virt}}}, \tag{5.71}$$

$$\underline{a}^{\text{Pulse}}(u) = \exp(j\, \underline{d}^{\text{Pulse}} u) \in \mathbb{C}^{N_{\text{Pulse}}}, \tag{5.72}$$

$$\underline{a}^{\text{Rx}}(u) = \exp(j\, \underline{d}^{\text{Rx}} u) \in \mathbb{C}^{N_{\text{Rx}}}. \tag{5.73}$$

As in Section 5.1.2.1, we express $\underline{b}(u, \omega)$ in another way:

$$\underline{b}(u, \omega) = \sqrt{\underline{\rho}^{\text{Virt}}} \odot \exp(j\, \underline{t}^{\text{Virt}}\omega) \odot \underline{a}^{\text{Virt}}(u) \in \mathbb{C}^{N_{\text{Virt}}}, \tag{5.74}$$

$$\underline{a}^{\text{Virt}}(u) = \underline{a}^{\text{Pulse}}(u) \otimes \underline{a}^{\text{Rx}}(u) = \exp(j\, \underline{d}^{\text{Virt}} u) \in \mathbb{C}^{N_{\text{Virt}}}, \tag{5.75}$$

$$\underline{d}^{\text{Virt}} = \underline{1}_{N_{\text{Pulse}}} \otimes \underline{d}^{\text{Rx}} + \underline{d}^{\text{Pulse}} \otimes \underline{1}_{N_{\text{Rx}}} \in \mathbb{R}^{N_{\text{Virt}}}. \tag{5.76}$$

The other variables remain the same as in Section 5.1.2.1, which we repeat here for convenience

$$s(l) \in \mathbb{C}, \tag{5.77}$$

$$\underline{\rho}^{\text{Virt}} = \underline{\rho} \otimes \underline{1}_{N_{\text{Rx}}} \in \mathbb{C}^{N_{\text{Virt}}}, \tag{5.78}$$

$$\underline{t}^{\text{Virt}} = \underline{t} \otimes \underline{1}_{N_{\text{Rx}}} \in \mathbb{C}^{N_{\text{Virt}}}. \tag{5.79}$$

Given the observations $\underline{x}(l)$, $l = 1, \ldots, L$, the unknown quantities $\underline{\Theta}$ to be estimated are

$$\underline{\Theta} = [u, \omega, s(1), \ldots, s(L), \sigma^2]^T. \tag{5.80}$$

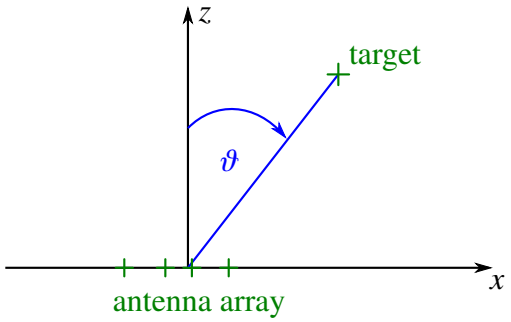

Figure 5.8.: Linear antenna array. The DOA ϑ is measured perpendicular to the antenna array.

5.1.2.4. TDM Scheme

The TDM scheme which is used in the TDM MIMO radar is characterized by the parameters

$$\psi^{\text{TDM}} = \left\{\mathbf{D}^{\text{Pulse}}, \underline{t}, \underline{\rho}, N_{\text{Pulse}}\right\} \tag{5.81}$$

with

$$\mathbf{D}^{\text{Pulse}} \in \mathbb{R}^{N_{\text{Pulse}} \times 2}, \ \underline{t}, \ \underline{\rho} \in \mathbb{R}^{N_{\text{Pulse}}}. \tag{5.82}$$

For a linear array, $\mathbf{D}^{\text{Pulse}}$ simplifies to $\underline{d}^{\text{Pulse}}$ and

$$\psi^{\text{TDM}} = \left\{\underline{d}^{\text{Pulse}}, \underline{t}, \underline{\rho}, N_{\text{Pulse}}\right\}. \tag{5.83}$$

N_{Pulse} are the number of transmitted chirps, $\underline{t}$ the transmission times and $\underline{\rho}$ the energy of the transmitted pulses. $\mathbf{D}^{\text{Pulse}}$ describes the sequence in which the Tx antennas transmit. $\mathbf{D}^{\text{Pulse}}$ contains also the number of used Tx antennas, since different positions in $\mathbf{D}^{\text{Pulse}}$ correspond to different Tx antennas. Note that ψ^{TDM} contains both discrete variables (N_{Pulse}) and continuous variables ($\underline{t}, \underline{\rho}$, positions in $\mathbf{D}^{\text{Pulse}}$).

In the following, we will see that the DOA performance of the TDM MIMO radar depends on the chosen TDM scheme, i. e. on ψ^{TDM}. Thus, for a good DOA performance, ψ^{TDM} has to be optimized.

5.2. One Moving Target

We study the performance in DOA estimation of one moving target. In Section 5.2.1 we derive the CRB for the DOA estimation using the model with a planar and linear array presented in Section 5.1.2. We discuss the properties of the CRB and compare it to a SIMO radar and a MIMO radar with a stationary target in Section 5.2.2. In Section 5.2.3, we present a theorem which gives sufficient conditions such that the CRB of the DOAs for a moving target equals the CRB of the DOAs for a stationary target, although the Doppler frequency of the target is not known. We investigate the MIMO radar with a linear Rx an Tx array in more detail in Section 5.2.4. We derive optimal TDM schemes in the sense that the CRB is minimized under different practical constraints.

5.2.1. Cramer Rao Bound

First we compute the CRB for a TDM MIMO radar with a planar array. After that we present the CRB for a linear array.

5.2.1.1. CRB for a Planar Array

The unknown parameter vector to be estimated is given in (5.62). We are interested in that part of the CRB of $\underline{\Theta}$ which corresponds to the parameters $\underline{u}$ and ω. Similar to Section 4.2.2.1, we have to obtain the FIM $\mathbf{J}$ of the whole parameter vector $\underline{\Theta}$ and determine its inverse. From $\mathbf{J}^{-1}$, we take the 3×3 block corresponding to $[u_x, u_y, \omega]^T$. This part is $\mathbf{CRB}_{\underline{u},\omega}$. Using the results from [Yau and Bresler, 1992],

$$\mathbf{CRB}_{\underline{u},\omega}^{-1} = 2\,L\,\frac{\sigma_s^2}{\sigma^2}\,\mathrm{Re}(\mathbf{C}) \in \mathbb{R}^{3\times 3} \tag{5.84}$$

where

$$\mathbf{C} = \mathbf{D}^H\,\mathbf{P}_{\underline{b}}^{\perp}\,\mathbf{D} \qquad \in \mathbb{C}^{3\times 3}, \tag{5.85}$$

$$\mathbf{D} = \left[\frac{\partial \underline{b}(\underline{u},\omega)}{\partial u_x}\ \frac{\partial \underline{b}(\underline{u},\omega)}{\partial u_y}\ \frac{\partial \underline{b}(\underline{u},\omega)}{\partial \omega}\right] \in \mathbb{C}^{N_{\mathrm{Virt}}\times 3}, \tag{5.86}$$

$$\mathbf{P}_{\underline{b}}^{\perp} = \mathbf{I} - \mathbf{P}_{\underline{b}} \qquad \in \mathbb{C}^{N_{\mathrm{Virt}}\times N_{\mathrm{Virt}}}, \tag{5.87}$$

$$\mathbf{P}_{\underline{b}} = \underline{b}\left(\underline{b}^H\,\underline{b}\right)^{-1}\underline{b}^H \qquad \in \mathbb{C}^{N_{\mathrm{Virt}}\times N_{\mathrm{Virt}}}, \tag{5.88}$$

$$\sigma_s^2 = \frac{1}{L}\sum_{l=1}^{L} |s(l)|^2 \qquad \in \mathbb{R}. \tag{5.89}$$

Note that $\mathbf{P}_{\underline{b}}$ is the projection matrix on the subspace spanned by $\underline{b}$. After some lengthy calculations, cf. Appendix H, we can show that $\mathbf{C}$ is real and

$$\mathbf{CRB}_{\underline{u},\omega}^{-1} = 2\,L\,\frac{\sigma_s^2}{\sigma^2}\,\mathbf{C}, \tag{5.90}$$

$$\mathbf{C} = N_{\mathrm{Rx}}\left(\underline{1}^T\underline{\rho}\right)\left\{\begin{bmatrix} \mathrm{Cov}^{\mathrm{S}}(\mathbf{D}^{\mathrm{Rx}}) & & 0 \\ & & 0 \\ 0 \quad 0 & & 0 \end{bmatrix} + \begin{bmatrix} \mathrm{Cov}^{\mathrm{WS}}(\mathbf{D}^{\mathrm{Pulse}},\underline{\rho}) & \mathrm{Cov}^{\mathrm{WS}}(\underline{t},\mathbf{D}^{\mathrm{Pulse}},\underline{\rho}) \\ \mathrm{Cov}^{\mathrm{WS}}(\mathbf{D}^{\mathrm{Pulse}},\underline{t},\underline{\rho}) & \mathrm{Var}^{\mathrm{WS}}(\underline{t},\underline{\rho}) \end{bmatrix}\right\}. \tag{5.91}$$

$\mathrm{Cov}^{\mathrm{S}}$ is the sample covariance or cross-covariance and $\mathrm{Cov}^{\mathrm{WS}}$ the weighted sample covariance or cross-covariance. $\mathrm{Var}^{\mathrm{WS}}$ is the weighted sample variance. The definitions and properties are given in Appendix A. As an example for the weighted sample variance, we consider $\mathrm{Var}^{\mathrm{WS}}(\underline{t},\underline{\rho})$. It can be written as

$$\mathrm{Var}^{\mathrm{WS}}(\underline{t},\underline{\rho}) = \frac{1}{\underline{1}^T\underline{\rho}}\sum_{i=1}^{N_{\mathrm{Pulse}}}\left(t_i - \mathrm{E}^{\mathrm{WS}}(\underline{t},\underline{\rho})\right)^2\rho_i, \tag{5.92}$$

$$\mathrm{E}^{\mathrm{WS}}(\underline{t},\underline{\rho}) = \frac{1}{\underline{1}^T\underline{\rho}}\sum_{i=1}^{N_{\mathrm{Pulse}}} t_i\,\rho_i. \tag{5.93}$$

It has a similar form as the usual sample variance, but each value is weighted by the transmission energy ρ_i of the i-th pulse.

5.2.1.2. CRB for a Linear Array

In the important case of a linear array of Tx and Rx antennas, the CRB can be computed completely analog to the planar case, or it can be derived as a special case of the CRB for the planar array. We use the latter approach which is much simpler. Setting

$$\mathbf{D}^{\mathrm{Rx}} = \left[\underline{d}^{\mathrm{Rx}} \quad \underline{0}\right], \tag{5.94}$$

$$\mathbf{D}^{\mathrm{Pulse}} = \left[\underline{d}^{\mathrm{Pulse}} \quad \underline{0}\right], \tag{5.95}$$

(5.91) reads

$$\mathbf{C} = N_{\mathrm{Rx}}\left(\underline{1}^T\underline{\rho}\right)\left\{\begin{bmatrix} \mathrm{Var}^{\mathrm{S}}(\underline{d}^{\mathrm{Rx}}) & 0 & 0 \\ 0 & 0 & 0 \\ 0 & 0 & 0 \end{bmatrix} + \begin{bmatrix} \mathrm{Cov}^{\mathrm{WS}}(\underline{d}^{\mathrm{Pulse}},\underline{\rho}) & 0 & \mathrm{Cov}^{\mathrm{WS}}(\underline{t},\underline{d}^{\mathrm{Pulse}},\underline{\rho}) \\ 0 & 0 & 0 \\ \mathrm{Cov}^{\mathrm{WS}}(\underline{d}^{\mathrm{Pulse}},\underline{t},\underline{\rho}) & 0 & \mathrm{Var}^{\mathrm{WS}}(\underline{t},\underline{\rho}) \end{bmatrix}\right\}. \tag{5.96}$$

Logically, there is no information about u_y, since the antennas are arranged on a linear array on the x-axes. The inverse of the CRB for the electrical angle $u = u_x$ and ω is

$$\mathbf{CRB}_{u,\omega}^{-1} = 2\,L\,\frac{\sigma_s^2}{\sigma^2}\,\mathrm{Re}(\mathbf{C}) \in \mathbb{R}^{2\times 2}, \tag{5.97}$$

with

$$\mathbf{C} = N_{\mathrm{Rx}}\left(\underline{1}^T\underline{\rho}\right)\left\{\begin{bmatrix}\mathrm{Var}^{\mathrm{S}}(\underline{d}^{\mathrm{Rx}}) & 0\\ 0 & 0\end{bmatrix} + \begin{bmatrix}\mathrm{Cov}^{\mathrm{WS}}(\underline{d}^{\mathrm{Pulse}},\underline{\rho}) & \mathrm{Cov}^{\mathrm{WS}}(\underline{t},\underline{d}^{\mathrm{Pulse}},\underline{\rho})\\ \mathrm{Cov}^{\mathrm{WS}}(\underline{d}^{\mathrm{Pulse}},\underline{t},\underline{\rho}) & \mathrm{Var}^{\mathrm{WS}}(\underline{t},\underline{\rho})\end{bmatrix}\right\}. \tag{5.98}$$

We are interested in the CRB CRB_u of the electrical angle u. Assuming

$$\det\left(\mathbf{CRB}_{u,\omega}^{-1}\right) \neq 0,$$

it is given by

$$\begin{aligned}\mathrm{CRB}_u &= \left[\mathbf{CRB}_{u,\omega}\right]_{1,1}\\ &= \frac{1}{2\,L}\frac{1}{S}\frac{1}{U} \qquad \in \mathbb{R}\end{aligned} \tag{5.99}$$

with

$$S = \frac{\sigma_s^2}{\sigma^2}\,N_{\mathrm{Rx}}\left(\underline{1}^T\underline{\rho}\right) \qquad \in \mathbb{R}, \tag{5.100}$$

$$U = \mathrm{Var}^{\mathrm{S}}(\underline{d}^{\mathrm{Rx}}) + \mathrm{Var}^{\mathrm{WS}}(\underline{d}^{\mathrm{Pulse}},\underline{\rho}) - \frac{\left(\mathrm{Cov}^{\mathrm{WS}}(\underline{d}^{\mathrm{Pulse}},\underline{t},\underline{\rho})\right)^2}{\mathrm{Var}^{\mathrm{WS}}(\underline{t},\underline{\rho})} \in \mathbb{R}. \tag{5.101}$$

Note that since $\rho_i > 0$, $i = 1,\ldots,N_{\mathrm{Pulse}}$, and all values in $\underline{t}$ have to be different for a meaningful physical system, $\mathrm{Var}^{\mathrm{WS}}(\underline{t},\underline{\rho}) \neq 0$.

5.2.2. Properties of the CRB

In the following, we discuss and interpret the derived CRB. Moreover, we proof important properties of the CRB.

5.2.2.1. Structure

$\mathbf{CRB}^{-1}_{\underline{u},\omega}$ in (5.90) has the structure

$$\mathbf{CRB}^{-1}_{\underline{u},\omega} = 2L\,\frac{\sigma_s^2}{\sigma^2}\,N_{\mathrm{Rx}}\left(\underline{1}^T\underline{\rho}\right)\cdot \left\{\left[\begin{array}{ccc|c} & & & 0 \\ & \text{Contribution of SIMO} & & 0 \\ & & & 0 \\ \hline 0 & 0 & 0 & \end{array}\right] + \left[\begin{array}{c|c} \text{Contribution of MIMO} & \text{moving} \\ \hline \text{moving} & \text{target} \end{array}\right]\right\} \tag{5.102}$$

The first part is determined by $\mathbf{D}^{\mathrm{Rx}}$, i. e. it is the contribution of the Rx array to the DOA estimation. This 2×2-block can be expressed as

$$\mathrm{Cov}^{\mathrm{S}}(\mathbf{D}^{\mathrm{Rx}}) = \begin{array}{c} \\ u_x \\ u_y \end{array} \begin{array}{c} \begin{array}{cc} \overset{u_x}{} & \overset{u_y}{} \end{array} \\ \begin{bmatrix} \mathrm{Var}^{\mathrm{S}}(\underline{d}^{\mathrm{Rx},x}) & \mathrm{Cov}^{\mathrm{S}}(\underline{d}^{\mathrm{Rx},x}, \underline{d}^{\mathrm{Rx},y}) \\ \mathrm{Cov}^{\mathrm{S}}(\underline{d}^{\mathrm{Rx},x}, \underline{d}^{\mathrm{Rx},y}) & \mathrm{Var}^{\mathrm{S}}(\underline{d}^{\mathrm{Rx},y}) \end{bmatrix} \end{array} \tag{5.103}$$

where $\underline{d}^{\mathrm{Rx},x}$ and $\underline{d}^{\mathrm{Rx},y}$ are the first and second column of $\mathbf{D}^{\mathrm{Rx}}$, respectively. They contain the x- and y-positions of the Rx antennas, respectively. The small variables u_x, u_y on the outside of the matrix in (5.103) depict the parameters to which the matrix entries correspond. $\mathrm{Var}^{\mathrm{S}}(\underline{d}^{\mathrm{Rx},x})$ describes the information on u_x gained by the different x-positions of the Rx antennas. It is the analog expression to (4.16), which appears in the CRB for DOA estimation of one stationary target using a SIMO radar. Analogously, $\mathrm{Var}^{\mathrm{S}}(\underline{d}^{\mathrm{Rx},y})$ denotes the information on u_y. $\mathrm{Cov}^{\mathrm{S}}(\underline{d}^{\mathrm{Rx},x}, \underline{d}^{\mathrm{Rx},y})$ describes the coupling between u_x and u_y due to the Rx antenna positions.

The matrix $\mathrm{Cov}^{\mathrm{WS}}(\mathbf{D}^{\mathrm{Pulse}}, \underline{\rho})$ in (5.91) contains the contributions of the different Tx antenna positions to the DOA estimation. It has the same structure as $\mathrm{Cov}^{\mathrm{S}}(\mathbf{D}^{\mathrm{Rx}})$, but the sample covariance is weighted with the transmission energies of the different antennas. The expressions $\mathrm{Cov}^{\mathrm{WS}}(\mathbf{D}^{\mathrm{Pulse}}, \underline{t}, \underline{\rho})$, $\mathrm{Cov}^{\mathrm{WS}}(\underline{t}, \mathbf{D}^{\mathrm{Pulse}}, \underline{\rho})$, and $\mathrm{Var}^{\mathrm{WS}}(\underline{t}, \underline{\rho})$ in the second matrix in (5.91) are related to the movement of the target. For convenience, we define $\underline{d}^{\mathrm{Pulse},x}$ and $\underline{d}^{\mathrm{Pulse},y}$ to be the first and second column of $\mathbf{D}^{\mathrm{Pulse}}$, respectively. Then the off-diagonal matrix block in (5.91) reads

$$\mathrm{Cov}^{\mathrm{WS}}(\underline{t}, \mathbf{D}^{\mathrm{Pulse}}, \underline{\rho}) = \begin{array}{c} \\ u_x \\ u_y \end{array} \begin{array}{c} \overset{\omega}{} \\ \begin{bmatrix} \mathrm{Cov}^{\mathrm{WS}}(\underline{t}, \underline{d}^{\mathrm{Pulse},x}, \underline{\rho}) \\ \mathrm{Cov}^{\mathrm{WS}}(\underline{t}, \underline{d}^{\mathrm{Pulse},y}, \underline{\rho}) \end{bmatrix} \end{array} \in \mathbb{R}^{2\times 1}. \tag{5.104}$$

It describes the coupling between ω and u_x and the coupling between ω and u_y. The term $\mathrm{Var}^{\mathrm{WS}}(\underline{t}, \underline{\rho})$ in (5.91) is the information on ω, gained by the different transmission times.

5.2.2.2. Comparison to CRB for a Stationary Target and to CRB for a SIMO Radar

We compute the CRB for DOA estimation of a stationary target and the CRB for a SIMO radar in order to compare them to the general CRB we have derived.

CRB for the TDM MIMO Radar and a Stationary Target If the target is stationary, i. e. it does not move relative to the radar, the Doppler frequency vanishes, i. e. $\omega = 0$. If this is known a priori, there is no need to estimate it. In this case, the CRB of the electrical angles $\mathbf{CRB}_{\underline{u},\mathrm{stat}}$ can be derived by using the model (5.55) with $\omega = 0$ and computing the CRB analogously to Section 5.2.1.1. In this case, the unknown parameter vector $\underline{\Theta}$ is

$$\underline{\Theta} = \left[u_x,\, u_y,\, s(1),\, \ldots,\, s(L),\, \sigma^2\right]^T \tag{5.105}$$

and the part of the CRB corresponding to $\underline{u}$ for the TDM MIMO radar for a stationary target is

$$\mathbf{CRB}^{-1}_{\underline{u},\mathrm{stat}} = 2\,L\,\frac{\sigma_s^2}{\sigma^2}\,\mathrm{Re}(\mathbf{C}_{\mathrm{stat}}) \in \mathbb{R}^{2\times 2} \tag{5.106}$$

with

$$\mathbf{C}_{\mathrm{stat}} = \mathbf{D}^H_{\mathrm{stat}}\,\mathbf{P}^{\perp}_{\underline{b}}\,\mathbf{D}_{\mathrm{stat}} \quad \in \mathbb{C}^{2\times 2}, \tag{5.107}$$

$$\mathbf{D}_{\mathrm{stat}} = \left[\frac{\partial \underline{b}(\underline{u})}{\partial u_x},\, \frac{\partial \underline{b}(\underline{u})}{\partial u_y}\right] \in \mathbb{C}^{N_{\mathrm{Virt}}\times 2}. \tag{5.108}$$

The other variables remain the same and are given in (5.87) to (5.89). Completely analogous computations to Appendix H yield

$$\mathbf{CRB}^{-1}_{\underline{u},\mathrm{stat}} = 2\,L\,\frac{\sigma_s^2}{\sigma^2}\,\mathbf{C}_{\mathrm{stat}} \quad \in \mathbb{R}^{2\times 2}, \tag{5.109}$$

$$\mathbf{C}_{\mathrm{stat}} = N_{\mathrm{Rx}}\left(\underline{1}^T\underline{\rho}\right)\left\{\mathrm{Cov}^{\mathrm{S}}(\mathbf{D}^{\mathrm{Rx}}) + \mathrm{Cov}^{\mathrm{WS}}(\mathbf{D}^{\mathrm{Pulse}},\underline{\rho})\right\} \in \mathbb{R}^{2\times 2}. \tag{5.110}$$

Here we see the information gain $\mathrm{Cov}^{\mathrm{S}}(\mathbf{D}^{\mathrm{Rx}})$ and $\mathrm{Cov}^{\mathrm{WS}}(\mathbf{D}^{\mathrm{Pulse}},\underline{\rho})$ due to the different Rx and Tx antenna positions, respectively. $\mathrm{Cov}^{\mathrm{WS}}(\mathbf{D}^{\mathrm{Pulse}},\underline{\rho})$ depends on the positions of the Tx antennas in $\mathbf{D}^{\mathrm{Pulse}}$, but not on the sequence in which they transmit, since $\mathrm{Cov}^{\mathrm{WS}}(\mathbf{D}^{\mathrm{Pulse}},\underline{\rho})$ remains the same if the elements in $\mathbf{D}^{\mathrm{Pulse}}$ and $\underline{\rho}$ are permuted in parallel.

In the case of a linear array, we substitute $\mathbf{D}^{\mathrm{Rx}}$ and $\mathbf{D}^{\mathrm{Pulse}}$ by $\underline{d}^{\mathrm{Rx}}$ and $\underline{d}^{\mathrm{Pulse}}$, respectively, as in Section 5.2.1.2. This results in

$$\mathrm{CRB}_{u,\mathrm{stat}} = \frac{1}{2L}\frac{1}{S}\frac{1}{U_{\mathrm{stat}}} \quad \in \mathbb{R}, \tag{5.111}$$

$$S = \frac{\sigma_s^2}{\sigma^2}\,N_{\mathrm{Rx}}\left(\underline{1}^T\underline{\rho}\right) \quad \in \mathbb{R}, \tag{5.112}$$

$$U_{\mathrm{stat}} = \mathrm{Var}^{\mathrm{S}}(\underline{d}^{\mathrm{Rx}}) + \mathrm{Var}^{\mathrm{WS}}(\underline{d}^{\mathrm{Pulse}},\underline{\rho}) \in \mathbb{R}. \tag{5.113}$$

Note that for pulses with equal transmission energy $\underline{\rho} \propto \underline{1}_{N_{\mathrm{Tx}}}$ and using the notation $\sigma^2_{s,\mathrm{MIMO}}$ instead of σ_s^2, this is the same expression as (4.29) in Section 4.3.2.

CRB for a SIMO Radar and a Moving Target The CRB for a SIMO radar and a moving target can be deduced from the CRB in (5.90) and (5.91) by using only one Tx antenna, i. e. setting

$$\mathbf{D}^{\mathrm{Pulse}} = \left[\underline{d}^{\mathrm{Tx},1}, \ldots, \underline{d}^{\mathrm{Tx},1}\right]^T \in \mathbb{R}^{N_{\mathrm{Pulse}} \times 2}. \tag{5.114}$$

Note that by doing so, we do not include the beamforming gain of a phased array with N_{Tx} Tx antennas, which can be achieved by sending the same waveform phase shifted with all Tx antennas. This is already discussed in Section 4.4.3.2. Due to (5.114), $\mathrm{Cov}^{\mathrm{WS}}(\mathbf{D}^{\mathrm{Pulse}}, \underline{\rho}) = \underline{0}_{2\times 2}$ and $\mathrm{Cov}^{\mathrm{WS}}(\underline{t}, \mathbf{D}^{\mathrm{Pulse}}, \underline{\rho}) = \underline{0}$ in (5.91), i. e. the DOAs always decouple from the Doppler frequency. This is logical since there is no information gain on the DOAs by different Tx positions. Thus the movement of the target has no influence on the CRB of the electrical angles. Due to (5.90) and (5.91), the part of the CRB corresponding to the electrical angles using a planar SIMO radar is given by

$$\mathbf{CRB}^{-1}_{\underline{u},\mathrm{SIMO}} = 2\,L\,\frac{\sigma_s^2}{\sigma^2}\,\mathbf{C}_{\mathrm{SIMO}} \qquad \in \mathbb{R}^{2\times 2}, \tag{5.115}$$

$$\mathbf{C}_{\mathrm{SIMO}} = N_{\mathrm{Rx}}\left(\underline{1}^T\underline{\rho}\right)\mathrm{Cov}^{\mathrm{S}}(\mathbf{D}^{\mathrm{Rx}}) \in \mathbb{R}^{2\times 2}, \tag{5.116}$$

regardless of the movement of the target.

For the special case of a linear Rx array, the CRB for the electrical angle u can be derived from (5.99) to (5.101) analogously. This results in

$$\mathrm{CRB}_{u,\mathrm{SIMO}} = \frac{1}{2\,L}\frac{1}{S}\frac{1}{U_{\mathrm{SIMO}}} \quad \in \mathbb{R}, \tag{5.117}$$

$$S = \frac{\sigma_s^2}{\sigma^2}\,N_{\mathrm{Rx}}\left(\underline{1}^T\underline{\rho}\right) \in \mathbb{R}, \tag{5.118}$$

$$U_{\mathrm{SIMO}} = \mathrm{Var}^{\mathrm{S}}(\underline{d}^{\mathrm{Rx}}) \qquad \in \mathbb{R}. \tag{5.119}$$

This is the same expressions as the CRB for a stationary target computed in Section 4.2.2.1, (4.13) if we use only one pulse with $\rho = 1$ and neglect the beampattern, i. e. $B(u) = 1$. Note that we used the same number of pulses and the same pulse energies $\underline{\rho}$ for the SIMO and MIMO radar. Due to this, the signal strength σ_s^2 is the same for the SIMO and MIMO radar in contrast to Section 4.

Comparison Let us compare the CRBs for the MIMO radar with a moving target, for the MIMO radar with a stationary target and for the SIMO radar given in (5.90), (5.109) and (5.115), respectively. They differ only in the matrix $\mathbf{C}$. For the sake of clarity, we repeat the matrices here without the factor $N_{\mathrm{Rx}}\left(\underline{1}^T\underline{\rho}\right)$

$$\mathbf{C}_{\mathrm{SIMO}} \propto \mathrm{Cov}^{\mathrm{S}}(\mathbf{D}^{\mathrm{Rx}}) \qquad \in \mathbb{R}^{2\times 2}, \tag{5.120}$$

$$\mathbf{C}_{\text{stat}} \propto \left\{\text{Cov}^{\text{S}}(\mathbf{D}^{\text{Rx}}) + \text{Cov}^{\text{WS}}(\mathbf{D}^{\text{Pulse}}, \underline{\rho})\right\} \in \mathbb{R}^{2\times 2}, \tag{5.121}$$

$$\mathbf{C} \propto \left\{\begin{bmatrix} \text{Cov}^{\text{S}}(\mathbf{D}^{\text{Rx}}) & & 0 \\ & & 0 \\ 0 & 0 & 0 \end{bmatrix} + \begin{bmatrix} \text{Cov}^{\text{WS}}(\mathbf{D}^{\text{Pulse}}, \underline{\rho}) & \text{Cov}^{\text{WS}}(\underline{t}, \mathbf{D}^{\text{Pulse}}, \underline{\rho}) \\ \text{Cov}^{\text{WS}}(\mathbf{D}^{\text{Pulse}}, \underline{t}, \underline{\rho}) & \text{Var}^{\text{WS}}(\underline{t}, \underline{\rho}) \end{bmatrix}\right\} \in \mathbb{R}^{3\times 3}. \tag{5.122}$$

Obviously, in the SIMO radar only the different Rx antenna positions $\mathbf{D}^{\text{Rx}}$ are relevant. In the stationary MIMO case, there is an additional gain $\text{Cov}^{\text{WS}}(\mathbf{D}^{\text{Pulse}}, \underline{\rho})$ due to the different Tx positions. The MIMO radar with a moving target has the same gain as well, but also receives an additional coupling term $\text{Cov}^{\text{WS}}(\underline{t}, \mathbf{D}^{\text{Pulse}}, \underline{\rho})$. In general, this term leads to a larger CRB of the electrical angles. The upper 2×2 block of $\mathbf{CRB}_{\underline{u},\omega}$ corresponds to $\underline{u}$. We denote this block by $\mathbf{CRB}_{\underline{u}}$. If the coupling term $\text{Cov}^{\text{WS}}(\underline{t}, \mathbf{D}^{\text{Pulse}}, \underline{\rho})$ vanishes, $\mathbf{CRB}_{\underline{u}}$ is equal to $\mathbf{CRB}_{\underline{u},\text{stat}}$, which is the following lemma. We use the following notation: "$A \implies B$" means "A is sufficient for B".

Lemma 5.2.1. $\text{Cov}^{\text{WS}}(\underline{t}, \mathbf{D}^{Pulse}, \underline{\rho}) = \mathbf{0}_{2\times 2} \implies \mathbf{CRB}_{\underline{u}} = \mathbf{CRB}_{\underline{u},stat}$.

Hence, the MIMO radar with the moving target can have the same DOA CRB as for a stationary target, despite the unknown Doppler frequency. We show in Section 5.2.3 under which conditions the coupling term vanishes and how the vanishing of the coupling can be interpreted.

Comparison: Linear Array We compare the CRBs in the special case of a radar system with a linear array. The CRBs are given in (5.99), (5.111), (5.117) and differ by the term U:

$$U_{\text{SIMO}} = \text{Var}^{\text{S}}(\underline{d}^{\text{Rx}}), \tag{5.123}$$

$$U_{\text{stat}} = \text{Var}^{\text{S}}(\underline{d}^{\text{Rx}}) + \text{Var}^{\text{WS}}(\underline{d}^{\text{Pulse}}, \underline{\rho}), \tag{5.124}$$

$$U = \text{Var}^{\text{S}}(\underline{d}^{\text{Rx}}) + \text{Var}^{\text{WS}}(\underline{d}^{\text{Pulse}}, \underline{\rho}) - U_{\text{penalty}}, \tag{5.125}$$

$$\text{with } U_{\text{penalty}} = \frac{\left(\text{Cov}^{\text{WS}}(\underline{d}^{\text{Pulse}}, \underline{t}, \underline{\rho})\right)^2}{\text{Var}^{\text{WS}}(\underline{t}, \underline{\rho})}. \tag{5.126}$$

In the moving target case, the performance degradation due to the coupling given by U_{penalty} can be seen explicitly, since we could easily invert the CRB. Moreover, the following theorem holds, where ψ^{TDM} is defined in (5.83).

Theorem 1. *For a radar system with a linear array and for a fixed ψ^{TDM}, the following inequalities hold for CRB_u*

$$CRB_{u,SIMO} \geq CRB_u \geq CRB_{u,stat}, \tag{5.127}$$

where $CRB_{u,SIMO}, CRB_u, CRB_{u,stat}$ are given in (5.117),(5.99) *and* (5.111)*, respectively. Moreover,*

$$CRB_u = CRB_{u,stat} \iff \text{Cov}^{\text{WS}}(\underline{d}^{Pulse}, \underline{t}, \underline{\rho}) = 0. \tag{5.128}$$

Here, the notation "$A \iff B$" stands for "A is necessary and sufficient for B". The proof is given in Appendix I.

Theorem 1 states that for a given TDM scheme, the CRB for a moving target is always bounded by the CRB of the corresponding SIMO radar and the CRB of the same MIMO radar with the same TDM scheme, but with a stationary target. Hence we can easily compute the MIMO gain compared to the SIMO radar and the loss in accuracy due to the movement of the target. By using the same MIMO radar hardware (N_{Tx} Tx antennas and N_{Rx} Rx antennas), the choice of the TDM scheme ψ^{TDM} has a significant impact on the DOA accuracy. In the worst case $\mathrm{CRB}_u = \mathrm{CRB}_{u,\mathrm{SIMO}}$, and in the best case $\mathrm{CRB}_u = \mathrm{CRB}_{u,\mathrm{stat}}$. The latter is achieved if the coupling term $\mathrm{Cov}^{\mathrm{WS}}(\underline{d}^{\mathrm{Pulse}}, \underline{t}, \underline{\rho})$ vanishes. This is only one condition on the TDM scheme. ψ^{TDM} has further degrees of freedom, i. e.

- the position of the Tx antennas and the sequence in which they transmit, given in $\underline{d}^{\mathrm{Pulse}}$,
- the transmitting times $\underline{t}$,
- the energy of the transmitted pulses $\underline{\rho}$, and
- the number of transmitted pulses N_{Pulse}.

In order to find TDM schemes which minimize CRB_u (5.99), ψ^{TDM} has to be optimized further. This is studied in detail in Section 5.2.4.

We present 2 examples of the TDM scheme which actually reach the bounds of Theorem 1. We consider an uniform linear array (ULA) of 4 Tx antennas with $N_{\mathrm{Pulse}} = 4$, $\underline{\rho} \propto \underline{1}$ and $\underline{t} \propto [0, 1, 2, 3]^T$.

Example 5.2.1 (Bad TDM Schemes)**.** We set $\underline{d}^{\mathrm{Pulse}} = c_1\,\underline{t} + c_2$ with constants c_1, c_2. In this case, $U_{\mathrm{penalty}} = \mathrm{Var}^{\mathrm{S}}(\underline{d}^{\mathrm{Pulse}})$ and $\mathrm{CRB}_u = \mathrm{CRB}_{u,\mathrm{SIMO}}$. This is the case if the Tx antennas transmit in the order of their geometric arrangement at equally spaced time instants, cf. Fig. 5.9.

Example 5.2.2 (Good TDM Scheme)**.** The lower bound in (5.127) is reached when using the TDM scheme $\underline{d}^{\mathrm{Pulse}} = [d_1^{\mathrm{Tx}}, d_4^{\mathrm{Tx}}, d_4^{\mathrm{Tx}}, d_1^{\mathrm{Tx}}]^T$, since $\mathrm{Cov}^{\mathrm{WS}}(\underline{d}^{\mathrm{Pulse}}, \underline{t}, \underline{\rho}) = 0$ is satisfied. This TDM scheme is also depicted in Fig. 5.9.

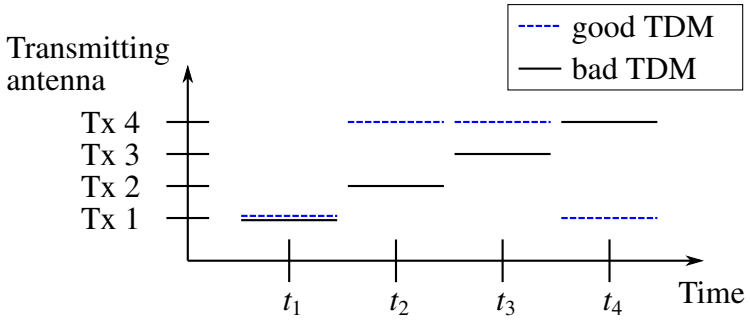

Figure 5.9.: Good and bad TDM scheme for an ULA of 4 Tx antennas and $\underline{t} \propto [0, 1, 2, 3]^T$

Simulations We present numerical simulations to verify and foster the understanding of the theoretical results. We examine a MIMO radar with a linear antenna array of Rx and Tx antennas and consider the maximum likelihood (ML) estimator of the unknown parameter vector $\underline{\Theta}$ in (5.80). We determine the root mean square error (RMSE) of the ML estimate $\hat{u}$ by doing Monte-Carlo simulations. We do this for different TDM schemes. According to (E.23), given the signal $\underline{x}$, the ML estimates $\hat{u}$, $\hat{\omega}$ can be computed by

$$\begin{bmatrix} \hat{u} \\ \hat{\omega} \end{bmatrix} = \arg\max_{u,\omega} |\,\underline{b}(u,\omega)^H \underline{x}\,|^2. \tag{5.129}$$

The MIMO radar under consideration consists of 4 Rx and 4 Tx antennas, uniformly spaced with an antenna distance of $\lambda/2$, i.e. $\underline{d}^{\mathrm{Rx}} = \underline{d}^{\mathrm{Tx}} = \pi \cdot [0,1,2,3]^T$. We choose $L = 1$ cycle with $N_{\mathrm{Pulse}} = 4$ pulses and set the transmitting time instants to $\underline{t} = [0,1,2,3]^T$, where $\underline{t}$ is normalized such that it is dimensionless. Moreover, $\underline{\rho} = \frac{1}{N_{\mathrm{Pulse}}}\underline{1}$, i. e. all pulses are transmitted with the same energy. The target's electrical angle u is set to $u = \sin(10°)$ and, for the non-stationary case, the Doppler frequency ω is chosen to be $\omega = 1.3$.

First we consider a TDM scheme with $\underline{d}^{\mathrm{Pulse}} = \underline{d}^{\mathrm{Tx}}$, i. e. it is has the form of the bad TDM scheme described in Example 5.2.1 and is depicted in Fig. 5.9. The CRB $\mathrm{CRB}_{u,\mathrm{SIMO}}$ of a SIMO radar with the same Rx antennas, using only one Tx antenna with $N_{\mathrm{Pulse}} = 4$, is computed as the upper bound for CRB_u. The CRB $\mathrm{CRB}_{u,\mathrm{stat}}$ of a MIMO radar and a stationary target with the same $\underline{d}^{\mathrm{Pulse}}$ is computed as the lower bound for CRB_u. The simulations are done for a total SNR S from 0 to 35 dB. 3000 Monte-Carlo simulations are carried out for each value of S in order to determine the RMSE of the ML estimator. The ML estimates are computed by doing a 2-dimensional search on a grid, with a resolution of $3.5 \cdot 10^{-4}$ for the electrical angle and $6 \cdot 10^{-4}\,\pi$ for the normalized Doppler frequency, followed by a quadratic interpolation. The simulations show that the modulus of the bias $|b_{\hat{u}}|$ is much smaller than the standard deviation $\sigma_{\hat{u}}$ and thus negligible. Fig. 5.10 shows that the ML estimator of the TDM MIMO radar with the bad TDM scheme achieves only the upper bound $\mathrm{CRB}_{u,\mathrm{SIMO}}$ as expected. Hence, in this case, there is no MIMO gain at all compared to the SIMO radar.

Next we consider a TDM scheme which uses only the two outermost Tx antennas $d_1^{\mathrm{Tx}}, d_4^{\mathrm{Tx}}$ and choose $\underline{d}^{\mathrm{Pulse}} = [d_1^{\mathrm{Tx}}, d_4^{\mathrm{Tx}}, d_4^{\mathrm{Tx}}, d_1^{\mathrm{Tx}}]^T$, i. e. the good TDM scheme of Example 5.2.2. The other parameters of the simulation are the same as in the former simulation. Again, we compute the upper bound $\mathrm{CRB}_{u,\mathrm{SIMO}}$, which is the same as in the former simulation, and the lower bound $\mathrm{CRB}_{u,\mathrm{stat}}$ using the same TDM scheme $\underline{d}^{\mathrm{Pulse}} = [d_1^{\mathrm{Tx}}, d_4^{\mathrm{Tx}}, d_4^{\mathrm{Tx}}, d_1^{\mathrm{Tx}}]^T$. For comparison, we carry out an additional simulation to compute the RMSE of $\hat{u}$ for the MIMO radar with a stationary target. Both simulations show that the bias is negligible compared to the standard deviation. The CRBs and the RMSE of the ML estimators are depicted in Fig. 5.11. It shows that the ML estimator with the good TDM scheme reaches indeed the lower bound $\mathrm{CRB}_{u,\mathrm{stat}}$, as does the ML estimator in the stationary case. The threshold values of S at which the ML estimators reach the CRB is approximately the same for the stationary and non-stationary case. Note that the ML estimator using the bad TDM scheme in

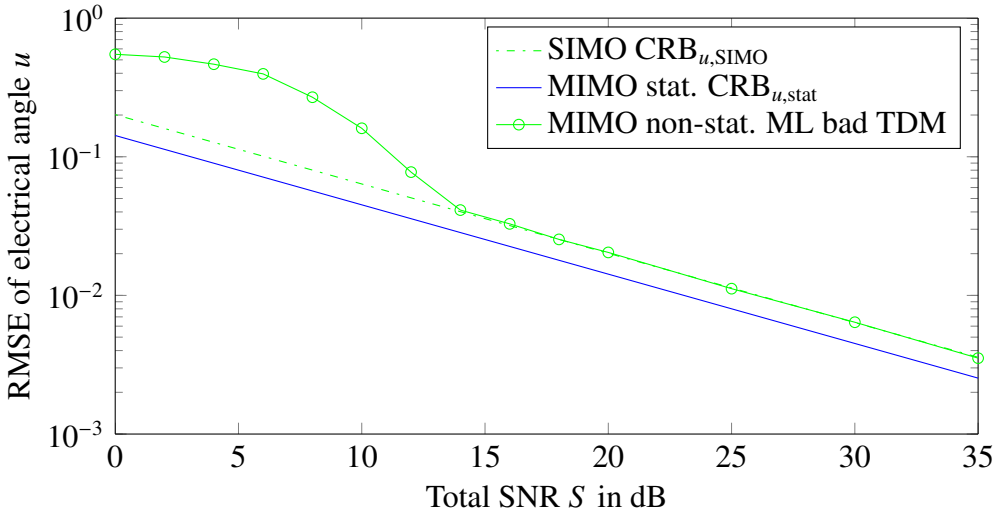

Figure 5.10.: MIMO radar DOA estimation with a bad TDM scheme. The ML estimator achieves only CRB$_{u,\mathrm{SIMO}}$

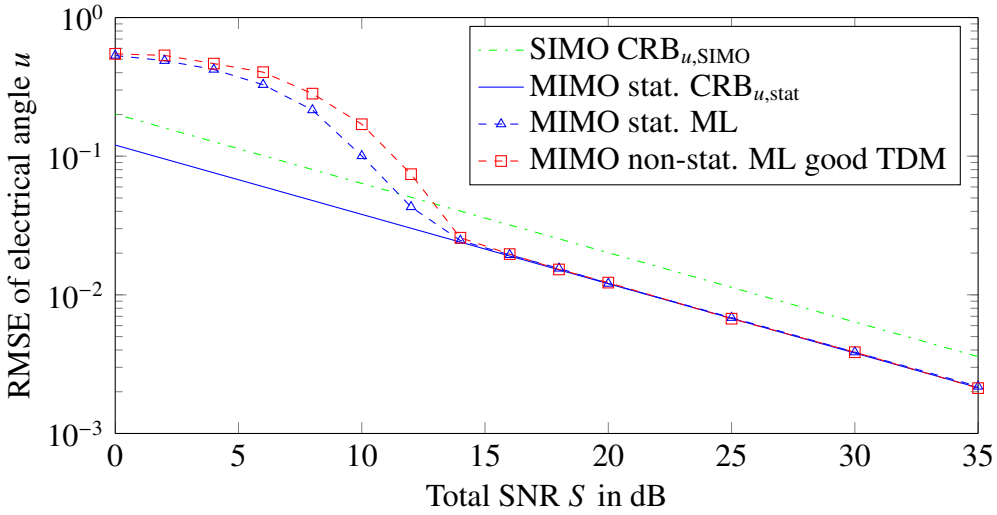

Figure 5.11.: MIMO radar DOA estimation with a good TDM scheme. The ML estimator achieves CRB$_{u,\mathrm{stat}}$

Fig. 5.10 achieves only CRB$_{u,\mathrm{SIMO}}$, which is the same in Fig. 5.10 and 5.11. Hence, with the same hardware platform, we can achieve a gain of 4.47 dB for the same DOA accuracy by just changing the transmission sequence $\underline{d}^{\mathrm{Pulse}}$ of the Tx antennas.

5.2.3. Decoupling of Electrical Angles from the Doppler Frequency

In the last section we have shown that if the coupling term vanishes, i. e. $\mathrm{Cov}^{\mathrm{WS}}(\mathbf{D}^{\mathrm{Pulse}}, \underline{t}, \underline{\rho}) = \underline{0}$, the electrical angles decouple from the Doppler frequency in the CRB. Moreover, the CRB of the electrical angles for the non-stationary and stationary target are equal. In the following, we present a theorem which gives conditions for a TDM scheme such that the coupling term $\mathrm{Cov}^{\mathrm{WS}}(\mathbf{D}^{\mathrm{Pulse}}, \underline{t}, \underline{\rho})$ vanishes. Moreover, we interpret the vanishing of the coupling term to improve the understanding.

We present several examples and some numerical simulations to verify the theoretical findings.

5.2.3.1. Theorem for Decoupling of the Electrical Angles from the Doppler Frequency

We denote by $\underline{t}^{(k)}$ the time instances when the k-th Tx antenna transmits and by $\underline{\rho}^{(k)}$ the corresponding energies of the transmitted pulses, cf. Fig. 5.12 for an example.

Theorem 2.

- *It holds*

$$\begin{aligned} &\mathrm{E}^{\mathrm{WS}}\left(\underline{t}^{(k)}, \underline{\rho}^{(k)}\right) = \mathrm{E}^{\mathrm{WS}}\left(\underline{t}^{(l)}, \underline{\rho}^{(l)}\right) \ \forall\, k, l \in \{1, \ldots, N_{Tx}\} \\ &\Longrightarrow \mathrm{Cov}^{\mathrm{WS}}\left(\mathbf{D}^{Pulse}, \underline{t}, \underline{\rho}\right) = \underline{0}. \end{aligned} \tag{5.130}$$

- *In the case of two transmitting Tx antennas, i. e.*

$$N_{Tx} = 2, \quad \underline{d}^{Tx,1} \neq \underline{d}^{Tx,2}, \quad \underline{1}^T \underline{\rho}^{(1)},\ \underline{1}^T \underline{\rho}^{(2)} > 0,$$

$$\mathrm{E}^{\mathrm{WS}}\left(\underline{t}^{(1)}, \underline{\rho}^{(1)}\right) = \mathrm{E}^{\mathrm{WS}}\left(\underline{t}^{(2)}, \underline{\rho}^{(2)}\right) \quad \Longleftrightarrow \quad \mathrm{Cov}^{\mathrm{WS}}\left(\mathbf{D}^{Pulse}, \underline{t}, \underline{\rho}\right) = \underline{0}. \tag{5.131}$$

Note that for a linear array, $\mathrm{Cov}^{\mathrm{WS}}\left(\mathbf{D}^{\mathrm{Pulse}}, \underline{t}, \underline{\rho}\right) = \underline{0}$ in (5.130) and (5.131) simplifies to $\mathrm{Cov}^{\mathrm{WS}}\left(\underline{d}^{\mathrm{Pulse}}, \underline{t}, \underline{\rho}\right) = 0$ and $\underline{d}^{\mathrm{Tx},1} \neq \underline{d}^{\mathrm{Tx},2}$ becomes $d_1^{\mathrm{Tx}} \neq d_2^{\mathrm{Tx}}$.

Proof. Here we present just the main idea of the proof. For the detailed proof see Appendix J. Let us consider the case of a linear array. $\underline{d}^{\mathrm{Pulse}}$ contains only N_{Tx} different values, the positions of the Tx antennas. It can be shown that $\mathrm{Cov}^{\mathrm{WS}}(\underline{d}^{\mathrm{Pulse}}, \underline{t}, \underline{\rho}) = \mathrm{Cov}^{\mathrm{WS}}(\underline{d}^{\mathrm{Tx}}, \widetilde{\underline{t}}, \widetilde{\underline{\rho}})$, where $\widetilde{\underline{t}}, \widetilde{\underline{\rho}} \in \mathbb{R}^{N_{\mathrm{Tx}}}$ can be computed from $\underline{t}, \underline{\rho}$. Thus, the weighted covariance of N_{Pulse}-dimensional vectors can be reformulated as weighted covariance of N_{Tx}-dimensional vectors. Therefore, the number of different elements in $\underline{d}^{\mathrm{Pulse}}$ is decisive. The elements of $\widetilde{\underline{t}}$ are $\widetilde{t}_k = \mathrm{E}^{\mathrm{WS}}(\underline{t}^{(k)}, \underline{\rho}^{(k)})$. If all elements in $\widetilde{\underline{t}}$ are equal, which is the condition in the theorem, $\widetilde{\underline{t}} \propto \underline{1}$ and therefore $\mathrm{Cov}^{\mathrm{WS}}(\underline{d}^{\mathrm{Tx}}, \widetilde{\underline{t}}, \widetilde{\underline{\rho}}) = \mathrm{Cov}^{\mathrm{WS}}(\underline{d}^{\mathrm{Pulse}}, \underline{t}, \underline{\rho}) = 0$. This is stated in (5.130).

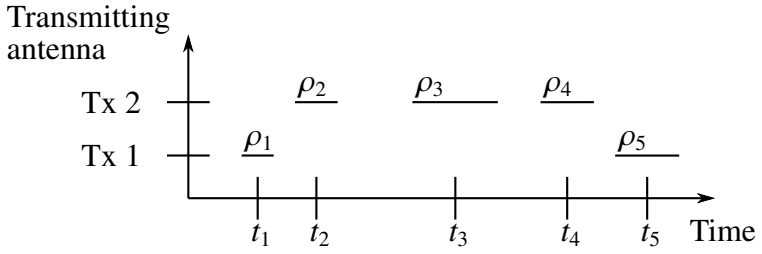

Figure 5.12.: Example of two transmitting antennas with $\underline{t}^{(1)} = [t_1, t_5]^T$, $\underline{\rho}^{(1)} = [\rho_1, \rho_5]^T$ and $\underline{t}^{(2)} = [t_2, t_3, t_4]^T$, $\underline{\rho}^{(2)} = [\rho_2, \rho_3, \rho_4]^T$

5.2.3.2. Discussion

In the following, we discuss some consequences of the theorem. First let us consider the case of equal transmission energy, i. e. $\underline{\rho} \propto \underline{1}$. Thus the weighted sample mean E^{WS} simplifies to simple sample mean E^{S}. From Theorem 2 it follows: If the mean transmission time of every Tx antenna is the same, then the electrical angles decouple from the Doppler frequency in the CRB. This can be roughly interpreted in the following way: The mean transmission time $\mathrm{E}^{\mathrm{S}}(\underline{t}^{(k)})$ is the effective measurement time instance of the data gained from Tx antenna k. Equal mean transmission times means that the effective measurement time instances of all Tx antennas are the same. In average, this results in the same Doppler phase for all Tx antennas. Therefore, the movement of the target does not influence the DOA estimation. This is what Theorem 2 tells us. If $\underline{\rho} \not\propto \underline{1}$, the transmission times of the k-th Tx antenna are weighted by the corresponding weights in $\underline{\rho}$ in order to compute the effective measurement time of the k-th antenna $\mathrm{E}^{\mathrm{WS}}(\underline{t}^{(k)}, \underline{\rho}^{(k)})$.

We illustrate this interpretation by the following examples. Consider a linear antenna array with 2 Rx and 4 Tx antennas. The antenna positions are $\underline{d}^{\mathrm{Rx}} = \Delta^{\mathrm{Rx}} \cdot [0,\ 1]^T$ and $\underline{d}^{\mathrm{Tx}} = \Delta^{\mathrm{Tx}} \cdot [0,\ 1,\ 2,\ 3]^T$, where Δ^{Rx} and Δ^{Tx} denotes the inter antenna spacing, cf. Fig. 5.13. We consider one cycle $L = 1$ and set $N_{\mathrm{Pulse}} = 4$, $\underline{\rho} \propto \underline{1}$ and $\underline{t} = \Delta t \cdot [0,\ 1,\ 2,\ 3]^T$, with Δt being the time difference between two successive pulses. The steering vector $\underline{b}(u, \omega)$ in (5.74) is written as

$$\underline{b}(u, \omega) = \sqrt{\underline{\rho}^{\mathrm{Virt}}} \odot \exp(j\, \underline{\phi}^{\mathrm{Virt}}) \tag{5.132}$$

with the definition of the phase of the virtual array

$$\underline{\phi}^{\mathrm{Virt}} = \underline{d}^{\mathrm{Virt}} u + \underline{t}^{\mathrm{Virt}} \omega. \tag{5.133}$$

We consider different TDM schemes. First we present the bad TDM scheme $\underline{d}^{\mathrm{Pulse}} = [d_1^{\mathrm{Tx}},\ d_2^{\mathrm{Tx}},\ d_3^{\mathrm{Tx}},\ d_4^{\mathrm{Tx}}]^T$ depicted in Fig. 5.9. In Fig. 5.14a and 5.14b, ϕ_i^{Virt} is shown for the different antenna positions of the virtual array for a stationary and a moving target, respectively. For the stationary target, $\omega = 0$, $\underline{\phi}^{\mathrm{Virt}}$ changes proportional to the antenna positions of the virtual array. If $\omega \neq 0$, the movement of the target introduces an additional stepwise increment of $\underline{\phi}^{\mathrm{Virt}}$ for every Tx antenna which transmits. Hence the phase change due to the different Tx antenna positions contains a phase change due to the DOA and due to Doppler effect. In this example, there is no information

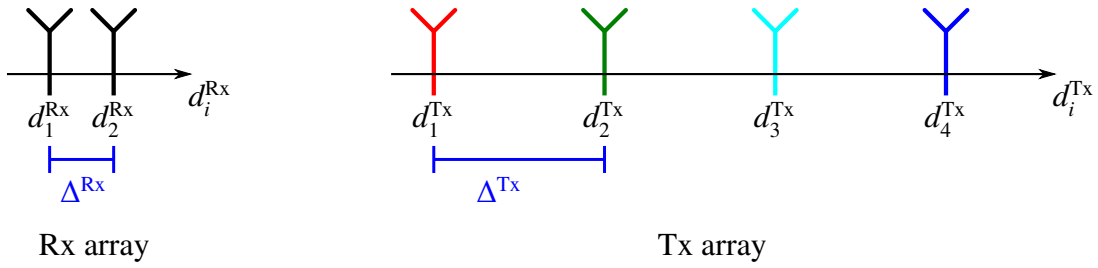

Rx array Tx array

Figure 5.13.: Rx and Tx antenna positions of the considered example

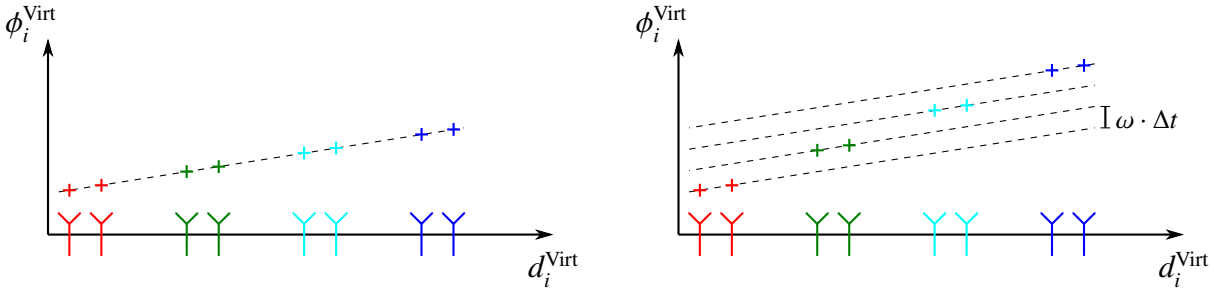

(a) $\omega = 0$ (b) $\omega \neq 0$

Figure 5.14.: Change of the virtual phase ϕ_i^{Virt}, bad TDM

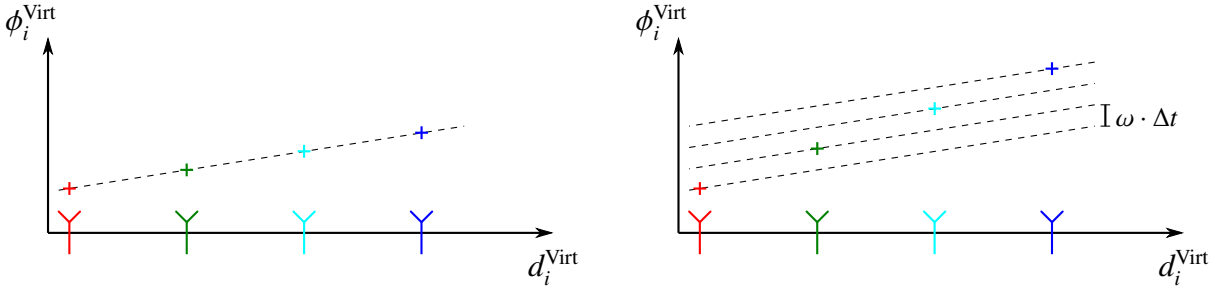

(a) $\omega = 0$ (b) $\omega \neq 0$

Figure 5.15.: Change of the virtual phase ϕ_i^{Virt}, bad TDM, with an Rx array containing only 1 Rx antenna

gain due to the different Tx antennas. This can be understood as follows: Let us assume that the Rx array contains only one Rx antenna. Then, the virtual array is the same as $\underline{d}^{\text{Pulse}}$. For this scenario, the changes of ϕ_i^{Virt} are depicted in Fig. 5.15. For a moving target, it cannot be distinguished if the phase change origins from an electrical angle $u \neq 0$, from the Doppler effect or from a combination of both. Hence the different Tx antennas do not yield additional information on the DOA estimation.

Next consider the good TDM scheme $\underline{d}^{\text{Pulse}} = [d_1^{\text{Tx}}, d_4^{\text{Tx}}, d_4^{\text{Tx}}, d_1^{\text{Tx}}]^T$ which is also shown in Fig. 5.9. The change of ϕ_i^{Virt} is plotted in Fig. 5.16. For $\omega = 0$, the virtual phases are located on a straight line. Some of the virtual antenna positions coincide, but are depicted just next to each other for illustrative purposes. The corresponding virtual phases are depicted in the same manner. For $\omega \neq 0$, there is again an additional Doppler phase change. The average phase change due to the Doppler effect for each Tx antenna is symbolized by the red and blue dot. In this example, the average transmission time for the first and fourth Tx antenna is $\text{E}^{\text{WS}}(\underline{t}^{(k)}, \underline{\rho}^{(k)}) = \text{E}^{\text{S}}(\underline{t}^{(k)}) = 1.5\,\Delta t$, $k = 1, 4$. Hence the average Doppler phase change is the same for both Tx antennas, as depicted in Fig. 5.16b, and equals $\omega \cdot 1.5\,\Delta t$. Then, due to Theorem 2, $\text{Cov}^{\text{WS}}(\underline{d}^{\text{Pulse}}, \underline{t}, \underline{\rho}) = 0$ and therefore, because of Theorem 1, $\text{CRB}_u = \text{CRB}_{u,\text{stat}}$. For comparison, we also plot the change ϕ_i^{Virt} for a SIMO radar in Fig. 5.17. Here, $\underline{d}^{\text{Pulse}} = [d_1^{\text{Tx}}, d_1^{\text{Tx}}, d_1^{\text{Tx}}, d_1^{\text{Tx}}]^T$, i. e. only one Tx antenna transmits.

Theorem 2 gives us an important design criterion for TDM schemes: If the TDM scheme satisfies the conditions in (5.130), then the CRB of the electrical angles for a moving target is as large as for a stationary target, despite the unknown Doppler frequency. Thus the whole virtual aperture of the MIMO radar can be used for the DOA estimation.

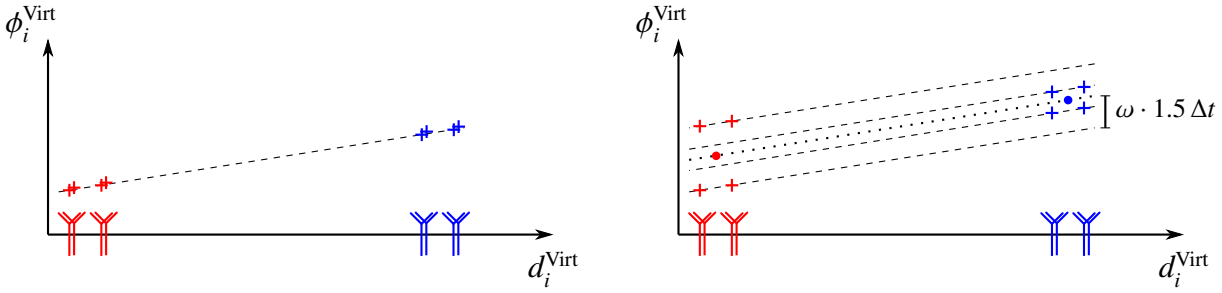

(a) $\omega = 0$ (b) $\omega \neq 0$

Figure 5.16.: Change of the virtual phase ϕ_i^{Virt}, good TDM

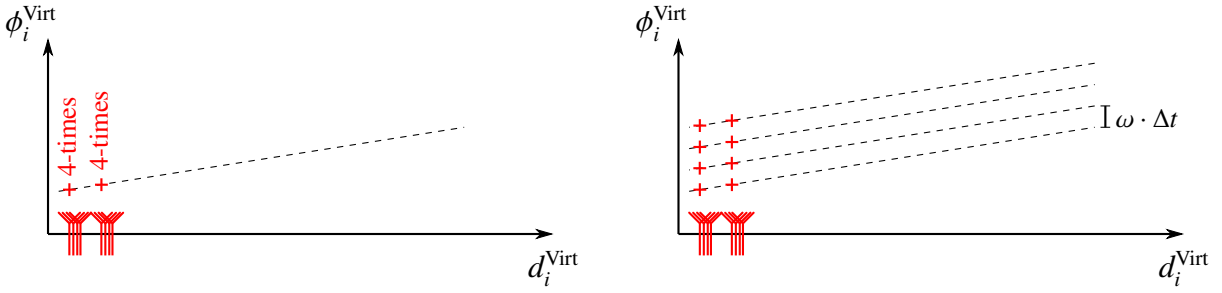

(a) $\omega = 0$ (b) $\omega \neq 0$

Figure 5.17.: Change of the virtual phase ϕ_i^{Virt}, SIMO array

Note that if the electrical angles are decoupled from the Doppler frequency in the CRB, then the DOAs ϑ, φ are decoupled from the Doppler frequency in the corresponding CRB as well. The Jacobian matrix of the transform $\underline{\psi} = \underline{\psi}(\underline{\Theta})$ with $\underline{\psi} = [\vartheta, \varphi, \omega, s(1), \ldots, s(L), \sigma^2]^T$ and $\underline{\Theta}$ given in (5.62) is used to compute the CRB of $\underline{\psi}$ from the CRB of $\underline{\Theta}$. The transform between u_x, u_y and ϑ, φ is given in (5.48). Since the Jacobian matrix is block diagonal, the statement "if u_x, u_y are decoupled from ω in the CRB, then ϑ, φ are decoupled from ω in the CRB as well" is obvious.

To foster the understanding, we present several examples.

Example: Planar Antenna Array. We investigate a radar system with an Rx array $\mathbf{D}^{\text{Rx}} = \pi \begin{bmatrix} 0 & 0 & 1 & 1 \\ 0 & 1 & 0 & 1 \end{bmatrix}^T$ and a Tx array $\mathbf{D}^{\text{Tx}} = \pi \begin{bmatrix} 0 & 0 \\ 0 & 2 \end{bmatrix}^T$ in the unit of $\frac{\lambda}{2\pi}$. The radar transmits at uni-

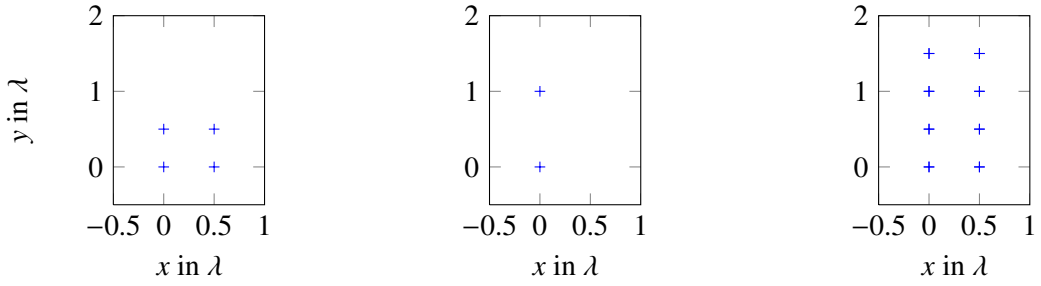

(a) Rx array (b) Tx array (c) Virtual array

Figure 5.18.: Positions of the antenna arrays

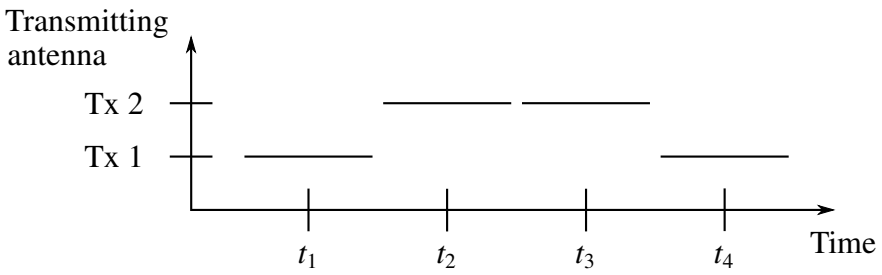

Figure 5.19.: Transmission sequence which satisfies the condition of Theorem 2

formly spaced times instances $\underline{t} \propto [0, \ldots, N_{\text{Pulse}} - 1]^T$ with equal pulse energies $\underline{\rho} \propto \underline{1}$. The antenna positions are depicted in Fig. 5.18. First consider the transmission sequence $\mathbf{D}^{\text{Pulse}} = \left[\underline{d}^{\text{Tx},1}, \underline{d}^{\text{Tx},2}\right]^T$, i. e. both Tx antennas transmit once, one after the other. This TDM sequence does not satisfy the condition of Theorem 2. By computing the CRB, we can show that the CRB of the electrical angles $\mathbf{CRB}_{\underline{u}}$ is the same as that of a SIMO radar with $\mathbf{D}^{\text{Pulse}} = \left[\underline{d}^{\text{Tx},1}, \underline{d}^{\text{Tx},1}\right]^T$, i. e. only one Tx antenna transmits twice. Thus the MIMO radar does not yield any gain despite of the different Tx antennas. The reason is that it cannot be distinguished if the phase difference of the received signals from the two different Tx antennas is due to the movement of the target or due to its DOAs. Now we consider the transmission sequence $\mathbf{D}^{\text{Pulse}} = \left[\underline{d}^{\text{Tx},1}, \underline{d}^{\text{Tx},2}, \underline{d}^{\text{Tx},2}, \underline{d}^{\text{Tx},1}\right]^T$, which is depicted in Fig. 5.19. Due to its symmetry, it satisfies the condition of the theorem and thus achieves the same $\mathbf{CRB}_{\underline{u}}$ as that of a MIMO radar with a stationary target. In other words, the choice of a suitable TDM sequence $\mathbf{D}^{\text{Pulse}}$ satisfying (5.130) can significantly increase the DOA accuracy without changing the Rx and Tx arrays.

Example: Local Decoupling of a Linear Array. We consider a linear Rx and Tx array. The Rx array is a 4 element ULA with half wavelength spacing, i. e. $\underline{d}^{\text{Rx}} = \pi \cdot [0, 1, 2, 3]^T$, and the positions of the Tx antennas are $\underline{d}^{\text{Tx}} = \pi \cdot [0, 3]^T$. We choose $L = 1$ cycle with $N_{\text{Pulse}} = 4$ pulses and set the transmitting time instants to $\underline{t} = [0, 1, 2, 3]^T$. Here $\underline{t}$ is normalized such that it is dimensionless. The trans-

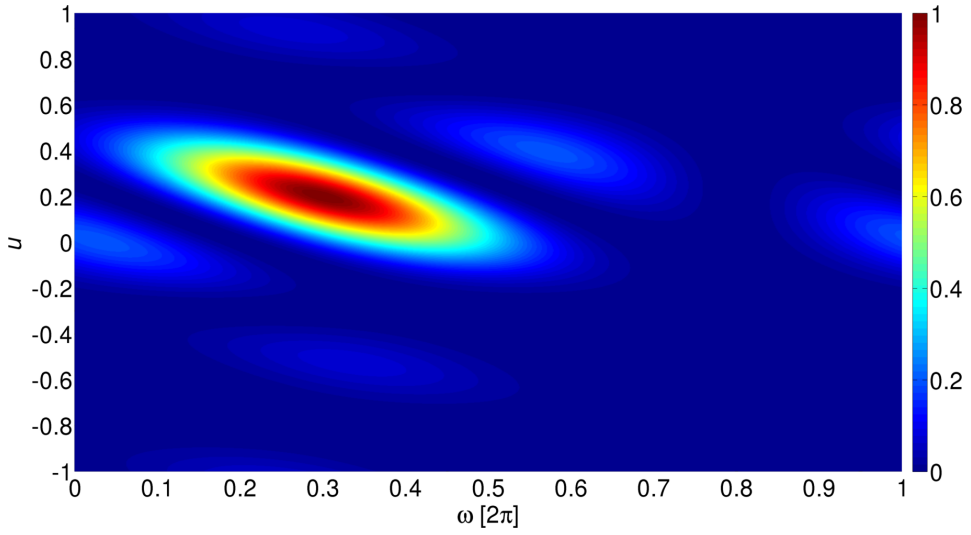

Figure 5.20.: Beampattern for $\underline{d}^{\text{Pulse},a}$. u and ω do not decouple.

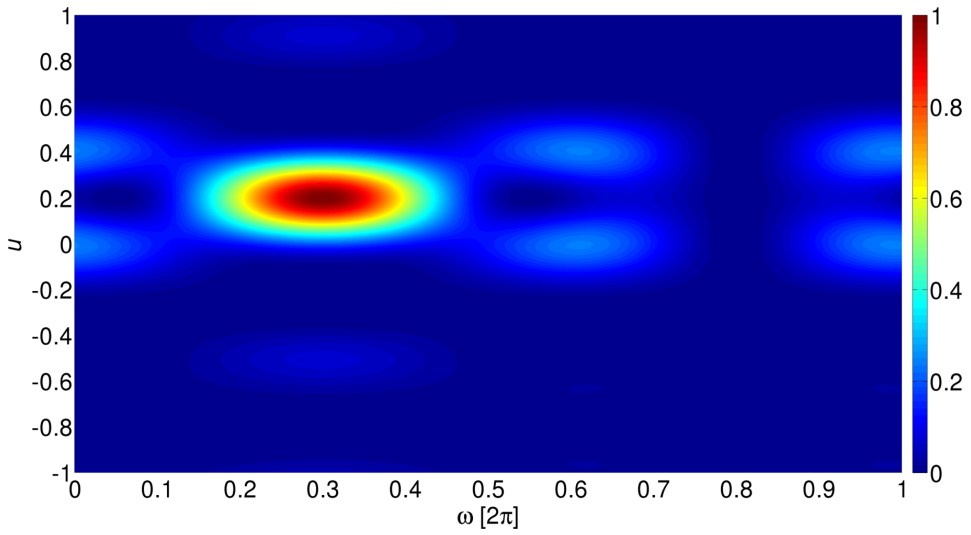

Figure 5.21.: Beampattern for $\underline{d}^{\text{Pulse},b}$. u and ω are decoupled in the vicinity of the global maximum.

mitted pulses have the same energy, $\underline{\rho} = \underline{1}$. The target's parameters are $u_0 = 0.2$ and $\omega_0 = 0.3 \cdot 2\pi$. We compare two TDM schemes $\underline{d}^{\text{Pulse},a} = \left[d_1^{\text{Tx}}, d_1^{\text{Tx}}, d_2^{\text{Tx}}, d_2^{\text{Tx}}\right]^T$ and $\underline{d}^{\text{Pulse},b} = \left[d_1^{\text{Tx}}, d_2^{\text{Tx}}, d_2^{\text{Tx}}, d_1^{\text{Tx}}\right]^T$. We consider the beampattern

$$B(\underline{\Theta}) = \left|\underline{a}^H(\underline{\Theta}_0)\,\underline{a}(\underline{\Theta})\right|^2 \frac{1}{\|\underline{a}(\underline{\Theta})\|^2} \tag{5.134}$$

with the parameter vector

$$\underline{\Theta} = [u, \omega]^T \tag{5.135}$$

and the true parameter vector

$$\underline{\Theta}_0 = [u_0, \omega_0]^T . \tag{5.136}$$

We normalize $B(\underline{\Theta})$ such that the maximum value equals 1. We denote this by $B_{\text{norm}}(\underline{\Theta})$. $B(\underline{\Theta})$ is the expression which is maximized to obtain the ML estimator $\hat{\underline{\Theta}}$ (E.23), if we replace the measured signal $\underline{x}(1)$ by $\underline{a}(\underline{\Theta}_0)\,s(1)$, i. e. we ignore the noise. In Fig. 5.20, B_{norm} is depicted for the TDM scheme $\underline{d}^{\text{Pulse},a}$. Note that this TDM scheme does not satisfy the decoupling condition (5.131). Fig. 5.20 shows that the contour lines of the main peak are ellipses and the main axes of the ellipses are rotated with respect to the coordinate axes, i. e. the electrical angle and the Doppler frequency are coupled. The TDM scheme $\underline{d}^{\text{Pulse},b}$ satisfies the decoupling condition. The normalized beampattern for this case is depicted in Fig. 5.21. Here the main axes of the elliptic contour lines are parallel to the coordinate axes, i. e. u and ω decouple. Since the decoupling condition is based on the CRB, it is only valid locally, i. e. in the vicinity of the main peak. This can also be seen in Fig. 5.21: There is no global decoupling. Hence, for a fixed $\omega \neq \omega_0$ the maximum w. r. t. u can be at a different value $u \neq u_0$. As long as the main peak is concerned, the maximum w. r. t. u is at the same value u_0 independent of ω. This property can be used to minimize the computational cost of estimation algorithms. For

example, only the data gained by one Tx antenna can be used to estimate ω roughly. Then, by an one-dimensional search in u, the main peak can be easily identified. With the knowledge of the local decoupling of u and ω, local optimization algorithms can be used to find the exact maximum.

5.2.3.3. Numerical Simulations

To verify the theoretical results of Theorem 2, we present numerical simulations. We study a planar antenna array with a single moving target in one experiment and a stationary target in a second experiment. For the moving target, the signal model (5.55) has the same structure as the model (E.1) in Appendix E. Therefore, according to (E.23), the deterministic ML estimates of u_x, u_y, ω can be computed by

$$\begin{bmatrix} \hat{u}_x \\ \hat{u}_y \\ \hat{\omega} \end{bmatrix} = \underset{u_x,u_y,\omega}{\arg\max} \sum_{l=1}^{L} |\underline{b}(u_x, u_y, \omega)^H \underline{x}(l)|^2. \tag{5.137}$$

Note that the unknown parameter vector of the ML estimator is $\underline{\Theta}$ in (5.62) and not only u_x, u_y and ω.

In the case of the stationary target, the signal model is given by (5.55) with $\omega = 0$. The ML estimates of u_x, u_y can be computed analogously

$$\begin{bmatrix} \hat{u}_x \\ \hat{u}_y \end{bmatrix} = \underset{u_x,u_y}{\arg\max} \sum_{l=1}^{L} |\underline{b}(u_x, u_y, \omega = 0)^H \underline{x}(l)|^2. \tag{5.138}$$

By doing Monte-Carlo simulations, we estimate the covariance matrix $\mathbf{C}_{\underline{\hat{u}}}$ of $\underline{\hat{u}}$. The error ellipse of $\underline{\hat{u}}$ is defined by $(\underline{\hat{u}} - \underline{u})^T \mathbf{C}_{\underline{\hat{u}}} (\underline{\hat{u}} - \underline{u}) = r^2$, where r is a constant. $\sqrt{\det \mathbf{C}_{\underline{\hat{u}}}}$ is proportional to the area of the error ellipse [McWhorter and Scharf, 1993]. Hence $\sqrt{\det \mathbf{C}_{\underline{\hat{u}}}}$ is a measure of the area of the region in which the target is supposed to be. It contains the variance of $\hat{u}_x$, of $\hat{u}_y$ as well as the correlation of both. Under some regularity conditions, $\mathbf{CRB}_{\underline{u}}$ is a lower bound for $\mathbf{C}_{\underline{\hat{u}}}$ for any unbiased estimator. The simulations show that the modulus of each element in $\underline{b}_{\underline{\hat{u}}} \underline{b}_{\underline{\hat{u}}}^T$ is much smaller then the modulus

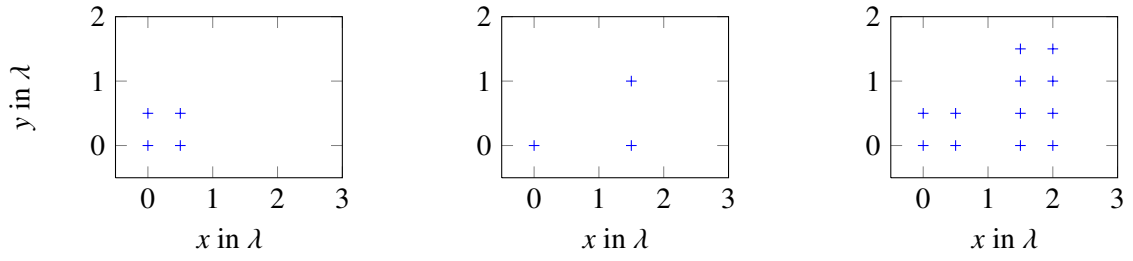

(a) Rx array (b) Tx array (c) Virtual array

Figure 5.22.: Positions of the antenna arrays used in the simulation

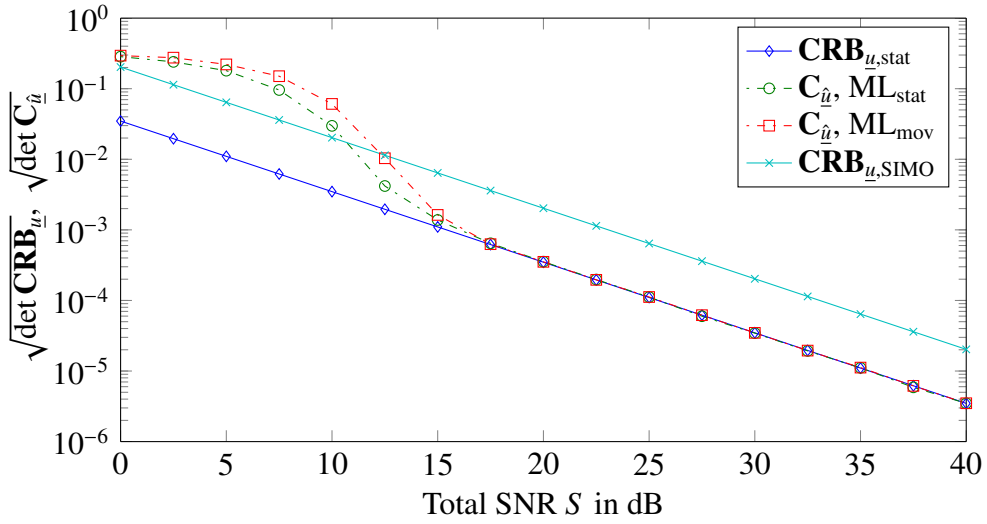

Figure 5.23.: Comparison: Estimation of DOAs of a moving target and stationary target. The TDM scheme satisfies the decoupling condition of Theorem 2.

of the corresponding element in the covariance matrix $\mathbf{C}_{\underline{\hat{u}}}$, where $\underline{b}_{\underline{\hat{u}}}$ is the bias of $\underline{\hat{u}}$. Therefore, $\underline{b}_{\underline{\hat{u}}}$ is negligible. Due to this, we compute $\sqrt{\det \mathbf{CRB}_{\underline{u}}}$ and compare it to $\sqrt{\det \mathbf{C}_{\underline{\hat{u}}}}$. The radar system has the following parameters: The number of measurement cycles is $L = 1$ and all pulses are transmitted with equal energy ($\underline{p} = \underline{1}$) and transmission times $\underline{t} = [0, \ldots, N_{\mathrm{Pulse}} - 1]^T$. $\underline{\rho}$ and $\underline{t}$ are normalized such that they are dimensionless. The Rx and Tx antenna arrays are given by $\mathbf{D}^{\mathrm{Rx}} = \pi \begin{bmatrix} 0 & 0 & 1 & 1 \\ 0 & 1 & 0 & 1 \end{bmatrix}^T$ and $\mathbf{D}^{\mathrm{Tx}} = \pi \begin{bmatrix} 0 & 3 & 3 \\ 0 & 0 & 2 \end{bmatrix}^T$, respectively. The positions of the antenna arrays are depicted in Fig. 5.22. The transmission sequence is $\mathbf{D}^{\mathrm{Pulse}} = \left[\underline{d}^{\mathrm{Tx},1}, \underline{d}^{\mathrm{Tx},2}, \underline{d}^{\mathrm{Tx},3}, \underline{d}^{\mathrm{Tx},3}, \underline{d}^{\mathrm{Tx},2}, \underline{d}^{\mathrm{Tx},1}\right]^T$. Since every Tx antenna transmits two times, all positions in $\mathbf{D}^{\mathrm{Virt}}$ appear twice. Due to the symmetry of the transmission sequence $\mathbf{D}^{\mathrm{Pulse}}$, the condition (5.130) of Theorem 2 is satisfied. Consequently, the CRB of the electrical angles for the moving and stationary target are equal. The target's DOAs are $\vartheta = 10.1°$, $\varphi = 4.3°$ and the normalized angular Doppler frequency is zero for the stationary target and $\omega = 0.4\,\pi$ for the moving target. For convenience, we define the total SNR

$$S = N_{\mathrm{Rx}} \left(\underline{1}^T \underline{\rho}\right) \frac{\sigma_s^2}{\sigma^2}. \tag{5.139}$$

The simulations are run for different values of S, where 3000 trials are done for each value of S. The ML estimates (5.137) and (5.138) are computed by a grid search followed by a local optimization. The grid resolution is $2 \cdot 10^{-2}$ for u_x and u_y, and $2\,\pi \cdot 10^{-2}$ for ω. We use a simplex search method for the local optimization, which is implemented in the programming language Matlab in the function fminsearch. The results are depicted in Fig. 5.23. The ML estimators with the stationary ($\mathrm{ML}_{\mathrm{stat}}$) and moving target ($\mathrm{ML}_{\mathrm{mov}}$) both achieve the CRB beyond the threshold point of approximately 15 dB.

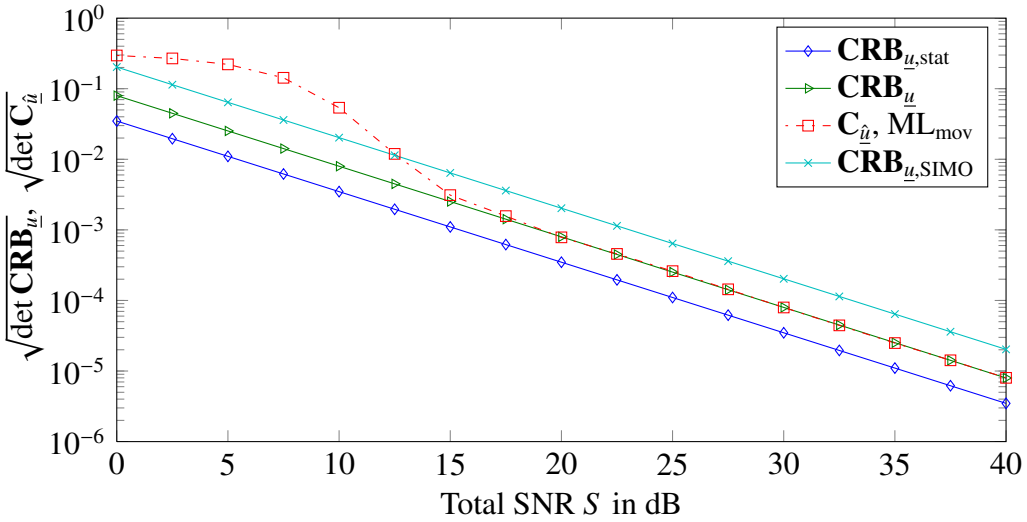

Figure 5.24.: Comparison: Estimation of DOAs of a moving target and stationary target. The TDM scheme does not satisfy the decoupling condition of Theorem 2.

Beyond the threshold point, $\mathrm{ML}_{\mathrm{mov}}$ achieves the same value of $\sqrt{\det \mathbf{C}_{\underline{\hat{u}}}}$ as $\mathrm{ML}_{\mathrm{stat}}$, despite of the unknown Doppler frequency.

Now we do the experiment for a moving target with the same radar system again, but this time we consider the TDM sequence $\mathbf{D}^{\mathrm{Pulse}} = \left[\underline{d}^{\mathrm{Tx},1}, \underline{d}^{\mathrm{Tx},1}, \underline{d}^{\mathrm{Tx},2}, \underline{d}^{\mathrm{Tx},2}, \underline{d}^{\mathrm{Tx},3}, \underline{d}^{\mathrm{Tx},3}\right]^T$. It does not satisfy the condition of Theorem 2. The bias is negligible as in the former simulation. For the stationary target, $\mathbf{CRB}_{\underline{u},\mathrm{stat}}$ and the performance of $\mathrm{ML}_{\mathrm{stat}}$ are the same as with the former sequence $\mathbf{D}^{\mathrm{Pulse}}$, since every Tx antenna transmits twice and the sequence in which they transmit is irrelevant. Fig. 5.24 shows that $\mathrm{ML}_{\mathrm{mov}}$ reaches the CRB at the threshold of approximately 15 dB. But this time $\sqrt{\det \mathbf{CRB}_{\underline{u},\mathrm{stat}}} < \sqrt{\det \mathbf{CRB}_{\underline{u}}} < \sqrt{\det \mathbf{CRB}_{\underline{u},\mathrm{SIMO}}}$, i. e. the radar system with a moving target does not reach the same CRB as with a stationary target.

Thus, using the same radar hardware, i. e. the same Rx and Tx antennas, the DOA accuracy can be significantly increased by choosing an appropriate TDM scheme.

5.2.4. Optimal TDM Schemes for Linear Arrays

We are interested in TDM schemes which minimize CRB_u in (5.99) for a linear antenna array. In the following, we call these schemes optimal TDM schemes. A TDM scheme is characterized by the parameters $\psi^{\mathrm{TDM}} = \left\{\underline{d}^{\mathrm{Pulse}}, \underline{t}, \underline{\rho}, N_{\mathrm{Pulse}}\right\}$ in (5.83). Theorem 2 states a sufficient condition under which $\mathrm{Cov}^{\mathrm{WS}}(\underline{d}^{\mathrm{Pulse}}, \underline{t}, \underline{\rho}) = 0$ and therefore, due to Theorem 1, $\mathrm{CRB}_u = \mathrm{CRB}_{u,\mathrm{stat}}$. ψ^{TDM} contains further degrees of freedom which can be optimized to minimize CRB_u.

Typically, applications introduce constraints on some of the parameters ψ^{TDM}. Important variables, which can be used to express constraints are

- the transmission energy of the pulses $\underline{\rho}$,

- the position of the Tx antennas in $\underline{d}^{\text{Pulse}}$,
- the transmission power of the pulses $\underline{p}$,
- the duration of the pulses $\underline{\Delta t}$,
- the minimal time gap between two successive pulses Δ_{gap}, and
- the overall transmission time of one cycle T_{cycle}.

Dependent on the application these parameters can be already fixed, constrained to a certain region, or they can be freely chosen. An example of a constrain is a limited transmission power or a limited geometrical size of the antenna array. As another example, a constraint on the transmission times $\underline{t}$ follows from a given $\underline{\Delta t}$ and a given minimal Δ_{gap}.

In general, different constraints result in different minimal values of CRB_u. In the next sections, we investigate optimal TDM schemes for two different cases. These sections are based on [Rambach et al., 2014] and on the master thesis [Vogel, 2013] which I supervised.[3]

5.2.4.1. Optimal TDM Schemes Under Limited Transmission Energy and Aperture Size

We determine the minimum value of CRB_u with respect to ψ^{TDM} (5.83) and derive conditions on ψ^{TDM} under which this minimum is reached. We consider TDM schemes which satisfy the energy constraint

$$\underline{1}^T \underline{\rho} \leq \rho^{\max}, \tag{5.140}$$

i. e. the transmitted energy per cycle is limited by $\rho^{\max}$. Note that CRB_u in (5.99) is scaled by $1/\left(\underline{1}^T \underline{\rho}\right)$. Obviously, (5.140) is a physically meaningful constraint. Moreover, the Tx antennas have to be placed within the real aperture range $\left[d_{\min}^{\text{Tx}}, d_{\max}^{\text{Tx}}\right]$, i. e.

$$d_{\min}^{\text{Tx}} \leq d_i^{\text{Pulse}} \leq d_{\max}^{\text{Tx}}, \quad i = 1, \ldots, N_{\text{Pulse}}. \tag{5.141}$$

Theorem 3.

1. *CRB_u is minimal w. r. t. ψ^{TDM} if and only if*
   a) *only the 2 outermost Tx antennas with $d_1^{Tx} = d_{min}^{Tx}$ and $d_2^{Tx} = d_{max}^{Tx}$ are used,*
   b) $\underline{1}^T \underline{\rho}^{(1)} = \underline{1}^T \underline{\rho}^{(2)}$,
   c) $\underline{1}^T \underline{\rho} = \rho^{max}$,
   d) $\text{E}^{\text{WS}}(\underline{t}^{(1)}, \underline{\rho}^{(1)}) = \text{E}^{\text{WS}}(\underline{t}^{(2)}, \underline{\rho}^{(2)})$,

[3] These sections contain quotations of our own published work [Rambach et al., 2014] which are not marked additionally.

where $\underline{t}^{(1)}$ and $\underline{t}^{(2)}$ are the time instances when the 1. and 2. Tx antenna transmit and $\underline{\rho}^{(1)}$ and $\underline{\rho}^{(2)}$ are the energies of their transmitted pulses, respectively.

2. *The minimal value of CRB_u w. r. t. ψ^{TDM} is given by*

$$CRB_{u,min} = \frac{1}{2L}\frac{1}{S_{max}}\frac{1}{U_{max}}, \tag{5.142}$$

$$S_{max} = \frac{\sigma_s^2}{\sigma^2} N_{Rx} \rho^{max}, \tag{5.143}$$

$$U_{max} = \mathrm{Var}^{\mathrm{S}}(\underline{d}^{Rx}) + \frac{1}{4}\left(d_{max}^{Tx} - d_{min}^{Tx}\right)^2. \tag{5.144}$$

Proof. 1. To minimize CRB_u in (5.99), S in (5.100) and U in (5.101) have to be maximized. S is maximal iff $\underline{1}^T\underline{\rho} = \rho^{\max}$, since the other variables are fixed. This is condition 1c. U is independent of a scaling of $\underline{\rho}$. To maximize U, we have to maximize

$$\Omega = \mathrm{Var}^{\mathrm{WS}}(\underline{d}^{\mathrm{Pulse}}, \underline{\rho}) - \frac{\left(\mathrm{Cov}^{\mathrm{WS}}(\underline{d}^{\mathrm{Pulse}}, \underline{t}, \underline{\rho})\right)^2}{\mathrm{Var}^{\mathrm{WS}}(\underline{t}, \underline{\rho})} \tag{5.145}$$

since $\underline{d}^{\mathrm{Rx}}$ is given. $\mathrm{Var}^{\mathrm{WS}}(\underline{d}^{\mathrm{Pulse}}, \underline{\rho})$ is maximal iff only the two outermost Tx antennas are used and $\underline{1}^T\underline{\rho}^{(1)} = \underline{1}^T\underline{\rho}^{(2)}$. This is proven in Appendix K. Using only two Tx antennas, due to Theorem 2 (5.131), $\mathrm{Cov}^{\mathrm{WS}}(\underline{d}^{\mathrm{Pulse}}, \underline{t}, \underline{\rho}) = 0$ iff $\mathrm{E}^{\mathrm{WS}}(\underline{t}^{(1)}, \underline{\rho}^{(1)}) = \mathrm{E}^{\mathrm{WS}}(\underline{t}^{(2)}, \underline{\rho}^{(2)})$. The two conditions $\underline{1}^T\underline{\rho}^{(1)} = \underline{1}^T\underline{\rho}^{(2)}$ and $\mathrm{E}^{\mathrm{WS}}(\underline{t}^{(1)}, \underline{\rho}^{(1)}) = \mathrm{E}^{\mathrm{WS}}(\underline{t}^{(2)}, \underline{\rho}^{(2)})$ do not contradict. An example which fulfills both conditions is presented below. Thus, $\max_{\underline{d}^{\mathrm{Pulse}}, \underline{\rho}} \mathrm{Var}^{\mathrm{WS}}(\underline{d}^{\mathrm{Pulse}}, \underline{\rho})$ is independent whether $\mathrm{Cov}^{\mathrm{WS}}(\underline{d}^{\mathrm{Pulse}}, \underline{t}, \underline{\rho}) = 0$ is fulfilled or not. Hence, $\mathrm{Var}^{\mathrm{WS}}(\underline{d}^{\mathrm{Pulse}}, \underline{\rho})$ can be maximized and $\mathrm{Cov}^{\mathrm{WS}}(\underline{d}^{\mathrm{Pulse}}, \underline{t}, \underline{\rho}) = 0$ at the same time. Consequently, Ω is maximal iff $\mathrm{Var}^{\mathrm{WS}}(\underline{d}^{\mathrm{Pulse}}, \underline{\rho})$ is maximal and at the same time $\mathrm{Cov}^{\mathrm{WS}}(\underline{d}^{\mathrm{Pulse}}, \underline{t}, \underline{\rho}) = 0$. Therefore, Ω is maximal iff conditions 1a, 1b and 1d are fulfilled.

2. The minimal value of CRB_u can be determined by choosing ψ^{TDM} such that the conditions of the 1. part of the Theorem are fulfilled.

□

The conditions of the theorem can be interpreted in the following way: Using the two outermost Tx antennas makes the virtual aperture as large as possible. $\underline{1}^T\underline{\rho}^{(1)} = \underline{1}^T\underline{\rho}^{(2)}$ means that the same amount of energy is transmitted from each Tx antenna. Roughly spoken, this yields the same amount of spatial information for both Tx antennas. $\underline{1}^T\underline{\rho} = \rho^{\max}$ states to transmit as much energy as possible, which obviously leads to the highest possible SNR. The condition $\mathrm{E}^{\mathrm{WS}}(\underline{t}^{(1)}, \underline{\rho}^{(1)}) = \mathrm{E}^{\mathrm{WS}}(\underline{t}^{(2)}, \underline{\rho}^{(2)})$ has already been interpreted in the context of Theorem 2. Due to this condition and with the help of Theorem 2 it follows that the minimal value of CRB_u w. r. t. ψ^{TDM} is as large as $\mathrm{CRB}_{u,\mathrm{stat}}$, the CRB of the electrical angle of a stationary target using the same radar and TDM scheme. Thus the achievable

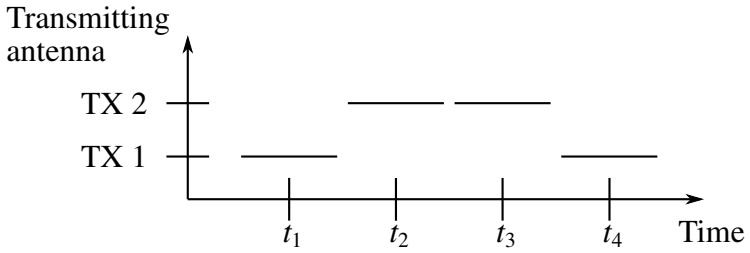

(a) TDM scheme with $\underline{d}^{\text{Pulse}} = [d^{\text{Tx}}_{\text{min}}, d^{\text{Tx}}_{\text{max}}, d^{\text{Tx}}_{\text{max}}, d^{\text{Tx}}_{\text{min}}]^T$, $\underline{t} \propto [0,1,2,3]^T$ and $\underline{\rho} \propto \underline{1}$

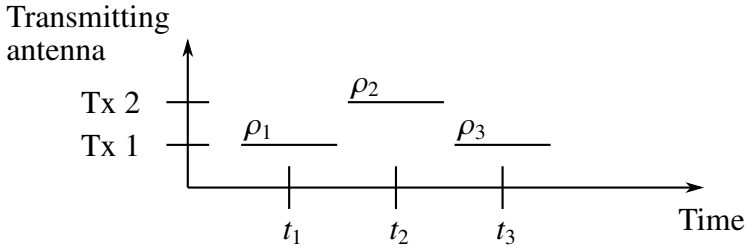

(b) TDM scheme with $\underline{d}^{\text{Pulse}} = [d^{\text{Tx}}_{\text{min}}, d^{\text{Tx}}_{\text{max}}, d^{\text{Tx}}_{\text{min}}]^T$, $\underline{t} \propto [0,1,2]^T$ and $\underline{\rho} \propto [1,2,1]^T$

Figure 5.25.: Examples of TDM schemes satisfying the conditions of Theorem 3

DOA accuracy is as large as if the target is not moving relative to the radar and the complete virtual aperture of the MIMO radar can be used as indicated in (5.144).

Theorem 3 helps us to find TDM schemes which achieve the smallest possible CRB_u. If we optimize ψ^{TDM}, this theorem tells us which conditions have to be fulfilled in order to yield an optimal TDM scheme.

We give two examples of optimal TDM schemes.

Example 5.2.3. The TDM scheme uses $N_{\text{Pulse}} = 4$ pulses and the same energy per pulse, $\underline{\rho} = \frac{\rho^{\max}}{4}\,\underline{1}$. Moreover, $\underline{d}^{\text{Pulse}} = [d^{\text{Tx}}_{\text{min}}, d^{\text{Tx}}_{\text{max}}, d^{\text{Tx}}_{\text{max}}, d^{\text{Tx}}_{\text{min}}]^T$, $\underline{t} \propto [0,1,2,3]^T$. The transmission sequence is depicted in Fig. 5.25a. Since the energy per pulse is constant, we can easily see that 1d is satisfied due to the symmetry in Fig. 5.25a.

Example 5.2.4. The radar transmits $N_{\text{Pulse}} = 3$ pulses with different pulse energies, $\underline{\rho} = \frac{\rho^{\max}}{4}\,[1,2,1]^T$, $\underline{d}^{\text{Pulse}} = [d^{\text{Tx}}_{\text{min}}, d^{\text{Tx}}_{\text{max}}, d^{\text{Tx}}_{\text{min}}]^T$ and $\underline{t} \propto [0,1,2]^T$. This is depicted in Fig. 5.25b.

5.2.4.2. Optimal TDM Schemes with Constant Transmission Energy and Equidistant Transmission Times

Theorem 3 states conditions for optimal TDM schemes under the two physically meaningful constraints of limited transmission energy (5.140) and limited geometrical size (5.141). Typical applications introduce additional constraints on the TDM scheme. In general, the additional constraints result in other optimal TDM schemes. In the following, we search for optimal TDM schemes under the constraints (5.140), (5.141) and additional practical constraints: We consider TDM schemes

which contain pulses transmitted at equidistant time instances with the same transmission energy per pulse, i. e. $\underline{\rho} \propto \underline{1}$. This is e. g. the case in automobile radar systems which transmit a sequence of identical chirps with the maximum available power $p^{\max}$. We consider two cases: a) the number of pulses N_{Pulse} in the TDM scheme is given and b) can be chosen freely.

For a given number of pulses N_{Pulse}, we derive the conditions a TDM scheme has to fulfill in order to minimize CRB_u. Dependent on N_{Pulse} the TDM schemes achieve different values of CRB_u. We show for which values of N_{Pulse} the smallest CRB_u is achieved, which is case b).

First we investigate case a). W. l. o. g. we set $d_{\min}^{\text{Tx}} = -1$ and $d_{\max}^{\text{Tx}} = +1$ and

$$\underline{t} = [1, \ldots, N_{\text{Pulse}}]^T - \text{E}^{\text{S}}\left([1, \ldots, N_{\text{Pulse}}]^T\right) \underline{1}, \tag{5.146}$$

i. e. $\text{E}^{\text{S}}(\underline{t}) = 0$. Here, $\underline{t}$ is normalized such that it is dimensionless. Analog to the proof of Theorem 3, to minimize CRB_u in (5.99), S in (5.100) and U in (5.101) have to be maximized. S is maximal iff $\underline{1}^T \underline{\rho} = \rho^{\max}$. Thus

$$\underline{\rho} = \frac{\rho^{\max}}{N_{\text{Pulse}}} \underline{1}. \tag{5.147}$$

To maximize U, we have to maximize Ω in (5.145). Since $\underline{\rho} \propto \underline{1}$, the functions E^{WS}, Var^{WS} and Cov^{WS} simplify to E^{S}, Var^{S} and Cov^{S}, respectively. Thus we have to maximize

$$\Omega(\underline{d}^{\text{Pulse}}) = \text{Var}^{\text{S}}(\underline{d}^{\text{Pulse}}) - \frac{\left(\text{Cov}^{\text{S}}(\underline{d}^{\text{Pulse}}, \underline{t})\right)^2}{\text{Var}^{\text{S}}(\underline{t})}. \tag{5.148}$$

The optimal solutions of $\underline{d}^{\text{Pulse}}$ are given by

$$\underline{d}^{\text{Pulse,opt}} = \arg\max_{\underline{d}^{\text{Pulse}}} \Omega(\underline{d}^{\text{Pulse}}). \tag{5.149}$$

Note that this optimization problem contains continuous variables (antenna positions in $\underline{d}^{\text{Pulse}}$) and discrete variables (N_{Pulse}).

Analog to Theorem 3 an optimum is achieved by using only the two outermost antennas [Vogel, 2013], i. e. $d_i^{\text{Pulse}} \in \left\{d_{\min}^{\text{Tx}}, d_{\max}^{\text{Tx}}\right\} \; \forall \, i$. This simplifies the optimization problem significantly, since the number and positions of the Tx antennas are already fixed. In contrast to Theorem 3, in general, for a fixed N_{Pulse}, we cannot maximize $\text{Var}^{\text{S}}(\underline{d}^{\text{Pulse}})$ and achieve $\text{Cov}^{\text{S}}(\underline{d}^{\text{Pulse}}, \underline{t}) = 0$ at the same time. For different N_{Pulse}, the maximal value of Ω and the criteria for an optimal TDM scheme differ. Therefore, we have to consider different cases of N_{Pulse}. This leads to the following Theorem. In the following, we use the short notation $N_{\text{Pulse}} \in 4\mathbb{N}$ instead of $N_{\text{Pulse}} \in 4n, n \in \mathbb{N}$. For the other cases, we use an analog notation. Moreover, we call a TDM scheme balanced, if only 2 Tx antennas are used and both antennas transmit equally often.

Theorem 4. *Under the constraints of limited transmission energy* (5.140)*, limited geometrical size* (5.141)*, same transmission energy per pulse,* $\underline{\rho} \propto \underline{1}$*, and equidistant transmission times, an optimal TDM scheme has to satisfy the conditions*

a) only the 2 outermost Tx antennas with $d_1^{Tx} = d_{min}^{Tx}$ *and* $d_2^{Tx} = d_{max}^{Tx}$ *are used,*

b) $\underline{\rho} = \frac{\rho^{max}}{N_{Pulse}} \underline{1}$.

Moreover, dependent on N_{Pulse}*, the following holds:*
$\underline{N_{Pulse} \in 4\mathbb{N}}$ *An optimal TDM scheme has to be balanced and fulfill* $\mathrm{Cov}^{\mathrm{S}}(\underline{d}^{Pulse}, \underline{t}) = 0$ *which is equivalent to* $\mathrm{E}^{\mathrm{S}}(\underline{t}^{(1)}) = \mathrm{E}^{\mathrm{S}}(\underline{t}^{(2)})$*. The optimal value for* Ω *is*

$$\Omega(\underline{d}^{Pulse,opt})\Big|_{N_{Pulse}\in 4\mathbb{N}} = 1. \tag{5.150}$$

$\underline{N_{Pulse} \in 4\mathbb{N} - 2}$ *An optimal TDM scheme has to be balanced and fulfill* $\mathrm{Cov}^{\mathrm{S}}(\underline{d}^{Pulse}, \underline{t}) = \pm\frac{1}{N_{Pulse}}$*. The maximum* Ω *for the minimal* CRB_u *is*

$$\Omega(\underline{d}^{Pulse,opt})\Big|_{N_{Pulse}\in(4\mathbb{N}-2)} = 1 - \frac{1}{N_{Pulse}^2} \cdot \frac{12}{N_{Pulse}^2 - 1}. \tag{5.151}$$

$\underline{N_{Pulse} \in 2\mathbb{N} + 1}$ *In an optimal TDM scheme, one Tx antenna has to transmit one pulse more than the other Tx antenna and the TDM scheme has to fulfill* $\mathrm{E}^{\mathrm{S}}(\underline{t}^{(1)}) = \mathrm{E}^{\mathrm{S}}(\underline{t}^{(2)})$*. The maximum* Ω *for the minimal* CRB_u *is*

$$\Omega(\underline{d}^{Pulse,opt})\Big|_{N_{Pulse}\in(2\mathbb{N}+1)} = 1 - \frac{1}{N_{Pulse}^2}. \tag{5.152}$$

Proof. In the following we present the reason for the case differentiation. The proof of the conditions on the TDM scheme for each case is shown in Appendix L. To maximize Ω, we have to maximize $\mathrm{Var}^{\mathrm{S}}(\underline{d}^{\mathrm{Pulse}})$ and to minimize $|\mathrm{Cov}^{\mathrm{S}}(\underline{d}^{\mathrm{Pulse}}, \underline{t})|$ at the same time. First we consider $\mathrm{Var}^{\mathrm{S}}(\underline{d}^{\mathrm{Pulse}})$. For even N_{Pulse}, both Tx antennas can be used equally often such that $\mathrm{Var}^{\mathrm{S}}(\underline{d}^{\mathrm{Pulse}})$ is maximal, $\mathrm{Var}^{\mathrm{S}}(\underline{d}^{\mathrm{Pulse}}) = 1$. For odd N_{Pulse}, one antenna is used more often than the other and a sample variance of 1 cannot be achieved. Hence optimal TDM schemes have to be determined for even and odd N_{Pulse} separately. A further case differentiation is required to minimize $\mathrm{Cov}^{\mathrm{S}}(\underline{d}^{\mathrm{Pulse}}, \underline{t})$. For odd N_{Pulse}, it can be shown that $\min|\mathrm{Cov}^{\mathrm{S}}(\underline{d}^{\mathrm{Pulse}}, \underline{t})| = 0$. For even N_{Pulse} with $N_{\mathrm{Pulse}} \in 4\mathbb{N}$, the minimum value is also $\min|\mathrm{Cov}^{\mathrm{S}}(\underline{d}^{\mathrm{Pulse}}, \underline{t})| = 0$. If N_{Pulse} is even with $N_{\mathrm{Pulse}} \in 4\mathbb{N} - 2$, then $\min|\mathrm{Cov}^{\mathrm{S}}(\underline{d}^{\mathrm{Pulse}}, \underline{t})| = 0.5$. Thus we have to make a second case differentiation for even N_{Pulse}. Therefore, we have to consider the cases $N_{\mathrm{Pulse}} \in 4\mathbb{N}$, $N_{\mathrm{Pulse}} \in 4\mathbb{N} - 2$ and $N_{\mathrm{Pulse}} \in 2\mathbb{N} + 1$. See [Vogel, 2013] for more details.

For a given number of pulses N_{Pulse}, Theorem 4 states the conditions a TDM has to satisfy in order to minimize CRB_u. Moreover, the maximum value of Ω and therefore the minimal value of CRB_u is specified. An overview of the optimal TDM schemes is shown in Tab. 5.2. It shows that the largest value of Ω is achieved for $N_{\mathrm{Pulse}} \in 4\mathbb{N}$. Note that the difference between Ω using $N_{\mathrm{Pulse}} \in 4\mathbb{N}$ pulses and using $N_{\mathrm{Pulse}} \notin 4\mathbb{N}$ pulses vanishes at least with $1/N_{\mathrm{Pulse}}^2$. Thus, the larger

Table 5.2.: Overview of the optimal TDM schemes

	$N_{\text{Pulse}} \in 4\mathbb{N}$	$N_{\text{Pulse}} \in (4\mathbb{N}-2)$	$N_{\text{Pulse}} \in (2\mathbb{N}+1)$
balanced $\text{Var}^{\text{S}}(\underline{d}^{\text{Pulse}})$	✓ 1	✓ 1	↯ $1-\frac{1}{N_{\text{Pulse}}^2}$
decoupling of u and ω $\frac{\left(\text{Cov}^{\text{WS}}(\underline{d}^{\text{Pulse,opt}},\underline{t})\right)^2}{\text{Var}^{\text{S}}(\underline{t})}$	✓ 0	↯ $\frac{1}{N_{\text{Pulse}}^2}\cdot\frac{12}{N_{\text{Pulse}}^2-1}$	✓ 0
$\Omega(\underline{d}^{\text{Pulse,opt}})$	1	$1-\frac{1}{N_{\text{Pulse}}^2}\cdot\frac{12}{N_{\text{Pulse}}^2-1}$	$1-\frac{1}{N_{\text{Pulse}}^2}$

N_{Pulse}, the smaller the difference. As an example, $N_{\text{Pulse}} = 6$ yields $\Omega(\underline{d}^{\text{Pulse,opt}}) \approx 0.99$ and $N_{\text{Pulse}} = 7$ yields $\Omega(\underline{d}^{\text{Pulse,opt}}) \approx 0.98$. Hence $\Omega(\underline{d}^{\text{Pulse,opt}})$ differs only by a few percent for different N_{Pulse}.

From the above findings follows: If N_{Pulse} can be chosen freely, which we denoted by case b), then an optimal TDM scheme has to use $N_{\text{Pulse}} \in 4\mathbb{N}$ pulses, be balanced and satisfy $\text{E}^{\text{S}}(\underline{t}^{(1)}) = \text{E}^{\text{S}}(\underline{t}^{(2)})$, since due to Theorem 4, it achieves the smallest CRB_u.

Thus for given or freely selectable N_{Pulse}, we have derived the conditions optimal TDM schemes have to fulfill. We present several examples of optimal TDM schemes for the different cases.

Example 5.2.5. $\underline{N_{\text{Pulse}} \in 4\mathbb{N}}$. Such optimal TDM schemes can be constructed by building schemes which are balanced and symmetric to the center index, i.e. $d_i^{\text{Pulse}} = d_{N_{\text{Pulse}}+1-i}^{\text{Pulse}}$. The symmetry ensures that $\text{E}^{\text{S}}(\underline{t}^{(1)}) = \text{E}^{\text{S}}(\underline{t}^{(2)})$. An example is $\underline{d}_1^{\text{Pulse,opt}} = [1,1,-1,-1,-1,-1,1,1]^T$. $\underline{d}_2^{\text{Pulse,opt}} = [1,-1,-1,1,-1,1,1,-1]^T$ is also optimal, but not of this structure. Both schemes are depicted in Fig. 5.26.

Example 5.2.6. $\underline{N_{\text{Pulse}} \in 4\mathbb{N}-2}$. Such optimal TDM schemes can be constructed by building schemes which are balanced and symmetric to the center index, except for the elements which are closest to the center of the sequence. An example of such an optimal TDM scheme is $\underline{d}_1^{\text{Pulse,opt}} = [-1,1,1,-1,1,-1]^T$. $\underline{d}_2^{\text{Pulse,opt}} = [-1,1,1,-1,-1,1]^T$ is also optimal, but of a different structure. These schemes are depicted in Fig. 5.27.

Example 5.2.7. $\underline{N_{\text{Pulse}} \in 2\mathbb{N}+1}$. Such optimal TDM schemes can be constructed by building schemes where one antenna transmits one pulse more than the other and which are symmetric to the center index. An example is $\underline{d}_1^{\text{Pulse,opt}} = [-1,-1,1,1,1,-1,-1]^T$. $\underline{d}_2^{\text{Pulse,opt}} = [-1,1,1,-1,-1,-1,1]^T$ is also optimal, but not of this structure. Both examples are illustrated in Fig. 5.28.

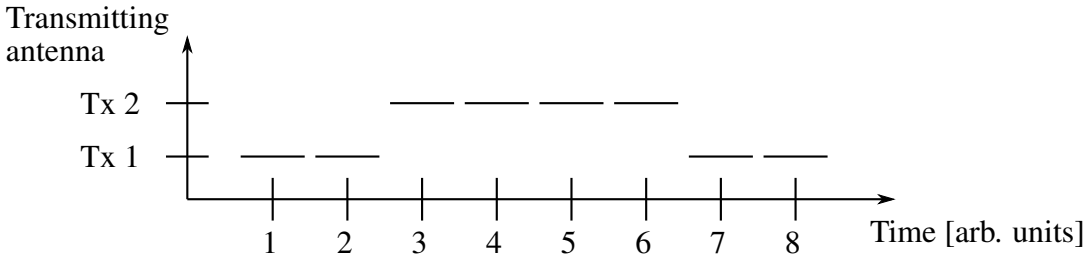

(a) Symmetric optimal TDM scheme

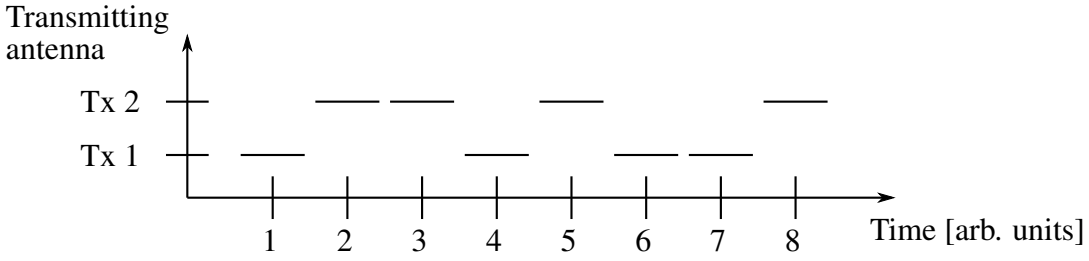

(b) Asymmetric optimal TDM scheme

Figure 5.26.: Example of optimal TDM schemes with $N_{\text{Pulse}} = 8$

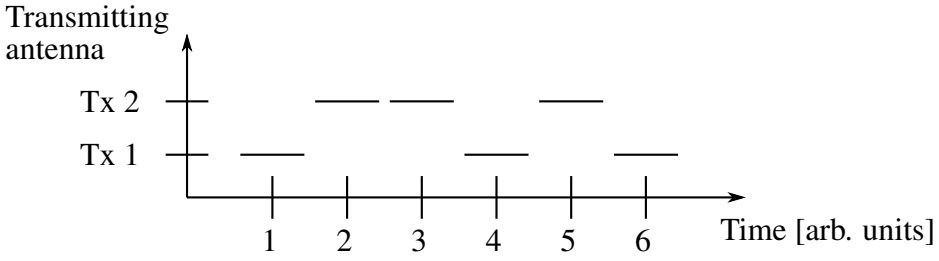

(a) Optimal symmetric TDM scheme except for the elements closest to the center of the sequence

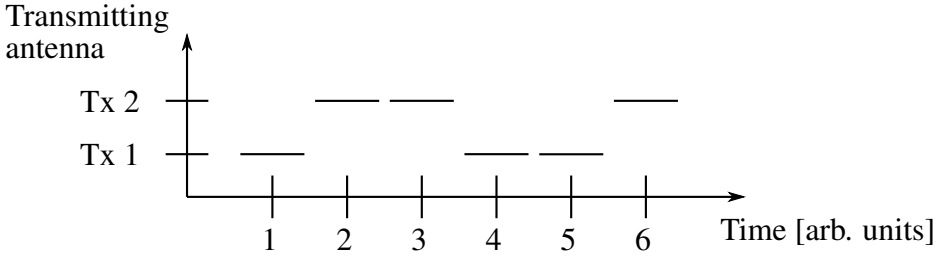

(b) Optimal TDM scheme of a different structure

Figure 5.27.: Example of optimal TDM schemes with $N_{\text{Pulse}} = 6$

In the examples, we have presented how to construct TDM schemes of a certain structure, which fulfill the conditions of Theorem 4. An algorithm which constructs all optimal TDM schemes is presented in [Vogel, 2013].

Simulations To verify and foster the understanding of the theoretical results, we present some numerical simulations.

We consider a MIMO radar which consists of 4 Rx and 4 Tx antennas. The antennas are uniformly spaced with an antenna distance of $\lambda/2$, i.e. $\underline{d}^{\text{Rx}} = \underline{d}^{\text{Tx}} = \pi \cdot [0, 1, 2, 3]^T$. We choose $L = 1$ cycle and consider optimal TDM schemes for 3 different values of N_{Pulse}, which corre-

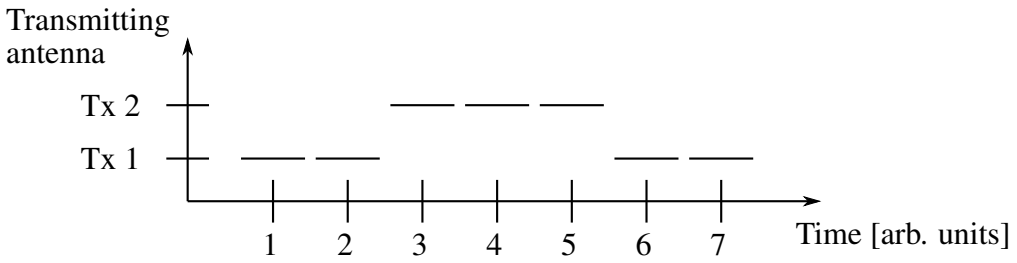

(a) Symmetric optimal TDM scheme

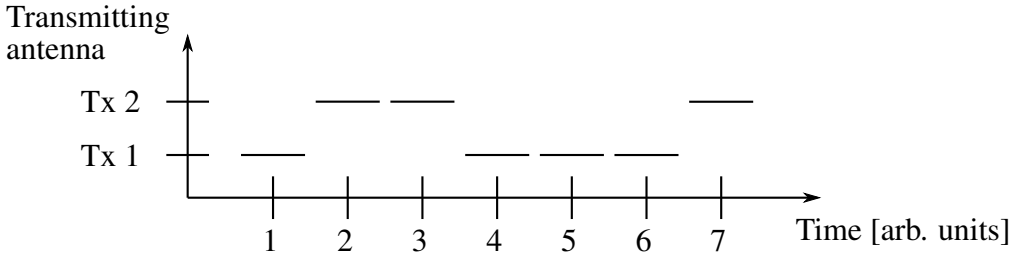

(b) Asymmetric optimal TDM scheme

Figure 5.28.: Example of optimal TDM-schemes with $N_{\text{Pulse}} = 7$

spond to the 3 different cases $N_{\text{Pulse}} \in 4\mathbb{N}$, $N_{\text{Pulse}} \in (4\mathbb{N} - 2)$ and $N_{\text{Pulse}} \in (2\mathbb{N} + 1)$. The transmitting time instants are $\underline{t} = [0, 1, \ldots, N_{\text{Pulse}} - 1]^T$, where we have normalized $\underline{t}$ such that it is dimensionless. The optimal TDM sequences, which we use for the simulations, are taken from the examples above: $\underline{d}^{\text{Pulse,opt}} = [1, -1, -1, 1, -1, 1, 1, -1]^T \in \mathbb{R}^8$, $\underline{d}^{\text{Pulse,opt}} = [-1, 1, 1, -1, -1, 1]^T \in \mathbb{R}^6$ and $\underline{d}^{\text{Pulse,opt}} = [-1, 1, 1, -1, -1, -1, 1]^T \in \mathbb{R}^7$. The target's electrical angle is $u = \sin(10°)$ and the Doppler frequency is $\omega = 1.3$. For each TDM scheme, we compute the RMSE of the deterministic ML estimate of u by doing Monte-Carlo simulations. Note that the unknown parameter vector of the ML estimator is $\underline{\Theta}$ in (5.80). We do this for different values of the total SNR S and compare the RMSE with CRB_u. The ML estimates are computed as in the former simulations, cf. (5.129).

The result is depicted in Fig. 5.29. The difference between the CRBs for the optimal TDM schemes is barely notable, since they differ only slightly, as computed above. The plot shows that the ML estimators achieve the corresponding CRBs above a threshold of approximately 16 dB. Hence, as long as an optimal TDM scheme is chosen, the number of chirps N_{Pulse} has only a small influence on the achievable accuracy. For comparison, $\text{CRB}_{u,\text{SIMO}}$, the CRB of the SIMO radar which uses the same antenna array but only one Tx antenna, is also depicted. $\text{CRB}_{u,\text{SIMO}}$ is achieved by a MIMO radar using a bad TDM scheme, cf. Theorem 1.

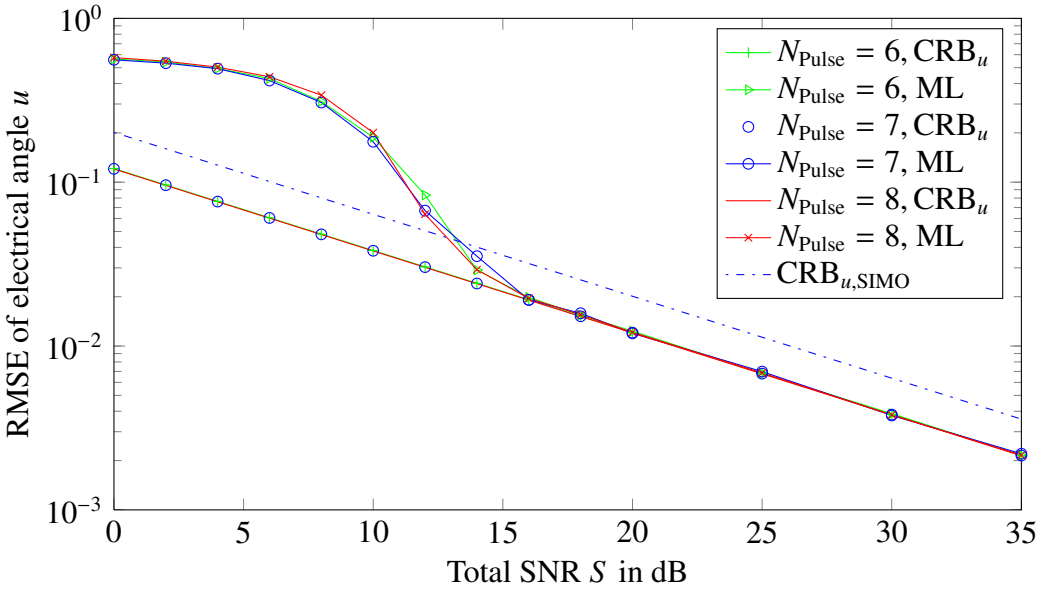

Figure 5.29.: RMSE of ML and CRB of optimal TDM schemes for different N_{Pulse}

5.3. Two Moving Targets

Consider a radar system which measures the signal of several targets, which have the same distance and relative radial velocity. The radar system cannot distinguish the targets in their distance and velocity, hence it has to estimate the DOAs of several targets. Since it is unlikely that more than two targets have nearly the same distance and velocity, we focus on the two target case. A typical automotive example, in which this situation arises, is depicted in Fig. 5.30: a car is driving in the middle of an alley, where other cars are parking on the left and right side. Due to the symmetry of the figure, the two cars which are located at the same distance have the same relative radial velocity.

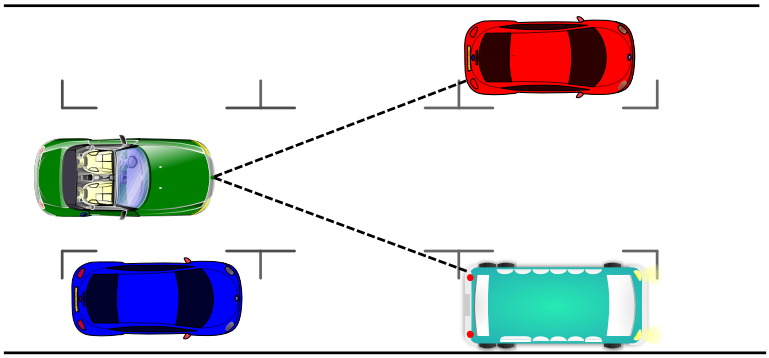

Figure 5.30.: Example of a scenario, in which two parking targets have the same distance. Due to the symmetry of the figure, they also have the same relative radial velocity v. [Openclipart, 2014, graphical parts used and adapted]

We are interested in the accuracy and resolution of a TDM MIMO radar system for the DOA estimation of two targets, which are moving relative to the radar. We want to compare different TDM MIMO radars, and compare the MIMO to a SIMO radar. We aim to find TDM schemes, which achieve a high accuracy and resolution. In [Li et al., 2008] and [Li and Stoica, 2009, Chapter 2], the CRB for the DOA of several stationary targets for a MIMO radar is computed. The authors use it to optimize the transmit waveform of the MIMO radar. Here, we derive and investigate the CRB for two non-stationary targets, i. e. targets moving relative to the radar, for a TDM MIMO radar. We derive conditions for TDM schemes such that the DOAs and Doppler frequencies decouple in the CRB. Hence the DOA estimation can be as accurate as if the Doppler frequencies are known a priori. Using the CRB, we define a statistical resolution limit to separate both targets. We show that the TDM MIMO radar can achieve a better resolution than the SIMO radar, despite the unknown Doppler frequencies. This section is based on [Rambach and Yang, 2014][4].

We introduce the signal model in Section 5.3.1. In Section 5.3.2 the CRB is computed and interpreted. We derive the conditions for the decoupling of the DOAs and Doppler frequencies in Sec-

[4]This section contains quotations of our own published work [Rambach and Yang, 2014] which are not marked additionally.

tion 5.3.3. To confirm the analytical results, numerical simulations are presented in Section 5.3.4. We investigate the angular resolution in Section 5.3.5 and summarize the results in Section 5.3.6.

5.3.1. Signal Model

Before we present the signal model, consider two targets which the radar system cannot separate in their distances or relative radial velocities. This does not necessarily mean that the relative velocities are equal, but the difference of the velocities is smaller than the velocity resolution of the radar system. A typical automotive radar system with a carrier frequency of 76.5 GHz achieves a resolution in the velocity of approximately $\delta_v = 1\,\mathrm{m/s}$ [Reiher, 2012]. The carrier wavelength is $\lambda \approx 3.9\,\mathrm{mm}$. Let us assume a measurement time of one cycle $T_{\mathrm{cycle}} = 5\,\mathrm{ms}$. The difference of the distance, the targets are moving during T_{cycle}, is up to $T_{\mathrm{cycle}} \cdot \delta_v = 5\,\mathrm{mm}$, which is larger than the carrier wavelength. Hence it is important to incorporate this in the signal model for the DOA estimation. Therefore, we have to introduce in the signal model an own Doppler frequency for every moving target.

We present the signal model for the DOA estimation of N_{Targets} moving targets for a TDM MIMO radar. The two target model is a special case which is obtained by setting $N_{\mathrm{Targets}} = 2$. The radar consists of a linear array with N_{Tx} Tx and N_{Rx} Rx colocated, isotropic antennas. As in Section 5.1.2 the targets are in the far field, are modeled as point targets and reflect the narrowband transmitted signal. To distinguish between the two dimensional electrical angle $\underline{u}$ of one target in Section 5.1.2.1, we denote the electrical angles of the targets by

$$\underline{U} = \left[U_1, \ldots, U_{N_{\mathrm{Targets}}}\right]^T \in \mathbb{R}^{N_{\mathrm{Targets}}}, \tag{5.153}$$

where U_i is the electrical angle of the i-th target. The Doppler frequencies and complex signal strengths of the targets are denoted by

$$\underline{\omega} = \left[\omega_1, \ldots, \omega_{N_{\mathrm{Targets}}}\right]^T \in \mathbb{R}^{N_{\mathrm{Targets}}}, \tag{5.154}$$

$$\underline{s}(l) = \left[s_1(l), \ldots, s_{N_{\mathrm{Targets}}}(l)\right]^T \in \mathbb{C}^{N_{\mathrm{Targets}}}, \quad l = 1, \ldots, L, \tag{5.155}$$

respectively. The signal is made up of the sum of the signals of each target. Hence, using the one target signal model for a linear array (5.70), we get

$$\begin{aligned} \underline{x}(l) &= \left(\sum_{k=1}^{N_{\mathrm{Targets}}} \underline{b}(U_k, \omega_k)\, s_k(l) \right) + \underline{n}(l) \\ &= \mathbf{B}(\underline{U}, \underline{\omega})\, \underline{s}(l) + \underline{n}(l), \quad l = 1, \ldots, L, \end{aligned} \tag{5.156}$$

with

$$\underline{b}(U, \omega) = \sqrt{\underline{\rho}^{\mathrm{Virt}}} \odot \exp(j \cdot \underline{t}^{\mathrm{Virt}} \omega) \odot \underline{a}^{\mathrm{Virt}}(U) \quad \in \mathbb{C}^{N_{\mathrm{Virt}}}, \tag{5.157}$$

$$\mathbf{B}(\underline{U}, \underline{\omega}) = \left[\underline{b}(U_1, \omega_1) \quad \ldots \quad \underline{b}(U_{N_{\text{Targets}}}, \omega_{N_{\text{Targets}}}) \right] \in \mathbb{C}^{N_{\text{Virt}} \times N_{\text{Targets}}}. \tag{5.158}$$

All other variables are given in (5.75) to (5.79). We make the same assumptions as stated in Section 5.1.2.1, where the assumptions concerning the target apply to all targets.

The unknown parameters $\underline{\Theta}$ to be estimated from $\underline{x}(l)$, $1 \leq l \leq L$, are

$$\underline{\Theta} = \left[\underline{U}^T, \underline{\omega}^T, \underline{s}^T(1), \ldots, \underline{s}^T(L), \sigma^2 \right]^T. \tag{5.159}$$

5.3.2. Cramer Rao Bound

We present the deterministic CRB for the DOAs and Doppler frequencies for the multiple target model (5.156) in Section 5.3.2.1 and simplify it further for the two target case, $N_{\text{Targets}} = 2$. In 5.3.2.2 we interpret the resulting formula of the CRB.

5.3.2.1. Derivation of the CRB

The unknown parameter vector is given in (5.159). We denote the electrical angle and Doppler frequency of each target by

$$\underline{\Theta}^{(i)} = [U_i,\ \omega_i]^T, \quad i = 1, \ldots, N_{\text{Targets}}. \tag{5.160}$$

We want to obtain the part of the CRB corresponding to the parameters $\underline{\Theta}^{(1)}, \ldots, \underline{\Theta}^{(N_{\text{Targets}})}$. This part is denoted by $\mathbf{CRB}_{\left(\underline{\Theta}^{(1)}, \ldots, \underline{\Theta}^{(N_{\text{Targets}})}\right)}$. Thus we have to compute the FIM $\mathbf{J}$ of the whole parameter vector $\underline{\Theta}$ and then its inverse $\mathbf{J}^{-1}$. We take that $2N_{\text{Targets}} \times 2N_{\text{Targets}}$ block of $\mathbf{J}^{-1}$ corresponding to $\underline{\Theta}^{(1)}, \ldots, \underline{\Theta}^{(N_{\text{Targets}})}$. This part is $\mathbf{CRB}_{\left(\underline{\Theta}^{(1)}, \ldots, \underline{\Theta}^{(N_{\text{Targets}})}\right)}$. Following [Yau and Bresler, 1992],

$$\mathbf{CRB}^{-1}_{\left(\underline{\Theta}^{(1)}, \ldots, \underline{\Theta}^{(N_{\text{Targets}})}\right)} = \frac{2\,L}{\sigma^2} \operatorname{Re}\left[\mathbf{C} \odot \left(\mathbf{S}^T \otimes \mathbf{1}_{2\times 2} \right) \right] \in \mathbb{R}^{2N_{\text{Targets}} \times 2N_{\text{Targets}}} \tag{5.161}$$

with

$$\mathbf{C} = \mathbf{D}^H\, \mathbf{P}_{\mathbf{B}}^{\perp}\, \mathbf{D} \qquad \in \mathbb{C}^{2N_{\text{Targets}} \times 2N_{\text{Targets}}}, \tag{5.162}$$

$$\mathbf{D} = \left[\mathbf{D}_1 \quad \ldots \quad \mathbf{D}_{N_{\text{Targets}}} \right] \qquad \in \mathbb{C}^{N_{\text{Virt}} \times 2N_{\text{Targets}}}, \tag{5.163}$$

$$\mathbf{D}_i = \left[\frac{\partial \underline{b}(U_i, \omega_i)}{\partial U_i} \ \frac{\partial \underline{b}(U_i, \omega_i)}{\partial \omega_i} \right] \in \mathbb{C}^{N_{\text{Virt}} \times 2},\ i = 1, \ldots, N_{\text{Targets}}, \tag{5.164}$$

$$\mathbf{P}_{\mathbf{B}}^{\perp} = \mathbf{I} - \mathbf{P}_{\mathbf{B}} \qquad \in \mathbb{C}^{N_{\text{Virt}} \times N_{\text{Virt}}}, \tag{5.165}$$

$$\mathbf{P}_{\mathbf{B}} = \mathbf{B} \left(\mathbf{B}^H\, \mathbf{B} \right)^{-1} \mathbf{B}^H \qquad \in \mathbb{C}^{N_{\text{Virt}} \times N_{\text{Virt}}}, \tag{5.166}$$

$$\mathbf{S} = \frac{1}{L} \sum_{l=1}^{L} \underline{s}(l)\, \underline{s}^H(l) \qquad \in \mathbb{C}^{N_{\text{Targets}} \times N_{\text{Targets}}}. \tag{5.167}$$

For the sake of clarity, we show which parameters the different elements of $\mathbf{CRB}^{-1}_{(\underline{\Theta}^{(1)},\underline{\Theta}^{(2)})}$ correspond to:

$$\mathbf{CRB}^{-1}_{\left(\underline{\Theta}^{(1)},\ldots,\underline{\Theta}^{(N_{\text{Targets}})}\right)} = \begin{array}{c} \\ U_1 \\ \omega_1 \\ \vdots \\ U_{N_{\text{Targets}}} \\ \omega_{N_{\text{Targets}}} \end{array} \begin{array}{c} \begin{array}{ccccc} U_1 & \omega_1 & \ldots & U_{N_{\text{Targets}}} & \omega_{N_{\text{Targets}}} \end{array} \\ \begin{bmatrix} \times & \times & \ldots & \times & \times \\ \times & \times & \ldots & \times & \times \\ \vdots & \vdots & \ddots & \vdots & \vdots \\ \times & \times & \ldots & \times & \times \\ \times & \times & \ldots & \times & \times \end{bmatrix} \end{array}$$

Further Analytical Computations for Two Targets To gain a deeper insight, we compute a more compact expression for the case of two targets, i. e. $N_{\text{Targets}} = 2$. In that case $\mathbf{CRB}_{(\underline{\Theta}^{(1)},\underline{\Theta}^{(2)})} \in \mathbb{C}^{4\times4}$. We abbreviate the matrix elements in $\mathbf{S}$ by

$$\mathbf{S} = \begin{bmatrix} \sigma^2_{s,1} & c_s \\ c_s^* & \sigma^2_{s,2} \end{bmatrix} \in \mathbb{C}^{2\times2}. \tag{5.168}$$

Hence

$$\sigma^2_{s,i} = \frac{1}{L}\sum_{l=1}^{L} |s_i(l)|^2 \tag{5.169}$$

is the mean of the i-th target's signal strength over all cycles and

$$c_s = \frac{1}{L}\sum_{l=1}^{L} s_1(l)s_2^*(l) \tag{5.170}$$

is the correlation coefficient between the two target signals. After some lengthy calculations, which are given in Appendix M, we can express the matrix $\mathbf{C} \in \mathbb{C}^{4\times4}$ by

$$\mathbf{C} = \mathbf{C}_1 + \mathbf{C}_2 - \mathbf{C}_3, \tag{5.171}$$

$$\mathbf{C}_1 = \begin{bmatrix} \rho^{\text{Virt}}_{\text{sum}} \operatorname{Cov}^{\text{S}}(\mathbf{V}_1) & b^*_{\Delta\text{sum}} \operatorname{Cov}^{\text{WS}}(\mathbf{V}_1, \underline{b}^*_{\Delta\text{Rx}}) \\ b_{\Delta\text{sum}} \operatorname{Cov}^{\text{WS}}(\mathbf{V}_1, \underline{b}_{\Delta\text{Rx}}) & \rho^{\text{Virt}}_{\text{sum}} \operatorname{Cov}^{\text{S}}(\mathbf{V}_1) \end{bmatrix}, \tag{5.172}$$

$$\mathbf{C}_2 = \begin{bmatrix} \rho^{\text{Virt}}_{\text{sum}} \operatorname{Cov}^{\text{WS}}(\mathbf{V}_2, \underline{\rho}) & b^*_{\Delta\text{sum}} \operatorname{Cov}^{\text{WS}}(\mathbf{V}_2, \underline{b}^*_{\Delta\text{Tx}}) \\ b_{\Delta\text{sum}} \operatorname{Cov}^{\text{WS}}(\mathbf{V}_2, \underline{b}_{\Delta\text{Tx}}) & \rho^{\text{Virt}}_{\text{sum}} \operatorname{Cov}^{\text{WS}}(\mathbf{V}_2, \underline{\rho}) \end{bmatrix}, \tag{5.173}$$

$$\mathbf{C}_3 = \frac{\rho^{\text{Virt}}_{\text{sum}}}{{\rho^{\text{Virt}}_{\text{sum}}}^2 - |b_{\Delta\text{sum}}|^2} \cdot \begin{bmatrix} |b_{\Delta\text{sum}}|^2\, \underline{m}^*\underline{m}^T & -\rho^{\text{Virt}}_{\text{sum}}\, b^*_{\Delta\text{sum}}\, \underline{m}^*\underline{m}^H \\ -\rho^{\text{Virt}}_{\text{sum}}\, b_{\Delta\text{sum}}\, \underline{m}\,\underline{m}^T & |b_{\Delta\text{sum}}|^2\, \underline{m}\,\underline{m}^H \end{bmatrix} \tag{5.174}$$

with

$$\rho_{\text{sum}}^{\text{Virt}} = \underline{1}^T \underline{\rho}^{\text{Virt}} = N_{\text{Rx}} \underline{1}^T \underline{\rho} \qquad \in \mathbb{R}, \tag{5.175}$$

$$\Delta U = U_1 - U_2 \qquad \in \mathbb{R}, \tag{5.176}$$

$$\Delta\omega = \omega_1 - \omega_2 \qquad \in \mathbb{R}, \tag{5.177}$$

$$\underline{b}_{\Delta\text{Tx}} = \underline{\rho} \odot \exp(j \cdot \underline{t}\, \Delta\omega) \odot \exp(j \cdot \underline{d}^{\text{Pulse}} \Delta U) \qquad \in \mathbb{C}^{N_{\text{Pulse}}}, \tag{5.178}$$

$$\underline{b}_{\Delta\text{Rx}} = \exp(j \cdot \underline{d}^{\text{Rx}} \Delta U) \qquad \in \mathbb{C}^{N_{\text{Rx}}}, \tag{5.179}$$

$$\underline{b}_{\Delta} = \underline{b}_{\Delta\text{Tx}} \otimes \underline{b}_{\Delta\text{Rx}} \qquad \in \mathbb{C}^{N_{\text{Virt}}}, \tag{5.180}$$

$$b_{\Delta\text{sum}} = \underline{1}^T \underline{b}_{\Delta} = \left(\underline{1}^T \underline{b}_{\Delta\text{Tx}}\right) \left(\underline{1}^T \underline{b}_{\Delta\text{Rx}}\right) \qquad \in \mathbb{C}, \tag{5.181}$$

$$\underline{m} = \left[\text{E}^{\text{S}}(\mathbf{V}_1) - \text{E}^{\text{WS}}(\mathbf{V}_1, \underline{b}_{\Delta\text{Rx}}) + \text{E}^{\text{WS}}(\mathbf{V}_2, \underline{\rho}) - \text{E}^{\text{WS}}(\mathbf{V}_2, \underline{b}_{\Delta\text{Tx}})\right]^T \in \mathbb{C}^2, \tag{5.182}$$

$$\mathbf{V}_1 = \left[\underline{d}^{\text{Rx}} \quad \underline{0}\right] \qquad \in \mathbb{C}^{N_{\text{Rx}} \times 2}, \tag{5.183}$$

$$\mathbf{V}_2 = \left[\underline{d}^{\text{Pulse}} \quad \underline{t}\right] \qquad \in \mathbb{C}^{N_{\text{Pulse}} \times 2}. \tag{5.184}$$

The definitions and properties of $\text{E}^{\text{WS}}, \text{E}^{\text{S}}, \text{Cov}^{\text{WS}}, \text{Cov}^{\text{S}}$ are given in Appendix A. Here we have assumed that all expressions are finite and no division by 0 occurs. Since $\text{E}^{\text{WS}}(., \underline{w})$, $\text{Cov}^{\text{WS}}(., \underline{w})$ with complex weight vector $\underline{w}$ contains the division by $\underline{1}^T \underline{w}$, this means that $\underline{1}^T \underline{w} \neq 0$ for all weight vectors.

5.3.2.2. Notes on the CRB

Interpretation of C The matrix $\mathbf{C}$ consists of 3 terms, $\mathbf{C}_1, \mathbf{C}_2$ and $\mathbf{C}_3$, which we interpret in the following.

$\mathbf{C}_1$ is especially determined by the Rx-array $\underline{d}^{\text{Rx}}$. The 2×2-blocks on the diagonal contain

$$\text{Cov}^{\text{S}}(\mathbf{V}_1) = \begin{matrix} \\ U_i \\ \omega_i \end{matrix} \begin{matrix} \begin{matrix} U_i & \omega_i \end{matrix} \\ \begin{bmatrix} \text{Var}^{\text{S}}(\underline{d}^{\text{Rx}}) & 0 \\ 0 & 0 \end{bmatrix} \end{matrix}. \tag{5.185}$$

It describes the influence of $\underline{d}^{\text{Rx}}$ on the estimation of U_1 and U_2. The 0 entries show that $\text{Cov}^{\text{S}}(\mathbf{V}_1)$ does not contain any information about $\underline{\omega}$. $\text{Var}^{\text{S}}(\underline{d}^{\text{Rx}})$ is the same expression as the one which appears in the CRB for a SIMO radar for the one target DOA estimation (4.16). The off-diagonal 2×2-blocks contain

$$\text{Cov}^{\text{WS}}(\mathbf{V}_1, \underline{b}_{\Delta\text{Rx}}) = \begin{matrix} \\ U_j \\ \omega_j \end{matrix} \begin{matrix} \begin{matrix} U_i & \omega_i \end{matrix} \\ \begin{bmatrix} \text{Var}^{\text{WS}}(\underline{d}^{\text{Rx}}, \underline{b}_{\Delta\text{Rx}}) & 0 \\ 0 & 0 \end{bmatrix} \end{matrix}, \; i \neq j, \tag{5.186}$$

or the complex conjugate of it. There is again no information about $\underline{\omega}$. $\mathrm{Var}^{\mathrm{WS}}(\underline{d}^{\mathrm{Rx}}, \underline{b}_{\Delta\mathrm{Rx}})$ expresses the coupling between the two electrical angles. The coupling depends on $\underline{d}^{\mathrm{Rx}}$ and the angle separation ΔU of the two targets.

$\mathbf{C}_2$ is particularly determined by the TDM sequence, namely $\underline{d}^{\mathrm{Pulse}}$ and $\underline{t}$.

$$\mathrm{Cov}^{\mathrm{WS}}(\mathbf{V}_2, \underline{\rho}) = \begin{matrix} \\ U_i \\ \omega_i \end{matrix} \begin{matrix} \begin{matrix} U_i & \omega_i \end{matrix} \\ \begin{bmatrix} \mathrm{Var}^{\mathrm{WS}}(\underline{d}^{\mathrm{Pulse}}, \underline{\rho}) & \mathrm{Cov}^{\mathrm{WS}}(\underline{d}^{\mathrm{Pulse}}, \underline{t}, \underline{\rho}) \\ \mathrm{Cov}^{\mathrm{WS}}(\underline{d}^{\mathrm{Pulse}}, \underline{t}, \underline{\rho}) & \mathrm{Var}^{\mathrm{WS}}(\underline{t}, \underline{\rho}) \end{bmatrix} \end{matrix} \tag{5.187}$$

is analog to the one-target DOA estimation, Section 5.2.2: $\mathrm{Var}^{\mathrm{WS}}(\underline{d}^{\mathrm{Pulse}}, \underline{\rho})$ describes the amount of information on U_1, U_2 due to the Tx antennas. $\mathrm{Var}^{\mathrm{WS}}(\underline{t}, \underline{\rho})$ contains the information for estimating ω_1 and ω_2 due to the different Tx times. $\mathrm{Cov}^{\mathrm{WS}}(\underline{d}^{\mathrm{Pulse}}, \underline{t}, \underline{\rho})$ is the coupling between U and ω of the same target. If $\underline{d}^{\mathrm{Pulse}}, \underline{t}$ and $\underline{\rho}$ are chosen in a suitable way, this coupling can be reduced to 0, cf. Section 5.2.3. The 2×2-block $b_{\Delta\mathrm{sum}}\,\mathrm{Cov}^{\mathrm{WS}}(\mathbf{V}_2, \underline{b}_{\Delta\mathrm{Tx}})$ expresses the coupling between both targets. Since

$$\mathrm{Cov}^{\mathrm{WS}}(\mathbf{V}_2, \underline{b}_{\Delta\mathrm{Tx}}) = \begin{matrix} \\ U_j \\ \omega_j \end{matrix} \begin{matrix} \begin{matrix} U_i & \omega_i \end{matrix} \\ \begin{bmatrix} \mathrm{Var}^{\mathrm{WS}}(\underline{d}^{\mathrm{Pulse}}, \underline{b}_{\Delta\mathrm{Tx}}) & \mathrm{Cov}^{\mathrm{WS}}(\underline{d}^{\mathrm{Pulse}}, \underline{t}, \underline{b}_{\Delta\mathrm{Tx}}) \\ \mathrm{Cov}^{\mathrm{WS}}(\underline{d}^{\mathrm{Pulse}}, \underline{t}, \underline{b}_{\Delta\mathrm{Tx}}) & \mathrm{Var}^{\mathrm{WS}}(\underline{t}, \underline{b}_{\Delta\mathrm{Tx}}) \end{bmatrix} \end{matrix}, \; i \neq j, \tag{5.188}$$

ΔU as well as $\Delta\omega$ affect the amount of coupling between the two targets' electrical angles and Doppler frequencies.

The matrix $\mathbf{C}_3$ can be interpreted in the following way: $\mathbf{C}_3$ origins from $\mathbf{D}^H\mathbf{P}_\mathbf{B}\mathbf{D}$. $\mathbf{P}_\mathbf{B}$ is the projector onto the subspace W spanned by the column vectors of $\mathbf{B}$, namely the steering vectors $\underline{b}(U_1, \omega_1), \underline{b}(U_2, \omega_2)$. $\mathbf{D}$ contains the derivatives of the steering vectors. Those vectors are perpendicular to the subspace W iff $\mathbf{D}^H\mathbf{P}_\mathbf{B}\mathbf{D} = \mathbf{0}$. It can be shown, without loss of generality, that this is equivalent to $\mathbf{C}_3 = \mathbf{0}$. Hence, roughly speaking, $\mathbf{C}_3$ denotes the part of the derivatives of the steering vectors which is in W. The smaller the diagonal elements of $\mathbf{C}_3$, the more information is contained in the diagonal elements of $\mathbf{C}$. This is in accordance to the geometrical interpretation: the radar system is sensitive if the change of the steering vectors, due to a change of parameters, is perpendicular to the steering vectors. Note that $\mathbf{C}_3$ has mixed contributions from both the Rx and Tx array and contains couplings of both targets' DOAs and Doppler frequencies.

All matrices $\mathbf{C}_1, \mathbf{C}_2$ and $\mathbf{C}_3$ contain $b_{\Delta\mathrm{sum}} = \left(\underline{1}^T \underline{b}_{\Delta\mathrm{Tx}}\right)\left(\underline{1}^T \underline{b}_{\Delta\mathrm{Rx}}\right)$. The factor

$$\underline{1}^T \underline{b}_{\Delta\mathrm{Rx}} = \sum_{i=1}^{N_{\mathrm{Rx}}} \exp(j \cdot d_i^{\mathrm{Rx}} \Delta U) \tag{5.189}$$

can be considered as the complex Rx beampattern at ΔU. Similarly,

$$\underline{1}^T \underline{b}_{\Delta\mathrm{Tx}} = \sum_{i=1}^{N_{\mathrm{Pulse}}} \rho_i \cdot \exp(j \cdot t_i \, \Delta\omega) \cdot \exp(j \cdot d_i^{\mathrm{Pulse}} \Delta U) \tag{5.190}$$

is the complex Tx beampattern at $\Delta U, \Delta\omega$ weighted with $\underline{\rho}$. Hence, $b_{\Delta\mathrm{sum}}$ is the product of these beampatterns.

Other notes on the CRB $\mathbf{CRB}_{(\underline{\Theta}^{(1)}, \underline{\Theta}^{(2)})}$ depends not only on the position of the Tx antennas, but also on the TDM scheme described by the transmitting order $\underline{d}^{\mathrm{Pulse}}$ and transmitting times $\underline{t}$. Hence, the choice of a good TDM scheme is crucial in order to achieve a high accuracy.

Moreover, $\mathbf{CRB}_{(\underline{\Theta}^{(1)}, \underline{\Theta}^{(2)})}$ is a function of ΔU, $\Delta\omega$, $\sigma_{s,1}^2$, $\sigma_{s,2}^2$, c_s

$$\mathbf{CRB}_{(\underline{\Theta}^{(1)}, \underline{\Theta}^{(2)})} = \mathbf{CRB}_{(\underline{\Theta}^{(1)}, \underline{\Theta}^{(2)})}(\Delta U, \, \Delta\omega, \, \sigma_{s,1}^2, \, \sigma_{s,2}^2, \, c_s). \tag{5.191}$$

Hence it does not depend on the absolute values of U_i, ω_i, but only on their differences. Moreover, it does not depend on $s_1(l), s_2(l)$, $l = 1, \ldots, L$, but on the mean signal strengths $\sigma_{s,1}^2$, $\sigma_{s,2}^2$ and the correlation coefficient c_s defined in (5.169) and (5.170), respectively. Note that for the important case of one cycle, i. e. $L = 1$, $\sigma_{s,i}^2 = |s_i|^2$ and $c_s = s_1 \, s_2^*$.

5.3.3. Decoupling of Electrical Angles and Doppler Frequencies

In Section 5.2, the DOA estimation of one moving target was investigated. It was shown that TDM schemes can be found such that the CRB of the DOA has the same value as for a stationary target. Similarly, we are interested here in TDM schemes which lead to a decoupling of the electrical angles and Doppler frequencies in the CRB. $\mathbf{CRB}_{(\underline{\Theta}^{(1)}, \underline{\Theta}^{(2)})}$ depends on several parameters of the targets cf. (5.191). Because of this, it is difficult to find good TDM schemes for a general setting. Therefore, we focus first on the case with $L = 1$ cycle and consider two targets, which have the same signal strength, i. e. $|s_1| = |s_2|$. Here we have abbreviated $s_i(1)$ by s_i, $i = 1, 2$. In Fig. 5.31, the element of the CRB which corresponds to the first target's electrical angle $\mathrm{CRB}_{U_1} = \left[\mathbf{CRB}_{(\underline{\Theta}^{(1)}, \underline{\Theta}^{(2)})}\right]_{1,1}$ is plotted for varying $\Delta\omega$ and ΔU. We have used the following parameters: $N_{\mathrm{Pulse}} = 4$, $\underline{\rho} = \frac{1}{N_{\mathrm{Pulse}}} \underline{1}$, the SNR defined as $\mathrm{SNR} = \frac{\sigma_{s,1}^2}{\sigma^2}$ is 30 dB, the Rx array is a 4-element ULA with half-wavelength spacing $\underline{d}^{\mathrm{Rx}} = \pi \cdot [-1.5, -0.5, 0.5, 1.5]^T$. Moreover, $\underline{d}^{\mathrm{Tx}} = \pi \cdot [-2, 2]^T$, $\underline{d}^{\mathrm{Pulse}} = [d_1^{\mathrm{Tx}}, d_2^{\mathrm{Tx}}, d_2^{\mathrm{Tx}}, d_1^{\mathrm{Tx}}]^T$, $\underline{t} = [0, 1, 2, 3]^T$, where $\underline{t}$ is normalized such that it is unitless, and $c_s = |s_1| \cdot |s_2| \, \mathrm{e}^{j \cdot 0.3\pi}$. Fig. 5.31 shows that for a fixed ΔU, CRB_{U_1} is maximal in the vicinity of $\Delta\omega = 0$. We have studied other TDM schemes and different values of c_s, which yield a qualitative similar result, i. e. for a fixed ΔU, the maximum of CRB_{U_1} is located in the vicinity of $\Delta\omega = 0$.

Due to this, we investigate in the following the case $\Delta\omega = 0$, i. e. the two targets have exactly the same Doppler frequency. Hence the two targets can be distinguished only by their DOAs. Note,

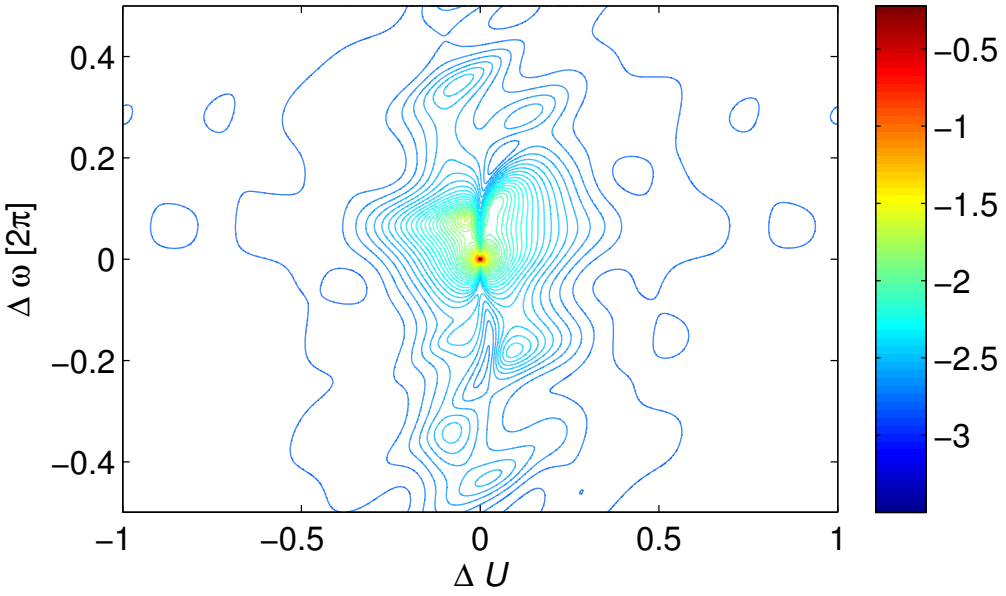

Figure 5.31.: $\log\left(\sqrt{\mathrm{CRB}_{U_1}}\right)$ for varying $\Delta\omega$ and ΔU

since the estimator does not know a priori $\Delta\omega = 0$, both Doppler frequencies ω_1 and ω_2 have to be estimated.

Theorem 5. *Let $\Delta\omega = 0$. The elements of $\mathbf{CRB}_{(\underline{\Theta}^{(1)},\underline{\Theta}^{(2)})}$ corresponding to U_1, U_2 decouple from the elements corresponding to ω_1, ω_2 if the TDM scheme satisfies*

$$\mathrm{E}^{\mathrm{WS}}\left(\underline{t}^{(k)},\underline{\rho}^{(k)}\right) = \mathrm{E}^{\mathrm{WS}}\left(\underline{t}^{(l)},\underline{\rho}^{(l)}\right)\ \forall k,l \in \{1,\ldots,N_{Tx}\}. \tag{5.192}$$

Here, $\underline{t}^{(k)}$ denotes the transmit times of the k-th Tx antenna and $\underline{\rho}^{(k)}$ the corresponding energies of the transmitted pulses.

Proof. This theorem is a special case of the more general Theorem 6 which we present and prove in Section 5.4.

The theorem gives a sufficient condition for the decoupling of the electrical angles and Doppler frequencies. The decoupling means that the CRB has the following form

$$\mathbf{CRB}_{(\underline{\Theta}^{(1)},\underline{\Theta}^{(2)})} = \begin{array}{c} \\ U_1 \\ \omega_1 \\ U_2 \\ \omega_2 \end{array} \begin{array}{c} \begin{array}{cccc} U_1 & \omega_1 & U_2 & \omega_2 \end{array} \\ \begin{bmatrix} . & 0 & . & 0 \\ 0 & . & 0 & . \\ . & 0 & . & 0 \\ 0 & . & 0 & . \end{bmatrix} \end{array}. \tag{5.193}$$

Thus, after a permutation of the parameters $U_1, U_2, \omega_1, \omega_2$, the CRB has a block diagonal structure. We denote the first 2×2 block for $\underline{U} = [U_1, U_2]^T$ by $\mathbf{CRB}_{\underline{U}}$. Moreover, due to the decoupling,

$\mathbf{CRB}_{\underline{U}}$ is equal to the CRB when the Doppler frequencies are known and do not have to be estimated

$$\mathbf{CRB}_{\underline{U}} = \mathbf{CRB}_{\underline{U},\,\text{known}\,\underline{\omega}}. \tag{5.194}$$

Hence, if a TDM scheme satisfying (5.192) is chosen, a DOA accuracy can be achieved which is as good as if the Doppler frequencies are known a priori.

Let us consider the case of two stationary targets, i. e. the targets do not move relative to the radar and that is known a priori. In that case, $\omega_1 = \omega_2 = 0$ and therefore $\Delta\omega = 0$. Since $\mathbf{CRB}_{(\underline{\Theta}^{(1)},\underline{\Theta}^{(2)})}$ only depends on $\Delta\omega$ and not on the absolute values ω_1, ω_2, cf. (5.191), $\mathbf{CRB}_{\underline{U}}$ and therefore $\mathbf{CRB}_{\underline{U},\,\text{known}\,\underline{\omega}}$ also depend on $\Delta\omega$. Hence the CRB for the two electrical angles of two stationary targets $\mathbf{CRB}_{\underline{U},\,\text{stat}}$ is the same as $\mathbf{CRB}_{\underline{U},\,\text{known}\,\underline{\omega}}$ with $\Delta\omega = 0$. Thus

$$\mathbf{CRB}_{\underline{U}} = \mathbf{CRB}_{\underline{U},\,\text{stat}}, \tag{5.195}$$

i. e. if the TDM scheme satisfies (5.192), the achievable DOA accuracy is as good as if the targets are not moving relative to the radar. Hence the complete virtual aperture can be used for the estimation of the electrical angles despite the unknown Doppler frequencies.

Note that (5.192) is the same condition as for the decoupling of electrical angle and Doppler frequency in the one target case, cf. Section 5.2.3.1 Theorem 2. Moreover, due to Theorem 2, from (5.192)

$$\text{Cov}^{\text{WS}}\left(\underline{d}^{\text{Pulse}}, \underline{t}, \underline{\rho}\right) = 0 \tag{5.196}$$

follows, and for two Tx antennas (5.192) and (5.196) are equivalent.

To illustrate the findings, we consider a radar system with the following parameters: The number of measurement cycles is $L = 1$ and the Rx array is $\underline{d}^{\text{Rx}} = \pi \cdot [-1.5, -0.5, 0.5, 1.5]^T$. The Tx antenna positions are $\underline{d}^{\text{Tx}} = \pi \cdot [-2, 2]^T$. Both targets have the same signal strength $s_1 = s_2 = 1$ and we set $\Delta\omega = 0$. The SNR is $\text{SNR} = |s_1|^2/\sigma^2 = 30\,\text{dB}$. The transmitted energy per pulse is $\underline{\rho} = \frac{1}{N_{\text{Pulse}}}\underline{1}$ ensuring a constant total transmitted energy independent of the number of pulses. The transmission times are $\underline{t} = [0, \ldots, N_{\text{Pulse}} - 1]^T$. Since both targets have the same signal strength and $\Delta\omega = 0$, the CRBs of their electrical angles are equal, which we denote by CRB_U in the following: $\text{CRB}_U = \left[\mathbf{CRB}_{\underline{U}}\right]_{1,1} = \left[\mathbf{CRB}_{\underline{U}}\right]_{2,2}$. In Fig. 5.32, $\sqrt{\text{CRB}_U}$ is depicted for varying ΔU. Three different TDM schemes are considered: TDM scheme 1, for which the electrical angles decouple from the Doppler frequencies, and TDM scheme 2 and 3 which do not satisfy condition (5.192). Moreover, the CRBs for one moving target, which are computed in Section 5.2.1, are depicted. Fig. 5.32 shows that for $\Delta\omega = 0$ in general $\text{CRB}_{U,\text{TDM 1}} \leq \text{CRB}_{U,\text{TDM 2}}$. For large ΔU, CRB_U for the two-target case reaches CRB_u for one moving target. TDM scheme 3 achieves the same CRB_U as using only one transmitter, i.e. the SIMO case, because the Doppler frequencies have to be estimated as well. Since both Tx transmit only once, it cannot be distinguished by the different Tx positions if the phase

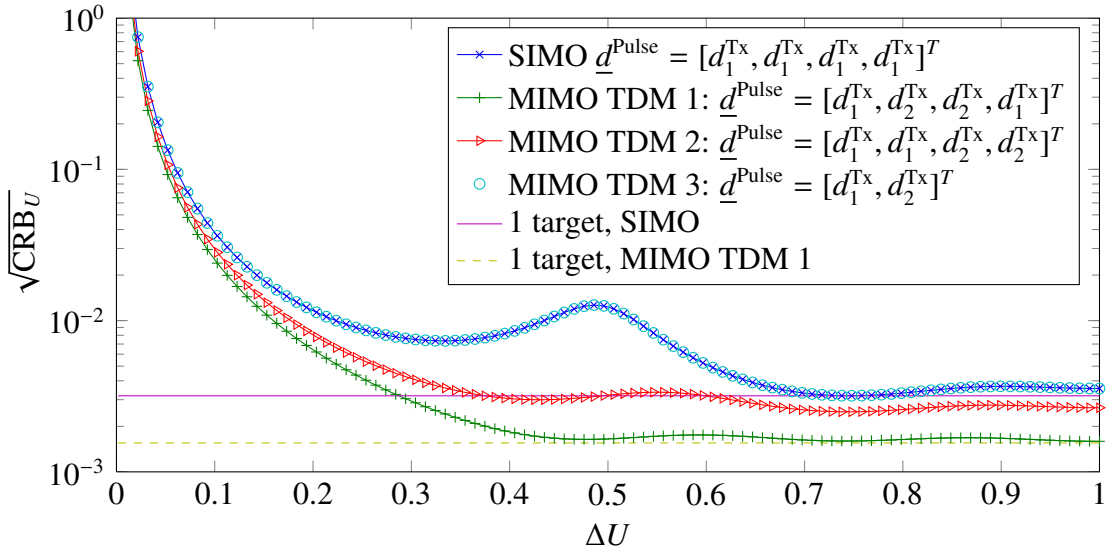

Figure 5.32.: $\sqrt{\mathrm{CRB}_U}$ for DOA estimation of two and one moving target

difference is due to the Doppler or due to the DOA. This is the same observation as in the one-target case.

We do the same investigation again but with a different correlation coefficient c_s, by setting $s_1 = 1$ and $s_2 = \mathrm{e}^{j\cdot 0.3\pi}$. This yields qualitatively the same result, i. e. in general $\mathrm{CRB}_{U,\mathrm{TDM\,1}} \leq \mathrm{CRB}_{U,\mathrm{TDM\,2}}$, but the absolute values of the CRBs are different compared to the case with $s_1 = s_2 = 1$.

In order to see if TDM schemes which satisfy the decoupling condition (5.192) yield also a small CRB for $\Delta\omega \neq 0$, we compute CRB_{U_1} for varying $\Delta\omega$ and fixed $\Delta U = 0.2$. The other parameters are the same as before, with $s_1 = s_2 = 1$. The CRB of the electrical angle of the first target CRB_{U_1} is depicted in Fig. 5.33 for three different TDM schemes. TDM scheme 1 satisfies the decoupling condition (5.192), TDM scheme 2 and 3 do not. The figure shows that $\mathrm{CRB}_{U_1,\mathrm{TDM\,1}}$ is smaller than $\mathrm{CRB}_{U_1,\mathrm{TDM\,2}}$ and $\mathrm{CRB}_{U_1,\mathrm{TDM\,3}}$ for a large part of the values of $\Delta\omega$, but not for all $\Delta\omega$. Moreover, for large $|\Delta\omega|$ TDM scheme 1 nearly achieves the CRB for one stationary target. As before, doing the same investigation with $s_1 = 1$ and $s_2 = \mathrm{e}^{j\cdot 0.3\pi}$ yields a qualitative similar result.

Hence, in general, a TDM scheme satisfying the decoupling condition (5.192) does not yield a smaller CRB than other TDM schemes for all possible target parameters. But for the important case $\Delta\omega = 0$, due to (5.194), such a TDM scheme yields a $\mathbf{CRB}_{\underline{U}}$ which is as small as if the Doppler frequencies are known a priori.

5.3.4. Numerical Simulation

In the following, we confirm the analytical findings by numerical simulations. We do a Monte-Carlo simulation to determine the RMSE of the ML estimator for the electrical angles U_1 and U_2 of the 1. and 2. target, respectively. We compare the RMSE to the computed CRB. The signal model (5.156)

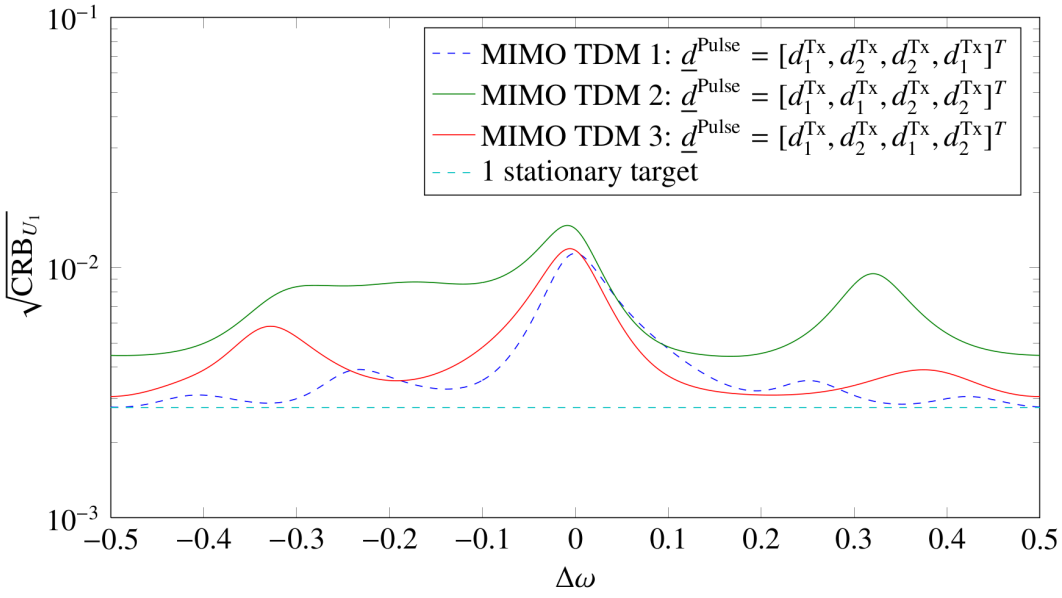

Figure 5.33.: $\sqrt{\text{CRB}_{U_1}}$ for varying $\Delta\omega$ and different TDM schemes

has the same structure as the one presented in Appendix E. Hence we can use the result (E.22) and the ML estimator $[\underline{\hat{U}}, \underline{\hat{\omega}}]^T$ of $[\underline{U}, \underline{\omega}]^T$ is given by

$$[\underline{\hat{U}}, \underline{\hat{\omega}}]^T = \arg\max_{\underline{U},\underline{\omega}} \text{Tr}\left(\mathbf{P}_{\mathbf{B}(\underline{U},\underline{\omega})}\,\hat{\mathbf{R}}\right) \tag{5.197}$$

with

$$\mathbf{P}_{\mathbf{B}(\underline{U},\underline{\omega})} = \mathbf{B}(\underline{U}, \underline{\omega})\,\mathbf{B}^{+}(\underline{U}, \underline{\omega}), \tag{5.198}$$

$$\hat{\mathbf{R}} = \frac{1}{L}\sum_{l=1}^{L} \underline{x}(l)\underline{x}^H(l). \tag{5.199}$$

$\mathbf{B}^+$ is the matrix pseudo inverse of $\mathbf{B}$, which can be computed by

$$\mathbf{B}^{+} = \left(\mathbf{B}^H\mathbf{B}\right)^{-1}\mathbf{B}^H, \tag{5.200}$$

under the assumption that $\mathbf{B}^H\mathbf{B}$ is invertible.

The parameters are the same as for the simulation presented in Fig. 5.32, but with SNR $= 25\,\text{dB}$. We consider TDM scheme 1 with $\underline{d}^{\text{Pulse}} = [d_1^{\text{Tx}}, d_2^{\text{Tx}}, d_2^{\text{Tx}}, d_1^{\text{Tx}}]^T$. 3000 Monte-Carlo simulations are done for every value of ΔU. Since the ML estimator (5.197) is nonlinear in $U_1, U_2, \omega_1, \omega_2$, the ML estimates are computed by a 4-dimensional grid search, in order to find the global maximum of the likelihood, followed by a local optimization. Since the grid search is computational expensive, for $\Delta U \geq 0.2$, the ML estimates are computed by a local optimization starting at the true value. This is possible, since the ML estimator already achieves the CRB, as shown in Fig. 5.34, and hence global errors are negligible. In this case, the number of Monte-Carlo simulations is 10000.

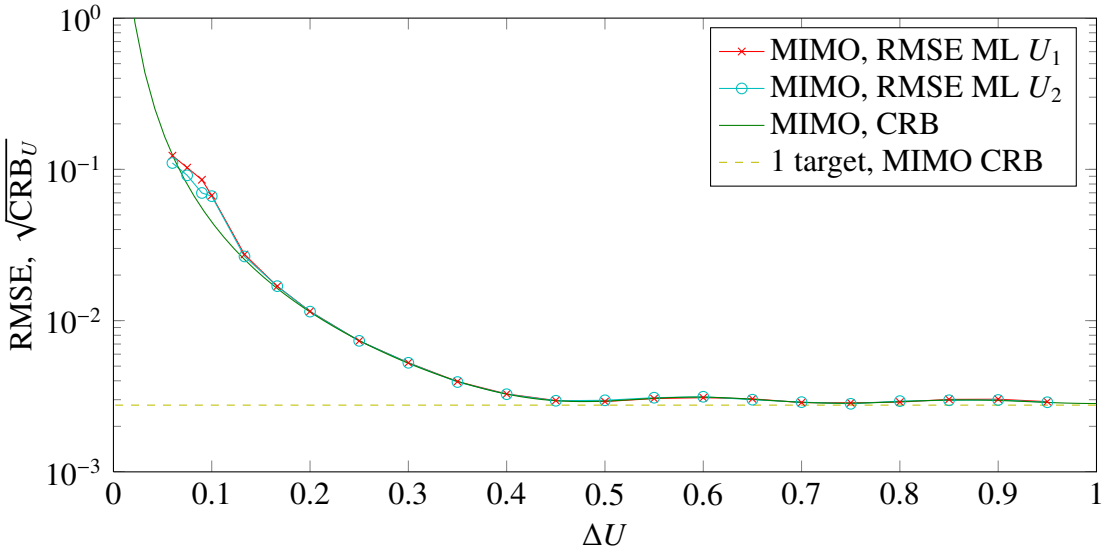

Figure 5.34.: DOA estimation of two moving targets with TDM scheme 1, $\underline{d}^{\mathrm{Pulse}} = [d_1^{\mathrm{Tx}}, d_2^{\mathrm{Tx}}, d_2^{\mathrm{Tx}}, d_1^{\mathrm{Tx}}]^T$. Comparison of $\sqrt{\mathrm{CRB}_U}$ and the RMSE of the maximum likelihood estimator for U_1 and U_2

Fig. 5.34 shows that for $\Delta U \geq 0.13$, the ML estimator reaches the CRB. For large ΔU, the one-target CRB is achieved. For $\Delta U < 0.13$, the ML deviates from the CRB due to global errors. If ΔU is very small, the RMSE of the U_1- and U_2-estimator differ. The reason is that for the computation of the RMSE, the smaller estimated electrical angle is always assigned to the 1. target. Note that for small ΔU the RMSE could be even smaller than the CRB, since the CRB does not incorporate the fact that the DOAs are always bounded by $-90°$ and $90°$ and therefore $-1 \leq U_1, U_2 \leq 1$.

With this, we have confirmed the derived CRB by simulations.

5.3.5. Angular Resolution

An important performance criterion of a radar system is its angular resolution, i.e. the angular separation at which two targets can be distinguished. In literature, there are several different definitions of the resolution, cf. Section 2.2.3. We use the definition of the resolution given in [El Korso et al., 2011], which works for multiple targets and multiple parameters of interest. Note that it is not clear yet, which estimators fulfill the conditions used in the definition in [El Korso et al., 2011] and which actually achieve the resolution. This is an ongoing research topic. The definition enables us to use the two-target CRB in order to define the angular resolution analytically. The unknown parameters of the signal model are given in (5.159). Instead of estimating $U_1, U_2, \omega_1, \omega_2$, we can also rewrite the model and estimate $U_1, \Delta U, \omega_1, \Delta\omega$. Hence the unknown parameters are

$$\underline{\Theta} = [U_1, \omega_1, \Delta U, \Delta\omega, \underline{s}(1), \ldots, \underline{s}(L), \sigma^2]^T. \tag{5.201}$$

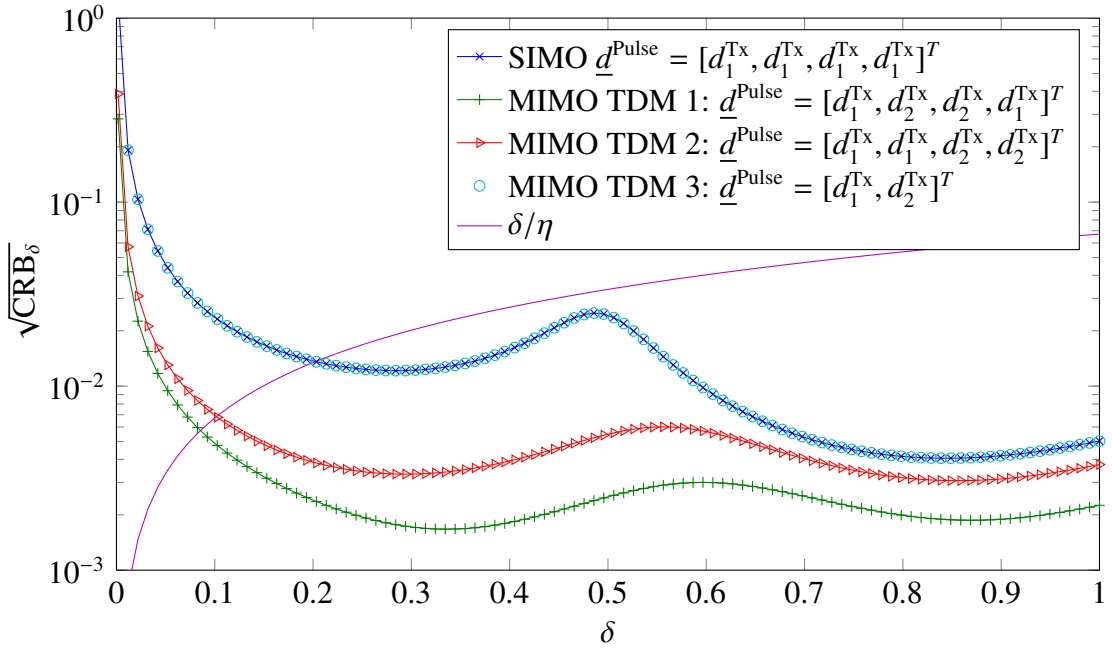

Figure 5.35.: Angular resolution for DOA estimation of two moving targets: it is obtained by the intersection of δ/η and $\sqrt{\text{CRB}_\delta(\delta)}$.

For the computation of the resolution, the parameters of interest are $\Delta U, \Delta\omega$ and the nuisance parameters are $[U_1, \omega_1, \underline{s}(1), \ldots, \underline{s}(L), \sigma^2]^T$. We investigate the case with $\Delta\omega = 0$ and equal signal strengths $s_1 = s_2$. Then, using (5.191) and due to symmetry, $\mathbf{CRB}_{(\underline{\Theta}^{(1)}, \underline{\Theta}^{(2)})}$ depends on $|\Delta U|$. The angular resolution δ_{ARL} is defined implicitly as the solution of [El Korso et al., 2011]

$$\delta_{\text{ARL}} = \eta \sqrt{\text{CRB}_\delta(\delta_{\text{ARL}})}. \tag{5.202}$$

Here, η is a factor which depends on the probability of false alarm P_{FA} and probability of detection P_{D}

$$\eta = \eta(P_{\text{FA}}, P_{\text{D}}) \tag{5.203}$$

and CRB_δ is the CRB of the parameter $\delta = |\Delta U|$. Note that CRB_δ is a function of δ, i. e. $\text{CRB}_\delta = \text{CRB}_\delta(\delta)$. It can be computed by using the rule of transformation of parameters [Kay, 1993] and is given by [El Korso et al., 2011]

$$\text{CRB}_\delta = \left[\mathbf{CRB}_{\underline{U}}\right]_{1,1} + \left[\mathbf{CRB}_{\underline{U}}\right]_{2,2} - 2\left[\mathbf{CRB}_{\underline{U}}\right]_{1,2}. \tag{5.204}$$

Using (5.202) the resolution can be obtained by the intersection of δ/η and $\sqrt{\text{CRB}_\delta(\delta)}$. We set $P_{\text{FA}} = 0.01$ and $P_{\text{D}} = 0.9$ which results in $\eta \approx 14.9$. For an interpretation of this resolution definition see Section 2.2.3.

δ/η and $\sqrt{\text{CRB}_\delta}$ are depicted in Fig. 5.35 for different TDM schemes. The parameters of the radar system are the same as in Fig. 5.34. The TDM scheme 1 with $\underline{d}^{\text{Pulse}} = [d_1^{\text{Tx}}, d_2^{\text{Tx}}, d_2^{\text{Tx}}, d_1^{\text{Tx}}]^T$ achieves

the best resolution $\delta_{\mathrm{ARL}} \approx 0.09$. In this case, $\underline{d}^{\mathrm{Pulse}}$ satisfies the condition of Theorem 5 which yields a decoupling of the electrical angles and Doppler frequencies. TDM scheme 2 does not satisfy the condition of Theorem 5. It achieves a worse resolution. TDM scheme 3 achieves the same resolution as the SIMO radar, i.e. using only one transmitter. In that case $\delta_{\mathrm{ARL}} \approx 0.2$. This behavior is similar to the CRBs depicted in Fig. 5.32 and explained there. Hence, the resolution of the MIMO radar using TDM scheme 1 is approximately half as large as the resolution of the SIMO radar or the MIMO radar using TDM scheme 3.

The resolution of a TDM MIMO radar depends crucially on the chosen TDM scheme and can be significantly improved compared to a SIMO radar by optimizing the TDM scheme.

5.3.6. Summary

We have investigated the DOA estimation of two moving targets for a TDM MIMO radar. After introducing the signal model, the CRB for the parameters of interest, the DOAs and Doppler frequencies, was derived and we interpreted the resulting equation. Since the CRB depends on many target parameters and due to the complexity of CRB, it is difficult to find general statements which are valid for all target parameters. Because of this, we investigated the important case where both targets have the same Doppler frequency, $\Delta\omega = 0$. For this case, conditions for TDM schemes were derived such that the CRB of the DOAs is decoupled from the CRB of the Doppler frequencies. These conditions can be used to find good TDM schemes. These TDM schemes achieve a DOA accuracy which is as good as if the Doppler frequencies are known a priori. We compared the CRB of MIMO radars using different TDM schemes. Moreover, we have confirmed the analytical computations by numerical simulations. These simulations show that the ML estimator indeed achieves the CRB. Moreover, the CRB was used to define the angular resolution. We have shown that the angular resolution depends on the chosen TDM scheme of the MIMO radar and can be better than that of the SIMO radar, despite the unknown Doppler frequencies. Moreover, in the investigated scenario, the TDM scheme which fulfills the decoupling condition achieves a high angular resolution.

5.4. Arbitrary Number of Moving Targets

In the previous sections, we have investigated the DOA estimation of one and two moving targets. In doing so, we have derived the CRB for the electrical angles and Doppler frequencies. One important result are the conditions which are sufficient for a decoupling of the electrical angles and Doppler frequencies in the CRB (Theorem 2 and 5). If these conditions are fulfilled, a DOA accuracy can be achieved as good as if the Doppler frequencies are already known a priori. The conditions are the same for the one target and two target case. Hence the question arises, if the same decoupling conditions are also true in the case of an arbitrary number of moving targets. The part of CRB which

corresponds to the electrical angles and Doppler frequencies $\mathbf{CRB}_{\left(\underline{\Theta}^{(1)},\ldots,\underline{\Theta}^{(N_{\text{Targets}})}\right)}$ is given in (5.161). A further simplified analytical expression as in the case of two targets is not feasible or only feasible with a high effort. We present and proof the conditions which lead to a decoupling by using the result (5.161). As we will see in the following, we do not need a more compact expression in order to state and prove the decoupling conditions.

Decoupling of Electrical Angles and Doppler Frequencies We denote the differences of the Doppler frequencies by

$$\Delta\omega_{qr} = \omega_q - \omega_r,\ q, r \in \{1, \ldots, N_{\text{Targets}}\}. \tag{5.205}$$

As in the two target case, we focus on the case in which the targets cannot be distinguished by their Doppler frequency, i. e. $\Delta\omega_{qr} = 0\ \forall\, q, r \in \{1, \ldots, N_{\text{Targets}}\}$. The following theorem gives sufficient conditions which lead to a decoupling in that case.

Theorem 6. *Let*

$$\Delta\omega_{qr} = 0\ \forall\, q, r \in \{1, \ldots, N_{Targets}\}. \tag{5.206}$$

If

$$\mathrm{E}^{\mathrm{WS}}\left(\underline{t}^{(k)}, \underline{\rho}^{(k)}\right) = \mathrm{E}^{\mathrm{WS}}\left(\underline{t}^{(l)}, \underline{\rho}^{(l)}\right)\ \forall k, l \in \{1, \ldots, N_{Tx}\}, \tag{5.207}$$

then the elements in $\mathbf{CRB}_{\left(\underline{\Theta}^{(1)},\ldots,\underline{\Theta}^{(N_{Targets})}\right)}$ *corresponding to the electrical angles* $\underline{U}$ *decouple from the elements corresponding to the Doppler frequencies* $\underline{\omega}$*.*

Here, $\underline{t}^{(k)}$ *denotes the transmit times of the k-th Tx antenna and* $\underline{\rho}^{(k)}$ *the corresponding energies of the transmitted pulses.*

Proof. The theorem states that if (5.206) and (5.207) are fulfilled, the elements marked with $\times$ are 0

$$\mathbf{CRB}_{\left(\underline{\Theta}^{(1)},\ldots,\underline{\Theta}^{(N_{\text{Targets}})}\right)} = \begin{array}{c} \\ U_1 \\ \omega_1 \\ U_2 \\ \omega_2 \\ \vdots \\ U_{N_{\text{Targets}}} \\ \omega_{N_{\text{Targets}}} \end{array} \begin{array}{c} \begin{array}{cccccccc} U_1 & \omega_1 & U_2 & \omega_2 & \ldots & U_{N_{\text{Targets}}} & \omega_{N_{\text{Targets}}} \end{array} \\ \begin{bmatrix} . & \times & . & \times & \ldots & . & \times \\ \times & . & \times & . & \ldots & \times & . \\ . & \times & . & \times & \ldots & . & \times \\ \times & . & \times & . & \ldots & \times & . \\ \vdots & \vdots & \vdots & \vdots & \ddots & \vdots & \vdots \\ . & \times & . & \times & \ldots & . & \times \\ \times & . & \times & . & \ldots & \times & . \end{bmatrix} \end{array}. \tag{5.208}$$

Thus after a reordering of the parameters $U_1, \ldots, U_{N_{\text{Targets}}}, \omega_1, \ldots, \omega_{N_{\text{Targets}}}$, the matrix $\mathbf{CRB}_{\left(\underline{\Theta}^{(1)}, \ldots, \underline{\Theta}^{(N_{\text{Targets}})}\right)}$ is block diagonal. Therefore, it is sufficient to prove that the corresponding elements in $\mathbf{CRB}^{-1}_{\left(\underline{\Theta}^{(1)}, \ldots, \underline{\Theta}^{(N_{\text{Targets}})}\right)}$ are 0, since the inversion keeps the block diagonal structure. In order to prove this, we express $\mathbf{C}$ in (5.161) by

$$\begin{aligned} \mathbf{C} &= \mathbf{D}^H \mathbf{P}_{\mathbf{B}}^{\perp} \mathbf{D} \\ &= \mathbf{C}^{(1)} - \mathbf{C}^{(2)} \end{aligned} \tag{5.209}$$

with the definitions

$$\mathbf{C}^{(1)} = \mathbf{D}^H \mathbf{D} \qquad \in \mathbb{C}^{2N_{\text{Targets}} \times 2N_{\text{Targets}}}, \tag{5.210}$$

$$\mathbf{C}^{(2)} = \mathbf{D}^H \mathbf{B} \left(\mathbf{B}^H \mathbf{B}\right)^{-1} \mathbf{B}^H \mathbf{D} \in \mathbb{C}^{2N_{\text{Targets}} \times 2N_{\text{Targets}}}. \tag{5.211}$$

We show that the relevant elements in $\mathbf{C}^{(1)}$ are 0. The computation and inversion of the matrix $\mathbf{B}^H \mathbf{B}$ is not feasible in general. Therefore, we show which elements in $\mathbf{B}^H \mathbf{D}$ are 0 in order to conclude that the relevant elements in $\mathbf{C}^{(2)}$ are 0 without the need to compute $\left(\mathbf{B}^H \mathbf{B}\right)^{-1}$. Hence, we can proof the theorem without computing the CRB in detail. See Appendix N for the detailed proof.

Interpretation and Discussion In the worst case, if all targets have the same Doppler frequency, Theorem 6 states that by choosing an appropriate TDM scheme, the CRB for the electrical angles is as large as if the Doppler frequencies are already known. Note that we do not assume that it is a priori known that the Doppler frequencies are equal, i. e. all Doppler frequencies have to be estimated. Hence the decoupling condition does not only work for one or two moving targets, but also for an arbitrary number of moving targets. A DOA accuracy can be achieved which is as large as if the Doppler frequencies are known a priori.

Note that it is not sufficient if only some of the Doppler frequencies are the same. For example, consider 3 moving targets with $\omega_1 = \omega_2 \neq \omega_3$. The theorem does not tell you anything about the decoupling in this case. In fact, the Doppler frequencies and electrical angles of the first and second target do not decouple in general. This can be easily verified by computing $\mathbf{CRB}_{\left(\underline{\Theta}^{(1)}, \ldots, \underline{\Theta}^{(N_{\text{Targets}})}\right)}$ (5.161) numerically for a specific counterexample with $N_{\text{Targets}} = 3$. Thus the influence of the third target prevents the decoupling of the first and second target.

5.5. Summary and Conclusions

In this chapter we have studied the DOA estimation of moving targets using a TDM MIMO radar. We derived the signal model and saw that the relative movement of the targets causes an additional phase shift due to the Doppler effect. Thus, the Doppler frequencies of the targets have to be estimated in addition to the DOAs. In general, this leads to a decrease in the DOA accuracy.

We analyzed the DOA estimation of one, two and several moving targets. In order to do that, we derived the CRB for these cases.

For one moving target, we compared the CRB of a SIMO radar to that of a MIMO radar with a stationary target. The results of the comparison for a planar array are given in Lemma 5.2.1 and for a linear array in Theorem 1. After that sufficient conditions were presented in Theorem 2 which lead to the vanishing of the coupling term between the electrical angles and the Doppler frequency in the CRB. If these conditions are satisfied, the CRB of the electrical angles for the moving target and the stationary target are equal. This theorem is the main result of this chapter. We demonstrated by numerical simulations that a DOA accuracy can be achieved, which is as good as if the Doppler frequencies are known a priori. Moreover we derived optimal TDM schemes which minimize the CRB of a linear MIMO array under different constraints. Theorem 3 states optimal TDM schemes under a limited transmission power and geometrical size of the antenna array. In Theorem 4 optimal TDM schemes are presented under the additional constraints of equidistant transmission times and equal transmission energy of the pulses.

For two moving targets, we investigated the decoupling condition for the special case, in which both targets have the same Doppler frequency (Theorem 5). We also investigated the resolution, which was defined using the two target CRB. Finally we extended the considerations to an arbitrary number of moving targets which is presented in Theorem 6.

6. Conclusions and Future Work

We summarize the presented work, draw conclusions and give an outlook on possible future work.

6.1. Conclusions

MIMO radars with colocated Tx and Rx antennas are a promising radar type to achieve a high performance in DOA estimation. They can be useful in automotive applications, which require good DOA estimates although the antenna arrays are limited to a small geometrical size and only a small number of antennas is used. We have investigated TDM MIMO radars and studied the DOA accuracy as well as the resolution.

The background and basics of radar systems have been presented in Chapter 2. We explained the working principle of a pulse Doppler, an FMCW, and a chirp sequence radar. After that we introduced the concept of parameter estimation and the statistical properties of an estimator: Bias, covariance and mean square error. We defined the accuracy and introduced the CRB as a lower bound on the covariance matrix. Finally, a definition of the resolution has been presented which is based on the CRB from estimation theory and the general likelihood ratio test (GLRT) from detection theory.

Chapter 3 gives an overview on MIMO radars and their current state of the art. First we introduced the two different types of MIMO radars: the MIMO radar with widely separated antennas and the MIMO radar with colocated antennas. We focused on the colocated MIMO radar and explained the concept of the virtual array. We gave an overview on the research which was already done on MIMO radars. After that different multiplexing techniques, frequency, code, and time division multiplexing, have been discussed. We explained their advantages and disadvantages. A TDM MIMO radar has low hardware requirements and can use the already optimized transmit waveforms used in SIMO radars. These are two important advantages for the use as an automobile radar system. Because of this, we focused on the investigation of TDM MIMO radars in this thesis. We described experimental investigations done with TDM MIMO radars and noted that quantitative and theoretical comparisons to different MIMO radars were still missing.

In Chapter 4, we investigated the DOA estimation of stationary targets. We introduced the signal models for the DOA estimation using a SIMO and MIMO radar, respectively. To study the maximal

achievable DOA accuracy, the CRB for the DOA has been derived for the SIMO and MIMO radar. In order to compare both systems, we computed the SNR after the baseband signal has been pulse compressed. This allows a quantitative comparison. The SIMO has the advantages of a Tx beamforming gain, if the beam is steered in the target's direction. To do this, the target's DOA has to be known approximately a priori. The MIMO radar offers a larger virtual aperture than the SIMO radar. Hence, dependent on the application and the positions of the Rx and Tx antennas, the MIMO or the SIMO radar can achieve a higher accuracy. In automotive applications, the advantage of a large aperture is important and due to this we focused our investigations on MIMO radars. Moreover, we compared the TDM to a CDM MIMO radar. We studied the case that one Tx antenna can transmit the maximal allowed total transmission power. In that case, the CRBs of the DOAs for both systems are equal. Moreover, we showed with the help of sufficient statistics that, for a certain structure of the noise covariance matrix, the received signals of both radar types contain the same amount of information on the DOA. Then, all properties which depend on the likelihood function, e. g. the sidelobe levels and resolution, are the same for the CDM and TDM MIMO radar.

The main part of our research is devoted to the study of DOA estimation of moving targets in Chapter 5. A target which is moving relative to the radar causes a phase shift in the baseband signal due to the Doppler effect in addition to the phase shift due to the DOA. In general, this leads to a decrease in the DOA accuracy, since the Doppler frequency has to be estimated as well. First we derived the signal model of the baseband signal of a transmitted chirp in order to compute the phase relation between the pulse compressed signal of successive chirps. Using this result, we introduced the signal model for DOA estimation of a moving target using a TDM MIMO radar. We computed the CRB for the DOA and Doppler frequency for planar Tx and Rx arrays in order to analyze the maximal achievable DOA accuracy. A theorem was deduced which characterized TDM schemes such that the DOA decouples from the Doppler frequency in the CRB. Hence, the CRB of the DOAs is as large as the CRB for the DOAs of a stationary target. Therefore, the whole virtual aperture of the MIMO radar can be used for the DOA estimation. Moreover, for linear arrays, we derived optimal TDM schemes which minimize the CRB of the DOA under different practical boundary conditions. Numerical simulations were presented, which confirmed the analytical findings.

We also investigated the DOA performance of a TDM MIMO radar in the estimation of the DOAs of several targets. We considered the two target case and computed the CRB of the DOAs and Doppler frequencies. For the case that both targets have the same Doppler frequency, TDM schemes were derived which result in a decoupling of the DOAs of the Doppler frequencies. In that case, similar to the one target DOA estimation, the CRB of the DOAs is the same as for stationary targets. Numerical simulations were carried out to verify the analytical computations. With the help of the two target CRB, we computed the DOA resolution of the TDM MIMO radar. Finally, we investigated the DOA estimation of more than two targets. Similar to the two target case, we derived a theorem which states conditions on the TDM schemes such that the DOAs decouple from the Doppler frequencies.

The results show that a TDM MIMO radar is a suitable system to be used in an automobile. It is

important to choose an appropriate TDM scheme. With a good TDM scheme, the TDM MIMO radar can achieve a high DOA performance despite a small geometrical size.

6.2. Future Work

We have investigated the DOA accuracy of a TDM MIMO radar. Another important property are the sidelobe levels in DOA and Doppler estimation. In a future work, the sidelobe levels of different TDM schemes can be studied and compared. Moreover, the Rx and Tx antenna positions, including the TDM scheme, can be optimized such that a high DOA accuracy is obtained under the constraint of a maximum sidelobe level. This ensures that the probability of outliers, i. e. completely wrong estimates, is small.

For stationary targets we have compared the TDM and CDM MIMO radars. The investigation can be generalized to moving targets, although an analytical comparison could be difficult to obtain.

Another issue is the robustness of a radar against different perturbation which are not considered in the model. For example, the positions of the Rx and Tx antennas may not coincide with the values used in the model due to fabrication uncertainties. It is interesting and important to know, how sensitive the radar reacts on perturbations. A first way to study the robustness can be achieved by numerical simulations: the estimator is evaluated with a signal which does not coincide with the modeled signal, but is a perturbed version of it.

Another topic is multipath propagation. The transmitted signal does not travel directly to the target and back, but is reflected one or several times in between. In an automotive environment, an additional reflection can occur at the traffic barrier for example. Then, in general the direction of departure (DOD) and the direction of arrival is not the same anymore. Therefore, the virtual array concept has to be modified to include this fact. This results in a new signal model for the DOA and the additional DOD estimation with a MIMO radar.

Moreover, in a future work the anisotropy of the Rx and Tx antennas can be incorporated in the signal model. This is important when evaluating measured signals, since real antennas do not have an isotropic characteristic. After measuring the antenna characteristics, the CRB of the DOA can be calculated by determining the derivatives of the measured steering vectors numerically. Then, the CRB can be compared to the experimentally determined MSE of the estimated DOA.

A. Sample Statistics

We define the sample statistics of matrices and vectors in Section A.1 and derive some properties in Section A.2.

A.1. Definitions

We define different sample statistics for two matrices $\mathbf{X} \in \mathbb{C}^{K \times N_1}, \mathbf{Y} \in \mathbb{C}^{K \times N_2}$ and one weight vector $\underline{w} \in \mathbb{C}^K$ with $\underline{1}^T \underline{w} \neq 0$. K can be regarded as the number of samples, N_1 and N_2 as the number of variables. We define the

- weighted sample mean

$$\underline{\mu}_{\mathbf{X}}^{\underline{w}} = \mathrm{E}^{\mathrm{WS}}(\mathbf{X}, \underline{w}) = \frac{1}{\underline{1}^T \underline{w}} \underline{w}^T \mathbf{X} \in \mathbb{C}^{1 \times N_1}, \tag{A.1}$$

- weighted sample cross-correlation

$$\mathrm{Corr}^{\mathrm{WS}}(\mathbf{X}, \mathbf{Y}, \underline{w}) = \frac{1}{\underline{1}^T \underline{w}} \mathbf{Y}^H \,\mathrm{diag}(\underline{w})\, \mathbf{X} \in \mathbb{C}^{N_2 \times N_1}, \tag{A.2}$$

- weighted sample cross-covariance

$$\mathrm{Cov}^{\mathrm{WS}}(\mathbf{X}, \mathbf{Y}, \underline{w}) = \mathrm{Corr}^{\mathrm{WS}}\left(\mathbf{X} - \underline{1}\ \mathrm{E}^{\mathrm{WS}}(\mathbf{X}, \underline{w}), \mathbf{Y} - \underline{1}\ \mathrm{E}^{\mathrm{WS}}(\mathbf{Y}, \underline{w}^*), \underline{w}\right) \in \mathbb{C}^{N_2 \times N_1}, \tag{A.3}$$

- weighted sample covariance

$$\mathrm{Cov}^{\mathrm{WS}}(\mathbf{X}, \underline{w}) = \mathrm{Cov}^{\mathrm{WS}}(\mathbf{X}, \mathbf{X}, \underline{w}) \in \mathbb{C}^{N_1 \times N_1}. \tag{A.4}$$

If $\underline{w} \propto \underline{1}_K$, all weights in $\underline{w}$ are equal and the above defined weighted sample mean, cross-correlation, cross-covariance and covariance simplify to the simple sample mean $\mathrm{E}^{\mathrm{S}}(\mathbf{X})$, sample cross-correlation

$\mathrm{Corr}^{\mathrm{S}}(\mathbf{X}, \mathbf{Y})$, sample cross-covariance $\mathrm{Cov}^{\mathrm{S}}(\mathbf{X}, \mathbf{Y})$ and sample covariance $\mathrm{Cov}^{\mathrm{S}}(\mathbf{X})$, respectively,

$$\mathrm{E}^{\mathrm{S}}(\mathbf{X}) = \frac{1}{K}\, \underline{1}_K^T \mathbf{X} \in \mathbb{C}^{1\times N_1}, \tag{A.5}$$

$$\mathrm{Corr}^{\mathrm{S}}(\mathbf{X}, \mathbf{Y}) = \frac{1}{K} \mathbf{Y}^H \mathbf{X} \in \mathbb{C}^{N_2\times N_1}, \tag{A.6}$$

$$\mathrm{Cov}^{\mathrm{S}}(\mathbf{X}, \mathbf{Y}) = \mathrm{Corr}^{\mathrm{S}}\left(\mathbf{X} - \underline{1}\ \mathrm{E}^{\mathrm{S}}(\mathbf{X})\,, \mathbf{Y} - \underline{1}\ \mathrm{E}^{\mathrm{S}}(\mathbf{Y})\right) \in \mathbb{C}^{N_2\times N_1}, \tag{A.7}$$

$$\mathrm{Cov}^{\mathrm{S}}(\mathbf{X}) = \mathrm{Cov}^{\mathrm{S}}(\mathbf{X}, \mathbf{X}) \in \mathbb{C}^{N_1\times N_1}. \tag{A.8}$$

In the special case of a vector $\underline{x} \in \mathbb{C}^K$, we write the weighted sample variance $\mathrm{Var}^{\mathrm{WS}}(\underline{x}, \underline{w})$ and the sample variance $\mathrm{Var}^{\mathrm{S}}(\underline{x})$ instead of $\mathrm{Cov}^{\mathrm{WS}}(\underline{x}, \underline{w})$ and $\mathrm{Cov}^{\mathrm{S}}(\underline{x})$, respectively, i. e.

$$\mathrm{Var}^{\mathrm{WS}}(\underline{x}, \underline{w}) = \mathrm{Cov}^{\mathrm{WS}}(\underline{x}, \underline{w}) \in \mathbb{C}, \tag{A.9}$$

$$\mathrm{Var}^{\mathrm{S}}(\underline{x}) = \mathrm{Cov}^{\mathrm{S}}(\underline{x}) \in \mathbb{C}. \tag{A.10}$$

A.2. Lemmas of the Sample Statistics

We state different lemmas of the sample statistics defined above. The proofs are given in Section A.2.5.

In the following, we assume

- $s, s_1, s_2 \in \mathbb{C}$.
- $\underline{w}, \underline{z} \in \mathbb{C}^K$ and $\underline{c} \in \mathbb{C}^M$, with $\underline{1}^T\underline{w}, \underline{1}^T\underline{z}, \underline{1}^T\underline{c} \neq 0$ and $\underline{1}^T(\underline{z} \otimes \underline{c}) \neq 0$.
- $\otimes$ is the Kronecker tensor product. For two matrices $\mathbf{C} \in \mathbb{C}^{S\times T}, \mathbf{D} \in \mathbb{C}^{U\times V}$ it is defined as $\mathbf{C} \otimes \mathbf{D} = \begin{bmatrix} C_{11}\mathbf{D} & \dots & C_{1T}\mathbf{D} \\ \vdots & \ddots & \vdots \\ C_{S1}\mathbf{D} & \dots & C_{ST}\mathbf{D} \end{bmatrix} \in \mathbb{C}^{S\cdot U\times T\cdot V}$. The Kronecker product of two vectors is a special case of this definition.
- $\mathbf{U}, \mathbf{X} \in \mathbb{C}^{K\times N_1}, \mathbf{V}, \mathbf{Y} \in \mathbb{C}^{K\times N_2}$ and $\mathbf{A} \in \mathbb{C}^{M\times P_1}, \mathbf{B} \in \mathbb{C}^{M\times P_2}$ (K, M can be regarded as the number of samples, N_1, N_2, P_1, P_2 as the number of variables).
- $\underline{1}_K \in \mathbb{R}^K$ is a vector with all elements equal 1. $\underline{1}$ is a shortcut with the dimension following from the context.
- $\mathbf{1}_{K\times M} \in \mathbb{R}^{K\times M}$ is a matrix with all elements equal 1. $\mathbf{1}$ is a shortcut with the dimensions following from the context.
- $\mathbf{0}_{K\times M} \in \mathbb{R}^{K\times M}$ is a matrix with all elements equal 0. $\mathbf{0}$ is a shortcut with the dimensions following from the context.

A.2.1. Lemmas of $\mathrm{E}^{\mathrm{S}}, \mathrm{Corr}^{\mathrm{S}}, \mathrm{Cov}^{\mathrm{S}}$

Lemma A.2.1. $\mathrm{E}^{\mathrm{S}}, \mathrm{Corr}^{\mathrm{S}}, \mathrm{Cov}^{\mathrm{S}}$ *are special cases of* $\mathrm{E}^{\mathrm{WS}}, \mathrm{Corr}^{\mathrm{WS}}, \mathrm{Cov}^{\mathrm{WS}}$ *respectively. Hence all properties of* $\mathrm{E}^{\mathrm{WS}}, \mathrm{Corr}^{\mathrm{WS}}, \mathrm{Cov}^{\mathrm{WS}}$ *apply to* $\mathrm{E}^{\mathrm{S}}, \mathrm{Corr}^{\mathrm{S}}, \mathrm{Cov}^{\mathrm{S}}$*, respectively, as well.*

A.2.2. Lemmas of E^{WS}

Lemma A.2.2. *From the definitions*

$$\mathrm{E}^{\mathrm{WS}}(\mathbf{X}, \underline{w}) = \mathrm{Corr}^{\mathrm{WS}}(\mathbf{X}, \underline{1}_K, \underline{w}),$$
$$\mathrm{E}^{\mathrm{WS}}(\mathbf{Y}, \underline{w})^H = \mathrm{Corr}^{\mathrm{WS}}(\underline{1}_K, \mathbf{Y}, \underline{w}^*)$$

follow.

Due to Lemma A.2.2 and the properties of $\mathrm{Corr}^{\mathrm{WS}}$ given in Section A.2.3, the subsequent lemmas follow:

Lemma A.2.3. E^{WS} *is linear in its first argument*

$$\mathrm{E}^{\mathrm{WS}}(s\,\mathbf{X}, \underline{w}) = s\ \mathrm{E}^{\mathrm{WS}}(\mathbf{X}, \underline{w})$$
$$\mathrm{E}^{\mathrm{WS}}(\mathbf{U} + \mathbf{X}, \underline{w}) = \mathrm{E}^{\mathrm{WS}}(\mathbf{U}, \underline{w}) + \mathrm{E}^{\mathrm{WS}}(\mathbf{X}, \underline{w})$$

Lemma A.2.4.

$$\mathrm{E}^{\mathrm{WS}}(\mathbf{X} \otimes \mathbf{A}, \underline{z} \otimes \underline{c}) = \mathrm{E}^{\mathrm{WS}}(\mathbf{X}, \underline{z}) \otimes \mathrm{E}^{\mathrm{WS}}(\mathbf{A}, \underline{c}) \in \mathbb{C}^{1 \times N_1 P_1}$$

Lemma A.2.5.

$$\mathrm{E}^{\mathrm{WS}}(\mathbf{X} \otimes \mathbf{1}_{M \times P_1}, \underline{z} \otimes \underline{c}) = \mathrm{E}^{\mathrm{WS}}(\mathbf{X}, \underline{z}) \otimes \underline{1}_{P_1}^T \in \mathbb{C}^{1 \times N_1 P_1}$$
$$\mathrm{E}^{\mathrm{WS}}(\mathbf{1}_{K \times N_1} \otimes \mathbf{A}, \underline{z} \otimes \underline{c}) = \underline{1}_{N_1}^T \otimes \mathrm{E}^{\mathrm{WS}}(\mathbf{A}, \underline{c}) \in \mathbb{C}^{1 \times N_1 P_1}$$

Lemma A.2.6.

$$\mathrm{E}^{\mathrm{WS}}(\mathbf{X} \otimes \mathbf{1}_{M \times P_1}, \underline{1}_K \otimes \underline{c}) = \mathrm{E}^{\mathrm{S}}(\mathbf{X}) \otimes \underline{1}_{P_1}^T$$
$$\mathrm{E}^{\mathrm{WS}}(\mathbf{1}_{K \times N_1} \otimes \mathbf{A}, \underline{z} \otimes \underline{1}_M) = \underline{1}_{N_1}^T \otimes \mathrm{E}^{\mathrm{S}}(\mathbf{A})$$

A.2.3. Lemmas of $\mathrm{Corr}^{\mathrm{WS}}$

Lemma A.2.7. *From the definition follows*

$$\mathrm{Corr}^{\mathrm{WS}}(\mathbf{X}, \mathbf{Y}, \underline{w}) = \mathrm{Corr}^{\mathrm{WS}}(\mathbf{Y}, \mathbf{X}, \underline{w}^*)^H$$

Lemma A.2.8. *From the definition follows that* $\mathrm{Corr}^{\mathrm{WS}}$ *is sesquilinear in its first two arguments*

$$\begin{aligned}
&\mathrm{Corr}^{\mathrm{WS}}(s_1\mathbf{X}, s_2\mathbf{Y}, \underline{w}) = s_1 s_2^* \,\mathrm{Corr}^{\mathrm{WS}}(\mathbf{X}, \mathbf{Y}, \underline{w}) \\
&\mathrm{Corr}^{\mathrm{WS}}(\mathbf{U} + \mathbf{X}, \mathbf{V} + \mathbf{Y}, \underline{w}) \\
&= \mathrm{Corr}^{\mathrm{WS}}(\mathbf{U}, \mathbf{V}, \underline{w}) + \mathrm{Corr}^{\mathrm{WS}}(\mathbf{U}, \mathbf{Y}, \underline{w}) + \mathrm{Corr}^{\mathrm{WS}}(\mathbf{X}, \mathbf{V}, \underline{w}) + \mathrm{Corr}^{\mathrm{WS}}(\mathbf{X}, \mathbf{Y}, \underline{w})
\end{aligned}$$

Lemma A.2.9.

$$\mathrm{Corr}^{\mathrm{WS}}(\mathbf{X} \otimes \mathbf{A}, \mathbf{Y} \otimes \mathbf{B}, \underline{z} \otimes \underline{c}) = \mathrm{Corr}^{\mathrm{WS}}(\mathbf{X}, \mathbf{Y}, \underline{z}) \otimes \mathrm{Corr}^{\mathrm{WS}}(\mathbf{A}, \mathbf{B}, \underline{c}) \in \mathbb{C}^{N_2P_2 \times N_1P_1}$$

Lemma A.2.10.

$$\begin{aligned}
\mathrm{Corr}^{\mathrm{WS}}(\mathbf{X} \otimes \mathbf{1}_{M\times P_1}, \mathbf{Y} \otimes \mathbf{1}_{M\times P_2}, \underline{z} \otimes \underline{c}) &= \mathrm{Corr}^{\mathrm{WS}}(\mathbf{X}, \mathbf{Y}, \underline{z}) \otimes \mathbf{1}_{P_2\times P_1} \in \mathbb{C}^{N_2P_2 \times N_1P_1} \\
\mathrm{Corr}^{\mathrm{WS}}(\mathbf{1}_{K\times N_1} \otimes \mathbf{A}, \mathbf{1}_{K\times N_2} \otimes \mathbf{B}, \underline{z} \otimes \underline{c}) &= \mathbf{1}_{N_2\times N_1} \otimes \mathrm{Corr}^{\mathrm{WS}}(\mathbf{A}, \mathbf{B}, \underline{c}) \in \mathbb{C}^{N_2P_2 \times N_1P_1}
\end{aligned}$$

Lemma A.2.11.

$$\begin{aligned}
\mathrm{Corr}^{\mathrm{WS}}(\mathbf{X} \otimes \mathbf{1}_{M\times P_1}, \mathbf{Y} \otimes \mathbf{1}_{M\times P_2}, \underline{1}_K \otimes \underline{c}) &= \mathrm{Corr}^{\mathrm{S}}(\mathbf{X}, \mathbf{Y}) \otimes \mathbf{1}_{P_2\times P_1} \in \mathbb{C}^{N_2P_2 \times N_1P_1} \\
\mathrm{Corr}^{\mathrm{WS}}(\mathbf{1}_{K\times N_1} \otimes \mathbf{A}, \mathbf{1}_{K\times N_2}\mathbf{B}, \underline{z} \otimes \underline{1}_M) &= \mathbf{1}_{N_2\times N_1} \otimes \mathrm{Corr}^{\mathrm{S}}(\mathbf{A}, \mathbf{B}) \in \mathbb{C}^{N_2P_2 \times N_1P_1}
\end{aligned}$$

A.2.4. Lemmas of $\mathrm{Cov}^{\mathrm{WS}}$

Lemma A.2.12.

$$\begin{aligned}
\mathrm{Cov}^{\mathrm{WS}}(\mathbf{X}, \mathbf{Y}, \underline{w}) &= \mathrm{Corr}^{\mathrm{WS}}(\mathbf{X}, \mathbf{Y}, \underline{w}) - \mathrm{E}^{\mathrm{WS}}(\mathbf{Y}, \underline{w}^*)^H \,\mathrm{E}^{\mathrm{WS}}(\mathbf{X}, \underline{w}) \\
&= \mathrm{Corr}^{\mathrm{WS}}(\mathbf{X}, \mathbf{Y}, \underline{w}) - \mathrm{E}^{\mathrm{WS}}(\mathbf{Y}^*, \underline{w})^T \,\mathrm{E}^{\mathrm{WS}}(\mathbf{X}, \underline{w})
\end{aligned}$$

Lemma A.2.13. *Due to Lemma A.2.12 and the properties of* E^{WS} *and* $\mathrm{Corr}^{\mathrm{WS}}$*, it follows that* $\mathrm{Cov}^{\mathrm{WS}}$ *is sesquilinear in its first two arguments*

$$\begin{aligned}
&\mathrm{Cov}^{\mathrm{WS}}(s_1\mathbf{X}, s_2\mathbf{Y}, \underline{w}) = s_1 s_2^* \,\mathrm{Cov}^{\mathrm{WS}}(\mathbf{X}, \mathbf{Y}, \underline{w}) \\
&\mathrm{Cov}^{\mathrm{WS}}(\mathbf{U} + \mathbf{X}, \mathbf{V} + \mathbf{Y}, \underline{w}) \\
&= \mathrm{Cov}^{\mathrm{WS}}(\mathbf{U}, \mathbf{V}, \underline{w}) + \mathrm{Cov}^{\mathrm{WS}}(\mathbf{U}, \mathbf{Y}, \underline{w}) + \mathrm{Cov}^{\mathrm{WS}}(\mathbf{X}, \mathbf{V}, \underline{w}) + \mathrm{Cov}^{\mathrm{WS}}(\mathbf{X}, \mathbf{Y}, \underline{w})
\end{aligned}$$

Lemma A.2.14. *Due to Lemma A.2.12 and the properties of* E^{WS} *and* $\mathrm{Corr}^{\mathrm{WS}}$

$$\begin{aligned}
&\mathrm{Cov}^{\mathrm{WS}}(\mathbf{X} \otimes \mathbf{A}, \mathbf{Y} \otimes \mathbf{B}, \underline{z} \otimes \underline{c}) \\
&= \mathrm{Corr}^{\mathrm{WS}}(\mathbf{X}, \mathbf{Y}, \underline{z}) \otimes \mathrm{Corr}^{\mathrm{WS}}(\mathbf{A}, \mathbf{B}, \underline{c}) - \left(\mathrm{E}^{\mathrm{WS}}(\mathbf{Y}, \underline{z}^*)^H \,\mathrm{E}^{\mathrm{WS}}(\mathbf{X}, \underline{z})\right) \otimes \left(\mathrm{E}^{\mathrm{WS}}(\mathbf{B}, \underline{c}^*)^H \,\mathrm{E}^{\mathrm{WS}}(\mathbf{A}, \underline{c})\right) \\
&\not\equiv \mathrm{Cov}^{\mathrm{WS}}(\mathbf{X}, \mathbf{Y}, \underline{z}) \otimes \mathrm{Cov}^{\mathrm{WS}}(\mathbf{A}, \mathbf{B}, \underline{c})
\end{aligned}$$

follows.

Lemma A.2.15.

$$\mathrm{Cov}^{\mathrm{WS}}(\mathbf{1}_{K\times N_1}\otimes\mathbf{A},\mathbf{Y}\otimes\mathbf{1}_{M\times P_2},\underline{z}\otimes\underline{c})=\mathbf{0}_{N_2P_2\times N_1P_1}$$

Lemma A.2.16. *Due to Lemma A.2.12 and the properties of* E^{WS} *and* $\mathrm{Corr}^{\mathrm{WS}}$*,*

$$\begin{aligned}\mathrm{Cov}^{\mathrm{WS}}(\mathbf{X}\otimes\mathbf{1}_{M\times P_1},\mathbf{Y}\otimes\mathbf{1}_{M\times P_2},\underline{z}\otimes\underline{c})&=\mathrm{Cov}^{\mathrm{WS}}(\mathbf{X},\mathbf{Y},\underline{z})\otimes\mathbf{1}_{P_2\times P_1}\in\mathbb{C}^{N_2P_2\times N_1P_1}\\ \mathrm{Cov}^{\mathrm{WS}}(\mathbf{1}_{K\times N_1}\otimes\mathbf{A},\mathbf{1}_{K\times N_2}\otimes\mathbf{B},\underline{z}\otimes\underline{c})&=\mathbf{1}_{N_2\times N_1}\otimes\mathrm{Cov}^{\mathrm{WS}}(\mathbf{A},\mathbf{B},\underline{c})\in\mathbb{C}^{N_2P_2\times N_1P_1}\end{aligned}$$

follow.

Lemma A.2.17. *From Lemma A.2.16,*

$$\begin{aligned}\mathrm{Cov}^{\mathrm{WS}}(\mathbf{X}\otimes\mathbf{1}_{M\times P_1},\mathbf{Y}\otimes\mathbf{1}_{M\times P_2},\underline{1}_K\otimes\underline{c})&=\mathrm{Cov}^{\mathrm{S}}(\mathbf{X},\mathbf{Y})\otimes\mathbf{1}_{P_2\times P_1}\in\mathbb{C}^{N_2P_2\times N_1P_1}\\ \mathrm{Cov}^{\mathrm{WS}}(\mathbf{1}_{K\times N_1}\otimes\mathbf{A},\mathbf{1}_{K\times N_2}\mathbf{B},\underline{z}\otimes\underline{1}_M)&=\mathbf{1}_{N_2\times N_1}\otimes\mathrm{Cov}^{\mathrm{S}}(\mathbf{A},\mathbf{B})\in\mathbb{C}^{N_2P_2\times N_1P_1}\end{aligned}$$

follow.

A.2.5. Proofs

A.2.5.1. Proofs of Lemmas of $\mathrm{Corr}^{\mathrm{WS}}$

Proof of A.2.9.

$$\begin{aligned}\mathrm{Corr}^{\mathrm{WS}}(\mathbf{X}\otimes\mathbf{A},\mathbf{Y}\otimes\mathbf{B},\underline{z}\otimes\underline{c})&=\frac{1}{(\underline{1}\otimes\underline{1})^T(\underline{z}\otimes\underline{c})}(\mathbf{Y}\otimes\mathbf{B})^H\left(\mathrm{diag}(\underline{z}\otimes\underline{c})\right)(\mathbf{X}\otimes\mathbf{A})\\ &=\frac{1}{\underline{1}^T\underline{z}\cdot\underline{1}^T\underline{c}}\left(\mathbf{Y}^H\otimes\mathbf{B}^H\right)\left(\mathrm{diag}(\underline{z})\otimes\mathrm{diag}(\underline{c})\right)(\mathbf{X}\otimes\mathbf{A})\\ &=\left(\frac{1}{\underline{1}^T\underline{z}}\mathbf{Y}^H\,\mathrm{diag}(\underline{z})\mathbf{X}\right)\otimes\left(\frac{1}{\underline{1}^T\underline{c}}\mathbf{B}^H\,\mathrm{diag}(\underline{c})\mathbf{A}\right)\\ &=\mathrm{Corr}^{\mathrm{WS}}(\mathbf{X},\mathbf{Y},\underline{z})\otimes\mathrm{Corr}^{\mathrm{WS}}(\mathbf{A},\mathbf{B},\underline{c})\end{aligned}$$

□

Proof of A.2.10. Using Lemma A.2.9 results in

$$\begin{aligned}\mathrm{Corr}^{\mathrm{WS}}(\mathbf{X}\otimes\mathbf{1}_{M\times P_1},\mathbf{Y}\otimes\mathbf{1}_{M\times P_2},\underline{z}\otimes\underline{c})&=\mathrm{Corr}^{\mathrm{WS}}(\mathbf{X},\mathbf{Y},\underline{z})\otimes\mathrm{Corr}^{\mathrm{WS}}(\mathbf{1}_{M\times P_1},\mathbf{1}_{M\times P_2},\underline{c})\\ &=\mathrm{Corr}^{\mathrm{WS}}(\mathbf{X},\mathbf{Y},\underline{z})\otimes\mathbf{1}_{P_2\times P_1}\end{aligned}$$

The other property follows analogously. □

Proof of A.2.11. Using Lemma A.2.9 we get

$$\begin{aligned}\operatorname{Corr}^{\mathrm{WS}}(\mathbf{X}\otimes\mathbf{1}_{M\times P_1},\mathbf{Y}\otimes\mathbf{1}_{M\times P_2},\underline{1}_K\otimes\underline{c}) &= \operatorname{Corr}^{\mathrm{WS}}(\mathbf{X},\mathbf{Y},\underline{1})\otimes\operatorname{Corr}^{\mathrm{WS}}(\mathbf{1}_{M\times P_1},\mathbf{1}_{M\times P_2},\underline{c})\\ &= \operatorname{Corr}^{\mathrm{S}}(\mathbf{X},\mathbf{Y})\otimes\mathbf{1}_{P_2\times P_1}\end{aligned}$$

The other property follows analogously. □

A.2.5.2. Proofs of Lemmas of $\mathrm{Cov}^{\mathrm{WS}}$

Proof of A.2.12.

$$\begin{aligned}&\operatorname{Cov}^{\mathrm{WS}}(\mathbf{X},\mathbf{Y},\underline{w})\\ &= \frac{1}{\underline{1}^T\underline{w}}\left(\mathbf{Y}-\underline{1}\,\mathrm{E}^{\mathrm{WS}}(\mathbf{Y},\underline{w}^*)\right)^H\operatorname{diag}(\underline{w})\left(\mathbf{X}-\underline{1}\,\mathrm{E}^{\mathrm{WS}}(\mathbf{X},\underline{w})\right)\\ &= \frac{1}{\underline{1}^T\underline{w}}\left(\mathbf{Y}^*-\underline{1}\,\mathrm{E}^{\mathrm{WS}}(\mathbf{Y}^*,\underline{w})\right)^T\operatorname{diag}(\underline{w})\left(\mathbf{X}-\underline{1}\,\mathrm{E}^{\mathrm{WS}}(\mathbf{X},\underline{w})\right)\\ &= \frac{1}{\underline{1}^T\underline{w}}\left(\mathbf{Y}^H\operatorname{diag}(\underline{w})\mathbf{X}-\mathbf{Y}^H\operatorname{diag}(\underline{w})\underline{1}\underline{\mu}_{\mathbf{X}}^{\underline{w}}-\underline{\mu}_{\mathbf{Y}^*}^{\underline{w}\,T}\underline{1}^T\operatorname{diag}(\underline{w})\mathbf{X}+\underline{\mu}_{\mathbf{Y}^*}^{\underline{w}\,T}\underline{1}^T\operatorname{diag}(\underline{w})\underline{1}\underline{\mu}_{\mathbf{X}}^{\underline{w}}\right)\\ &= \operatorname{Corr}^{\mathrm{WS}}(\mathbf{X},\mathbf{Y},\underline{w})-\underline{\mu}_{\mathbf{Y}^*}^{\underline{w}\,T}\underline{\mu}_{\mathbf{X}}^{\underline{w}}-\underline{\mu}_{\mathbf{Y}^*}^{\underline{w}\,T}\underline{\mu}_{\mathbf{X}}^{\underline{w}}+\underline{\mu}_{\mathbf{Y}^*}^{\underline{w}\,T}\underline{\mu}_{\mathbf{X}}^{\underline{w}}\\ &= \operatorname{Corr}^{\mathrm{WS}}(\mathbf{X},\mathbf{Y},\underline{w})-\mathrm{E}^{\mathrm{WS}}(\mathbf{Y}^*,\underline{w})^T\,\mathrm{E}^{\mathrm{WS}}(\mathbf{X},\underline{w})\\ &= \operatorname{Corr}^{\mathrm{WS}}(\mathbf{X},\mathbf{Y},\underline{w})-\mathrm{E}^{\mathrm{WS}}(\mathbf{Y},\underline{w}^*)^H\,\mathrm{E}^{\mathrm{WS}}(\mathbf{X},\underline{w})\end{aligned}$$

□

Proof of A.2.15. Due to Lemma A.2.14 and A.2.2

$$\begin{aligned}&\operatorname{Cov}^{\mathrm{WS}}(\mathbf{1}_{K\times N_1}\otimes\mathbf{A},\mathbf{Y}\otimes\mathbf{1}_{M\times P_2},\underline{z}\otimes\underline{c})\\ &= \operatorname{Corr}^{\mathrm{WS}}(\mathbf{1}_{K\times N_1},\mathbf{Y},\underline{z})\otimes\operatorname{Corr}^{\mathrm{WS}}(\mathbf{A},\mathbf{1}_{M\times P_2},\underline{c})\\ &\quad-\left(\mathrm{E}^{\mathrm{WS}}(\mathbf{Y},\underline{z}^*)^H\,\mathrm{E}^{\mathrm{WS}}(\mathbf{1}_{K\times N_1},\underline{z})\right)\otimes\left(\mathrm{E}^{\mathrm{WS}}(\mathbf{1}_{M\times P_2},\underline{c}^*)^H\,\mathrm{E}^{\mathrm{WS}}(\mathbf{A},\underline{c})\right)\\ &= \left(\mathrm{E}^{\mathrm{WS}}(\mathbf{Y},\underline{z}^*)^H\underline{1}_{N_1}^T\right)\otimes\left(\underline{1}_{P_2}\,\mathrm{E}^{\mathrm{WS}}(\mathbf{A},\underline{c})\right)-\left(\mathrm{E}^{\mathrm{WS}}(\mathbf{Y},\underline{z}^*)^H\underline{1}_{N_1}^T\right)\otimes\left(\underline{1}_{P_2}\,\mathrm{E}^{\mathrm{WS}}(\mathbf{A},\underline{c})\right)\\ &= \mathbf{0}\end{aligned}$$

□

B. Derivation of the Cramer-Rao Bound for a SIMO Radar

We derive the Cramer-Rao bound $\mathrm{CRB}_{u,\mathrm{SIMO}}$ in (4.13) for the electrical angle u using a SIMO radar, cf. Section 4.2.2.1.

We set

$$C_1 = \underline{D}^H \underline{D} \tag{B.1}$$

$$C_2 = \underline{D}^H \underline{g} (\underline{g}^H \underline{g})^{-1} \underline{g}^H \underline{D}. \tag{B.2}$$

Hence

$$C = C_1 - C_2. \tag{B.3}$$

We use the notation

$$\underline{a} = \underline{a}^{\mathrm{Rx}} = \exp(j\, \underline{d}^{\mathrm{Rx}} u), \tag{B.4}$$

$$B(u) = f(u) \cdot \mathrm{e}^{\,j\beta(u)} \tag{B.5}$$

with $f(u) \in \mathbb{R},\ f(u) \geq 0,\ \beta(u) \in \mathbb{R}$. Hence,

$$\underline{g}(u) = B(u)\, \underline{a}(u). \tag{B.6}$$

In the following, we use an upper dot to denote the derivative with respect to u, e. g. $\dot{f} = \frac{\partial f}{\partial u}$. With (4.11) and (4.5), $\underline{D}$ can be computed by

$$\underline{D} = \dot{\underline{g}} = \dot{B}\underline{a} + B\dot{\underline{a}}. \tag{B.7}$$

In the following, $\odot$ denotes the entrywise Hadamard product, i. e. $\underline{x} = \underline{y} \odot \underline{z}$ means $x_i = y_i \cdot z_i \forall i$. We need the following identities for further computations:

$$\underline{a}^H \underline{a} = N_{\mathrm{Rx}}, \tag{B.8}$$

$$\dot{\underline{a}} = j\underline{d}^{\mathrm{Rx}} \odot \underline{a}, \tag{B.9}$$

$$\underline{a}^H \underline{\dot{a}} = jN_{\mathrm{Rx}}\,\mathrm{E}^{\mathrm{S}}(\underline{d}^{\mathrm{Rx}}), \tag{B.10}$$

$$\underline{\dot{a}}^H \underline{\dot{a}} = N_{\mathrm{Rx}}\,\mathrm{Corr}^{\mathrm{S}}(\underline{d}^{\mathrm{Rx}}, \underline{d}^{\mathrm{Rx}}), \tag{B.11}$$

$$\dot{B} = \dot{f}\,\mathrm{e}^{j\beta} + jf\dot{\beta}\,\mathrm{e}^{j\beta} = \mathrm{e}^{j\beta}(\dot{f} + jf\dot{\beta}), \tag{B.12}$$

$$\left|\dot{B}\right|^2 = \dot{f}^2 + f^2\dot{\beta}^2, \tag{B.13}$$

$$B^*\dot{B} = f\dot{f} + jf^2\dot{\beta}, \tag{B.14}$$

where E^{S} and $\mathrm{Corr}^{\mathrm{S}}$ are defined in (A.5) and (A.6), respectively. Then

$$\begin{aligned}
C_1 &= \underline{\dot{g}}^H \underline{\dot{g}} \\
&= (\dot{B}\underline{a} + B\underline{\dot{a}})^H(\dot{B}\underline{a} + B\underline{\dot{a}}) \\
&= \left|\dot{B}\right|^2 \underline{a}^H\underline{a} + \dot{B}^*B\underline{a}^H\underline{\dot{a}} + B^*\dot{B}\underline{\dot{a}}^H\underline{a} + |B|^2\underline{\dot{a}}^H\underline{\dot{a}} \\
&= \left|\dot{B}\right|^2 N_{\mathrm{Rx}} + j\dot{B}^*BN_{\mathrm{Rx}}\,\mathrm{E}^{\mathrm{S}}(\underline{d}^{\mathrm{Rx}}) - jB^*\dot{B}N_{\mathrm{Rx}}\,\mathrm{E}^{\mathrm{S}}(\underline{d}^{\mathrm{Rx}}) + |B|^2N_{\mathrm{Rx}}\,\mathrm{Corr}^{\mathrm{S}}(\underline{d}^{\mathrm{Rx}}, \underline{d}^{\mathrm{Rx}}) \\
&= \left|\dot{B}\right|^2 N_{\mathrm{Rx}} + j\left(f\dot{f} - jf^2\dot{\beta} - (f\dot{f} + jf^2\dot{\beta})\right)N_{\mathrm{Rx}}\,\mathrm{E}^{\mathrm{S}}(\underline{d}^{\mathrm{Rx}}) + |B|^2N_{\mathrm{Rx}}\,\mathrm{Corr}^{\mathrm{S}}(\underline{d}^{\mathrm{Rx}}, \underline{d}^{\mathrm{Rx}}) \\
&= (\dot{f}^2 + f^2\dot{\beta}^2)N_{\mathrm{Rx}} + 2f^2\dot{\beta}N_{\mathrm{Rx}}\,\mathrm{E}^{\mathrm{S}}(\underline{d}^{\mathrm{Rx}}) + f^2N_{\mathrm{Rx}}\,\mathrm{Corr}^{\mathrm{S}}(\underline{d}^{\mathrm{Rx}}, \underline{d}^{\mathrm{Rx}}).
\end{aligned} \tag{B.15}$$

C_2 can be computed by

$$\begin{aligned}
C_2 &= \underline{D}^H\underline{g}\left(\underline{g}^H\underline{g}\right)^{-1}\underline{g}^H\underline{D} \\
&= \underline{\dot{g}}^H\underline{g}\left(\underline{g}^H\underline{g}\right)^{-1}\underline{g}^H\underline{\dot{g}} \\
&= \left(\underline{g}^H\underline{\dot{g}}\right)^*\left(\underline{g}^H\underline{g}\right)^{-1}\underline{g}^H\underline{\dot{g}} \\
&= \frac{1}{\|\underline{g}\|^2}\left|\underline{g}^H\underline{\dot{g}}\right|^2,
\end{aligned} \tag{B.16}$$

$$\begin{aligned}
\underline{g}^H\underline{\dot{g}} &= (B\underline{a})^H(\dot{B}\underline{a} + B\underline{\dot{a}}) \\
&= B^*\dot{B}N_{\mathrm{Rx}} + j|B|^2N_{\mathrm{Rx}}\,\mathrm{E}^{\mathrm{S}}(\underline{d}^{\mathrm{Rx}}) \\
&= f\dot{f}N_{\mathrm{Rx}} + jN_{\mathrm{Rx}}\left(f^2\dot{\beta} + f^2\,\mathrm{E}^{\mathrm{S}}(\underline{d}^{\mathrm{Rx}})\right),
\end{aligned} \tag{B.17}$$

$$\|\underline{g}\|^2 = f^2N_{\mathrm{Rx}}, \tag{B.18}$$

$$\begin{aligned}
C_2 &= \frac{{N_{\mathrm{Rx}}}^2}{f^2N_{\mathrm{Rx}}}\left[\left(f\dot{f}\right)^2 + \left(f^2\dot{\beta} + f^2\,\mathrm{E}^{\mathrm{S}}(\underline{d}^{\mathrm{Rx}})\right)^2\right] \\
&= \dot{f}^2N_{\mathrm{Rx}} + f^2N_{\mathrm{Rx}}\left(\dot{\beta} + \mathrm{E}^{\mathrm{S}}(\underline{d}^{\mathrm{Rx}})\right)^2 \\
&= \dot{f}^2N_{\mathrm{Rx}} + f^2N_{\mathrm{Rx}}\left(\dot{\beta}^2 + 2\dot{\beta}\,\mathrm{E}^{\mathrm{S}}(\underline{d}^{\mathrm{Rx}}) + \mathrm{E}^{\mathrm{S}}(\underline{d}^{\mathrm{Rx}})^2\right).
\end{aligned} \tag{B.19}$$

Putting the expressions (B.15) and (B.19) in (B.3) yields

$$\begin{aligned}
C &= f^2N_{\mathrm{Rx}}\left(\mathrm{Corr}^{\mathrm{S}}(\underline{d}^{\mathrm{Rx}}, \underline{d}^{\mathrm{Rx}}) - \mathrm{E}^{\mathrm{S}}(\underline{d}^{\mathrm{Rx}})^2\right) \\
&= f^2N_{\mathrm{Rx}}\,\mathrm{Var}^{\mathrm{S}}(\underline{d}^{\mathrm{Rx}}),
\end{aligned} \tag{B.20}$$

where we have used the property of $\mathrm{Var}^{\mathrm{S}}$ given in Lemma A.2.1 and A.2.12. Since all variables in (B.20) are real, $C \in \mathbb{R}$. Using (4.8) and substituting f by $|B|$ results in

$$\mathrm{CRB}^{-1}_{u,\mathrm{SIMO}} = 2L \, \frac{\sigma^2_{s,\mathrm{SIMO}}}{\sigma^2} |B(u)|^2 N_{\mathrm{Rx}} \, \mathrm{Var}^{\mathrm{S}}(\underline{d}^{\mathrm{Rx}}), \tag{B.21}$$

from which (4.13) follows.

C. Maximal Beamforming Gain

We derive the maximal achievable beamforming gain for a SIMO radar with N_{Tx} Tx antennas which transmit the same waveform $s(t)$ up to a complex scaling factor. The transmitted signal of the i-th Tx antenna can be written as

$$s_i^{\mathrm{Tx}}(t) = c_i s(t) \tag{C.1}$$

with the complex scaling factor c_i. We put the scaling factors c_i in a vector $\underline{c}$. Then, the overall transmitted signal at the target's electrical angle u is

$$s^{\mathrm{Tx}}(t) = \left(\underline{a}^{\mathrm{Tx}}(u)\right)^T \underline{c} s(t) \tag{C.2}$$

with the Tx steering vector $\underline{a}^{\mathrm{Tx}}(u)$.

W. l. o. g. , we set the target's electrical angle $u = 0$. Then

$$s^{\mathrm{Tx}}(t) = s(t)\underline{1}^T \underline{c}. \tag{C.3}$$

Thus the beampattern is

$$B(0) = \underline{1}^T \underline{c}. \tag{C.4}$$

To find the maximal value $B_{\max}$ of $|B(0)|$

$$B_{\max} = \max_{\underline{c}} |B(0)|, \tag{C.5}$$

$\underline{1}^T \underline{c}$ has to be maximal or minimal. Obviously, $B(0)$ has an extremum, if the phase of c_i is the same for all i. W. l. o. g. we choose $c_i \in \mathbb{R}$, $i = 1, \ldots N_{\mathrm{Tx}}$.

The total transmission power has to be kept constant. In the case of one transmitter ($N_{\mathrm{Tx}} = 1$), $|c_1|^2 = 1$. Hence the total power constraint reads

$$\sum_{i=1}^{N_{\mathrm{Tx}}} |c_i|^2 = 1 \tag{C.6}$$

and since $c_i \in \mathbb{R}$

$$\sum_{i=1}^{N_{\mathrm{Tx}}} c_i^2 = 1. \tag{C.7}$$

Thus, we have to find the extremum of the function $f(\underline{c})$

$$f(\underline{c}) = \underline{1}^T \underline{c} \tag{C.8}$$

$$\text{s.t. } g(\underline{c}) = \sum_{i=1}^{N_{\mathrm{Tx}}} c_i^2 = 1. \tag{C.9}$$

We use the method of Lagrange Multipliers [Bronstein et al., 2008] with the Lagrangian multiplier λ and set

$$\Lambda(\underline{c}) = f(\underline{c}) + \lambda \Big(g(\underline{c}) - 1 \Big). \tag{C.10}$$

Taking the derivate of $\Lambda(\underline{c})$ with respect to $\underline{c}$ and setting it to 0 yields

$$\frac{\partial \Lambda}{\partial \underline{c}} = \underline{1} + \lambda 2 \underline{c} \stackrel{!}{=} 0. \tag{C.11}$$

Hence

$$\lambda = -\frac{1}{2c_i},\ i = 1, \dots N_{\mathrm{Tx}}. \tag{C.12}$$

Therefore

$$c_i = c_j,\ i, j = 1, \dots N_{\mathrm{Tx}}. \tag{C.13}$$

Thus, with (C.9) follows

$$\sum_{i=1}^{N_{\mathrm{Tx}}} c_i^2 = N_{\mathrm{Tx}} c_i^2 = 1,\ i = 1, \dots N_{\mathrm{Tx}}, \tag{C.14}$$

$$\text{and } c_i = \pm \sqrt{\frac{1}{N_{\mathrm{Tx}}}},\ i = 1, \dots N_{\mathrm{Tx}}. \tag{C.15}$$

This yields for $B_{\max}$ in (C.5)

$$\begin{aligned} B_{\max} &= |\underline{1}^T \underline{c}| \\ &= N_{\mathrm{Tx}} \sqrt{\frac{1}{N_{\mathrm{Tx}}}} = \sqrt{N_{\mathrm{Tx}}}. \end{aligned} \tag{C.16}$$

Thus, the maximal achievable beamforming gain for a SIMO radar using N_{Tx} antennas is $\sqrt{N_{\mathrm{Tx}}}$.

D. Computation of the SNR after a Discrete Fourier Transform

We consider a complex oscillation $\exp(j(\omega_{\text{diff}} n + \varphi))$ and compute the DFT of it. We derive the SNR of the complex amplitude of the highest peak in the spectrum as explained in Section 4.4.1. Then, we compute the SNR gain of the DFT.

The SNR after the DFT is (4.47)

$$\text{SNR}_{\text{after}} = \frac{\rho_s |S_w(\omega_{\max})|^2}{\text{Var}(N_w(\omega_{\max}))} \tag{D.1}$$

and since $\omega_{\max} = \omega_{\text{diff}}$

$$\text{SNR}_{\text{after}} = \frac{\rho_s |S_w(\omega_{\text{diff}})|^2}{\text{Var}(N_w(\omega_{\text{diff}}))}. \tag{D.2}$$

We first compute $|S_w(\omega_{\text{diff}})|^2$. Since $w(n)$ is nonzero only for $0 \leq n \leq N-1$ and using the convolution theorem [Kammeyer and Kroschel, 2012], $S_w(\omega)$ in (4.43) can be written as

$$\begin{aligned} S_w(\omega) &= \sum_{n=0}^{N-1} w(n) s(n) \, \mathrm{e}^{-j\omega n} \\ &= \sum_{n=-\infty}^{\infty} w(n) s(n) \, \mathrm{e}^{-j\omega n} \\ &= (W * S)(\omega) \end{aligned} \tag{D.3}$$

where the DTFT of $w(n)$ is

$$W(\omega) = \sum_{n=-\infty}^{\infty} w(n) \, \mathrm{e}^{-j\omega n} = \sum_{n=0}^{N-1} w(n) \, \mathrm{e}^{-j\omega n} \tag{D.4}$$

and

$$\begin{aligned} S(\omega) &= \sum_{n=-\infty}^{\infty} s(n) \, \mathrm{e}^{-j\omega n} \\ &= s_0 \, 2\pi \, \mathrm{e}^{j\varphi} \, \delta(\omega - \omega_{\text{diff}}). \end{aligned} \tag{D.5}$$

Hence

$$\begin{aligned} S_w(\omega) &= \frac{1}{2\pi}\int_{-\pi}^{\pi} W(\tilde{\omega}) S(\omega-\tilde{\omega})\,\mathrm{d}\tilde{\omega} \\ &= \frac{1}{2\pi}\int_{-\pi}^{\pi} W(\tilde{\omega})\, s_0\, 2\pi\, \mathrm{e}^{j\varphi}\,\delta(\omega-\tilde{\omega}-\omega_{\text{diff}})\,\mathrm{d}\tilde{\omega} \\ &= s_0 W(\omega-\omega_{\text{diff}})\,\mathrm{e}^{j\varphi} \end{aligned} \tag{D.6}$$

and thus

$$S_w(\omega_{\text{diff}}) = s_0 W(0)\,\mathrm{e}^{j\varphi}\,. \tag{D.7}$$

From (D.4) follows

$$W(0) = \sum_{n=0}^{N-1} w(n) \tag{D.8}$$

and therefore, since $w(n) \in \mathbb{R}$,

$$|S_w(\omega_{\text{diff}})|^2 = s_0^2\left(\sum_{n=0}^{N-1} w(n)\right)^2. \tag{D.9}$$

Next, we compute the variance of the noise. With $N_w(\omega)$ in (4.44) and using (4.39) we get

$$\begin{aligned} \mathrm{Var}(N_w(\omega)) &= \mathrm{E}\left(|N_w(\omega)|^2\right) \\ &= \sum_{m=0}^{N-1}\sum_{n=0}^{N-1} w(m)w(n)\,\mathrm{e}^{-j\omega(m-n)}\,\mathrm{E}\left[n(m)n^*(n)\right] \\ &= \sum_{m=0}^{N-1}\sum_{n=0}^{N-1} w(m)w(n)\,\mathrm{e}^{-j\omega(m-n)}\,\sigma_n^2\delta(m-n) \\ &= \sigma_n^2\sum_{n=0}^{N-1} w(n)^2. \end{aligned} \tag{D.10}$$

Plugging the expressions in (D.2) and using (4.40) yields

$$\begin{aligned} \mathrm{SNR}_{\text{after}} &= \frac{\rho_{\mathrm{s}} s_0^2}{\sigma_n^2}\frac{\left(\sum_{n=0}^{N-1} w(n)\right)^2}{\sum_{n=0}^{N-1} w(n)^2} \\ &= \mathrm{SNR}_{\text{before}}\cdot\mathrm{SNR}_{\text{gain}} \end{aligned} \tag{D.11}$$

with the SNR gain

$$\mathrm{SNR}_{\text{gain}} = \frac{\left(\sum_{n=0}^{N-1} w(n)\right)^2}{\sum_{n=0}^{N-1} w(n)^2}. \tag{D.12}$$

E. Maximum Likelihood Estimator for an N_{Targets} Target Model

We present the Maximum Likelihood (ML) estimator for the estimation of the unknown parameters of N_{Targets} targets with the following signal model

$$\underline{x}(l) = \sum_{k=1}^{N_{\text{Targets}}} \underline{a}\left(\underline{\Theta}_k\right) s_k(l) + \underline{n}(l), \quad l = 1, \ldots, L \tag{E.1}$$

where $L \in \mathbb{R}$ is the number of measurement cycles, $\underline{x}(l) \in \mathbb{C}^{N_{\text{ant}}}$ is the complex signal of the N_{ant} antennas. $s_k(l) \in \mathbb{C}$ is the unknown deterministic complex signal strength of the k-th target of measurement cycle l. $\underline{n}(l) \in \mathbb{C}^{N_{\text{ant}}}$ is the additional complex noise. $\underline{a}\left(\underline{\Theta}_k\right)$ is a function which depends on the k-th target's unknown parameter vector $\underline{\Theta}_k \in \mathbb{R}^M$. Hence, M is the number of unknowns per target in addition to the unknown signal strengths $s_k(l)$. $\underline{a}\left(\underline{\Theta}_k\right)$ can be e. g. the usual array steering vector which depends on the DOA of a target, but it can also be a more general function which depends on other parameters like the target's Doppler frequency.

In literature, such an ML estimator is called deterministic maximum likelihood (DML) estimator [Krim and Viberg, 1996], since the unknown signal strengths do not have a probability density function but are assumed to be deterministic.

The noise $\underline{n}(l)$ is assumed to be circular complex Gaussian with zero mean, spatially and temporally uncorrelated with

$$\mathrm{E}\left(\underline{n}(l)\,\underline{n}^H(m)\right) = \delta_{l,m}\,\sigma^2\,\mathbf{I}_{N_{\text{ant}}\times N_{\text{ant}}}. \tag{E.2}$$

Here, σ^2 is the unknown variance.

We stack the signal strengths in a vector

$$\underline{s}(l) = \left[s_1(l), \ldots, s_{N_{\text{Targets}}}(l)\right]^T \in \mathbb{C}^{N_{\text{Targets}}}, \quad l = 1, \ldots, L. \tag{E.3}$$

Hence, the unknown quantities $\underline{\Theta}$ to be estimated from $\underline{x}(l)$, $l = 1, \ldots, L$, are given by

$$\underline{\Theta} = \left[\underline{\Theta}_1^T, \ldots, \underline{\Theta}_{N_{\text{Targets}}}^T, \underline{s}^T(1), \ldots, \underline{s}^T(L), \sigma^2\right]^T. \tag{E.4}$$

To compute the ML estimator of $\underline{\Theta}$, we write the signal model in a more compact form. We define the unknown parameter matrix

$$\mathbf{\Theta} = \left[\underline{\Theta}_1 \quad \dots \quad \underline{\Theta}_{N_{\text{Targets}}}\right] \in \mathbb{R}^{M \times N_{\text{Targets}}} \tag{E.5}$$

and the matrix

$$\mathbf{A}\left(\mathbf{\Theta}\right) = \left[\underline{a}\left(\underline{\Theta}_1\right) \quad \dots \quad \underline{a}\left(\underline{\Theta}_{N_{\text{Targets}}}\right)\right] \in \mathbb{C}^{N_{\text{ant}} \times N_{\text{Targets}}}. \tag{E.6}$$

Then

$$\underline{x}(l) = \mathbf{A}\left(\mathbf{\Theta}\right) \underline{s}(l) + \underline{n}(l). \tag{E.7}$$

We give an overview how to derive the ML estimator of $\mathbf{\Theta}$ similar to [Krim and Viberg, 1996; Böhme, 1985]. The likelihood function $f_{\underline{x}(l)}\left(\underline{x}(l); \mathbf{\Theta},\ \underline{s}(l),\ \sigma^2\right)$ of $\underline{x}(l)$ is complex normal distributed

$$f_{\underline{x}(l)}\left(\underline{x}(l); \mathbf{\Theta},\ \underline{s}(l),\ \sigma^2\right) \sim \mathcal{CN}\left(\mathbf{A}(\mathbf{\Theta})\underline{s}(l), \sigma^2\, \mathbf{I}_{N_{\text{ant}} \times N_{\text{ant}}}\right). \tag{E.8}$$

Thus the pdf is given by [Kay, 1993]

$$\begin{aligned} f_{\underline{x}(l)}\left(\underline{x}(l);\ \mathbf{\Theta},\ \underline{s}(l),\ \sigma^2\right) &= \frac{1}{\pi^{N_{\text{ant}}} \det(\sigma^2\, \mathbf{I}_{N_{\text{ant}} \times N_{\text{ant}}})} \cdot \\ &\quad \exp\left\{-\left(\underline{x}(l) - \mathbf{A}(\mathbf{\Theta})\underline{s}(l)\right)^H \left(\sigma^2\, \mathbf{I}\right)^{-1} \left(\underline{x}(l) - \mathbf{A}(\mathbf{\Theta})\underline{s}(l)\right)\right\} \\ &= \frac{1}{\pi^{N_{\text{ant}}} \sigma^{2N_{\text{ant}}}} \exp\left(-\frac{\|\underline{x}(l) - \mathbf{A}(\mathbf{\Theta})\underline{s}(l)\|^2}{\sigma^2}\right). \end{aligned} \tag{E.9}$$

Since the observations $\underline{x}(l)$ are independent, the likelihood of all observations

$$\mathbf{X} = \left[\underline{x}(1) \quad \dots \quad \underline{x}(L)\right] \in \mathbb{C}^{N_{\text{ant}} \times L} \tag{E.10}$$

is

$$\begin{aligned} f\left(\mathbf{X};\ \underline{\Theta}\right) &= \prod_{l=1}^{L} f_{\underline{x}(l)}\left(\underline{x}(l); \mathbf{\Theta},\ \underline{s}(l),\ \sigma^2\right) \\ &= \frac{1}{\pi^{L\, N_{\text{ant}}} \sigma^{2\, L\, N_{\text{ant}}}} \exp\left(-\sum_{l=1}^{L} \frac{\|\underline{x}(l) - \mathbf{A}(\mathbf{\Theta})\underline{s}(l)\|^2}{\sigma^2}\right). \end{aligned} \tag{E.11}$$

The ML estimate $\hat{\underline{\Theta}}$ of $\underline{\Theta}$ are the arguments which maximize $f\left(\mathbf{X};\ \underline{\Theta}\right)$, given the observations $\mathbf{X}$

$$\hat{\underline{\Theta}} = \arg\max_{\underline{\Theta}}\ f\left(\mathbf{X};\ \underline{\Theta}\right). \tag{E.12}$$

Since the logarithm is strictly monotonically increasing, $\hat{\underline{\Theta}}$ can also be computed by minimizing the

negative logarithm of the likelihood, called log-likelihood l_{ML}.

$$\hat{\underline{\Theta}} = \arg\min_{\underline{\Theta}} l_{\mathrm{ML}}\left(\mathbf{X};\, \underline{\Theta}\right) \tag{E.13}$$

with

$$\begin{aligned} l_{\mathrm{ML}}\left(\mathbf{X};\, \underline{\Theta}\right) &= -\ln f\left(\mathbf{X};\, \underline{\Theta}\right) \\ &= -L\, N_{\mathrm{ant}} \ln\left(\pi\sigma^2\right) + \frac{1}{\sigma^2}\sum_{l=1}^{L} \|\underline{x}(l) - \mathbf{A}(\mathbf{\Theta})\underline{s}(l)\|^2. \end{aligned} \tag{E.14}$$

The minima with respect to $\underline{s}(l)$ and σ^2 can be computed explicitly [Krim and Viberg, 1996]. A convenient way to derive the minima with respect to the complex vectors $\underline{s}(l)$ is the use of Wirtinger derivatives introduced by Wirtinger [Wirtinger, 1927]. The ML estimates are

$$\hat{\sigma^2} = \frac{1}{N_{\mathrm{ant}}} \mathrm{Tr}\left(\mathbf{P}^{\perp}_{\mathbf{A}(\mathbf{\Theta})}\, \hat{\mathbf{R}}\right), \tag{E.15}$$

$$\hat{\underline{s}}(l) = \mathbf{A}^{+}(\mathbf{\Theta})\, \underline{x}(l), \quad l = 1, \ldots, L, \tag{E.16}$$

with the sample correlation matrix $\hat{\mathbf{R}}$

$$\hat{\mathbf{R}} = \frac{1}{L}\sum_{l=1}^{L} \underline{x}(l)\underline{x}^{H}(l) = \frac{1}{L}\mathbf{X}\,\mathbf{X}^{H} \in \mathbb{C}^{N_{\mathrm{ant}} \times N_{\mathrm{ant}}}. \tag{E.17}$$

$\mathbf{A}^{+}$ is the Moore-Penrose pseudo-inverse of $\mathbf{A}$,

$$\mathbf{A}^{+} = \left(\mathbf{A}^{H}\mathbf{A}\right)^{-1}\mathbf{A}^{H} \in \mathbb{C}^{N_{\mathrm{Targets}} \times N_{\mathrm{ant}}}, \tag{E.18}$$

and $\mathbf{P}^{\perp}_{\mathbf{A}}$ is the orthogonal projector onto the nullspace of $\mathbf{A}^{H}$,

$$\mathbf{P}_{\mathbf{A}} = \mathbf{A}\,\mathbf{A}^{+} \in \mathbb{C}^{N_{\mathrm{ant}} \times N_{\mathrm{ant}}}, \tag{E.19}$$

$$\mathbf{P}^{\perp}_{\mathbf{A}} = \mathbf{I} - \mathbf{P}_{\mathbf{A}} \in \mathbb{C}^{N_{\mathrm{ant}} \times N_{\mathrm{ant}}}. \tag{E.20}$$

Plugging these ML estimates in (E.14) and (E.13), we can compute the ML estimates $\hat{\mathbf{\Theta}}$ of the parameters $\mathbf{\Theta}$. This results in

$$\hat{\mathbf{\Theta}} = \arg\min_{\mathbf{\Theta}}\ \mathrm{Tr}\left(\mathbf{P}^{\perp}_{\mathbf{A}(\mathbf{\Theta})}\hat{\mathbf{R}}\right) \tag{E.21}$$

or equivalently

$$\hat{\mathbf{\Theta}} = \arg\max_{\mathbf{\Theta}}\ \mathrm{Tr}\left(\mathbf{P}_{\mathbf{A}(\mathbf{\Theta})}\hat{\mathbf{R}}\right). \tag{E.22}$$

In general, this is a nonlinear function of $\mathbf{\Theta}$ which cannot be simplified further.

For the special case of one target, $N_{\text{Targets}} = 1$, $\mathbf{\Theta} = \underline{\Theta}_1$, (E.22) can be simplified further and the ML estimator $\hat{\underline{\Theta}}_1$ of $\underline{\Theta}_1$ reads

$$\begin{aligned}\hat{\underline{\Theta}}_1 &= \arg\max_{\underline{\Theta}_1} \; \text{Tr}\left(\underline{a}\left(\underline{a}^H\underline{a}\right)^{-1}\underline{a}^H\,\mathbf{X}\,\mathbf{X}^H\right) \\ &= \arg\max_{\underline{\Theta}_1} \; \sum_{l=1}^{L}\left|\underline{a}^H(\underline{\Theta}_1)\,\underline{x}(l)\right|^2 \frac{1}{\|\underline{a}(\underline{\Theta}_1)\|^2}. \end{aligned} \tag{E.23}$$

F. Asymptotic Properties of Maximum Likelihood Estimators

The deterministic CRB is a lower bound for unbiased estimators [Kay, 1993]. In general, the deterministic maximum likelihood (ML) estimator is not unbiased and we cannot conclude that the CRB is a lower bound for the ML estimator. Because of this, we carry out numerical simulations to see if the ML estimator achieves the CRB. In the considered radar applications, we investigate this for increasing SNR. Analytical results can be obtained for an increasing number of observations [Böhme, 1998; Yang, 2011]. We briefly present them here.

We consider a sequence of ML estimators, where the number of observations increases. Let $\underline{X}_1, \ldots, \underline{X}_N$ be N independent identically distributed random observations. The pdf of each observation is $f_n(\underline{x}_n; \underline{\Theta})$ with the unknown deterministic parameter $\underline{\Theta}$. Let $\mathbf{J}$ be the Fisher information matrix (FIM) for one observation. Let $\hat{\underline{\Theta}}_N$ be the ML estimator of $\underline{\Theta}$ given N observations. Under some regularity conditions, the following properties hold:

- $\hat{\underline{\Theta}}_N$ is consistent: $\hat{\underline{\Theta}}_N$ converges for $N \to \infty$ to $\underline{\Theta}$ in probability.
- $\hat{\underline{\Theta}}_N$ is asymptotically unbiased: $\lim_{N\to\infty} \mathrm{E}(\hat{\underline{\Theta}}_N) = \underline{\Theta}$.
- $\hat{\underline{\Theta}}_N$ is asymptotically normal distributed: the cumulative distribution function of $\sqrt{N}(\hat{\underline{\Theta}}_N - \underline{\Theta})$ converges for $N \to \infty$ to the cumulative distribution function of a normal distributed, zero mean random vector with covariance matrix $\mathbf{C}$.
- $\hat{\underline{\Theta}}_N$ is asymptotically efficient: $\mathbf{C} = \mathbf{J}^{-1}$, where $\mathbf{C}$ is the covariance matrix of the asymptotic distribution.

G. Baseband Signal Model for a Moving Target in the Time Domain

Here we present the calculations used to derive the baseband signal $s(t)$ and the phase difference $\Delta\varphi$ presented in Section 5.1.1.

G.1. Computation of the Received Signal

To compute the signal $s_{\mathrm{Rx}}(t)$ which is received by the radar, we first compute the Doppler frequency change of the wave $\exp(j\,\omega t)$ as explained in Section 5.1.1.2. After that we use the result to calculate $s_{\mathrm{Rx}}(t)$.

Consider the transmitted wave $\exp(j\,\omega t)$. We compute the frequency change of the signal which reaches the target. Note that in classical physics, the change in frequency of a sound signal is different for the following two cases: a) the Rx is at rest relative to the transmission medium and the Tx is moving and b) the Rx is moving relative to the transmission medium and the Tx is at rest. Here, we consider electromagnetic waves which do not need a transmission medium. For an exact derivation, we have to use theory of relativity. From that it follows: In the frame of reference of the target, the target receives a signal with the angular frequency [Rebhan, 2001]

$$\omega' = \sqrt{\zeta}\,\omega, \tag{G.1}$$

$$\zeta = \frac{1-\beta}{1+\beta}, \tag{G.2}$$

$$\beta = \frac{v}{c}, \tag{G.3}$$

where the relative velocity v is defined to be positive if the target moves away from the radar. c is the speed of light. The signal is reflected at the target. We treat this as a signal which is transmitted from the target to the radar with transmission frequency ω'. Since the target moves relative to the radar, the frequency changes once again by the same factor. Thus the radar system receives a signal with the angular frequency

$$\omega'' = \sqrt{\zeta}\,\omega' = \zeta\,\omega. \tag{G.4}$$

Computing the Taylor series of ζ w. r. t. β at $\beta = 0$ yields

$$\zeta(\beta) = 1 - 2\beta + O(\beta^2). \tag{G.5}$$

Thus the angular frequency changes by

$$\omega_{\text{Doppler}} = \omega - \omega'' \approx 2\,\frac{v}{c}\,\omega \tag{G.6}$$

for $|v| \ll c$. Now we compute the received signal. Let us ignore the phase jump at the reflection at the target and let us ignore the time delay between the transmitted and received signal for a moment. Then, with (5.10), the radar receives

$$s_{\text{Rx0}}(t) \propto \int_{-\infty}^{\infty} S_{\text{Tx}}(\omega)\,\mathrm{e}^{j\omega'' t}\,\frac{1}{2\pi}\mathrm{d}\omega \tag{G.7}$$

$$= \int_{-\infty}^{\infty} S_{\text{Tx}}(\omega)\,\mathrm{e}^{j\zeta\omega t}\,\frac{1}{2\pi}\mathrm{d}\omega \tag{G.8}$$

$$= s_{\text{Tx}}(\zeta t). \tag{G.9}$$

Now we compute the time delay. In the frame of reference of the radar, the target's position $x_{\text{target}}(t)$ is given by

$$x_{\text{target}}(t) = d_0 + vt, \tag{G.10}$$

where d_0 is the distance of the target at the start of the transmission of the chirp, i. e. $t = 0$. Consider a short electromagnetic pulse which is transmitted from the radar at $t = 0$. It's position $x_{\text{em}}(t)$ is

$$x_{\text{em}}(t) = ct. \tag{G.11}$$

The time t_0 at which the pulse reaches the target is the solution of

$$x_{\text{em}}(t_0) = x_{\text{target}}(t_0). \tag{G.12}$$

It follows

$$t_0 = \frac{d_0}{c - v}. \tag{G.13}$$

The pulse is reflected at the target and needs to travel back exactly the same distance $x_{\text{target}}(t_0)$. Thus the radar receives the reflected pulse at

$$\tau = 2\,t_0 = 2\,\frac{d_0}{c - v} = \kappa\,\tau_0, \tag{G.14}$$

$$\tau_0 = 2\,\frac{d_0}{c}, \tag{G.15}$$

$$\kappa = \frac{1}{1-\beta}, \tag{G.16}$$

where τ_0 is the time delay of a stationary target at distance d_0. Thus the received signal, including the time delay, is given by

$$s_{\mathrm{Rx}}(t) = s_{\mathrm{Rx0}}(t-\tau) \propto s_{\mathrm{Tx}}\left(\zeta(t-\tau)\right). \tag{G.17}$$

The transmitted signal $s_{\mathrm{Tx}}(t)$ is defined in (5.5). The amplitude of the received signal is smaller than the transmitted one due to the damping and the radar cross section of the target. Furthermore, the duration of the signal changes due to relativistic reasons, and since the energy has to be conserved, the amplitude changes as well. We include all these effects in the amplitude A_{Rx}. Moreover, in general a phase jump occurs at the reflection of the signal which we denote by $\varphi_{\mathrm{target}}$. Thus the received signal is

$$s_{\mathrm{Rx}}(t) = A_{\mathrm{Rx}} \cos\left(\varphi_{\mathrm{Rx}}(t)\right) \tag{G.18}$$

with

$$\varphi_{\mathrm{Rx}}(t) = \varphi_{\mathrm{Tx}}\left(\zeta(t-\tau)\right) + \varphi_0 + \varphi_{\mathrm{target}} \tag{G.19}$$

and $\varphi_{\mathrm{Tx}}(t)$ in (5.8) is the time dependent phase of the transmitted signal and φ_0 the phase of the transmitted signal at $t = 0$. Now we compute

$$\varphi_{\mathrm{Tx}}\left(\zeta(t-\tau)\right) = \varphi_{\mathrm{Tx}}\left(\zeta(t-\kappa\tau_0)\right) \tag{G.20}$$

in more detail. Plugging in (5.8) yields

$$\varphi_{\mathrm{Tx}}\left(\zeta(t-\kappa\tau_0)\right) = \omega_0\left(\zeta(t-\kappa\tau_0)\right) + \frac{1}{2}\chi\left(\zeta(t-\kappa\tau_0)\right)^2. \tag{G.21}$$

We compute the first order truncated Taylor series of (G.21) w. r. t. β at $\beta = 0$. With

$$\zeta(\beta) = 1 - 2\beta + O(\beta^2), \tag{G.22}$$

$$\kappa(\beta) = 1 + \beta + O(\beta^2), \tag{G.23}$$

this results in

$$\varphi_{\mathrm{Tx}}\left(\zeta(t-\kappa\tau_0)\right) = \varphi_{\mathrm{Tx}}(t) - \varphi_{\mathrm{base}}(t) + O(\beta^2), \tag{G.24}$$

with

$$\varphi_{\mathrm{base}}(t) = \omega_0\,\tau_0\,(1-\beta) - \frac{1}{2}\chi\,\tau_0^2\,(1-2\beta) + t\left[\omega_0\,2\beta + \chi\,\tau_0\,(1-3\beta)\right] + t^2 2\chi\beta. \tag{G.25}$$

Thus the phase of the received signal is

$$\varphi_{\mathrm{Rx}}(t) = \varphi_{\mathrm{Tx}}(t) - \varphi_{\mathrm{base}}(t) + \varphi_0 + \varphi_{\mathrm{target}}. \tag{G.26}$$

G.2. Baseband Signal After the IQ-Mixer

We consider an IQ-mixer which mixes the received signal $s_{\mathrm{Rx}}(t)$ (G.18) with the transmitted one, i. e. it is mixed with $A_{\mathrm{Tx}} \cos(\varphi_{\mathrm{Tx}}(t) + \varphi_0)$ and $A_{\mathrm{Tx}} \sin(\varphi_{\mathrm{Tx}}(t) + \varphi_0)$. We assume the signal to be narrowband, i. e. the bandwidth is much smaller than the carrier frequency. Thus the phase of the complex baseband signal is given as the difference of the Tx phase $\varphi_{\mathrm{Tx}}(t) + \varphi_0$ and the Rx phase $\varphi_{\mathrm{Rx}}(t)$ in (G.26). Hence the complex baseband signal is

$$\begin{aligned} s(t) &= \frac{1}{2} A_{\mathrm{Rx}} A_{\mathrm{Tx}} \exp\left(j\left[\,\varphi_{\mathrm{Tx}}(t) + \varphi_0 - \varphi_{\mathrm{Rx}}(t)\,\right]\right) \\ &= \frac{1}{2} A_{\mathrm{Rx}} A_{\mathrm{Tx}} \exp\Big(j\left[\varphi_{\mathrm{base}}(t) - \varphi_{\mathrm{target}}\right]\Big) \\ &= A \exp\left(\, j\, \varphi_{\mathrm{base}}(t)\,\right), \end{aligned} \tag{G.27}$$

where we have defined

$$A = \frac{1}{2} A_{\mathrm{Rx}} A_{\mathrm{Tx}} \exp(-j\, \varphi_{\mathrm{target}}). \tag{G.28}$$

For convenience, we express $\varphi_{\mathrm{base}}(t)$ in (G.25) as

$$\varphi_{\mathrm{base}}(t) = \varphi_{\mathrm{base},a} + \varphi_{\mathrm{base},b}(t) + \varphi_{\mathrm{base},c}(t), \tag{G.29}$$

$$\varphi_{\mathrm{base},a} = \omega_0\, \tau_0\, (1 - \beta) - \frac{1}{2} \chi\, \tau_0^2\, (1 - 2\beta), \tag{G.30}$$

$$\varphi_{\mathrm{base},b}(t) = t\, [\omega_0\, 2\beta + \chi\, \tau_0\, (1 - 3\beta)], \tag{G.31}$$

$$\varphi_{\mathrm{base},c}(t) = t^2 2\, \chi\, \beta. \tag{G.32}$$

(G.29) is the same result as the one derived in [Stove, 1992] up to differences in some of the factors in front of β. The reason is that in [Stove, 1992] a classical derivation is used for the Doppler effect instead of the relativistic one and therefore it is not exactly correct. Usually these differences do not matter for the DOA estimation.

In the following, we show that one of the terms in (G.30) is negligible. In order to do that, we have to compute how much a phase error influences the error in the electrical angle. In Appendix G.3, it is shown that for a typical radar system with a DOA accuracy of $\sigma_\vartheta = 0.1^\circ \approx 1.7 \cdot 10^{-3}$ rad and an observed DOA region with $|\vartheta| \leq 30^\circ$, phase errors smaller than $5 \cdot 10^{-3}$ are negligible. We compute the order of magnitude of $\chi\, \tau_0^2 \beta$ in (G.30) using the values given in Tab. 5.1 as maximal values for the different parameters. For an FMCW radar, $\chi\, \tau_0^2 \beta$ is of order of magnitude 10^{-6} and for a chirp

sequence radar 10^{-5}. Note that β and τ_0 are given by (5.17) and (5.18), respectively. Therefore, the term $\chi\,\tau_0^2\beta$ is negligible and

$$\varphi_{\text{base},a} = \omega_0\,\tau_0\,(1-\beta) - \frac{1}{2}\chi\,\tau_0^2. \tag{G.33}$$

G.3. Influence of the Phase Error on the Error in the Electrical Angle

In order to know which terms of the phase of the baseband signal are negligible, we have to know how much a phase error influences the error in the electrical angle. To compute this, we consider two antennas with an antenna spacing Δd. The relation between the phase difference $\Delta\varphi_{2\text{ antennas}}$ between the two antennas and the electrical angle u of the target is given by

$$\Delta\varphi_{2\text{ antennas}} = 2\,\pi\frac{\Delta d}{\lambda}u \tag{G.34}$$

with the carrier wavelength λ. Hence

$$u = \frac{\Delta\varphi_{2\text{ antennas}}}{2\pi\frac{\Delta d}{\lambda}}. \tag{G.35}$$

The error σ_u of u due to an error $\sigma_{\Delta\varphi_{2\text{ antennas}}}$ of the phase difference $\Delta\varphi_{2\text{ antennas}}$ is therefore

$$\sigma_u = \frac{\sigma_{\Delta\varphi_{2\text{ antennas}}}}{2\pi\frac{\Delta d}{\lambda}}. \tag{G.36}$$

The smaller the distance Δd between two antennas, the larger the error σ_u due to an error $\sigma_{\Delta\varphi_{2\text{ antennas}}}$. We consider the worst case: the smallest distance Δd between two antennas is typically $\frac{\lambda}{2}$. Hence

$$\sigma_u \approx \frac{\sigma_{\Delta\varphi_{2\text{ antennas}}}}{\pi}. \tag{G.37}$$

Thus, errors $\sigma_{\Delta\varphi_{2\text{ antennas}}}$ smaller than $\pi\cdot\sigma_u$ are negligible.

A typical long range radar system achieves a DOA accuracy $\sigma_\vartheta = 0.1^\circ \approx 1.7\cdot 10^{-3}$ rad [Reiher, 2012]. Since $u = \sin(\vartheta)$,

$$\mathrm{d}u = \mathrm{d}\vartheta\cdot\cos(\vartheta). \tag{G.38}$$

Short, mid, and long range radars for automotive applications have different field of views. A short range radar observes nearly the whole DOA region, i. e. $-90^\circ \le \vartheta \le 90^\circ$, for a mid range radar $-50^\circ \le \vartheta \le 50^\circ$ and a long range radar observes typically $\pm 10^\circ$ to $\pm 20^\circ$[Schoor, 2010]. A high DOA accuracy is important for long range radars, because for a target at a large distance, a small

error in the DOA estimation can lead to a large lateral displacement. Because of this we consider a long range radar and set the observed DOA region to $|\vartheta| \leq 30°$ to include the worst case. Hence, in order to yield at DOA accuracy $\sigma_\vartheta = 0.1°$, the accuracy σ_u of the electrical angle has to satisfy

$$\sigma_u \leq \sigma_\vartheta \cdot |\cos(\vartheta)| \quad \forall\, |\vartheta| \leq 30°, \tag{G.39}$$

and therefore, plugging in the worst case,

$$\sigma_u = \sigma_\vartheta \cdot |\cos(30°)| \approx 1.5 \cdot 10^{-3}. \tag{G.40}$$

Plugging this in (G.37) yields

$$\sigma_{\Delta\varphi_{2\text{ antennas}}} \approx 5 \cdot 10^{-3}. \tag{G.41}$$

Hence, phase errors $\sigma_{\Delta\varphi_{2\text{ antennas}}}$ smaller than $5 \cdot 10^{-3}$ are negligible.

G.4. Phase Difference Between Two Chirps

We calculate the difference $\Delta\varphi_{1k}$ of the phases of the baseband signals of the first and k-th chirp at the time in the middle of the chirps. As explained in Section 5.1.1.2, we investigate chirps which have the same carrier frequency in the middle of the chirp

$$\omega_1(t_{\mathrm{M},1}) = \omega_k(t_{\mathrm{M},k}) = \omega_{0\mathrm{M}} \tag{G.42}$$

as depicted in Fig. 5.4. The subscript $i = 1, k$, denotes that the corresponding variable belongs to chirp i. The angular frequencies of the chirps can be expressed as

$$\omega_i(t) = \omega_{0\mathrm{M}} + \chi_i \left(t - t_{\mathrm{start},i} - \frac{1}{2} T_i \right), \quad t \in [t_{\mathrm{start},i}, t_{\mathrm{start},i} + T_i]. \tag{G.43}$$

We rewrite it as

$$\omega_i(t) = \omega_{0,i} + \chi_i\,(t - t_{\mathrm{start},i}), \tag{G.44}$$

$$\omega_{0,i} = \omega_{0\mathrm{M}} - \frac{1}{2}\chi_i\, T_i. \tag{G.45}$$

$\omega_{0,i}$ is the angular frequency at the start of the i-th chirp. An example of a chirp with these parameters is depicted in Fig. G.1. Hence it has the same form as (5.7) but with $\omega_{0,i}$ instead of ω_0 and the start of the chirp is set to $t_{\mathrm{start},i}$. Thus we can use the result (5.13) replacing t by $t - t_{\mathrm{start},i}$. Moreover, the chirp dependent parameters ω_0, τ_0, χ in (5.14) to (5.16) have to be replaced by $\omega_{0,i}, \tau_{0,i}, \chi_i$, respectively.

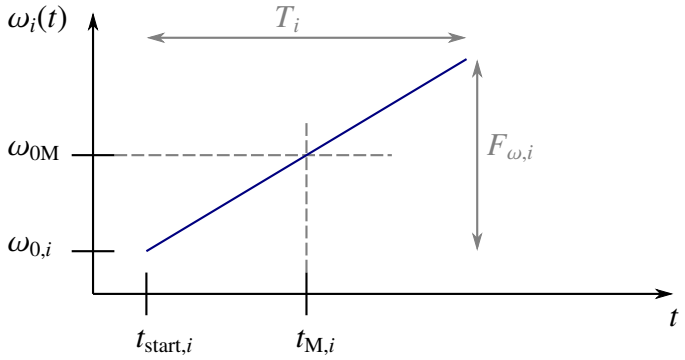

Figure G.1.: Example of a linear chirp i and its parameters

Thus, the phase $\varphi_{\text{base},i}(t)$ of the received baseband signal of the i-th chirp is

$$\varphi_{\text{base},i}(t) = \varphi^{(i)}_{\text{base}}(t - t_{\text{start},i}), \tag{G.46}$$

where

$$\varphi^{(i)}_{\text{base}}(t) = \varphi^{(i)}_{\text{base},a} + \varphi^{(i)}_{\text{base},b}(t) + \varphi^{(i)}_{\text{base},c}(t), \tag{G.47}$$

$$\varphi^{(i)}_{\text{base},a} = \omega_{0,i}\,\tau_{0,i}\,(1-\beta) - \frac{1}{2}\chi_i\,\tau^2_{0,i} \tag{G.48}$$

$$\varphi^{(i)}_{\text{base},b}(t) = t\,[\omega_{0,i}\,2\beta + \chi_i\,\tau_{0,i}\,(1-3\beta)], \tag{G.49}$$

$$\varphi^{(i)}_{\text{base},c}(t) = t^2 2\chi_i\beta. \tag{G.50}$$

Now we can write the phase difference $\Delta\varphi_{1k}$ we want to derive as

$$\Delta\varphi_{1k} = \varphi_{\text{base},k}(t_{\text{M},k}) - \varphi_{\text{base},1}(t_{\text{M},1}). \tag{G.51}$$

We compute $\varphi_{\text{base},i}(t_{\text{M},i})$ in more detail.

$$\begin{aligned}
\varphi_{\text{base},i}(t_{\text{M},i}) &= \varphi^{(i)}_{\text{base}}(t_{\text{M},i} - t_{\text{start},i}) \\
&= \varphi^{(i)}_{\text{base}}\left(\frac{T_i}{2}\right) \\
&= \omega_{0,i}\,\tau_{0,i}\,(1-\beta) - \frac{1}{2}\chi_i\,\tau^2_{0,i} + \frac{T_i}{2}\,[\omega_{0,i}\,2\beta + \chi_i\,\tau_{0,i}\,(1-3\beta)] + \frac{1}{2}\,T_i^2\,\chi_i\beta.
\end{aligned} \tag{G.52}$$

Inserting (G.45) results in

$$\varphi_{\text{base},i}(t_{\text{M},i}) = \omega_{0\text{M}}\,\tau_{0,i}\,(1-\beta) - \frac{1}{2}\chi_i\,\tau^2_{0,i} + \omega_{0\text{M}}\beta\,T_i - \beta\,T_i\chi_i\,\tau_{0,i}. \tag{G.53}$$

By using (5.29), the round trip time $\tau_{M,i}$ at the middle of chirp i, defined in (5.30), can be written as

$$\tau_{M,i} = 2\,\frac{d_{0,i} + v\,T_i/2}{c} = \tau_{0,i} + \beta\,T_i. \tag{G.54}$$

Hence

$$\tau_{0,i} = \tau_{M,i} - \beta\, T_i. \tag{G.55}$$

Inserting this in (G.53) yields

$$\varphi_{\text{base},i}(t_{\text{M},i}) = \omega_{0\text{M}}\, \tau_{M,i}\, (1-\beta) - \frac{1}{2}\chi_i\, \tau_{M,i}^2 + \omega_{0\text{M}} \beta^2\, T_i + \frac{1}{2}\chi_i \beta^2\, T_i^2. \tag{G.56}$$

Using the maximum values of Tab. 5.1, we compute the order of magnitude of the two terms including β^2: $\omega_{0\text{M}} \beta^2\, T_i$ and $\frac{1}{2}\chi_i \beta^2\, T_i^2 = \frac{1}{2}\beta^2\, F_{\omega,i}\, T_i$. For an FMCW radar, they are of order of magnitude 10^{-4} and 10^{-6}, respectively, and for a chirp sequence radar of order of magnitude 10^{-6} and 10^{-8}, respectively. Hence these terms are negligible and

$$\varphi_{\text{base},i}(t_{\text{M},i}) = \omega_{0\text{M}}\, \tau_{M,i}\, (1-\beta) - \frac{1}{2}\chi_i\, \tau_{M,i}^2. \tag{G.57}$$

The time delay $\tau_{M,k}$ can be written as

$$\tau_{M,k} = \frac{2}{c}\, d_{M,k} = \frac{2}{c}\, (d_{M,1} + v\, \Delta t_{\text{M},1k}) \tag{G.58}$$

with

$$\Delta t_{\text{M},1k} = t_{\text{M},k} - t_{\text{M},1}. \tag{G.59}$$

Thus, the difference of the time delays is

$$\tau_{M,k} - \tau_{M,1} = 2\beta\, \Delta t_{\text{M},1k}. \tag{G.60}$$

Plugging (G.57) in (G.51) yields

$$\Delta\varphi_{1k} = \omega_{0\text{M}}\, 2\beta\, \Delta t_{\text{M},1k}\, (1-\beta) - \left(\frac{1}{2}\chi_k\, \tau_{M,k}^2 - \frac{1}{2}\chi_1\, \tau_{M,1}^2\right). \tag{G.61}$$

The term $\omega_{0\text{M}}\, 2\, \Delta t_{\text{M},1k}\, \beta^2$ is negligible since with the maximum values given in Tab. 5.1 it is smaller than $3 \cdot 10^{-3}$ for both the FMCW and chirp sequence radar. Hence

$$\Delta\varphi_{1k} = \omega_{\text{Doppler}}\, \Delta t_{\text{M},1k} - \left(\frac{1}{2}\chi_k\, \tau_{M,k}^2 - \frac{1}{2}\chi_1\, \tau_{M,1}^2\right), \tag{G.62}$$

with

$$\omega_{\text{Doppler}} = \omega_{0\text{M}}\, 2\, \frac{v}{c}. \tag{G.63}$$

G.5. Simplification of $\Delta\varphi_{1k}$ for a Chirp Sequence Radar

We simplify $\Delta\varphi_{1k}$ in (G.62) for a chirp sequence radar. A chirp sequence radar transmits several equal chirps with $\chi_1 = \chi_k = \chi$. Thus we can write

$$\Delta\varphi_{1k} = \omega_{\text{Doppler}}\,\Delta t_{\text{M},1k} - \frac{1}{2}\chi\left(\tau_{M,k}^2 - \tau_{M,1}^2\right). \tag{G.64}$$

From (G.60) follows $\tau_{M,k} = \tau_{M,1} + 2\beta\,\Delta t_{\text{M},1k}$ and thus

$$\tau_{M,k}^2 - \tau_{M,1}^2 = 4\,\tau_{M,1}\,\beta\,\Delta t_{\text{M},1k} + 4\beta^2\Delta t_{\text{M},1k}^2. \tag{G.65}$$

Hence

$$\Delta\varphi_{1k} = \omega_{\text{Doppler}}\,\Delta t_{\text{M},1k} - 2\chi\left(\tau_{M,1}\,\beta\,\Delta t_{\text{M},1k} + \beta^2\Delta t_{\text{M},1k}^2\right). \tag{G.66}$$

We use the maximum values given in Tab. 5.1 to compute the maximum value of $2\chi\beta^2\Delta t_{\text{M},1k}^2$. Consider a measurement with overall measurement time of 20 ms. This time is approximately the time difference $\Delta t_{\text{M},1k}$ between the last and the first chirp. Hence we set $\Delta t_{\text{M},1k} = 20\,\text{ms}$. Then $2\chi\beta^2\Delta t_{\text{M},1k}^2 \approx 3.6\cdot 10^{-3}$ and can be neglected. The other term $2\chi\,\tau_{M,1}\,\beta\,\Delta t_{\text{M},1k}$ is in general larger and cannot be neglected, but it can be incorporated together with the first term by defining a new unknown pseudo Doppler frequency

$$\begin{aligned}\omega_{\text{pseudoDoppler}} &= \omega_{\text{Doppler}} - 2\chi\,\tau_{M,1}\,\beta \\ &= 2\,\frac{v}{c}\left(\omega_{0\text{M}} - \chi\,\tau_{M,1}\right).\end{aligned} \tag{G.67}$$

Then $\Delta\varphi_{1k}$ has the simple form

$$\Delta\varphi_{1k} = \omega_{\text{pseudoDoppler}}\,\Delta t_{\text{M},1k}. \tag{G.68}$$

Since $\omega_{\text{pseudoDoppler}}$ contains only the round trip time $\tau_{M,1}$ of the first chirp, $\omega_{\text{pseudoDoppler}}$ stays the same if we consider the phase difference $\Delta\varphi_{1k}$ between any chirp k and the first chirp.

G.6. Estimation of the Error in $\Delta\varphi_{\textbf{corrected},1k}$

We compute the error in $\Delta\varphi_{\text{corrected},1k}$ which arises since not the exact values $d_{M,1}, d_{M,k}$ are used in (5.34) but their estimates $\hat{d}_{M,1}, \hat{d}_{M,k}$. Typically, an FMCW radar achieves a distance accuracy $\sigma_d = 0.1\,\text{m}$ [Reiher, 2012]. We define

$$\Delta\tilde{\varphi} = \frac{2}{c^2}\left(\chi_1 d_{M,1}^2 - \chi_k d_{M,k}^2\right). \tag{G.69}$$

Then the error $\sigma_{\Delta\tilde{\varphi}}$ in $\Delta\varphi_{\text{corrected},1k}$ due to the estimation error of $\hat{d}_{M,1}$ and $\hat{d}_{M,k}$ can be computed by

$$\sigma_{\Delta\tilde{\varphi}} = \frac{\partial\Delta\tilde{\varphi}}{\partial d_{M,1}}\sigma_{d_{M,1}} + \frac{\partial\Delta\tilde{\varphi}}{\partial d_{M,k}}\sigma_{d_{M,k}}, \tag{G.70}$$

with $\sigma_{d_{M,i}}$ being the accuracy of $d_{M,i}$. Hence

$$\left|\sigma_{\Delta\tilde{\varphi}}\right| \leq \left|\frac{\partial\Delta\tilde{\varphi}}{\partial d_{M,1}}\right|\sigma_{d_{M,1}} + \left|\frac{\partial\Delta\tilde{\varphi}}{\partial d_{M,k}}\right|\sigma_{d_{M,k}}, \tag{G.71}$$

We set $\sigma_{d_{M,i}} = 0.1\,\text{m}$, $i = 1, 2$. This yields

$$\left|\sigma_{\Delta\tilde{\varphi}}\right| = \frac{2}{c^2}\left(|2\chi_1 d_{M,1}|\,\sigma_{d_{M,1}} + |2\chi_k d_{M,k}|\,\sigma_{d_{M,k}}\right) \approx 3\cdot 10^{-3}, \tag{G.72}$$

where we have plugged in the values of the FMCW radar parameters and the target parameters given in Tab. 5.1. As shown above, such a phase error is negligible for a typical radar system. If an even higher chirp rate than the one given in Tab. 5.1 is used and/or the distance estimations $\hat{d}_{M,1}, \hat{d}_{M,k}$ are very imprecise, the error might have to be considered.

H. Derivation of the Cramer-Rao Bound for a Planar TDM MIMO Radar with a Non-Stationary Target

We compute the CRB for the electrical angles and Doppler frequency of a non-stationary target using a TDM MIMO radar, cf. Section 5.2.1. We have to derive (5.91) and show that $\mathbf{C} \in \mathbb{R}^{3\times 3}$. We define

$$\mathbf{C} = \mathbf{C}^{(1)} - \mathbf{C}^{(2)} \tag{H.1}$$

with

$$\mathbf{C}^{(1)} = \mathbf{D}^H \mathbf{D}, \tag{H.2}$$

$$\begin{aligned}\mathbf{C}^{(2)} &= \mathbf{D}^H \mathbf{P}_{\underline{b}} \mathbf{D} \\ &= \mathbf{D}^H \underline{b} \frac{1}{\|\underline{b}\|^2} \underline{b}^H \mathbf{D}.\end{aligned} \tag{H.3}$$

Computation of D We compute $\mathbf{D}$ defined in (5.86). With $\underline{b}$ given in (5.56), the derivative with respect to ω reads

$$\frac{\partial \underline{b}}{\partial \omega} = j\, \underline{t}^{\text{Virt}} \odot \underline{b}. \tag{H.4}$$

The derivatives with respect to $\underline{u}$ can be computed by

$$\begin{aligned}\frac{\partial \underline{b}}{\partial \underline{u}^T} &= \begin{bmatrix} \frac{\partial \underline{b}}{\partial u_x} & \frac{\partial \underline{b}}{\partial u_y} \end{bmatrix} \\ &= \sqrt{\underline{\rho}^{\text{Virt}}} \odot \exp(j\, \underline{t}^{\text{Virt}} \omega) \odot \frac{\partial}{\partial \underline{u}^T} \exp(j\, \mathbf{D}^{\text{Virt}} \underline{u}),\end{aligned} \tag{H.5}$$

$$\frac{\partial}{\partial \underline{u}^T} \exp(j\, \mathbf{D}^{\text{Virt}} \underline{u}) = \begin{bmatrix} \exp(j\, \mathbf{D}^{\text{Virt}} \underline{u}) & \exp(j\, \mathbf{D}^{\text{Virt}} \underline{u}) \end{bmatrix} \odot j\, \mathbf{D}^{\text{Virt}}, \tag{H.6}$$

$$\frac{\partial \underline{b}}{\partial \underline{u}^T} = \begin{bmatrix} \underline{b} & \underline{b} \end{bmatrix} \odot j\, \mathbf{D}^{\text{Virt}}. \tag{H.7}$$

Plugging this in (5.86) yields

$$\begin{aligned}\mathbf{D} &= j\begin{bmatrix}\underline{b} & \underline{b} & \underline{b}\end{bmatrix} \odot \begin{bmatrix}\mathbf{D}^{\text{Virt}} & \underline{t}^{\text{Virt}}\end{bmatrix} \\ &= j\begin{bmatrix}\underline{b} & \underline{b} & \underline{b}\end{bmatrix} \odot \mathbf{V}, \qquad \text{(H.8)}\\ \text{with} \quad \mathbf{V} &= \begin{bmatrix}\mathbf{D}^{\text{Virt}} & \underline{t}^{\text{Virt}}\end{bmatrix}. \qquad \text{(H.9)}\end{aligned}$$

Computation of $\mathbf{C}^{(1)}$ From (5.56) follows

$$\underline{b} \odot \underline{b}^* = \underline{\rho}^{\text{Virt}}, \qquad \text{(H.10)}$$

$$\|\underline{b}\|^2 = \left(\underline{1}^T \underline{\rho}^{\text{Virt}}\right). \qquad \text{(H.11)}$$

For some matrices $\mathbf{X} \in \mathbb{C}^{N_{\text{Virt}} \times K_1}$ and $\mathbf{Y} \in \mathbb{C}^{N_{\text{Virt}} \times K_2}$ holds

$$\begin{aligned}\left[\left(\left(\underline{b}\ \underline{1}_{K_2}^T\right) \odot \mathbf{Y}\right)^H \left(\left(\underline{b}\ \underline{1}_{K_1}^T\right) \odot \mathbf{X}\right)\right]_{kl} &= \sum_{m=1}^{N_{\text{Virt}}} \left[\left(\underline{b}\ \underline{1}_{K_2}^T\right)^H\right]_{km} \left[\mathbf{Y}^H\right]_{km} \left[\left(\underline{b}\ \underline{1}_{K_1}^T\right)\right]_{ml} [\mathbf{X}]_{ml} \\ &= \sum_m \left[\mathbf{Y}^H\right]_{km} b_m^* b_m [\mathbf{X}]_{ml} \\ &= \left[\mathbf{Y}^H \operatorname{diag}(\underline{\rho}^{\text{Virt}})\mathbf{X}\right]_{kl}. \qquad \text{(H.12)}\end{aligned}$$

Hence, using (H.11) and the definition of Corr^{WS} in (A.2) gives

$$\left[\left(\underline{b}\ \underline{1}_{K_2}^T\right) \odot \mathbf{Y}\right]^H \left[\left(\underline{b}\ \underline{1}_{K_1}^T\right) \odot \mathbf{X}\right] = \|\underline{b}\|^2 \,\text{Corr}^{\text{WS}}(\mathbf{X}, \mathbf{Y}, \underline{\rho}^{\text{Virt}}). \qquad \text{(H.13)}$$

Thus with (H.8) follows

$$\begin{aligned}\mathbf{C}^{(1)} &= \mathbf{D}^H\mathbf{D} \\ &= \left[\left(\underline{b}\ \underline{1}_3^T\right) \odot \mathbf{V}\right]^H \left[\left(\underline{b}\ \underline{1}_3^T\right) \odot \mathbf{V}\right] \\ &= \|\underline{b}\|^2 \,\text{Corr}^{\text{WS}}(\mathbf{V}, \mathbf{V}, \underline{\rho}^{\text{Virt}}) \qquad \text{(H.14)}\end{aligned}$$

Computation of $\mathbf{C}^{(2)}$ $\mathbf{C}^{(2)}$ is defined in (H.3). With the help of (H.13), setting $\mathbf{Y} = \underline{1}_{N_{\text{Virt}}}$, we get

$$\begin{aligned}\underline{b}^H\mathbf{D} &= [\underline{b} \odot \underline{1}_{N_{\text{Virt}}}]^H j\left[\left(\underline{b}\ \underline{1}_3^T\right) \odot \mathbf{V}\right] \\ &= j\,\|\underline{b}\|^2 \,\text{Corr}^{\text{WS}}(\mathbf{V}, \underline{1}_{N_{\text{Virt}}}, \underline{\rho}^{\text{Virt}}) \\ &= j\,\|\underline{b}\|^2 \,\text{E}^{\text{WS}}(\mathbf{V}, \underline{\rho}^{\text{Virt}}), \qquad \text{(H.15)}\end{aligned}$$

where we have used Lemma A.2.2. Putting this in (H.3) yields

$$\mathbf{C}^{(2)} = \|\underline{b}\|^2 \,\text{E}^{\text{WS}}(\mathbf{V}, \underline{\rho}^{\text{Virt}})^H \,\text{E}^{\text{WS}}(\mathbf{V}, \underline{\rho}^{\text{Virt}}). \qquad \text{(H.16)}$$

Plugging the results in C With the property of $\mathrm{Cov}^{\mathrm{WS}}$ in Lemma A.2.12 we get

$$\begin{aligned}\mathbf{C} &= \mathbf{C}^{(1)} - \mathbf{C}^{(2)} \\ &= \|\underline{b}\|^2 \left[\mathrm{Corr}^{\mathrm{WS}}(\mathbf{V}, \mathbf{V}, \underline{\rho}^{\mathrm{Virt}}) - \mathrm{E}^{\mathrm{WS}}(\mathbf{V}, \underline{\rho}^{\mathrm{Virt}})^H \mathrm{E}^{\mathrm{WS}}(\mathbf{V}, \underline{\rho}^{\mathrm{Virt}})\right] \\ &= \|\underline{b}\|^2 \mathrm{Cov}^{\mathrm{WS}}(\mathbf{V}, \mathbf{V}, \underline{\rho}^{\mathrm{Virt}}) \\ &= \|\underline{b}\|^2 \mathrm{Cov}^{\mathrm{WS}}(\mathbf{V}, \underline{\rho}^{\mathrm{Virt}}). \end{aligned} \tag{H.17}$$

Using (H.11) and the definition of $\underline{\rho}^{\mathrm{Virt}}$ (5.57) yields

$$\mathbf{C} = N_{\mathrm{Rx}} \left(\underline{1}^T \underline{\rho}\right) \mathrm{Cov}^{\mathrm{WS}}(\mathbf{V}, \underline{\rho}^{\mathrm{Virt}}). \tag{H.18}$$

Since all variables in (H.18) are real, $\mathbf{C} \in \mathbb{R}^{3\times 3}$.

Simplifying C in (H.18)

$$\begin{aligned}\mathbf{V} &= \begin{bmatrix} \mathbf{D}^{\mathrm{Virt}} & \underline{t}^{\mathrm{Virt}} \end{bmatrix} \\ &= \begin{bmatrix} \underline{1}_{N_{\mathrm{Pulse}}} \otimes \mathbf{D}^{\mathrm{Rx}} + \mathbf{D}^{\mathrm{Pulse}} \otimes \underline{1}_{N_{\mathrm{Rx}}} & \underline{t} \otimes \underline{1}_{N_{\mathrm{Rx}}} \end{bmatrix} \\ &= \underline{1}_{N_{\mathrm{Pulse}}} \otimes \begin{bmatrix} \mathbf{D}^{\mathrm{Rx}} & \underline{0} \end{bmatrix} + \begin{bmatrix} \mathbf{D}^{\mathrm{Pulse}} & \underline{t} \end{bmatrix} \otimes \underline{1}_{N_{\mathrm{Rx}}} \\ &= \underline{1}_{N_{\mathrm{Pulse}}} \otimes \mathbf{V}_1 + \mathbf{V}_2 \otimes \underline{1}_{N_{\mathrm{Rx}}} \end{aligned} \tag{H.19}$$

with

$$\mathbf{V}_1 = \begin{bmatrix} \mathbf{D}^{\mathrm{Rx}} & \underline{0} \end{bmatrix}, \tag{H.20}$$

$$\mathbf{V}_2 = \begin{bmatrix} \mathbf{D}^{\mathrm{Pulse}} & \underline{t} \end{bmatrix}. \tag{H.21}$$

Using the properties of $\mathrm{Cov}^{\mathrm{WS}}$, cf. Appendix A.2.4, we get

$$\begin{aligned}\mathrm{Cov}^{\mathrm{WS}}(\mathbf{V}, \underline{\rho}^{\mathrm{Virt}}) &= \mathrm{Cov}^{\mathrm{WS}}(\mathbf{V}, \mathbf{V}, \underline{\rho}^{\mathrm{Virt}}) \\ &= \mathrm{Cov}^{\mathrm{WS}}(\underline{1}_{N_{\mathrm{Pulse}}} \otimes \mathbf{V}_1 + \mathbf{V}_2 \otimes \underline{1}_{N_{\mathrm{Rx}}}, \underline{1}_{N_{\mathrm{Pulse}}} \otimes \mathbf{V}_1 + \mathbf{V}_2 \otimes \underline{1}_{N_{\mathrm{Rx}}}, \underline{\rho} \otimes \underline{1}_{N_{\mathrm{Rx}}}) \\ &= \mathrm{Cov}^{\mathrm{WS}}(\underline{1}_{N_{\mathrm{Pulse}}} \otimes \mathbf{V}_1, \underline{1}_{N_{\mathrm{Pulse}}} \otimes \mathbf{V}_1, \underline{\rho} \otimes \underline{1}_{N_{\mathrm{Rx}}}) \\ &+ \mathrm{Cov}^{\mathrm{WS}}(\underline{1}_{N_{\mathrm{Pulse}}} \otimes \mathbf{V}_1, \mathbf{V}_2 \otimes \underline{1}_{N_{\mathrm{Rx}}}, \underline{\rho} \otimes \underline{1}_{N_{\mathrm{Rx}}}) \\ &+ \mathrm{Cov}^{\mathrm{WS}}(\mathbf{V}_2 \otimes \underline{1}_{N_{\mathrm{Rx}}}, \underline{1}_{N_{\mathrm{Pulse}}} \otimes \mathbf{V}_1, \underline{\rho} \otimes \underline{1}_{N_{\mathrm{Rx}}}) \\ &+ \mathrm{Cov}^{\mathrm{WS}}(\mathbf{V}_2 \otimes \underline{1}_{N_{\mathrm{Rx}}}, \mathbf{V}_2 \otimes \underline{1}_{N_{\mathrm{Rx}}}, \underline{\rho} \otimes \underline{1}_{N_{\mathrm{Rx}}}) \\ &= \mathrm{Cov}^{\mathrm{S}}(\mathbf{V}_1, \mathbf{V}_1) + \mathbf{0} + \mathbf{0} + \mathrm{Cov}^{\mathrm{WS}}(\mathbf{V}_2, \mathbf{V}_2, \underline{\rho}) \\ &= \mathrm{Cov}^{\mathrm{S}}(\mathbf{V}_1, \mathbf{V}_1) + \mathrm{Cov}^{\mathrm{WS}}(\mathbf{V}_2, \mathbf{V}_2, \underline{\rho}). \end{aligned} \tag{H.22}$$

Hence

$$\mathrm{Cov}^{\mathrm{WS}}(\mathbf{V}, \underline{\rho}^{\mathrm{Virt}}) = \begin{bmatrix} \mathrm{Cov}^{\mathrm{S}}(\mathbf{D}^{\mathrm{Rx}}) & & 0 \\ & & 0 \\ 0 \quad & 0 \quad & 0 \end{bmatrix} + \begin{bmatrix} \mathrm{Cov}^{\mathrm{WS}}(\mathbf{D}^{\mathrm{Pulse}}, \underline{\rho}) & \mathrm{Cov}^{\mathrm{WS}}(\underline{t}, \mathbf{D}^{\mathrm{Pulse}}, \underline{\rho}) \\ \mathrm{Cov}^{\mathrm{WS}}(\mathbf{D}^{\mathrm{Pulse}}, \underline{t}, \underline{\rho}) & \mathrm{Var}^{\mathrm{WS}}(\underline{t}, \underline{\rho}) \end{bmatrix}. \tag{H.23}$$

Putting this in (H.18) gives (5.91), which we wanted to derive.

I. Proof of Theorem 1

As shown in Section 5.2.2.2, $\mathrm{CRB}_{u,\mathrm{SIMO}}, \mathrm{CRB}_u$ and $\mathrm{CRB}_{u,\mathrm{stat}}$ differ by the terms U given in (5.123) to (5.126). The expression $\left(\mathrm{Cov}^{\mathrm{WS}}(\underline{d}^{\mathrm{Pulse}}, \underline{t}, \underline{\rho})\right)^2$ appears in U_{penalty} (5.126). We show that

$$\left(\mathrm{Cov}^{\mathrm{WS}}(\underline{d}^{\mathrm{Pulse}}, \underline{t}, \underline{\rho})\right)^2 \leq |\,\mathrm{Var}^{\mathrm{WS}}(\underline{d}^{\mathrm{Pulse}}, \underline{\rho})| \cdot |\,\mathrm{Var}^{\mathrm{WS}}(\underline{t}, \underline{\rho})|, \tag{I.1}$$

for any $\underline{d}^{\mathrm{Pulse}}, \underline{t}, \underline{\rho}$. For arbitrary but fixed $\underline{\rho}$, we assume w. l. o. g. $\mathrm{E}^{\mathrm{WS}}(\underline{d}^{\mathrm{Pulse}}, \underline{\rho}) = \mathrm{E}^{\mathrm{WS}}(\underline{t}, \underline{\rho}) = 0$. This can always be achieved by shifting the spatial or temporal coordinate system by a constant, which is physically irrelevant. Then, due to Lemma A.2.12,

$$\mathrm{Cov}^{\mathrm{WS}}(\underline{d}^{\mathrm{Pulse}}, \underline{t}, \underline{\rho}) = \mathrm{Corr}^{\mathrm{WS}}(\underline{d}^{\mathrm{Pulse}}, \underline{t}, \underline{\rho}), \tag{I.2}$$

$$\mathrm{Var}^{\mathrm{WS}}(\underline{d}^{\mathrm{Pulse}}, \underline{\rho}) = \mathrm{Corr}^{\mathrm{WS}}(\underline{d}^{\mathrm{Pulse}}, \underline{d}^{\mathrm{Pulse}}, \underline{\rho}), \tag{I.3}$$

$$\mathrm{Var}^{\mathrm{WS}}(\underline{t}, \underline{\rho}) = \mathrm{Corr}^{\mathrm{WS}}(\underline{t}, \underline{t}, \underline{\rho}). \tag{I.4}$$

Note that $\rho_i \in \mathbb{R}$, $\underline{\rho}_i > 0$, $i = 1, \ldots, N_{\mathrm{Pulse}}$. For fixed $\underline{\rho}$ and vectors $\underline{x}, \underline{y}, \in \mathbb{R}^{N_{\mathrm{Pulse}}}$, $\mathrm{Corr}^{\mathrm{WS}}(\underline{x}, \underline{y}, \underline{\rho})$ is an inner product

$$\langle \underline{x}, \underline{y} \rangle := \mathrm{Corr}^{\mathrm{WS}}(\underline{x}, \underline{y}, \underline{\rho}), \tag{I.5}$$

since it fulfills all axioms of an inner product, i. e. it is symmetric in $\underline{x}, \underline{y}$, linear in its first argument and positive definite [Poole, 2011]. Thus the Cauchy Schwarz inequality holds [Poole, 2011]

$$|\,\mathrm{Corr}^{\mathrm{WS}}(\underline{x}, \underline{y}, \underline{\rho})|^2 \leq |\,\mathrm{Corr}^{\mathrm{WS}}(\underline{x}, \underline{x}, \underline{\rho})| \cdot |\,\mathrm{Corr}^{\mathrm{WS}}(\underline{y}, \underline{y}, \underline{\rho})|. \tag{I.6}$$

Therefore

$$|\,\mathrm{Corr}^{\mathrm{WS}}(\underline{d}^{\mathrm{Pulse}}, \underline{t}, \underline{\rho})|^2 \leq |\,\mathrm{Corr}^{\mathrm{WS}}(\underline{d}^{\mathrm{Pulse}}, \underline{d}^{\mathrm{Pulse}}, \underline{\rho})| \cdot |\,\mathrm{Corr}^{\mathrm{WS}}(\underline{t}, \underline{t}, \underline{\rho})|, \tag{I.7}$$

from which follows (I.1). Plugging (I.1) in (5.126) yields $0 \leq U_{\mathrm{penalty}} \leq \mathrm{Var}^{\mathrm{WS}}(\underline{d}^{\mathrm{Pulse}}, \underline{\rho})$. With (5.123) to (5.125) follows $U_{\mathrm{SIMO}} \leq U \leq U_{\mathrm{stat}}$ and thus (5.127).

The second part of the theorem (5.128) follows immediately from (5.125). □

J. Proof of Theorem 2: Weighted Mean Transmit Times and Decoupling of Electrical Angles from the Doppler Frequency

We prove Theorem 2 in Section 5.2.3.1. For that purpose, we first state and prove different lemmas of $\mathrm{Cov}^{\mathrm{WS}}$.

J.1. Lemmas of the Weighted Sample Covariance of Clustered Values

Lemma J.1.1 ($\mathrm{Cov}^{\mathrm{WS}}$ of clustered values)**.** *Let $\underline{x}, \underline{y}, \in \mathbb{R}^K$ and $\underline{w} \in \mathbb{C}^K$. Let*

$$\underline{x} = \begin{bmatrix} \tilde{x}_1 \, \underline{1}_{M_1} \\ \vdots \\ \tilde{x}_C \, \underline{1}_{M_C} \end{bmatrix} = \begin{bmatrix} \underline{x}^{(1)} \\ \vdots \\ \underline{x}^{(C)} \end{bmatrix} \in \mathbb{R}^K,$$

with $\underline{x}^{(i)} \in \mathbb{R}^{M_i}$ and $\sum_{i=1}^{C} M_i = K$. Thus $\underline{x}$ contains at most $1 \leq C \leq K$ different cluster values $\tilde{x}_1, \ldots, \tilde{x}_C$. Some of them can be identical. Similarly, we write

$$\underline{y} = \begin{bmatrix} \underline{y}^{(1)} \\ \vdots \\ \underline{y}^{(C)} \end{bmatrix}, \quad \underline{w} = \begin{bmatrix} \underline{w}^{(1)} \\ \vdots \\ \underline{w}^{(C)} \end{bmatrix},$$

with $\underline{y}^{(i)} \in \mathbb{R}^{M_i}$ and $\underline{w}^{(i)} \in \mathbb{C}^{M_i}$. Note that in general, only $\underline{x}$ contains cluster values and $\underline{y}, \underline{w}$ do not. We define

$$\underline{\tilde{x}} = \begin{bmatrix} \tilde{x}_1 & \ldots & \tilde{x}_C \end{bmatrix}^T, \tag{J.1}$$

$$\underline{\tilde{y}} = \begin{bmatrix} \tilde{y}_1 & \dots & \tilde{y}_C \end{bmatrix}^T, \tag{J.2}$$

$$\tilde{y}_i = \frac{1}{\underline{1}^T \underline{w}^{(i)}} \underline{w}^{(i)T} \underline{y}^{(i)} = \mathrm{E}^{\mathrm{WS}}\left(\underline{y}^{(i)}, \underline{w}^{(i)}\right), \tag{J.3}$$

$$\underline{\tilde{w}} = \begin{bmatrix} \tilde{w}_1 & \dots & \tilde{w}_C \end{bmatrix}^T, \tag{J.4}$$

$$\tilde{w}_i = \underline{1}^T \underline{w}^{(i)}. \tag{J.5}$$

Then

$$\mathrm{Cov}^{\mathrm{WS}}(\underline{x}, \underline{y}, \underline{w}) = \mathrm{Cov}^{\mathrm{WS}}(\underline{\tilde{x}}, \underline{\tilde{y}}, \underline{\tilde{w}}). \tag{J.6}$$

Here we assume $\underline{1}^T \underline{w} \neq 0$ *and* $\underline{1}^T \underline{w}^{(i)} \neq 0$, $i \in \{1, \dots, C\}$.

This lemma states that due to the clustering $\underline{x}^{(\mathrm{i})} = \tilde{x}_i \underline{1}$, the weighted covariance of a K-point problem $(\underline{x}, \underline{y}, \underline{w})$ can be reformulated as the weighted covariance of a C-point problem $(\underline{\tilde{x}}, \underline{\tilde{y}}, \underline{\tilde{w}})$. The values of $\underline{y}$ corresponding to cluster i are represented by their weighted mean $\tilde{y}_i = \mathrm{E}^{\mathrm{WS}}(\underline{y}^{(\mathrm{i})}, \underline{w}^{(\mathrm{i})})$ and the corresponding values of $\underline{w}$ by the sum of all weights of that cluster $\tilde{w}_i = \underline{1}^T \underline{w}^{(\mathrm{i})}$.

Proof. We define

$$S = \underline{1}^T \underline{w} = \underline{1}^T \underline{\tilde{w}}. \tag{J.7}$$

We use Lemma A.2.12 and get

$$\begin{aligned}
\mathrm{Cov}^{\mathrm{WS}}(\underline{x}, \underline{y}, \underline{w}) &= \mathrm{Corr}^{\mathrm{WS}}(\underline{x}, \underline{y}, \underline{w}) - \mathrm{E}^{\mathrm{WS}}(\underline{y}, \underline{w})\, \mathrm{E}^{\mathrm{WS}}(\underline{x}, \underline{w}) \\
&= \frac{1}{S} \sum_{k=1}^{K} w_k\, x_k\, y_k - \left(\frac{1}{S} \sum_{k=1}^{K} w_k\, x_k\right)\left(\frac{1}{S} \sum_{k=1}^{K} w_k\, y_k\right) \qquad \text{(J.8)} \\
&= \frac{1}{S} \sum_{i=1}^{C} \underline{w}^{(\mathrm{i})T} \underline{y}^{(\mathrm{i})} \tilde{x}_i - \left(\frac{1}{S} \sum_{i=1}^{C} \underline{1}^T \underline{w}^{(\mathrm{i})} \tilde{x}_i\right)\left(\frac{1}{S} \sum_{i=1}^{C} \underline{w}^{(\mathrm{i})T} \underline{y}^{(\mathrm{i})}\right) \\
&= \frac{1}{S} \sum_{i=1}^{C} \tilde{w}_i\, \tilde{y}_i\, \tilde{x}_i - \left(\frac{1}{S} \sum_{i=1}^{C} \tilde{w}_i\, \tilde{x}_i\right)\left(\frac{1}{S} \sum_{i=1}^{C} \tilde{w}_i\, \tilde{y}_i\right) \\
&= \mathrm{Cov}^{\mathrm{WS}}(\underline{\tilde{x}}, \underline{\tilde{y}}, \underline{\tilde{w}}). \qquad \text{(J.9)}
\end{aligned}$$

□

Lemma J.1.2. *Let* $\underline{\tilde{x}}, \underline{\tilde{y}} \in \mathbb{R}^C$, $\underline{\tilde{w}} \in \mathbb{C}^C$, $\tilde{w}_i \neq 0$ *and* $\underline{1}^T \underline{\tilde{w}} \neq 0$. *Then*

$$\underline{\tilde{y}} \propto \underline{1} \Longrightarrow \mathrm{Cov}^{\mathrm{WS}}(\underline{\tilde{x}}, \underline{\tilde{y}}, \underline{\tilde{w}}) = 0. \tag{J.10}$$

Moreover, if $C = 2$ *and* $\tilde{x}_1 \neq \tilde{x}_2$

$$\underline{\tilde{y}} \propto \underline{1} \iff \mathrm{Cov}^{\mathrm{WS}}(\underline{\tilde{x}}, \underline{\tilde{y}}, \underline{\tilde{w}}) = 0. \tag{J.11}$$

Proof. Since $\underline{\tilde{y}} \propto \underline{1}$ implies $\tilde{y}_k = \tilde{y}_l \; \forall \, k, l \in \{1, \ldots, C\}$, (J.10) follows immediately from (J.9). If $C = 2$ and $\tilde{x}_1 \neq \tilde{x}_2$,

$$\begin{aligned}
\mathrm{Cov}^{\mathrm{WS}}(\underline{\tilde{x}}, \underline{\tilde{y}}, \underline{\tilde{w}}) &= \mathrm{Corr}^{\mathrm{WS}}(\underline{\tilde{x}}, \underline{\tilde{y}}, \underline{\tilde{w}}) - \mathrm{E}^{\mathrm{WS}}(\underline{\tilde{y}}, \underline{\tilde{w}})\, \mathrm{E}^{\mathrm{WS}}(\underline{\tilde{x}}, \underline{\tilde{w}}) \\
&= \frac{1}{\underline{1}^T \underline{\tilde{w}}} \sum_{k=1}^{C} \tilde{w}_k \, \tilde{x}_k \, \tilde{y}_k - \left(\frac{1}{S} \sum_{k=1}^{C} \tilde{w}_k \, \tilde{x}_k \right) \left(\frac{1}{S} \sum_{k=1}^{C} \tilde{w}_k \, \tilde{y}_k \right) \qquad \text{(J.12)} \\
&= \frac{1}{\left(\underline{1}^T \underline{\tilde{w}} \right)^2} \left[\left(\sum_{k=1}^{C} \tilde{w}_k \right) \left(\sum_{k=1}^{C} \tilde{w}_k \, \tilde{x}_k \, \tilde{y}_k \right) - \left(\sum_{k=1}^{C} \tilde{w}_k \, \tilde{x}_k \right) \left(\sum_{k=1}^{C} \tilde{w}_k \, \tilde{y}_k \right) \right] \\
&= \frac{1}{\left(\underline{1}^T \underline{\tilde{w}} \right)^2} \sum_{k=1}^{C} \sum_{l=1}^{C} \underbrace{\left(\tilde{w}_k \, \tilde{w}_l \, \tilde{x}_l \, \tilde{y}_l - \tilde{w}_k \, \tilde{w}_l \, \tilde{x}_k \, \tilde{y}_l \right)}_{=0 \text{ if } k=l} \\
&= \frac{1}{\left(\underline{1}^T \underline{\tilde{w}} \right)^2} \tilde{w}_1 \, \tilde{w}_2 \left(\tilde{x}_1 \, \tilde{y}_1 + \tilde{x}_2 \, \tilde{y}_2 - \tilde{x}_1 \, \tilde{y}_2 - \tilde{x}_2 \, \tilde{y}_1 \right) \\
&= \frac{1}{\left(\underline{1}^T \underline{\tilde{w}} \right)^2} \tilde{w}_1 \, \tilde{w}_2 \left(\tilde{x}_1 - \tilde{x}_2 \right) \left(\tilde{y}_1 - \tilde{y}_2 \right) \\
&= 0 \iff \tilde{y}_1 = \tilde{y}_2, \qquad \text{(J.13)}
\end{aligned}$$

since $\tilde{x}_1 \neq \tilde{x}_2$ and $\tilde{w}_1, \, \tilde{w}_2 \neq 0$. □

Combining both lemmas, we get the following lemma.

Lemma J.1.3. *Let* $\underline{x} \in \mathbb{R}^K, \underline{y} \in \mathbb{R}^K$ *and the weight vector* $\underline{w} \in \mathbb{C}^K$*. Moreover, let* $\underline{x}$ *contain at most* $1 \leq C \leq K$ *different values. Since* $\mathrm{Cov}^{\mathrm{WS}}(\underline{x}, \underline{y}, \underline{w})$ *is invariant w. r. t. a synchronous sorting of the elements of* $\underline{x}, \underline{y}, \underline{w}$*, we sort* $\underline{x}, \underline{y}, \underline{w}$ *such that*

$$\underline{x} = \begin{bmatrix} \tilde{x}_1 \, \underline{1}_{M_1} \\ \vdots \\ \tilde{x}_C \, \underline{1}_{M_C} \end{bmatrix} = \begin{bmatrix} \underline{x}^{(1)} \\ \vdots \\ \underline{x}^{(C)} \end{bmatrix} \in \mathbb{R}^K,$$

with $\underline{x}^{(i)} \in \mathbb{R}^{M_i}$ *and* $\sum_{i=1}^{C} M_i = K$*. Hence, we have C clusters,* $\tilde{x}_1 \underline{1}_{M_1}, \ldots, \tilde{x}_C \underline{1}_{M_C}$*, where the i-th cluster of* $\underline{x}$ *contains one value* $\tilde{x}_i$*. Some of the values* $\tilde{x}_i$*,* $i = 1, \ldots, C$*, can be identical. Similarly*

$$\underline{y} = \begin{bmatrix} \underline{y}^{(1)} \\ \vdots \\ \underline{y}^{(C)} \end{bmatrix}, \quad \underline{w} = \begin{bmatrix} \underline{w}^{(1)} \\ \vdots \\ \underline{w}^{(C)} \end{bmatrix}.$$

Then

$$\begin{aligned} &\mathrm{E}^{\mathrm{WS}}\left(\underline{y}^{(k)}, \underline{w}^{(k)}\right) = \mathrm{E}^{\mathrm{WS}}\left(\underline{y}^{(l)}, \underline{w}^{(l)}\right) \ \forall\, k, l \in \{1, \ldots, C\} \\ &\Longrightarrow \mathrm{Cov}^{\mathrm{WS}}\left(\underline{x}, \underline{y}, \underline{w}\right) = 0. \end{aligned} \tag{J.14}$$

Moreover, for $C = 2$, $\tilde{x}_1 \neq \tilde{x}_2$ *and* $\underline{1}^T \underline{w}^{(k)} \neq 0$, $k = 1, 2$,

$$\mathrm{E}^{\mathrm{WS}}\left(\underline{y}^{(1)}, \underline{w}^{(1)}\right) = \mathrm{E}^{\mathrm{WS}}\left(\underline{y}^{(2)}, \underline{w}^{(2)}\right) \quad \Longleftrightarrow \quad \mathrm{Cov}^{\mathrm{WS}}\left(\underline{x}, \underline{y}, \underline{w}\right) = 0. \tag{J.15}$$

Here we assume $\underline{1}^T \underline{w} \neq 0$ *and* $\underline{1}^T \underline{w}^{(i)} \neq 0$, $i \in \{1, \ldots, C\}$.

Proof. This lemma follows directly from Lemma J.1.1 and J.1.2. □

J.2. Proof of Theorem 2

We apply Lemma J.1.3 to prove Theorem 2. First we consider the case of a linear array. We set $\underline{x} = \underline{d}^{\mathrm{Pulse}}$, $\underline{y} = \underline{t}$, $\underline{w} = \underline{\rho}$. Here, $\underline{d}^{\mathrm{Pulse}}$ contains N_{Tx} different antenna positions. Hence the synchronous sorting with $C = N_{\mathrm{Tx}}$ clusters yields

$$\underline{\tilde{x}} = \underline{d}^{\mathrm{Tx}}, \tag{J.16}$$

$$\underline{y}^{(\mathrm{i})} = \underline{t}^{(i)}, \tag{J.17}$$

$$\underline{w}^{(\mathrm{i})} = \underline{\rho}^{(i)}. \tag{J.18}$$

Therefore, for a linear array Theorem 2 follows directly from Lemma J.1.3.

Now we consider the planar array. First we show (5.130) in Theorem 2. Since

$$\mathrm{Cov}^{\mathrm{WS}}(\mathbf{D}^{\mathrm{Pulse}}, \underline{t}, \underline{\rho}) = \begin{bmatrix} \mathrm{Cov}^{\mathrm{WS}}(\underline{d}^{\mathrm{Pulse},x}, \underline{t}, \underline{\rho}) \\ \mathrm{Cov}^{\mathrm{WS}}(\underline{d}^{\mathrm{Pulse},y}, \underline{t}, \underline{\rho}) \end{bmatrix} \tag{J.19}$$

we have to show

$$\mathrm{E}^{\mathrm{WS}}\left(\underline{t}^{(k)}, \underline{\rho}^{(k)}\right) = \mathrm{E}^{\mathrm{WS}}\left(\underline{t}^{(l)}, \underline{\rho}^{(l)}\right) \ \forall k, l \in \{1, \ldots, N_{\mathrm{Tx}}\} \quad \Longrightarrow \quad \mathrm{Cov}^{\mathrm{WS}}\left(\underline{d}^{\mathrm{Pulse},x}, \underline{t}, \underline{\rho}\right) = 0 \tag{J.20}$$

for the x-coordinate $\underline{d}^{\mathrm{Pulse},x}$ of the Tx antennas and at the same time

$$\mathrm{E}^{\mathrm{WS}}\left(\underline{t}^{(k)}, \underline{\rho}^{(k)}\right) = \mathrm{E}^{\mathrm{WS}}\left(\underline{t}^{(l)}, \underline{\rho}^{(l)}\right) \ \forall k, l \in \{1, \ldots, N_{\mathrm{Tx}}\} \quad \Longrightarrow \quad \mathrm{Cov}^{\mathrm{WS}}\left(\underline{d}^{\mathrm{Pulse},y}, \underline{t}, \underline{\rho}\right) = 0 \tag{J.21}$$

for the y-coordinate $\underline{d}^{\mathrm{Pulse},y}$. First we prove (J.20). We set $\underline{x} = \underline{d}^{\mathrm{Pulse},x}$, $\underline{y} = \underline{t}$, $\underline{w} = \underline{\rho}$ and apply Lemma J.1.3 with $C = N_{\mathrm{Tx}}$ clusters, where each cluster contains x-coordinate of one Tx antenna. From that (J.20) follows. Analogously we prove (J.21) in the same way. Hence we have shown

(5.130). The reason is that the MIMO-TDM scheme implies a reuse of individual Tx antenna which corresponds to a synchronous clustering of the x/y- coordinates of the Tx antennas regardless of the dimension of the Tx array (1D, 2D).

Now we prove (5.131) in Theorem 2 for 2 Tx antennas. The implication "$\Longrightarrow$" in (5.131) follows from (5.130). Hence we have to show the other implication "$\Longleftarrow$":

$$\mathrm{E}^{\mathrm{WS}}\left(\underline{t}^{(1)},\underline{\rho}^{(1)}\right)=\mathrm{E}^{\mathrm{WS}}\left(\underline{t}^{(2)},\underline{\rho}^{(2)}\right)\quad\Longleftarrow\quad\mathrm{Cov}^{\mathrm{WS}}\left(\mathbf{D}^{\mathrm{Pulse}},\underline{t},\underline{\rho}\right)=\underline{0}. \tag{J.22}$$

Since $\underline{d}^{\mathrm{Tx},1}\neq\underline{d}^{\mathrm{Tx},2}$, the Tx antennas differ in their x-coordinate or their y-coordinate or both. We assume w. l. o. g. $d_x^{\mathrm{Tx},1}\neq d_x^{\mathrm{Tx},2}$. We set $\underline{x}=\underline{d}^{\mathrm{Pulse},x}$, $\underline{y}=\underline{t}$, $\underline{w}=\underline{\rho}$ and use Lemma J.1.3 with $C=2$ clusters. From (J.15) follows

$$\mathrm{E}^{\mathrm{WS}}\left(\underline{t}^{(1)},\underline{\rho}^{(1)}\right)=\mathrm{E}^{\mathrm{WS}}\left(\underline{t}^{(2)},\underline{\rho}^{(2)}\right)\quad\Longleftarrow\quad\mathrm{Cov}^{\mathrm{WS}}\left(\underline{d}^{\mathrm{Pulse},x},\underline{t},\underline{\rho}\right)=0 \tag{J.23}$$

and therefore (J.22). Thus we have shown (5.131). □

K. Proof of Theorem 3: Optimal TDM Schemes for Constrained Transmission Energy and Constrained Aperture Size

We prove the part which is missing in the proof of Theorem 3 on p. 109 in the following section. In Section K.2 we state and prove several lemmas which we use for the proof.

K.1. Missing Part of the Proof of Theorem 3

We have to show:

$$\begin{aligned}&\mathrm{Var}^{\mathrm{WS}}(\underline{d}^{\mathrm{Pulse}}, \underline{\rho}) \text{ is maximal iff}\\ &\text{only the two outermost Tx antennas are used and } \underline{1}^T\underline{\rho}^{(1)} = \underline{1}^T\underline{\rho}^{(2)}.\end{aligned} \tag{K.1}$$

We abbreviate the assertions by

$$A: \quad \mathrm{Var}^{\mathrm{WS}}(\underline{d}^{\mathrm{Pulse}}, \underline{\rho}) \text{ is maximal,} \tag{K.2}$$

$$B: \quad \text{only the two outermost Tx antennas are used and } \underline{1}^T\underline{\rho}^{(1)} = \underline{1}^T\underline{\rho}^{(2)}. \tag{K.3}$$

Thus we have to show

$$A \iff B, \tag{K.4}$$

where " $\iff$ " is an abbreviation for "if and only if". We consider an arbitrary TDM scheme characterized by $\underline{d}^{\mathrm{Pulse}}$, $\underline{\rho}$, N_{Pulse}, which does not fulfill B, i. e. it uses not only the two outermost antennas and/or $\underline{1}^T\underline{\rho}^{(1)} \neq \underline{1}^T\underline{\rho}^{(2)}$.

First we consider the case that the TDM scheme does not use only the two outermost antennas. Afterwards, we consider the case that $\underline{1}^T\underline{\rho}^{(1)} = \underline{1}^T\underline{\rho}^{(2)}$ is not satisfied.

Case 1: The TDM scheme does not use only the two outermost antennas. In the trivial case, when the TDM scheme uses only 1 Tx antenna, $\underline{d}^{\text{Pulse}} \propto \underline{1}$ and obviously $\text{Var}^{\text{WS}}(\underline{d}^{\text{Pulse}}, \underline{\rho}) = 0$.

If the TDM scheme uses more than 2 Tx antennas, there exists at least one $k \in \{1, \ldots, N_{\text{Pulse}}\}$ with $d_k^{\text{Pulse}} \neq d_{\min}^{\text{Pulse}}, d_{\max}^{\text{Pulse}}$, where $d_{\min}^{\text{Pulse}} = \min(\underline{d}^{\text{Pulse}})$ and $d_{\max}^{\text{Pulse}} = \max(\underline{d}^{\text{Pulse}})$. Using Lemma K.2.1 we can increase $\text{Var}^{\text{WS}}(\underline{d}^{\text{Pulse}}, \underline{\rho})$ by substituting the element d_k^{Pulse} in $\underline{d}^{\text{Pulse}}$ by $d_{\min}^{\text{Pulse}}$, appending $d_{\max}^{\text{Pulse}}$ to $\underline{d}^{\text{Pulse}}$ while keeping the overall transmitting energy $\underline{1}^T \underline{\rho}$ constant. We call the resulting vectors $\underline{d}_{(a)}^{\text{Pulse}}$ and $\underline{\rho}_{(a)}$, respectively. Hence

$$\text{Var}^{\text{WS}}\left(\underline{d}^{\text{Pulse}}, \underline{\rho}\right) < \text{Var}^{\text{WS}}\left(\underline{d}_{(a)}^{\text{Pulse}}, \underline{\rho}_{(a)}\right). \tag{K.5}$$

We do this repeatedly until $\underline{d}_{(a)}^{\text{Pulse}}$ consists only of the elements $d_{\min}^{\text{Pulse}}$ and $d_{\max}^{\text{Pulse}}$, i. e. it uses only 2 Tx antennas. The resulting vectors are denoted by $\underline{d}_{(2\text{ Tx})}^{\text{Pulse}}$ and $\underline{\rho}_{(2\text{ Tx})}$, respectively. Thus

$$\text{Var}^{\text{WS}}\left(\underline{d}^{\text{Pulse}}, \underline{\rho}\right) < \text{Var}^{\text{WS}}\left(\underline{d}_{(2\text{ Tx})}^{\text{Pulse}}, \underline{\rho}_{(2\text{ Tx})}\right). \tag{K.6}$$

Now let us assume that the TDM scheme uses 2 Tx antennas, but not the two outermost ones. Hence all elements in $\underline{d}^{\text{Pulse}}$ equal $d_{\min}^{\text{Pulse}}$ or $d_{\max}^{\text{Pulse}}$ and

$$\begin{bmatrix} d_{\min}^{\text{Pulse}} \\ d_{\max}^{\text{Pulse}} \end{bmatrix} \neq \begin{bmatrix} d_{\min}^{\text{Tx}} \\ d_{\max}^{\text{Tx}} \end{bmatrix}. \tag{K.7}$$

The pulse energies are denoted by $\underline{\rho} = \underline{\rho}_{(2\text{ Tx})}$, since the TDM scheme uses only 2 Tx antennas. Let $\underline{d}_{(2\text{ Tx, outermost})}^{\text{Pulse}}$ be the same as $\underline{d}^{\text{Pulse}}$, but with $d_{\min}^{\text{Pulse}}$ and $d_{\max}^{\text{Pulse}}$ replaced by $d_{\min}^{\text{Tx}}$ and $d_{\max}^{\text{Tx}}$, respectively. Hence, the transmission sequence in $\underline{d}_{(2\text{ Tx, outermost})}^{\text{Pulse}}$ is the same as in $\underline{d}^{\text{Pulse}}$ but only the two outermost antenna positions are used. We can express

$$\underline{d}_{(2\text{ Tx, outermost})}^{\text{Pulse}} = a \cdot \underline{d}^{\text{Pulse}} + b \cdot \underline{1} \tag{K.8}$$

with $a \in \mathbb{R}$, $a > 1$ and $b \in \mathbb{R}$ chosen appropriately. Hence

$$\begin{aligned} \text{Var}^{\text{WS}}\left(\underline{d}_{(2\text{ Tx, outermost})}^{\text{Pulse}}, \underline{\rho}_{(2\text{ Tx})}\right) &= \text{Var}^{\text{WS}}\left(a\,\underline{d}^{\text{Pulse}}, \underline{\rho}_{(2\text{ Tx})}\right) + \text{Var}^{\text{WS}}\left(b\,\underline{1}, \underline{\rho}_{(2\text{ Tx})}\right) \\ &= a^2\ \text{Var}^{\text{WS}}\left(\underline{d}^{\text{Pulse}}, \underline{\rho}_{(2\text{ Tx})}\right) \\ &> \text{Var}^{\text{WS}}\left(\underline{d}^{\text{Pulse}}, \underline{\rho}_{(2\text{ Tx})}\right). \end{aligned} \tag{K.9}$$

Note that for $\underline{d}_{(2\text{ Tx})}^{\text{Pulse}}$ in (K.6),

$$\text{Var}^{\text{WS}}\left(\underline{d}_{(2\text{ Tx})}^{\text{Pulse}}, \underline{\rho}_{(2\text{ Tx})}\right) \leq \text{Var}^{\text{WS}}\left(\underline{d}_{(2\text{ Tx, outermost})}^{\text{Pulse}}, \underline{\rho}_{(2\text{ Tx})}\right) \tag{K.10}$$

holds, with the equality iff $\underline{d}^{\text{Pulse}}_{(2\text{ Tx})}$ contains only the outermost positions.

Thus we have shown that for any TDM scheme $\underline{d}^{\text{Pulse}}, \underline{\rho}$, which does not use only the two outermost antennas

$$\text{Var}^{\text{WS}}\left(\underline{d}^{\text{Pulse}}, \underline{\rho}\right) < \text{Var}^{\text{WS}}\left(\underline{d}^{\text{Pulse}}_{(2\text{ Tx, outermost})}, \underline{\rho}_{(2\text{ Tx})}\right), \tag{K.11}$$

where $\underline{d}^{\text{Pulse}}_{(2\text{ Tx, outermost})}$ and $\underline{\rho}_{(2\text{ Tx})}$ are constructed from $\underline{d}^{\text{Pulse}}, \underline{\rho}$ as described above.

Case 2: $\underline{1}^T\underline{\rho}^{(1)} \neq \underline{1}^T\underline{\rho}^{(2)}$**.** Now let us assume that the TDM scheme uses only the two outermost Tx antennas but $\underline{1}^T\underline{\rho}^{(1)} \neq \underline{1}^T\underline{\rho}^{(2)}$. We denote $\underline{d}^{\text{Pulse}}$ by $\underline{d}^{\text{Pulse}}_{(2\text{ Tx, outermost})}$ and $\underline{\rho}$ by $\underline{\rho}_{(2\text{ Tx})}$. Since $\text{Var}^{\text{WS}}(\underline{d}^{\text{Pulse}}_{(2\text{ Tx, outermost})}, \underline{\rho}_{(2\text{ Tx})})$ is invariant w. r. t. a synchronous sorting of the elements in $\underline{d}^{\text{Pulse}}_{(2\text{ Tx, outermost})}$ and $\underline{\rho}_{(2\text{ Tx})}$, we sort $\underline{d}^{\text{Pulse}}_{(2\text{ Tx, outermost})}$ and $\underline{\rho}_{(2\text{ Tx})}$ such that we have two clusters in $\underline{d}^{\text{Pulse}}_{(2\text{ Tx, outermost})}$

$$\underline{d}^{\text{Pulse}}_{(2\text{ Tx, outermost})} = \begin{bmatrix} d^{\text{Tx}}_{\text{min}}\,\underline{1} \\ d^{\text{Tx}}_{\text{max}}\,\underline{1} \end{bmatrix}, \tag{K.12}$$

$$\underline{\rho}_{(2\text{ Tx})} = \begin{bmatrix} \underline{\rho}^{(1)}_{(2\text{ Tx})} \\ \underline{\rho}^{(2)}_{(2\text{ Tx})} \end{bmatrix}. \tag{K.13}$$

Now we can apply Lemma J.1.1 for Cov^{WS} of clustered values. From that follows

$$\text{Var}^{\text{WS}}\left(\underline{d}^{\text{Pulse}}_{(2\text{ Tx, outermost})}, \underline{\rho}_{(2\text{ Tx})}\right) = \text{Var}^{\text{WS}}\left(\underline{\widetilde{d}}^{\text{Pulse}}_{(2\text{ Tx, outermost})}, \underline{\widetilde{\rho}}_{(2\text{ Tx})}\right) \tag{K.14}$$

with

$$\underline{\widetilde{d}}^{\text{Pulse}}_{(2\text{ Tx, outermost})} = \begin{bmatrix} d^{\text{Tx}}_{\text{min}} \\ d^{\text{Tx}}_{\text{max}} \end{bmatrix}, \tag{K.15}$$

$$\underline{\widetilde{\rho}}_{(2\text{ Tx})} = \begin{bmatrix} \underline{1}^T\underline{\rho}^{(1)}_{(2\text{ Tx})} \\ \underline{1}^T\underline{\rho}^{(2)}_{(2\text{ Tx})} \end{bmatrix}. \tag{K.16}$$

Now we use Lemma K.2.3, which states that $\text{Var}^{\text{WS}}(\underline{\widetilde{d}}^{\text{Pulse}}_{(2\text{ Tx, outermost})}, \underline{\widetilde{\rho}}_{(2\text{ Tx})})$ is maximal iff $\underline{\widetilde{\rho}}_{(2\text{ Tx})} \propto [1, 1]^T$. Since we assumed $\underline{1}^T\underline{\rho}^{(1)}_{(2\text{ Tx})} \neq \underline{1}^T\underline{\rho}^{(2)}_{(2\text{ Tx})}$

$$\text{Var}^{\text{WS}}\left(\underline{\widetilde{d}}^{\text{Pulse}}_{(2\text{ Tx, outermost})}, \underline{\widetilde{\rho}}_{(2\text{ Tx})}\right) < \text{Var}^{\text{WS}}\left(\underline{\widetilde{d}}^{\text{Pulse}}_{(2\text{ Tx, outermost})}, \underline{\widetilde{\rho}}_{(\text{equal energy})}\right) \tag{K.17}$$

with

$$\underline{\widetilde{\rho}}_{(\text{equal energy})} = [1,\ 1]^T. \tag{K.18}$$

Obviously

$$\mathrm{Var}^{\mathrm{WS}}\left(\underline{\widetilde{d}}^{\mathrm{Pulse}}_{(2\ \mathrm{Tx,\ outermost})}, \underline{\widetilde{\rho}}_{(\mathrm{equal\ energy})}\right) = \frac{1}{4}\left(d^{\mathrm{Tx}}_{\mathrm{max}} - d^{\mathrm{Tx}}_{\mathrm{min}}\right)^2. \tag{K.19}$$

Note that all vectors $\underline{\rho}_{(\mathrm{equal\ energy})} \in \mathbb{R}^{N_{\mathrm{Pulse}}}$ which satisfy

$$\underline{1}^T \underline{\rho}^{(1)}_{(\mathrm{equal\ energy})} = \underline{1}^T \underline{\rho}^{(2)}_{(\mathrm{equal\ energy})} \tag{K.20}$$

end up in $\underline{\widetilde{\rho}}_{(\mathrm{equal\ energy})}$ after sorting and clustering (up to a scaling factor). Here $\underline{\rho}^{(1)}_{(\mathrm{equal\ energy})}$ and $\underline{\rho}^{(2)}_{(\mathrm{equal\ energy})}$ denote the energies of the pulses which the first and second antenna transmits, respectively. Thus we have shown that

$$\mathrm{Var}^{\mathrm{WS}}\left(\underline{d}^{\mathrm{Pulse}}_{(2\ \mathrm{Tx,\ outermost})}, \underline{\rho}_{(2\ \mathrm{Tx})}\right) < \mathrm{Var}^{\mathrm{WS}}\left(\underline{d}^{\mathrm{Pulse}}_{(2\ \mathrm{Tx,\ outermost})}, \underline{\rho}_{(\mathrm{equal\ energy})}\right) \tag{K.21}$$

$$= \frac{1}{4}\left(d^{\mathrm{Tx}}_{\mathrm{max}} - d^{\mathrm{Tx}}_{\mathrm{min}}\right)^2, \tag{K.22}$$

where $\underline{\rho}_{(\mathrm{equal\ energy})} \in \mathbb{R}^{N_{\mathrm{Pulse}}}$ is any vector satisfying (K.20).

Result: Summarizing the results of case 1 and 2, we have shown that for any TDM scheme $\underline{d}^{\mathrm{Pulse}}, \underline{\rho}$ which does not satisfy assertion *B* (K.3),

$$\mathrm{Var}^{\mathrm{WS}}\left(\underline{d}^{\mathrm{Pulse}}, \underline{\rho}\right) < \mathrm{Var}^{\mathrm{WS}}\left(\underline{\widetilde{d}}^{\mathrm{Pulse}}_{(2\ \mathrm{Tx,\ outermost})}, \underline{\widetilde{\rho}}_{(\mathrm{equal\ energy})}\right) \tag{K.23}$$

holds, where $\underline{\widetilde{d}}^{\mathrm{Pulse}}_{(2\ \mathrm{Tx,\ outermost})}, \underline{\widetilde{\rho}}_{(\mathrm{equal\ energy})}$ is any TDM scheme satisfying *B*.

From that follows that if *B* is not satisfied, $\mathrm{Var}^{\mathrm{WS}}(\underline{d}^{\mathrm{Pulse}}, \underline{\rho})$ is not maximal. Written in shorter notation

$$\neg B \Longrightarrow \neg A \tag{K.24}$$

where "¬" means negation and "$\Longrightarrow$" is an abbreviation for "is sufficient for". This is equivalent to

$$A \Longrightarrow B. \tag{K.25}$$

On the other hand, if *B* is satisfied, $\mathrm{Var}^{\mathrm{WS}}(\underline{d}^{\mathrm{Pulse}}, \underline{\rho}) = \frac{1}{4}\left(d^{\mathrm{Tx}}_{\mathrm{max}} - d^{\mathrm{Tx}}_{\mathrm{min}}\right)^2$ due to (K.22), i. e. all TDM schemes satisfying *B* yield the same value for $\mathrm{Var}^{\mathrm{WS}}(\underline{d}^{\mathrm{Pulse}}, \underline{\rho})$. Since all TDM schemes which do not satisfy *B* yield a smaller value, $\mathrm{Var}^{\mathrm{WS}}(\underline{d}^{\mathrm{Pulse}}, \underline{\rho})$ is maximal, i. e.

$$B \Longrightarrow A. \tag{K.26}$$

Thus we have shown (K.4). □

K.2. Lemmas

Lemma K.2.1. *Let $\underline{d}^{Pulse}, \underline{\rho} \in \mathbb{R}^{N_{Pulse}}$. We define*

$$d_{min}^{Pulse} = \min\left(\underline{d}^{Pulse}\right),\ d_{max}^{Pulse} = \max\left(\underline{d}^{Pulse}\right). \tag{K.27}$$

Let $d_{min}^{Pulse} < d_{max}^{Pulse}$. Let there be at least one $k \in \{1, \ldots, N_{Pulse}\}$ with $d_k^{Pulse} \neq d_{min}^{Pulse}, d_{max}^{Pulse}$. We can increase $\mathrm{Var}^{\mathrm{WS}}(\underline{d}^{Pulse}, \underline{\rho})$ by substituting d_k^{Pulse} in $\underline{d}^{Pulse}$ by d_{min}^{Pulse}, adding an additional element d_{max}^{Pulse} and keeping the overall transmission energy constant.

More precisely: Let N_{Pulse} be arbitrary and

$$\begin{aligned}
\underline{d}^{Pulse} &= \left[d_1^{Pulse}, \ldots, d_k^{Pulse}, \ldots, d_{N_{Pulse}}^{Pulse}\right]^T, \\
\underline{\rho} &= \left[\rho_1, \ldots, \rho_{N_{Pulse}}\right], \\
\rho_i &> 0, \quad i = 1, \ldots, N_{Pulse}.
\end{aligned}$$

Then

$$\mathrm{Var}^{\mathrm{WS}}(\underline{d}^{Pulse}, \underline{\rho}) < \mathrm{Var}^{\mathrm{WS}}(\widetilde{\underline{d}^{Pulse}}, \widetilde{\underline{\rho}})$$

where

$$\widetilde{N_{Pulse}} = N_{Pulse} + 1, \tag{K.28}$$

$$\widetilde{\underline{d}^{Pulse}} \in \mathbb{R}^{\widetilde{N_{Pulse}}}, \tag{K.29}$$

$$\widetilde{d_i^{Pulse}} = d_i^{Pulse}, i = 1, \ldots, N_{Pulse} \wedge i \neq k, \tag{K.30}$$

$$\widetilde{d_k^{Pulse}} = d_{min}^{Pulse}, \tag{K.31}$$

$$\widetilde{d_{\widetilde{N_{Pulse}}}^{Pulse}} = d_{max}^{Pulse}, \tag{K.32}$$

$$\widetilde{\underline{\rho}} \in \mathbb{R}^{\widetilde{N_{Pulse}}}, \tag{K.33}$$

$$\widetilde{\rho_i} = \rho_i,\ i = 1, \ldots, N_{Pulse} \wedge i \neq k, \tag{K.34}$$

$$\underline{1}^T \underline{\rho} = \underline{1}^T \widetilde{\underline{\rho}}. \tag{K.35}$$

Proof.

$$\mathrm{E}^{\mathrm{WS}}(\widetilde{\underline{d}^{\mathrm{Pulse}}}, \widetilde{\underline{\rho}}) = \frac{1}{\underline{1}^T \widetilde{\underline{\rho}}} \sum_{i=1}^{\widetilde{N_{\mathrm{Pulse}}}} \widetilde{d_i^{\mathrm{Pulse}}}\, \widetilde{\rho_i} \tag{K.36}$$

$$= \frac{1}{\underline{1}^T \widetilde{\underline{\rho}}} \left\{ \left[\sum_{i=1, i\neq k}^{N_{\mathrm{Pulse}}} d_i^{\mathrm{Pulse}} \rho_i \right] + d_{\mathrm{min}}^{\mathrm{Pulse}} \widetilde{\rho}_k + d_{\mathrm{max}}^{\mathrm{Pulse}} \widetilde{\rho}_{\widetilde{N_{\mathrm{Pulse}}}} \right\} \tag{K.37}$$

We choose $\widetilde{\rho}_k$ and $\widetilde{\rho}_{\widetilde{N_{\text{Pulse}}}}$ such that

$$d_k^{\text{Pulse}}\,\rho_k = d_{\min}^{\text{Pulse}}\,\widetilde{\rho}_k + d_{\max}^{\text{Pulse}}\,\widetilde{\rho}_{\widetilde{N_{\text{Pulse}}}} \tag{K.38}$$

while

$$\rho_k = \widetilde{\rho}_k + \widetilde{\rho}_{\widetilde{N_{\text{Pulse}}}} \tag{K.39}$$

in order to fulfill (K.35). This is always uniquely possible since these are two linear independent equations for the two unknowns $\widetilde{\rho}_k$ and $\widetilde{\rho}_{\widetilde{N_{\text{Pulse}}}}$.

Putting (K.38) in (K.37) yields

$$\mathrm{E}^{\mathrm{WS}}(\widetilde{\underline{d}^{\text{Pulse}}}, \underline{\widetilde{\rho}}) = \mathrm{E}^{\mathrm{WS}}(\underline{d}^{\text{Pulse}}, \underline{\rho}). \tag{K.40}$$

Now we can compute $\mathrm{Var}^{\mathrm{WS}}(\widetilde{\underline{d}^{\text{Pulse}}}, \underline{\widetilde{\rho}})$ using (K.40)

$$\mathrm{Var}^{\mathrm{WS}}(\widetilde{\underline{d}^{\text{Pulse}}}, \underline{\widetilde{\rho}}) = \frac{1}{\underline{1}^T \underline{\widetilde{\rho}}} \sum_{i=1}^{\widetilde{N_{\text{Pulse}}}} \left[\widetilde{d_i^{\text{Pulse}}} - \mathrm{E}^{\mathrm{WS}}(\widetilde{\underline{d}^{\text{Pulse}}}, \underline{\widetilde{\rho}})\right]^2 \widetilde{\rho}_i \tag{K.41}$$

$$= \frac{1}{\underline{1}^T \underline{\rho}} \sum_{i=1}^{\widetilde{N_{\text{Pulse}}}} \left[\widetilde{d_i^{\text{Pulse}}} - \mathrm{E}^{\mathrm{WS}}(\underline{d}^{\text{Pulse}}, \underline{\rho})\right]^2 \widetilde{\rho}_i. \tag{K.42}$$

We compare this to

$$\mathrm{Var}^{\mathrm{WS}}(\underline{d}^{\text{Pulse}}, \underline{\rho}) = \frac{1}{\underline{1}^T \underline{\rho}} \sum_{i=1}^{N_{\text{Pulse}}} \left[d_i^{\text{Pulse}} - \mathrm{E}^{\mathrm{WS}}(\underline{d}^{\text{Pulse}}, \underline{\rho})\right]^2 \rho_i. \tag{K.43}$$

We set $c = \mathrm{E}^{\mathrm{WS}}(\underline{d}^{\text{Pulse}}, \underline{\rho})$. Note since $d_{\min}^{\text{Pulse}} < d_{\max}^{\text{Pulse}}$

$$d_{\min}^{\text{Pulse}} < c < d_{\max}^{\text{Pulse}}. \tag{K.44}$$

Hence

$$\sum_{i=1}^{\widetilde{N_{\text{Pulse}}}} (\widetilde{d_i^{\text{Pulse}}} - c)^2\,\widetilde{\rho}_i = \sum_{i=1, i\neq k}^{N_{\text{Pulse}}} (d_i^{\text{Pulse}} - c)^2\,\rho_i + (d_{\min}^{\text{Pulse}} - c)^2\,\widetilde{\rho}_k + (d_{\max}^{\text{Pulse}} - c)^2\,\widetilde{\rho}_{\widetilde{N_{\text{Pulse}}}}. \tag{K.45}$$

Using Lemma K.2.2 yields

$$\sum_{i=1}^{\widetilde{N_{\text{Pulse}}}} (\widetilde{d_i^{\text{Pulse}}} - c)^2\,\widetilde{\rho}_i > \sum_{i=1, i\neq k}^{N_{\text{Pulse}}} (d_i^{\text{Pulse}} - c)^2\,\rho_i + (d_k^{\text{Pulse}} - c)^2\,\rho_k \tag{K.46}$$

$$= \sum_{i=1}^{N_{\text{Pulse}}} (d_i^{\text{Pulse}} - c)^2\,\rho_i. \tag{K.47}$$

Thus

$$\mathrm{Var}^{\mathrm{WS}}(\widetilde{\underline{d}^{\mathrm{Pulse}}}, \widetilde{\underline{\rho}}) > \mathrm{Var}^{\mathrm{WS}}(\underline{d}^{\mathrm{Pulse}}, \underline{\rho}). \tag{K.48}$$

□

Lemma K.2.2. *Let* w_{sum}, w_1, w_2, a, a_{min}, a_{max}, $c \in \mathbb{R}$, *then*

$$(a-c)^2\, w_{sum} < (a_{min}-c)^2\, w_1 + (a_{max}-c)^2\, w_2$$

with

$$\begin{aligned} w_{sum} &= w_1 + w_2, \\ a_{min} &< c < a_{max}, \\ a\, w_{sum} &= a_{min}\, w_1 + a_{max}\, w_2, \\ w_1,\, w_2 &> 0. \end{aligned}$$

Proof.

$$\begin{aligned} (a-c)^2 w_{\mathrm{sum}} &= (a\, w_{\mathrm{sum}} - c\, w_{\mathrm{sum}})^2\, \frac{1}{w_{\mathrm{sum}}} \\ &= (a_{\mathrm{min}}\, w_1 - c\, w_1 + a_{\mathrm{max}}\, w_2 - c\, w_2)^2\, \frac{1}{w_{\mathrm{sum}}} \\ &= [(a_{\mathrm{min}} - c)\, w_1 + (a_{\mathrm{max}} - c)\, w_2]^2\, \frac{1}{w_{\mathrm{sum}}}. \end{aligned}$$

Since $a_{\mathrm{min}} < c < a_{\mathrm{max}}$ and $w_1,\, w_2 > 0$, we get

$$\begin{aligned} (a-c)^2 w_{\mathrm{sum}} &< \left\{[(a_{\mathrm{min}} - c)\, w_1]^2 + [(a_{\mathrm{max}} - c)\, w_2]^2\right\}\, \frac{1}{w_{\mathrm{sum}}} \\ &= \frac{(a_{\mathrm{min}} - c)^2\, w_1^2}{w_1 + w_2} + \frac{(a_{\mathrm{max}} - c)^2\, w_2^2}{w_1 + w_2} \\ &< (a_{\mathrm{min}} - c)^2\, w_1 + (a_{\mathrm{max}} - c)^2\, w_2. \end{aligned}$$

□

Lemma K.2.3. *Let* $\underline{a}, \underline{w} \in \mathbb{R}^2, a_1 \neq a_2$. *Then for fixed* $\underline{a}$, $\mathrm{Var}^{\mathrm{WS}}(\underline{a}, \underline{w})$ *is maximal iff* $\underline{w} \propto [1,1]^T$. *Moreover,* $\max_{\underline{w}} \mathrm{Var}^{\mathrm{WS}}(\underline{a}, \underline{w}) = \mathrm{Var}^{\mathrm{S}}(\underline{a})$.

Proof. Since

$$\mathrm{Var}^{\mathrm{WS}}(\underline{a}, \underline{w}) = \mathrm{Var}^{\mathrm{WS}}(\underline{a}, s\, \underline{w}), \tag{K.49}$$

where $s \in \mathbb{R}, s \neq 0$, we set w. l. o. g. $\underline{1}^T \underline{w} = 1$. Since $\mathrm{Var}^{\mathrm{WS}}(\underline{a} - s\, \underline{1}, \underline{w}) = \mathrm{Var}^{\mathrm{WS}}(\underline{a}, \underline{w})$, where $s \in \mathbb{R}$, we set w. l. o. g. $\underline{a} = [0, a_2]^T, a_2 \neq 0$.

Let $\underline{w} = [w_1, w_2]^T$. With Lemma A.2.12 follows

$$\begin{aligned} \mathrm{Var}^{\mathrm{WS}}(\underline{a}, \underline{w}) &= \mathrm{Corr}^{\mathrm{WS}}(\underline{a}, \underline{a}, \underline{w}) - \mathrm{E}^{\mathrm{WS}}(\underline{a}, \underline{w})^2 && \text{(K.50)} \\ &= \frac{1}{\underline{1}^T \underline{w}} a_2^2 w_2 - \left(\frac{1}{\underline{1}^T \underline{w}} a_2 w_2 \right)^2 && \text{(K.51)} \\ &= a_2^2 (w_2 - w_2^2). && \text{(K.52)} \end{aligned}$$

Computing the 1. and 2. derivative with respect to w_2, we see that $\mathrm{Var}^{\mathrm{WS}}(\underline{a}, \underline{w})$ has got one global maximum at $w_2 = 0.5$. With $\underline{1}^T \underline{w} = 1$ follows $w_1 = 0.5$ and thus $\underline{w} = [0.5, 0.5]^T$. Due to (K.49), $\mathrm{Var}^{\mathrm{WS}}(\underline{a}, \underline{w})$ is maximal iff $\underline{w} \propto [1, 1]^T$. Moreover,

$$\max_{\underline{w}} \mathrm{Var}^{\mathrm{WS}}(\underline{a}, \underline{w}) = \mathrm{Var}^{\mathrm{WS}}(\underline{a}, [1, 1]^T) = \mathrm{Var}^{\mathrm{S}}(\underline{a}). \tag{K.53}$$

□

L. Proof of Theorem 4: Optimal TDM Schemes Under Additional Constraints

In the following, we call a TDM scheme which is not balanced an imbalanced TDM scheme.

1. $N_{\text{Pulse}} \in 4\mathbb{N}$. In this case Theorem 3 can be applied, since the conditions 1a to 1d can be fulfilled, where $\underline{\rho}$ is already given. Note that $\underline{\rho}$ is normalized such that $\underline{1}^T\underline{\rho} = \rho^{\max}$, i. e. it fulfills 1c. As already noted, and due to 1a, an optimal TDM scheme has to use only the two outermost antennas. Since $\underline{\rho} \propto \underline{1}$, from 1b follows that both Tx antennas are used equally often. Moreover, the TDM scheme has to satisfy 1d, $\mathrm{E}^{\mathrm{S}}(\underline{t}^{(1)}) = \mathrm{E}^{\mathrm{S}}(\underline{t}^{(2)})$. Since the TDM scheme is balanced, $\mathrm{Var}^{\mathrm{S}}(\underline{d}^{\text{Pulse}}) = 1$. Moreover, due to Theorem 2, $\mathrm{E}^{\mathrm{S}}(\underline{t}^{(1)}) = \mathrm{E}^{\mathrm{S}}(\underline{t}^{(2)})$ is equivalent to $\mathrm{Cov}^{\mathrm{S}}(\underline{d}^{\text{Pulse}}, \underline{t}) = 0$. Thus the optimal value of Ω is

$$\Omega(\underline{d}^{\text{Pulse,opt}})\Big|_{N_{\text{Pulse}} \in 4\mathbb{N}} = 1. \tag{L.1}$$

2. $N_{\text{Pulse}} \in 4\mathbb{N} - 2$. In this case the maximum value $\mathrm{Var}^{\mathrm{S}}(\underline{d}^{\text{Pulse}}) = 1$ and $\mathrm{Cov}^{\mathrm{S}}(\underline{d}^{\text{Pulse}}, \underline{t}) = 0$ in (5.148) cannot be achieved at the same time. An optimal TDM scheme has to be balanced and fulfill $|\mathrm{Cov}^{\mathrm{S}}(\underline{d}^{\text{Pulse,opt}}, \underline{t})| = \pm\frac{1}{N_{\text{Pulse}}}$. Since it is balanced, $\mathrm{Var}^{\mathrm{S}}(\underline{d}^{\text{Pulse}}) = 1$. It can be shown that these TDM schemes yield a lower CRB_u than an imbalanced sequence which uses one antenna twice more often than the other and achieves $\mathrm{Cov}^{\mathrm{S}}(\underline{d}^{\text{Pulse}}, \underline{t}) = 0$. Any other sequence either makes the variance smaller and/or the covariance larger or improves the covariance and is of the second type. Therefore, a sequence of the proposed structure is optimal. Since $\mathrm{Var}^{\mathrm{S}}(\underline{t}) = \frac{N_{\text{Pulse}}^2 - 1}{12}$, the contribution of Ω to the minimal CRB_u is

$$\Omega(\underline{d}^{\text{Pulse,opt}})\Big|_{N_{\text{Pulse}} \in (4\mathbb{N}-2)} = 1 - \frac{1}{N_{\text{Pulse}}^2} \cdot \frac{12}{N_{\text{Pulse}}^2 - 1}. \tag{L.2}$$

3. $N_{\text{Pulse}} \in 2\mathbb{N} + 1$. Since N_{Pulse} is odd, each TDM scheme is imbalanced. Let the imbalance be the number of pulses one antenna transmits more often than the other. To maximize $\mathrm{Var}^{\mathrm{S}}(\underline{d}^{\text{Pulse}})$, the imbalance has to be as small as possible, i. e. 1. Moreover, the condition $\mathrm{Cov}^{\mathrm{S}}(\underline{d}^{\text{Pulse}}, \underline{t}) = 0$ has to be satisfied. Due to Theorem 2 this condition is equivalent to $\mathrm{E}^{\mathrm{S}}(\underline{t}^{(1)}) = \mathrm{E}^{\mathrm{S}}(\underline{t}^{(2)})$. Hence an optimal TDM scheme has an imbalance of 1 and satisfies $\mathrm{E}^{\mathrm{S}}(\underline{t}^{(1)}) = \mathrm{E}^{\mathrm{S}}(\underline{t}^{(2)})$. Any other TDM scheme yields a lower value for Ω since it either makes the

sample variance smaller and/or the covariance larger. The value for Ω of the optimal TDM schemes is

$$\Omega(\underline{d}^{\mathrm{Pulse}})\Big|_{N_{\mathrm{Pulse}} \in (2\mathbb{N}+1)} = 1 - \frac{1}{N_{\mathrm{Pulse}}^2}. \tag{L.3}$$

M. Derivation of the Cramer-Rao Bound for a TDM MIMO Radar with Two Non-Stationary Targets

The matrix $\mathbf{C}$ in (5.171) appears in the CRB of the electrical angles and Doppler frequencies for a TDM MIMO radar with several non-stationary targets. We give the derivation of $\mathbf{C}$ in (5.171), with $\mathbf{C}_1, \mathbf{C}_2, \mathbf{C}_3$ defined in (5.172) to (5.174).

We compute a part of the formulas for an arbitrary number of targets N_{Targets}, since we need these formulas in a further proof as well. According to (5.162)

$$\begin{aligned} \mathbf{C} &= \mathbf{D}^H \mathbf{P}_{\mathbf{B}}^{\perp} \mathbf{D} \\ &= \mathbf{C}^{(1)} - \mathbf{C}^{(2)} \end{aligned} \tag{M.1}$$

with the definitions

$$\mathbf{C}^{(1)} = \mathbf{D}^H \mathbf{D} \qquad \in \mathbb{C}^{2N_{\text{Targets}} \times 2N_{\text{Targets}}}, \tag{M.2}$$

$$\mathbf{C}^{(2)} = \mathbf{D}^H \mathbf{B} \left(\mathbf{B}^H \mathbf{B} \right)^{-1} \mathbf{B}^H \mathbf{D} \in \mathbb{C}^{2N_{\text{Targets}} \times 2N_{\text{Targets}}}. \tag{M.3}$$

First we compute $\mathbf{D}$, then $\mathbf{C}^{(1)}$ and $\mathbf{C}^{(2)}$ and simplify the formulas afterwards.

Computation of $\mathbf{D}_i$ From (5.157) follows

$$\frac{\partial \underline{b}(U, \omega)}{\partial U} = \underline{b}(U, \omega) \odot j \, \underline{d}^{\text{Virt}}, \tag{M.4}$$

$$\frac{\partial \underline{b}(U, \omega)}{\partial \omega} = \underline{b}(U, \omega) \odot j \, \underline{t}^{\text{Virt}}. \tag{M.5}$$

We define

$$\mathbf{V} = \begin{bmatrix} \underline{d}^{\text{Virt}} & \underline{t}^{\text{Virt}} \end{bmatrix} \in \mathbb{R}^{N_{\text{Virt}} \times 2}. \tag{M.6}$$

Then $\mathbf{D}_i$ in (5.164) equals

$$\mathbf{D}_i = j\left[\underline{b}(\underline{\Theta}^{(i)}) \quad \underline{b}(\underline{\Theta}^{(i)})\right] \odot \mathbf{V} \in \mathbb{C}^{N_{\text{Virt}} \times 2},\ i = 1, \ldots, N_{\text{Targets}}, \tag{M.7}$$

with $\underline{\Theta}^{(i)}$ defined in (5.160). Thus, with the abbreviation

$$\underline{b}^{(i)} = \underline{b}(\underline{\Theta}^{(i)}),\ i = 1, \ldots, N_{\text{Targets}}, \tag{M.8}$$

$\mathbf{D}_i$ can be written as

$$\begin{aligned}\mathbf{D}_i &= j\left[\underline{b}^{(i)} \quad \underline{b}^{(i)}\right] \odot \mathbf{V} \\ &= j\left[\underline{b}^{(i)} \underline{1}_2^T\right] \odot \mathbf{V},\ i = 1, \ldots, N_{\text{Targets}}.\end{aligned} \tag{M.9}$$

Computation of $\mathbf{C}^{(1)}$ Due to (M.2) and (5.163), we can express $\mathbf{C}^{(1)}$ as

$$\begin{aligned}\mathbf{C}^{(1)} &= \mathbf{D}^H \mathbf{D} \\ &= \begin{bmatrix} \mathbf{D}_1^H \\ \vdots \\ \mathbf{D}_{N_{\text{Targets}}}^H \end{bmatrix} \begin{bmatrix} \mathbf{D}_1 & \ldots & \mathbf{D}_{N_{\text{Targets}}} \end{bmatrix} \\ &= \begin{bmatrix} \mathbf{D}_1^H \mathbf{D}_1 & \ldots & \mathbf{D}_1^H \mathbf{D}_{N_{\text{Targets}}} \\ \vdots & \ddots & \vdots \\ \mathbf{D}_{N_{\text{Targets}}}^H \mathbf{D}_1 & \ldots & \mathbf{D}_{N_{\text{Targets}}}^H \mathbf{D}_{N_{\text{Targets}}} \end{bmatrix}.\end{aligned} \tag{M.10}$$

Next we simplify the expressions $\mathbf{D}_q^H \mathbf{D}_r$, $q, r \in \{1, \ldots, N_{\text{Targets}}\}$. We investigate the following expression: for some matrices $\mathbf{X} \in \mathbb{C}^{N_{\text{Virt}} \times K_1}$ and $\mathbf{Y} \in \mathbb{C}^{N_{\text{Virt}} \times K_2}$ and $q, r \in \{1, \ldots, N_{\text{Targets}}\}$ holds

$$\begin{aligned}\left[\left(\left(\underline{b}^{(q)} \underline{1}_{K_2}^T\right) \odot \mathbf{Y}\right)^H \left(\left(\underline{b}^{(r)} \underline{1}_{K_1}^T\right) \odot \mathbf{X}\right)\right]_{kl} &= \sum_{m=1}^{N_{\text{Virt}}} \left[\left(\underline{b}^{(q)}\ \underline{1}_{K_2}^T\right)^H\right]_{km} \left[\mathbf{Y}^H\right]_{km} \left[\left(\underline{b}^{(r)}\ \underline{1}_{K_1}^T\right)\right]_{ml} [\mathbf{X}]_{ml} \\ &= \sum_m \left[\mathbf{Y}^H\right]_{km} {b^{(q)}}^*{}_m b^{(r)}{}_m [\mathbf{X}]_{ml} \\ &= \left[\mathbf{Y}^H \operatorname{diag}\left(\underline{b}^{(q)*} \odot \underline{b}^{(r)}\right) \mathbf{X}\right]_{kl}.\end{aligned} \tag{M.11}$$

Hence, with the definition of Corr^{WS} in (A.2) we get

$$\left[\left(\underline{b}^{(q)} \underline{1}_{K_2}^T\right) \odot \mathbf{Y}\right]^H \left[\left(\underline{b}^{(r)} \underline{1}_{K_1}^T\right) \odot \mathbf{X}\right] = \underline{1}^T \left(\underline{b}^{(q)*} \odot \underline{b}^{(r)}\right) \cdot \text{Corr}^{\text{WS}}\left(\mathbf{X}, \mathbf{Y}, \underline{b}^{(q)*} \odot \underline{b}^{(r)}\right). \tag{M.12}$$

Moreover,

$$\begin{aligned}\underline{b}^{(q)} \odot \underline{b}^{(r)*} &\overset{(5.157)}{=} \left(\sqrt{\underline{\rho}^{\text{Virt}}} \odot \exp(j\,\underline{t}^{\text{Virt}}\omega_q) \odot \underline{a}^{\text{Virt}}(U_q)\right) \odot \left(\sqrt{\underline{\rho}^{\text{Virt}}} \odot \exp(-j\,\underline{t}^{\text{Virt}}\omega_r) \odot \left(\underline{a}^{\text{Virt}}(U_r)\right)^*\right) \\ &\overset{(5.75)}{=} \underline{\rho}^{\text{Virt}} \odot \exp(j\,\underline{t}^{\text{Virt}}\omega_q) \odot \exp(j\,\underline{d}^{\text{Virt}}U_q) \odot \exp(-j\,\underline{t}^{\text{Virt}}\omega_r) \odot \exp(-j\,\underline{d}^{\text{Virt}}U_r) \\ &= \underline{\rho}^{\text{Virt}} \odot \exp(j\,\underline{t}^{\text{Virt}}\Delta\omega_{qr}) \odot \exp(j\,\underline{d}^{\text{Virt}}\Delta U_{qr}), \end{aligned} \tag{M.13}$$

with the definitions

$$\Delta\omega_{qr} = \omega_q - \omega_r, \tag{M.14}$$

$$\Delta U_{qr} = U_q - U_r,\ q, r \in \{1, \ldots, N_{\text{Targets}}\}. \tag{M.15}$$

In addition, we define

$$\underline{b}^{(qr)}_{\Delta\text{Tx}} = \underline{\rho} \odot \exp(j \cdot \underline{t}\,\Delta\omega_{qr}) \odot \exp(j \cdot \underline{d}^{\text{Pulse}}\Delta U_{qr}) \qquad \in \mathbb{C}^{N_{\text{Pulse}}}, \tag{M.16}$$

$$\underline{b}^{(qr)}_{\Delta\text{Rx}} = \exp(j \cdot \underline{d}^{\text{Rx}}\Delta U_{qr}) \qquad \in \mathbb{C}^{N_{\text{Rx}}}, \tag{M.17}$$

$$\underline{b}^{(qr)}_{\Delta} = \underline{b}^{(qr)}_{\Delta\text{Tx}} \otimes \underline{b}^{(qr)}_{\Delta\text{Rx}} \qquad \in \mathbb{C}^{N_{\text{Virt}}}, \tag{M.18}$$

$$b^{(qr)}_{\Delta\text{sum}} = \underline{1}^T \underline{b}^{(qr)}_{\Delta} = \left(\underline{1}^T \underline{b}^{(qr)}_{\Delta\text{Tx}}\right)\left(\underline{1}^T \underline{b}^{(qr)}_{\Delta\text{Rx}}\right) \qquad \in \mathbb{C}. \tag{M.19}$$

Note that for $q = 1$, $r = 2$ these definitions simplify to the definitions without the superscript "(qr)" given in (5.176) to (5.181). Using these definitions yields

$$\begin{aligned}\underline{b}^{(qr)}_{\Delta} &= \left(\underline{\rho} \odot \exp(j\,\underline{t}\,\Delta\omega_{qr}) \odot \exp(j\,\underline{d}^{\text{Pulse}}\Delta U_{qr})\right) \otimes \exp(j\,\underline{d}^{\text{Rx}}\Delta U_{qr}) \\ &= \left(\underline{\rho} \odot \exp(j\,\underline{t}\,\Delta\omega_{qr}) \odot \exp(j\,\underline{d}^{\text{Pulse}}\Delta U_{qr})\right) \otimes \left(\underline{1}_{N_{\text{Rx}}} \odot \underline{1}_{N_{\text{Rx}}} \odot \exp(j\,\underline{d}^{\text{Rx}}\Delta U_{qr})\right) \\ &= \left(\underline{\rho} \otimes \underline{1}_{N_{\text{Rx}}}\right) \odot \left(\exp(j\,\underline{t}\,\Delta\omega_{qr}) \otimes \underline{1}_{N_{\text{Rx}}}\right) \odot \left(\exp(j\,\underline{d}^{\text{Pulse}}\Delta U_{qr}) \otimes \exp(j\,\underline{d}^{\text{Rx}}\Delta U_{qr})\right) \\ &= \underline{\rho}^{\text{Virt}} \odot \exp(j\,\underline{t}^{\text{Virt}}\Delta\omega_{qr}) \odot \exp(j\,\underline{d}^{\text{Virt}}\Delta U_{qr}), \end{aligned} \tag{M.20}$$

where we have used (5.75), (5.78) and (5.79) in the last line. Comparing (M.13) with (M.20) yields

$$\underline{b}^{(q)} \odot \underline{b}^{(r)*} = \underline{b}^{(qr)}_{\Delta}. \tag{M.21}$$

Note that

$$\underline{b}^{(rq)}_{\Delta} = \underline{b}^{(qr)*}_{\Delta} \tag{M.22}$$

and

$$\underline{b}^{(qq)}_{\Delta} = \underline{\rho}^{\text{Virt}}. \tag{M.23}$$

Plugging (M.21) in (M.12) yields

$$\left[\left(\underline{b}^{(q)}\underline{1}_{K_2}^T\right)\odot\mathbf{Y}\right]^H\left[\left(\underline{b}^{(r)}\underline{1}_{K_1}^T\right)\odot\mathbf{X}\right]=b_{\Delta\text{sum}}^{(qr)\ *}\,\text{Corr}^{\text{WS}}\left(\mathbf{X},\mathbf{Y},\underline{b}_{\Delta}^{(qr)*}\right),\ q,r\in\{1,\ldots,N_{\text{Targets}}\}. \tag{M.24}$$

Therefore, using (M.9) results in

$$\begin{aligned}\mathbf{D}_q^H\mathbf{D}_r&=\left[\left(\underline{b}^{(q)}\underline{1}_2^T\right)\odot\mathbf{V}\right]^H\left[\left(\underline{b}^{(r)}\underline{1}_2^T\right)\odot\mathbf{V}\right]\\&=b_{\Delta\text{sum}}^{(qr)\ *}\,\text{Corr}^{\text{WS}}\left(\mathbf{V},\mathbf{V},\underline{b}_{\Delta}^{(qr)*}\right)\in\mathbb{C}^{2\times2}.\end{aligned} \tag{M.25}$$

Note that swapping q and r gives

$$\mathbf{D}_r^H\mathbf{D}_q=b_{\Delta\text{sum}}^{(qr)}\,\text{Corr}^{\text{WS}}\left(\mathbf{V},\mathbf{V},\underline{b}_{\Delta}^{(qr)}\right). \tag{M.26}$$

Thus (M.10) reads

$$\mathbf{C}^{(1)}=\begin{bmatrix}b_{\Delta\text{sum}}^{(11)}\,\text{Corr}^{\text{WS}}\left(\mathbf{V},\mathbf{V},\underline{b}_{\Delta}^{(11)}\right) & \ldots & b_{\Delta\text{sum}}^{(1N_{\text{Targets}})*}\,\text{Corr}^{\text{WS}}\left(\mathbf{V},\mathbf{V},\underline{b}_{\Delta}^{(1N_{\text{Targets}})*}\right)\\ \vdots & \ddots & \vdots\\ b_{\Delta\text{sum}}^{(1N_{\text{Targets}})}\,\text{Corr}^{\text{WS}}\left(\mathbf{V},\mathbf{V},\underline{b}_{\Delta}^{(1N_{\text{Targets}})}\right) & \ldots & b_{\Delta\text{sum}}^{(N_{\text{Targets}}N_{\text{Targets}})}\,\text{Corr}^{\text{WS}}\left(\mathbf{V},\mathbf{V},\underline{b}_{\Delta}^{(N_{\text{Targets}}N_{\text{Targets}})}\right)\end{bmatrix}. \tag{M.27}$$

For $N_{\text{Targets}}=2$, keeping (M.23) in mind and using the definition (5.175), we can simplify it to

$$\mathbf{C}^{(1)}=\begin{bmatrix}\rho_{\text{sum}}^{\text{Virt}}\,\text{Corr}^{\text{WS}}(\mathbf{V},\mathbf{V},\underline{\rho}^{\text{Virt}}) & b_{\Delta\text{sum}}^{*}\,\text{Corr}^{\text{WS}}(\mathbf{V},\mathbf{V},\underline{b}_{\Delta}^{*})\\ b_{\Delta\text{sum}}\,\text{Corr}^{\text{WS}}(\mathbf{V},\mathbf{V},\underline{b}_{\Delta}) & \rho_{\text{sum}}^{\text{Virt}}\,\text{Corr}^{\text{WS}}(\mathbf{V},\mathbf{V},\underline{\rho}^{\text{Virt}})\end{bmatrix}\in\mathbb{C}^{2\times2}. \tag{M.28}$$

Computation of $\mathbf{C}^{(2)}$ First we compute $\mathbf{B}^H\,\mathbf{D}$. With the above abbreviations $\underline{b}^{(i)}$

$$\mathbf{B}=\begin{bmatrix}\underline{b}^{(1)} & \ldots & \underline{b}^{(N_{\text{Targets}})}\end{bmatrix}\in\mathbb{C}^{N_{\text{Virt}}\times N_{\text{Targets}}}. \tag{M.29}$$

Hence

$$\begin{aligned}\mathbf{B}^H\,\mathbf{D}&=\begin{bmatrix}\underline{b}^{(1)H}\\ \vdots\\ \underline{b}^{(N_{\text{Targets}})H}\end{bmatrix}\begin{bmatrix}\mathbf{D}_1 & \ldots & \mathbf{D}_{N_{\text{Targets}}}\end{bmatrix}\\&=\begin{bmatrix}\underline{b}^{(1)H}\mathbf{D}_1 & \ldots & \underline{b}^{(1)H}\mathbf{D}_{N_{\text{Targets}}}\\ \vdots & \ddots & \vdots\\ \underline{b}^{(N_{\text{Targets}})H}\mathbf{D}_1 & \ldots & \underline{b}^{(N_{\text{Targets}})H}\mathbf{D}_{N_{\text{Targets}}}\end{bmatrix}\in\mathbb{C}^{N_{\text{Targets}}\times2N_{\text{Targets}}}.\end{aligned} \tag{M.30}$$

Using (M.9) results in

$$\underline{b}^{(q)H}\mathbf{D}_r=j\,\underline{b}^{(q)H}\left[\left(\underline{b}^{(r)}\underline{1}_2^T\right)\odot\mathbf{V}\right]. \tag{M.31}$$

This is of the form (M.24) with $K_2 = 1$, $\mathbf{Y} = \underline{1}_{N_{\text{Virt}}}$. Thus

$$\begin{aligned} \underline{b}^{(q)H}\mathbf{D}_r &= j\, b_{\Delta\text{sum}}^{(qr)\ *}\ \text{Corr}^{\text{WS}}\left(\mathbf{V}, \underline{1}_{N_{\text{Virt}}}, \underline{b}_{\Delta}^{(qr)*}\right) \\ &= j\, b_{\Delta\text{sum}}^{(qr)\ *}\ \text{E}^{\text{WS}}\left(\mathbf{V}, \underline{b}_{\Delta}^{(qr)*}\right), \end{aligned} \tag{M.32}$$

where we have used Lemma A.2.2 in the last line. Hence (M.30) reads

$$\mathbf{B}^H\mathbf{D} = j \begin{bmatrix} b_{\Delta\text{sum}}^{(11)}\,\text{E}^{\text{WS}}\left(\mathbf{V}, \underline{b}_{\Delta}^{(11)}\right) & \dots & b_{\Delta\text{sum}}^{(1N_{\text{Targets}})^*}\,\text{E}^{\text{WS}}\left(\mathbf{V}, \underline{b}_{\Delta}^{(1N_{\text{Targets}})^*}\right) \\ \vdots & \ddots & \vdots \\ b_{\Delta\text{sum}}^{(1N_{\text{Targets}})}\,\text{E}^{\text{WS}}\left(\mathbf{V}, \underline{b}_{\Delta}^{(1N_{\text{Targets}})}\right) & \dots & b_{\Delta\text{sum}}^{(N_{\text{Targets}}N_{\text{Targets}})^*}\,\text{E}^{\text{WS}}\left(\mathbf{V}, \underline{b}_{\Delta}^{(N_{\text{Targets}}N_{\text{Targets}})^*}\right) \end{bmatrix}. \tag{M.33}$$

For two targets, $N_{\text{Targets}} = 2$, this simplifies to

$$\mathbf{B}^H\mathbf{D} = j \begin{bmatrix} \rho_{\text{sum}}^{\text{Virt}}\,\text{E}^{\text{WS}}(\mathbf{V}, \underline{\rho}^{\text{Virt}}) & b_{\Delta\text{sum}}^{*}\,\text{E}^{\text{WS}}(\mathbf{V}, \underline{b}_{\Delta}^{*}) \\ b_{\Delta\text{sum}}\,\text{E}^{\text{WS}}(\mathbf{V}, \underline{b}_{\Delta}) & \rho_{\text{sum}}^{\text{Virt}}\,\text{E}^{\text{WS}}(\mathbf{V}, \underline{\rho}^{\text{Virt}}) \end{bmatrix}. \tag{M.34}$$

In the following we stick to the case $N_{\text{Targets}} = 2$. We compute $\left(\mathbf{B}^H\mathbf{B}\right)^{-1}$.

$$\begin{aligned} \mathbf{B}^H\mathbf{B} &= \begin{bmatrix} \underline{b}^{(1)H} \\ \underline{b}^{(2)H} \end{bmatrix} \begin{bmatrix} \underline{b}^{(1)} & \underline{b}^{(2)} \end{bmatrix} \\ &= \begin{bmatrix} \rho_{\text{sum}}^{\text{Virt}} & b_{\Delta\text{sum}}^{*} \\ b_{\Delta\text{sum}} & \rho_{\text{sum}}^{\text{Virt}} \end{bmatrix} \in \mathbb{C}^{2\times 2}. \end{aligned} \tag{M.35}$$

Thus the inverse is given by

$$\left(\mathbf{B}^H\mathbf{B}\right)^{-1} = \frac{1}{{\rho_{\text{sum}}^{\text{Virt}}}^2 - |b_{\Delta\text{sum}}|^2} \begin{bmatrix} \rho_{\text{sum}}^{\text{Virt}} & -b_{\Delta\text{sum}}^{*} \\ -b_{\Delta\text{sum}} & \rho_{\text{sum}}^{\text{Virt}} \end{bmatrix} \in \mathbb{C}^{2\times 2}. \tag{M.36}$$

From (M.3) follows that

$$\mathbf{C}^{(2)} = \left(\mathbf{C}^{(2)}\right)^H. \tag{M.37}$$

Hence it is sufficient to compute the 2×2 matrices $\mathbf{C}_1^{(2)}, \mathbf{C}_2^{(2)}, \mathbf{C}_3^{(2)}$, where

$$\mathbf{C}^{(2)} = \begin{bmatrix} \mathbf{C}_1^{(2)} & \mathbf{C}_2^{(2)} \\ \left(\mathbf{C}_2^{(2)}\right)^H & \mathbf{C}_3^{(2)} \end{bmatrix}. \tag{M.38}$$

In the following, we use the abbreviations

$$\tau = \rho_{\text{sum}}^{\text{Virt}} \qquad \in \mathbb{R}, \tag{M.39}$$

$$\varphi = b_{\Delta\text{sum}} \qquad \in \mathbb{C}, \tag{M.40}$$

$$\underline{\chi} = \mathrm{E}^{\text{WS}}(\mathbf{V}, \underline{\rho}^{\text{Virt}})^T \in \mathbb{R}^2, \tag{M.41}$$

$$\underline{\Psi} = \mathrm{E}^{\text{WS}}(\mathbf{V}, \underline{b}_\Delta)^T \quad \in \mathbb{C}^2. \tag{M.42}$$

Note, since $\mathbf{V}$ and $\underline{\rho}^{\text{Virt}}$ are real, $\underline{\chi}$ is real. Moreover, since $\mathbf{V}$ is real

$$\mathrm{E}^{\text{WS}}(\mathbf{V}, \underline{b}_\Delta^*) = \mathrm{E}^{\text{WS}}(\mathbf{V}, \underline{b}_\Delta)^* \tag{M.43}$$

and hence

$$\underline{\Psi}^H = \mathrm{E}^{\text{WS}}(\mathbf{V}, \underline{b}_\Delta^*). \tag{M.44}$$

Then $\mathbf{C}^{(2)}$ in (M.3) reads

$$\begin{aligned}
\mathbf{C}^{(2)} &= \mathbf{D}^H \mathbf{B} \left(\mathbf{B}^H \mathbf{B}\right)^{-1} \mathbf{B}^H \mathbf{D} \\
&= \frac{1}{\tau^2 - |\varphi|^2} \begin{bmatrix} \tau\underline{\chi} & \varphi^*\underline{\Psi}^* \\ \varphi\underline{\Psi} & \tau\underline{\chi} \end{bmatrix} \begin{bmatrix} \tau & -\varphi^* \\ -\varphi & \tau \end{bmatrix} \begin{bmatrix} \tau\underline{\chi}^T & \varphi^*\underline{\Psi}^H \\ \varphi\underline{\Psi}^T & \tau\underline{\chi}^T \end{bmatrix} \\
&= \frac{1}{\tau^2 - |\varphi|^2} \begin{bmatrix} \tau\underline{\chi} & \varphi^*\underline{\Psi}^* \\ \varphi\underline{\Psi} & \tau\underline{\chi} \end{bmatrix} \begin{bmatrix} \tau^2\underline{\chi}^T - |\varphi|^2\underline{\Psi}^T & \tau\varphi^*\underline{\Psi}^H - \tau\varphi^*\underline{\chi}^T \\ -\tau\varphi\underline{\chi}^T + \tau\varphi\underline{\Psi}^T & -|\varphi|^2\underline{\Psi}^H + \tau^2\underline{\chi}^T \end{bmatrix}.
\end{aligned} \tag{M.45}$$

Hence, using the notation given in (M.38) yields

$$\mathbf{C}_1^{(2)} = \frac{1}{\tau^2 - |\varphi|^2} \left\{\tau\underline{\chi}\left(\tau^2\underline{\chi}^T - |\varphi|^2\underline{\Psi}^T\right) + \varphi^*\underline{\Psi}^*\left(-\tau\varphi\underline{\chi}^T + \tau\varphi\underline{\Psi}^T\right)\right\}, \tag{M.46}$$

$$\mathbf{C}_2^{(2)} = \frac{1}{\tau^2 - |\varphi|^2} \left\{\tau\underline{\chi}\left(\tau\varphi^*\underline{\Psi}^H - \tau\varphi^*\underline{\chi}^T\right) + \varphi^*\underline{\Psi}^*\left(-|\varphi|^2\underline{\Psi}^H + \tau^2\underline{\chi}^T\right)\right\}, \tag{M.47}$$

$$\mathbf{C}_3^{(2)} = \frac{1}{\tau^2 - |\varphi|^2} \left\{\varphi\underline{\Psi}\left(\tau\varphi^*\underline{\Psi}^H - \tau\varphi^*\underline{\chi}^T\right) + \tau\underline{\chi}\left(-|\varphi|^2\underline{\Psi}^H + \tau^2\underline{\chi}^T\right)\right\}. \tag{M.48}$$

We note, that

$$\left(\mathbf{C}_3^{(2)}\right)^* = \mathbf{C}_1^{(2)}. \tag{M.49}$$

$\mathbf{C}_1^{(2)}$ can be expressed as

$$\begin{aligned}
\mathbf{C}_1^{(2)} &= \frac{1}{\tau^2 - |\varphi|^2} \left\{\tau^3\underline{\chi}\underline{\chi}^T - \tau|\varphi|^2\underline{\chi}\underline{\Psi}^T + \tau|\varphi|^2\left(-\underline{\Psi}^*\underline{\chi}^T + \underline{\Psi}^*\underline{\Psi}^T\right)\right\} \\
&= \tau\underline{\chi}\underline{\chi}^T + \frac{\tau|\varphi|^2}{\tau^2 - |\varphi|^2}\left(\underline{\chi}\underline{\chi}^T - \underline{\chi}\underline{\Psi}^T - \underline{\Psi}^*\underline{\chi}^T + \underline{\Psi}^*\underline{\Psi}^T\right).
\end{aligned} \tag{M.50}$$

Since $\underline{\chi}$ is real, this can be rewritten as

$$\mathbf{C}_1^{(2)} = \tau \underline{\chi}\,\underline{\chi}^T + \frac{\tau|\varphi|^2}{\tau^2 - |\varphi|^2}\,\underline{\widetilde{m}}^*\underline{\widetilde{m}}^T \tag{M.51}$$

with the definition

$$\underline{\widetilde{m}} = \underline{\chi} - \underline{\Psi}. \tag{M.52}$$

Due to (M.49), $\mathbf{C}_3^{(2)}$ is given by

$$\mathbf{C}_3^{(2)} = \tau \underline{\chi}\,\underline{\chi}^T + \frac{\tau|\varphi|^2}{\tau^2 - |\varphi|^2}\underline{\widetilde{m}}\,\underline{\widetilde{m}}^H. \tag{M.53}$$

Analog computations yield for $\mathbf{C}_2^{(2)}$

$$\begin{aligned}
\mathbf{C}_2^{(2)} &= \frac{1}{\tau^2 - |\varphi|^2}\left\{-\varphi^*|\varphi|^2\,\underline{\Psi}^*\underline{\Psi}^H + \tau^2\varphi^*\,\underline{\Psi}^*\underline{\chi}^T + \tau^2\varphi^*\left(\underline{\chi}\,\underline{\Psi}^H - \underline{\chi}\,\underline{\chi}^T\right)\right\} \\
&= \varphi^*\,\underline{\Psi}^*\underline{\Psi}^H - \frac{\tau^2\varphi^*}{\tau^2 - |\varphi|^2}\left(\underline{\Psi}^*\underline{\Psi}^H - \underline{\chi}\,\underline{\Psi}^H - \underline{\Psi}^*\underline{\chi}^T + \underline{\chi}\,\underline{\chi}^T\right) \\
&= \varphi^*\,\underline{\Psi}^*\underline{\Psi}^H - \frac{\tau^2\varphi^*}{\tau^2 - |\varphi|^2}\,\underline{\widetilde{m}}^*\underline{\widetilde{m}}^H.
\end{aligned} \tag{M.54}$$

Putting the results in (M.38) yields

$$\begin{aligned}
\mathbf{C}^{(2)} &= \begin{bmatrix} \tau\underline{\chi}\,\underline{\chi}^T + \frac{\tau|\varphi|^2}{\tau^2-|\varphi|^2}\,\underline{\widetilde{m}}^*\underline{\widetilde{m}}^T & \varphi^*\,\underline{\Psi}^*\underline{\Psi}^H - \frac{\tau^2\varphi^*}{\tau^2-|\varphi|^2}\,\underline{\widetilde{m}}^*\underline{\widetilde{m}}^H \\ \left(\varphi^*\,\underline{\Psi}^*\underline{\Psi}^H - \frac{\tau^2\varphi^*}{\tau^2-|\varphi|^2}\,\underline{\widetilde{m}}^*\underline{\widetilde{m}}^H\right)^H & \tau\underline{\chi}\,\underline{\chi}^T + \frac{\tau|\varphi|^2}{\tau^2-|\varphi|^2}\underline{\widetilde{m}}\,\underline{\widetilde{m}}^H \end{bmatrix} \\
&= \begin{bmatrix} \tau\underline{\chi}\,\underline{\chi}^T + \frac{\tau|\varphi|^2}{\tau^2-|\varphi|^2}\,\underline{\widetilde{m}}^*\underline{\widetilde{m}}^T & \varphi^*\,\underline{\Psi}^*\underline{\Psi}^H - \frac{\tau^2\varphi^*}{\tau^2-|\varphi|^2}\,\underline{\widetilde{m}}^*\underline{\widetilde{m}}^H \\ \varphi\,\underline{\Psi}\,\underline{\Psi}^T - \frac{\tau^2\varphi}{\tau^2-|\varphi|^2}\,\underline{\widetilde{m}}\,\underline{\widetilde{m}}^T & \tau\underline{\chi}\,\underline{\chi}^T + \frac{\tau|\varphi|^2}{\tau^2-|\varphi|^2}\underline{\widetilde{m}}\,\underline{\widetilde{m}}^H \end{bmatrix} \\
&= \begin{bmatrix} \tau\underline{\chi}\,\underline{\chi}^T & \varphi^*\,\underline{\Psi}^*\underline{\Psi}^H \\ \varphi\,\underline{\Psi}\,\underline{\Psi}^T & \tau\underline{\chi}\,\underline{\chi}^T \end{bmatrix} + \frac{\tau}{\tau^2 - |\varphi|^2}\begin{bmatrix} |\varphi|^2\,\underline{\widetilde{m}}^*\underline{\widetilde{m}}^T & -\tau\varphi^*\,\underline{\widetilde{m}}^*\underline{\widetilde{m}}^H \\ -\tau\varphi\,\underline{\widetilde{m}}\,\underline{\widetilde{m}}^T & |\varphi|^2\underline{\widetilde{m}}\,\underline{\widetilde{m}}^H \end{bmatrix}.
\end{aligned} \tag{M.55}$$

Simplification of the formulas Now we put (M.28) and (M.55) in (M.1). We substitute some of the used abbreviations:

$$\begin{aligned}
\mathbf{C} = &\begin{bmatrix} \rho_{\mathrm{sum}}^{\mathrm{Virt}}\,\mathrm{Corr}^{\mathrm{WS}}(\mathbf{V},\mathbf{V},\underline{\rho}^{\mathrm{Virt}}) & b_{\Delta\mathrm{sum}}^*\,\mathrm{Corr}^{\mathrm{WS}}(\mathbf{V},\mathbf{V},\underline{b}_\Delta^*) \\ b_{\Delta\mathrm{sum}}\,\mathrm{Corr}^{\mathrm{WS}}(\mathbf{V},\mathbf{V},\underline{b}_\Delta) & \rho_{\mathrm{sum}}^{\mathrm{Virt}}\,\mathrm{Corr}^{\mathrm{WS}}(\mathbf{V},\mathbf{V},\underline{\rho}^{\mathrm{Virt}}) \end{bmatrix} \\
&- \begin{bmatrix} \rho_{\mathrm{sum}}^{\mathrm{Virt}}\,\mathrm{E}^{\mathrm{WS}}(\mathbf{V},\underline{\rho}^{\mathrm{Virt}})^T\,\mathrm{E}^{\mathrm{WS}}(\mathbf{V},\underline{\rho}^{\mathrm{Virt}}) & b_{\Delta\mathrm{sum}}^*\,\mathrm{E}^{\mathrm{WS}}(\mathbf{V},\underline{b}_\Delta)^H\,\mathrm{E}^{\mathrm{WS}}(\mathbf{V},\underline{b}_\Delta)^* \\ b_{\Delta\mathrm{sum}}\,\mathrm{E}^{\mathrm{WS}}(\mathbf{V},\underline{b}_\Delta)^T\,\mathrm{E}^{\mathrm{WS}}(\mathbf{V},\underline{b}_\Delta) & \rho_{\mathrm{sum}}^{\mathrm{Virt}}\,\mathrm{E}^{\mathrm{WS}}(\mathbf{V},\underline{\rho}^{\mathrm{Virt}})^T\,\mathrm{E}^{\mathrm{WS}}(\mathbf{V},\underline{\rho}^{\mathrm{Virt}}) \end{bmatrix} \\
&- \frac{\tau}{\tau^2 - |\varphi|^2}\begin{bmatrix} |\varphi|^2\,\underline{\widetilde{m}}^*\underline{\widetilde{m}}^T & -\tau\varphi^*\,\underline{\widetilde{m}}^*\underline{\widetilde{m}}^H \\ -\tau\varphi\,\underline{\widetilde{m}}\,\underline{\widetilde{m}}^T & |\varphi|^2\underline{\widetilde{m}}\,\underline{\widetilde{m}}^H \end{bmatrix}.
\end{aligned} \tag{M.56}$$

Keeping in mind that $\mathbf{V}$ is real, with the help of Lemma A.2.12, the equation can be simplified to

$$\mathbf{C} = \begin{bmatrix} \rho_{\text{sum}}^{\text{Virt}} \operatorname{Cov}^{\text{WS}}(\mathbf{V}, \mathbf{V}, \underline{\rho}^{\text{Virt}}) & b_{\Delta\text{sum}}^{*} \operatorname{Cov}^{\text{WS}}(\mathbf{V}, \mathbf{V}, \underline{b}_{\Delta}^{*}) \\ b_{\Delta\text{sum}} \operatorname{Cov}^{\text{WS}}(\mathbf{V}, \mathbf{V}, \underline{b}_{\Delta}) & \rho_{\text{sum}}^{\text{Virt}} \operatorname{Cov}^{\text{WS}}(\mathbf{V}, \mathbf{V}, \underline{\rho}^{\text{Virt}}) \end{bmatrix} - \frac{\tau}{\tau^2 - |\varphi|^2} \begin{bmatrix} |\varphi|^2 \, \widetilde{\underline{m}}^{*} \widetilde{\underline{m}}^{T} & -\tau\varphi^{*} \, \widetilde{\underline{m}}^{*} \widetilde{\underline{m}}^{H} \\ -\tau\varphi \, \widetilde{\underline{m}} \, \widetilde{\underline{m}}^{T} & |\varphi|^2 \widetilde{\underline{m}} \, \widetilde{\underline{m}}^{H} \end{bmatrix}. \tag{M.57}$$

We simplify the expressions of the weighted sample covariances. Therefore using (M.6), (5.76) and (5.79) we compute

$$\begin{aligned} \mathbf{V} &= \begin{bmatrix} \underline{d}^{\text{Virt}} & \underline{t}^{\text{Virt}} \end{bmatrix} \\ &= \begin{bmatrix} \underline{1}_{N_{\text{Pulse}}} \otimes \underline{d}^{\text{Rx}} + \underline{d}^{\text{Pulse}} \otimes \underline{1}_{N_{\text{Rx}}} & \underline{t} \otimes \underline{1}_{N_{\text{Rx}}} \end{bmatrix} \\ &= \underline{1}_{N_{\text{Pulse}}} \otimes \begin{bmatrix} \underline{d}^{\text{Rx}} & \underline{0} \end{bmatrix} + \begin{bmatrix} \underline{d}^{\text{Pulse}} & \underline{t} \end{bmatrix} \otimes \underline{1}_{N_{\text{Rx}}} \\ &= \underline{1}_{N_{\text{Pulse}}} \otimes \mathbf{V}_1 + \mathbf{V}_2 \otimes \underline{1}_{N_{\text{Rx}}}, \end{aligned} \tag{M.58}$$

where $\mathbf{V}_1$ and $\mathbf{V}_2$ are defined in (5.183) and (5.184), respectively. Let $\underline{c} \in \mathbb{C}^{N_{\text{Rx}}}$ and $\underline{z} \in \mathbb{C}^{N_{\text{Pulse}}}$, $\underline{c}, \underline{z} \neq \underline{0}$. Then, using the properties of $\operatorname{Cov}^{\text{WS}}$, cf. Appendix A.2.4, we get

$$\begin{aligned} \operatorname{Cov}^{\text{WS}}(\mathbf{V}, \mathbf{V}, \underline{z} \otimes \underline{c}) &= \operatorname{Cov}^{\text{WS}}(\underline{1}_{N_{\text{Pulse}}} \otimes \mathbf{V}_1 + \mathbf{V}_2 \otimes \underline{1}_{N_{\text{Rx}}}, \underline{1}_{N_{\text{Pulse}}} \otimes \mathbf{V}_1 + \mathbf{V}_2 \otimes \underline{1}_{N_{\text{Rx}}}, \underline{z} \otimes \underline{c}) \\ &= \operatorname{Cov}^{\text{WS}}(\underline{1}_{N_{\text{Pulse}}} \otimes \mathbf{V}_1, \underline{1}_{N_{\text{Pulse}}} \otimes \mathbf{V}_1, \underline{z} \otimes \underline{c}) \\ &+ \operatorname{Cov}^{\text{WS}}(\underline{1}_{N_{\text{Pulse}}} \otimes \mathbf{V}_1, \mathbf{V}_2 \otimes \underline{1}_{N_{\text{Rx}}}, \underline{z} \otimes \underline{c}) \\ &+ \operatorname{Cov}^{\text{WS}}(\mathbf{V}_2 \otimes \underline{1}_{N_{\text{Rx}}}, \underline{1}_{N_{\text{Pulse}}} \otimes \mathbf{V}_1, \underline{z} \otimes \underline{c}) \\ &+ \operatorname{Cov}^{\text{WS}}(\mathbf{V}_2 \otimes \underline{1}_{N_{\text{Rx}}}, \mathbf{V}_2 \otimes \underline{1}_{N_{\text{Rx}}}, \underline{z} \otimes \underline{c}) \\ &= \operatorname{Cov}^{\text{WS}}(\mathbf{V}_1, \mathbf{V}_1, \underline{c}) + \mathbf{0} + \mathbf{0} + \operatorname{Cov}^{\text{WS}}(\mathbf{V}_2, \mathbf{V}_2, \underline{z}) \\ &= \operatorname{Cov}^{\text{WS}}(\mathbf{V}_1, \underline{c}) + \operatorname{Cov}^{\text{WS}}(\mathbf{V}_2, \underline{z}). \end{aligned} \tag{M.59}$$

Since $\underline{\rho}^{\text{Virt}} = \underline{\rho} \otimes \underline{1}_{N_{\text{Rx}}}$ and $\underline{b}_{\Delta} = \underline{b}_{\Delta\text{Tx}} \otimes \underline{b}_{\Delta\text{Rx}}$, we can apply this result to (M.57) and get

$$\begin{aligned} \mathbf{C} = &\begin{bmatrix} \rho_{\text{sum}}^{\text{Virt}} \operatorname{Cov}^{\text{S}}(\mathbf{V}_1) & b_{\Delta\text{sum}}^{*} \operatorname{Cov}^{\text{WS}}(\mathbf{V}_1, \underline{b}_{\Delta\text{Rx}}^{*}) \\ b_{\Delta\text{sum}} \operatorname{Cov}^{\text{WS}}(\mathbf{V}_1, \underline{b}_{\Delta\text{Rx}}) & \rho_{\text{sum}}^{\text{Virt}} \operatorname{Cov}^{\text{S}}(\mathbf{V}_1) \end{bmatrix} \\ &+ \begin{bmatrix} \rho_{\text{sum}}^{\text{Virt}} \operatorname{Cov}^{\text{WS}}(\mathbf{V}_2, \underline{\rho}) & b_{\Delta\text{sum}}^{*} \operatorname{Cov}^{\text{WS}}(\mathbf{V}_2, \underline{b}_{\Delta\text{Tx}}^{*}) \\ b_{\Delta\text{sum}} \operatorname{Cov}^{\text{WS}}(\mathbf{V}_2, \underline{b}_{\Delta\text{Tx}}) & \rho_{\text{sum}}^{\text{Virt}} \operatorname{Cov}^{\text{WS}}(\mathbf{V}_2, \underline{\rho}) \end{bmatrix} \\ &- \frac{\tau}{\tau^2 - |\varphi|^2} \begin{bmatrix} |\varphi|^2 \, \widetilde{\underline{m}}^{*} \widetilde{\underline{m}}^{T} & -\tau\varphi^{*} \, \widetilde{\underline{m}}^{*} \widetilde{\underline{m}}^{H} \\ -\tau\varphi \, \widetilde{\underline{m}} \, \widetilde{\underline{m}}^{T} & |\varphi|^2 \widetilde{\underline{m}} \, \widetilde{\underline{m}}^{H} \end{bmatrix} \end{aligned} \tag{M.60}$$

$$= \mathbf{C}_1 + \mathbf{C}_2 - \frac{\tau}{\tau^2 - |\varphi|^2} \begin{bmatrix} |\varphi|^2 \, \widetilde{\underline{m}}^{*} \widetilde{\underline{m}}^{T} & -\tau\varphi^{*} \, \widetilde{\underline{m}}^{*} \widetilde{\underline{m}}^{H} \\ -\tau\varphi \, \widetilde{\underline{m}} \, \widetilde{\underline{m}}^{T} & |\varphi|^2 \widetilde{\underline{m}} \, \widetilde{\underline{m}}^{H} \end{bmatrix}, \tag{M.61}$$

where $\mathbf{C}_1$ and $\mathbf{C}_2$ are defined in (5.172) and (5.173), respectively. Now we express $\widetilde{\underline{m}}$ differently. With (M.52), (M.41) and (M.42) follows

$$\widetilde{\underline{m}} = \mathrm{E}^{\mathrm{WS}}(\mathbf{V}, \underline{\rho}^{\mathrm{Virt}})^T - \mathrm{E}^{\mathrm{WS}}(\mathbf{V}, \underline{b}_{\Delta})^T. \tag{M.62}$$

Let $\underline{c} \in \mathbb{C}^{N_{\mathrm{Rx}}}$ and $\underline{z} \in \mathbb{C}^{N_{\mathrm{Pulse}}}$, $\underline{c}, \underline{z} \neq \underline{0}$. Using the properties of E^{WS}, cf. Appendix A.2.2, and (M.58) we get

$$\begin{aligned}
\mathrm{E}^{\mathrm{WS}}(\mathbf{V}, \underline{z} \otimes \underline{c}) &= \mathrm{E}^{\mathrm{WS}}(\underline{1}_{N_{\mathrm{Pulse}}} \otimes \mathbf{V}_1 + \mathbf{V}_2 \otimes \underline{1}_{N_{\mathrm{Rx}}}, \underline{z} \otimes \underline{c}) \\
&= \mathrm{E}^{\mathrm{WS}}(\underline{1}_{N_{\mathrm{Pulse}}} \otimes \mathbf{V}_1, \underline{z} \otimes \underline{c}) + \mathrm{E}^{\mathrm{WS}}(\mathbf{V}_2 \otimes \underline{1}_{N_{\mathrm{Rx}}}, \underline{z} \otimes \underline{c}) \\
&= \mathrm{E}^{\mathrm{WS}}(\mathbf{V}_1, \underline{c}) + \mathrm{E}^{\mathrm{WS}}(\mathbf{V}_2, \underline{z}).
\end{aligned} \tag{M.63}$$

Applying this result to (M.62) yields

$$\begin{aligned}
\widetilde{\underline{m}} &= \mathrm{E}^{\mathrm{S}}(\mathbf{V}_1)^T + \mathrm{E}^{\mathrm{WS}}(\mathbf{V}_2, \underline{\rho})^T - \left(\mathrm{E}^{\mathrm{WS}}(\mathbf{V}_1, \underline{b}_{\Delta\mathrm{Rx}})^T + \mathrm{E}^{\mathrm{WS}}(\mathbf{V}_2, \underline{b}_{\Delta\mathrm{Tx}})^T\right) \\
&= \underline{m},
\end{aligned} \tag{M.64}$$

where $\underline{m}$ is defined in (5.182). We plug this result in (M.61) and substitute the abbreviations τ and φ, defined in (M.39) and (M.40), respectively. This results in

$$\mathbf{C} = \mathbf{C}_1 + \mathbf{C}_2 - \mathbf{C}_3, \tag{M.65}$$

where $\mathbf{C}_3$ is defined in (5.174). This is what we wanted to derive.

N. Proof of Theorem 6: Decoupling of Electrical Angles and Doppler Frequencies for Arbitrary Number of Moving Targets

We prove Theorem 6 as described in the overview of the proof on p. 132. Thus we have to show that the relevant elements in $\mathbf{C}^{(1)}$ and $\mathbf{C}^{(2)}$ are 0. We use some of the results derived in Appendix M.

First we derive some relations which we need in the further computations. Since the condition (5.207) has to be fulfilled, we abbreviate

$$\mathrm{E}^{\mathrm{WS}}\left(\underline{t}^{(i)}, \underline{\rho}^{(i)}\right) = \tilde{t} \quad \forall\, i \in \{1, \ldots, N_{\mathrm{Tx}}\}. \tag{N.1}$$

With (5.206) and $\Delta\omega_{qr} = 0$,

$$\underline{b}_{\Delta\mathrm{Tx}}^{(qr)} = \underline{\rho} \odot \exp(j \cdot \underline{d}^{\mathrm{Pulse}} \Delta U_{qr}) \tag{N.2}$$

follows from (M.16). Defining

$$\underline{c}^{(qr)} = \exp(j \cdot \underline{d}^{\mathrm{Pulse}} \Delta U_{qr}) \tag{N.3}$$

yields

$$\underline{b}_{\Delta\mathrm{Tx}}^{(qr)} = \underline{\rho} \odot \underline{c}^{(qr)}. \tag{N.4}$$

Analogously to $\underline{t}^{(i)}$ and $\underline{\rho}^{(i)}$ we define

$$\underline{b}_{\Delta\mathrm{Tx}}^{(i),(qr)} = \underline{\rho}^{(i)} \cdot c^{(i),(qr)}, \tag{N.5}$$

$$c^{(i),(qr)} = \exp(j \cdot d_i^{\mathrm{Tx}} \Delta U_{qr}). \tag{N.6}$$

$\underline{b}_{\Delta\mathrm{Tx}}^{(i),(qr)}$ denotes the complex weights of the i-th Tx antenna which transmits at the time instances $\underline{t}^{(i)}$

for the q-th and r-th target. Using these notations

$$\mathrm{E}^{\mathrm{WS}}\left(\underline{t}^{(i)}, \underline{b}_{\Delta\mathrm{Tx}}^{(i),(qr)}\right) = \mathrm{E}^{\mathrm{WS}}\left(\underline{t}^{(i)}, c^{(i),(qr)} \cdot \underline{\rho}^{(i)}\right). \tag{N.7}$$

$c^{(i),(qr)}$ is a complex scalar unequal 0. Hence, from the definition of E^{WS} follows

$$\mathrm{E}^{\mathrm{WS}}\left(\underline{t}^{(i)}, \underline{b}_{\Delta\mathrm{Tx}}^{(i),(qr)}\right) = \mathrm{E}^{\mathrm{WS}}\left(\underline{t}^{(i)}, \underline{\rho}^{(i)}\right) = \tilde{t} \quad \forall\, i. \tag{N.8}$$

Next we show that $\mathrm{Cov}^{\mathrm{WS}}\left(\underline{d}^{\mathrm{Pulse}}, \underline{t}, \underline{b}_{\Delta\mathrm{Tx}}^{(qr)}\right) = 0$. We use Lemma J.1.3 with $\underline{x} = \underline{d}^{\mathrm{Pulse}}$, $\underline{y} = \underline{t}$, $\underline{w} = \underline{b}_{\Delta\mathrm{Tx}}^{(qr)}$ and with N_{Tx} clusters, corresponding to the N_{Tx} Tx antennas. Here, we keep q, r fixed. Then, with the notation of Lemma J.1.3,

$$\tilde{\underline{x}} = \underline{d}^{\mathrm{Tx}}, \tag{N.9}$$

$$\underline{y}^{(\mathrm{i})} = \underline{t}^{(i)}, \tag{N.10}$$

$$\underline{w}^{(\mathrm{i})} = \underline{b}_{\Delta\mathrm{Tx}}^{(i),(qr)}. \tag{N.11}$$

Due to (N.8)

$$\mathrm{E}^{\mathrm{WS}}\left(\underline{t}^{(k)}, \underline{b}_{\Delta\mathrm{Tx}}^{(k),(qr)}\right) = \mathrm{E}^{\mathrm{WS}}\left(\underline{t}^{(l)}, \underline{b}_{\Delta\mathrm{Tx}}^{(l),(qr)}\right) \ \forall k, l \in \{1, \ldots, N_{\mathrm{Tx}}\}. \tag{N.12}$$

Hence, from Lemma J.1.3

$$\mathrm{Cov}^{\mathrm{WS}}\left(\underline{d}^{\mathrm{Pulse}}, \underline{t}, \underline{b}_{\Delta\mathrm{Tx}}^{(qr)}\right) = 0 \tag{N.13}$$

follows. Moreover

$$\begin{aligned}
\mathrm{E}^{\mathrm{WS}}\left(\underline{t}, \underline{b}_{\Delta\mathrm{Tx}}^{(qr)}\right) &= \frac{1}{\underline{1}^T \underline{b}_{\Delta\mathrm{Tx}}^{(qr)}} \underline{b}_{\Delta\mathrm{Tx}}^{(qr)\,T}\, \underline{t} \\
&= \frac{1}{\underline{1}^T \underline{b}_{\Delta\mathrm{Tx}}^{(qr)}} \sum_{i=1}^{N_{\mathrm{Tx}}} \left(\underline{b}_{\Delta\mathrm{Tx}}^{(i),(qr)}\right)^T \underline{t}^{(i)} \\
&= \frac{1}{\underline{1}^T \underline{b}_{\Delta\mathrm{Tx}}^{(qr)}} \sum_{i=1}^{N_{\mathrm{Tx}}} \underline{1}^T \underline{b}_{\Delta\mathrm{Tx}}^{(i),(qr)}\, \mathrm{E}^{\mathrm{WS}}\left(\underline{t}^{(i)}, \underline{b}_{\Delta\mathrm{Tx}}^{(i),(qr)}\right)
\end{aligned} \tag{N.14}$$

and using (N.8) yields

$$\begin{aligned}
\mathrm{E}^{\mathrm{WS}}\left(\underline{t}, \underline{b}_{\Delta\mathrm{Tx}}^{(qr)}\right) &= \frac{1}{\underline{1}^T \underline{b}_{\Delta\mathrm{Tx}}^{(qr)}} \sum_{i=1}^{N_{\mathrm{Tx}}} \underline{1}^T \underline{b}_{\Delta\mathrm{Tx}}^{(i),(qr)} \cdot \tilde{t} \\
&= \tilde{t}.
\end{aligned} \tag{N.15}$$

W. l. o. g. we set the time origin such that $\tilde{t} = 0$. Hence

$$\mathrm{E}^{\mathrm{WS}}\left(\underline{t}, \underline{b}_{\Delta\mathrm{Tx}}^{(qr)}\right) = 0. \tag{N.16}$$

Due to this

$$\begin{aligned}\mathrm{Cov}^{\mathrm{WS}}\left(\underline{d}^{\mathrm{Pulse}}, \underline{t}, \underline{b}_{\Delta\mathrm{Tx}}^{(qr)}\right) &= \mathrm{Corr}^{\mathrm{WS}}\left(\underline{d}^{\mathrm{Pulse}}, \underline{t}, \underline{b}_{\Delta\mathrm{Tx}}^{(qr)}\right) - \mathrm{E}^{\mathrm{WS}}\left(\underline{t}, \underline{b}_{\Delta\mathrm{Tx}}^{(qr)}\right)\mathrm{E}^{\mathrm{WS}}\left(\underline{d}^{\mathrm{Pulse}}, \underline{b}_{\Delta\mathrm{Tx}}^{(qr)}\right) \\ &= \mathrm{Corr}^{\mathrm{WS}}\left(\underline{d}^{\mathrm{Pulse}}, \underline{t}, \underline{b}_{\Delta\mathrm{Tx}}^{(qr)}\right).\end{aligned} \tag{N.17}$$

With (N.13)

$$\mathrm{Corr}^{\mathrm{WS}}\left(\underline{d}^{\mathrm{Pulse}}, \underline{t}, \underline{b}_{\Delta\mathrm{Tx}}^{(qr)}\right) = 0 \tag{N.18}$$

follows.

Investigation of $\mathbf{C}^{(1)}$ $\mathbf{C}^{(1)}$ is given by (M.10)

$$\mathbf{C}^{(1)} = \begin{bmatrix} \mathbf{D}_1^H\mathbf{D}_1 & \dots & \mathbf{D}_1^H\mathbf{D}_{N_{\mathrm{Targets}}} \\ \vdots & \ddots & \vdots \\ \mathbf{D}_{N_{\mathrm{Targets}}}^H\mathbf{D}_1 & \dots & \mathbf{D}_{N_{\mathrm{Targets}}}^H\mathbf{D}_{N_{\mathrm{Targets}}} \end{bmatrix} \tag{N.19}$$

with $\mathbf{D}_q^H\mathbf{D}_r$ computed in (M.25)

$$\mathbf{D}_q^H\mathbf{D}_r = {b_{\Delta\mathrm{sum}}^{(qr)}}^{*}\,\mathrm{Corr}^{\mathrm{WS}}\left(\mathbf{V}, \mathbf{V}, \underline{b}_{\Delta}^{(qr)*}\right) \in \mathbb{C}^{2\times 2},\ q, r \in \{1, \dots, N_{\mathrm{Targets}}\}. \tag{N.20}$$

We show that the elements of $\mathbf{C}^{(1)}$ at the positions marked with $\times$ in (5.208) are 0. Thus we have to show that the off-diagonal elements of $\mathbf{D}_q^H\mathbf{D}_r$ are 0, $\forall q, r \in \{1, \dots, N_{\mathrm{Targets}}\}$. Plugging in the definition of $\mathbf{V}$ (M.6) yields

$$\mathrm{Corr}^{\mathrm{WS}}\left(\mathbf{V}, \mathbf{V}, \underline{b}_{\Delta}^{(qr)}\right) = \begin{bmatrix} \mathrm{Corr}^{\mathrm{WS}}\left(\underline{d}^{\mathrm{Virt}}, \underline{d}^{\mathrm{Virt}}, \underline{b}_{\Delta}^{(qr)}\right) & \mathrm{Corr}^{\mathrm{WS}}\left(\underline{d}^{\mathrm{Virt}}, \underline{t}^{\mathrm{Virt}}, \underline{b}_{\Delta}^{(qr)}\right) \\ \mathrm{Corr}^{\mathrm{WS}}\left(\underline{d}^{\mathrm{Virt}}, \underline{t}^{\mathrm{Virt}}, \underline{b}_{\Delta}^{(qr)}\right) & \mathrm{Corr}^{\mathrm{WS}}\left(\underline{t}^{\mathrm{Virt}}, \underline{t}^{\mathrm{Virt}}, \underline{b}_{\Delta}^{(qr)}\right) \end{bmatrix}. \tag{N.21}$$

With the definition of $\underline{b}_{\Delta}^{(qr)}$ (M.18) and some properties of $\mathrm{Corr}^{\mathrm{WS}}$ given in Appendix A.2.3, the off-diagonal element can be expressed as

$$\begin{aligned}\mathrm{Corr}^{\mathrm{WS}}\left(\underline{d}^{\mathrm{Virt}}, \underline{t}^{\mathrm{Virt}}, \underline{b}_{\Delta}^{(qr)}\right) &= \mathrm{Corr}^{\mathrm{WS}}\left(\underline{1}_{N_{\mathrm{Pulse}}} \otimes \underline{d}^{\mathrm{Rx}} + \underline{d}^{\mathrm{Pulse}} \otimes \underline{1}_{N_{\mathrm{Rx}}}, \underline{t} \otimes \underline{1}_{N_{\mathrm{Rx}}}, \underline{b}_{\Delta\mathrm{Tx}}^{(qr)} \otimes \underline{b}_{\Delta\mathrm{Rx}}^{(qr)}\right) \\ &= \mathrm{Corr}^{\mathrm{WS}}\left(\underline{1}_{N_{\mathrm{Pulse}}} \otimes \underline{d}^{\mathrm{Rx}}, \underline{t} \otimes \underline{1}_{N_{\mathrm{Rx}}}, \underline{b}_{\Delta\mathrm{Tx}}^{(qr)} \otimes \underline{b}_{\Delta\mathrm{Rx}}^{(qr)}\right) \\ &+ \mathrm{Corr}^{\mathrm{WS}}\left(\underline{d}^{\mathrm{Pulse}} \otimes \underline{1}_{N_{\mathrm{Rx}}}, \underline{t} \otimes \underline{1}_{N_{\mathrm{Rx}}}, \underline{b}_{\Delta\mathrm{Tx}}^{(qr)} \otimes \underline{b}_{\Delta\mathrm{Rx}}^{(qr)}\right) \\ &= \mathrm{Corr}^{\mathrm{WS}}\left(\underline{1}_{N_{\mathrm{Pulse}}}, \underline{t}, \underline{b}_{\Delta\mathrm{Tx}}^{(qr)}\right) \cdot \mathrm{Corr}^{\mathrm{WS}}\left(\underline{d}^{\mathrm{Rx}}, \underline{1}_{N_{\mathrm{Rx}}}, \underline{b}_{\Delta\mathrm{Rx}}^{(qr)}\right) \\ &+ \mathrm{Corr}^{\mathrm{WS}}\left(\underline{d}^{\mathrm{Pulse}}, \underline{t}, \underline{b}_{\Delta\mathrm{Tx}}^{(qr)}\right)\end{aligned}$$

$$= \mathrm{E}^{\mathrm{WS}}\left(\underline{t}, \underline{b}_{\Delta\mathrm{Tx}}^{(qr)}\right) \mathrm{Corr}^{\mathrm{WS}}\left(\underline{d}^{\mathrm{Rx}}, \underline{1}_{N_{\mathrm{Rx}}}, \underline{b}_{\Delta\mathrm{Rx}}^{(qr)}\right)$$
$$+ \mathrm{Corr}^{\mathrm{WS}}\left(\underline{d}^{\mathrm{Pulse}}, \underline{t}, \underline{b}_{\Delta\mathrm{Tx}}^{(qr)}\right). \tag{N.22}$$

Due to (N.16) and (N.18)

$$\mathrm{Corr}^{\mathrm{WS}}\left(\underline{d}^{\mathrm{Virt}}, \underline{t}^{\mathrm{Virt}}, \underline{b}_{\Delta}^{(qr)}\right) = 0. \tag{N.23}$$

Thus, we have shown that the off-diagonal elements of $\mathbf{D}_q^H \mathbf{D}_r$ equal 0 and therefore the relevant elements in $\mathbf{C}^{(1)}$ are 0.

Investigation of $\mathbf{C}^{(2)}$ $\mathbf{C}^{(2)}$ is defined in (5.211),

$$\mathbf{C}^{(2)} = \mathbf{D}^H \mathbf{B} \left(\mathbf{B}^H \mathbf{B}\right)^{-1} \mathbf{B}^H \mathbf{D}. \tag{N.24}$$

$\mathbf{B}^H \mathbf{D}$ is given in (M.30)

$$\mathbf{B}^H \mathbf{D} = j \begin{bmatrix} \underline{b}^{(1)H}\mathbf{D}_1 & \dots & \underline{b}^{(1)H}\mathbf{D}_{N_{\mathrm{Targets}}} \\ \vdots & \ddots & \vdots \\ \underline{b}^{(N_{\mathrm{Targets}})H}\mathbf{D}_1 & \dots & \underline{b}^{(N_{\mathrm{Targets}})H}\mathbf{D}_{N_{\mathrm{Targets}}} \end{bmatrix} \tag{N.25}$$

with (M.32)

$$\underline{b}^{(q)H}\mathbf{D}_r = j\, b_{\Delta\mathrm{sum}}^{(qr)\ *}\ \mathrm{E}^{\mathrm{WS}}\left(\mathbf{V}, \underline{b}_{\Delta}^{(qr)*}\right) \in \mathbb{C}^{1\times 2}. \tag{N.26}$$

Using the definition of $\mathbf{V}$ and $\underline{b}_{\Delta}^{(qr)}$ yields

$$\begin{aligned} \mathrm{E}^{\mathrm{WS}}\left(\mathbf{V}, \underline{b}_{\Delta}^{(qr)}\right) &= \mathrm{E}^{\mathrm{WS}}\left(\underline{1}_{N_{\mathrm{Pulse}}} \otimes \mathbf{V}_1 + \mathbf{V}_2 \otimes \underline{1}_{N_{\mathrm{Rx}}}, \underline{b}_{\Delta\mathrm{Tx}}^{(qr)} \otimes \underline{b}_{\Delta\mathrm{Rx}}^{(qr)}\right) \\ &= \mathrm{E}^{\mathrm{WS}}\left(\mathbf{V}_1, \underline{b}_{\Delta\mathrm{Rx}}^{(qr)}\right) + \mathrm{E}^{\mathrm{WS}}\left(\mathbf{V}_2, \underline{b}_{\Delta\mathrm{Tx}}^{(qr)}\right) \\ &= \left[\mathrm{E}^{\mathrm{WS}}\left(\underline{d}^{\mathrm{Rx}}, \underline{b}_{\Delta\mathrm{Rx}}^{(qr)}\right) \quad \mathrm{E}^{\mathrm{WS}}\left(0, \underline{b}_{\Delta\mathrm{Rx}}^{(qr)}\right)\right] + \left[\mathrm{E}^{\mathrm{WS}}\left(\underline{d}^{\mathrm{Pulse}}, \underline{b}_{\Delta\mathrm{Tx}}^{(qr)}\right) \quad \mathrm{E}^{\mathrm{WS}}\left(\underline{t}, \underline{b}_{\Delta\mathrm{Tx}}^{(qr)}\right)\right] \\ &= \left[\mathrm{E}^{\mathrm{WS}}\left(\underline{d}^{\mathrm{Rx}}, \underline{b}_{\Delta\mathrm{Rx}}^{(qr)}\right) + \mathrm{E}^{\mathrm{WS}}\left(\underline{d}^{\mathrm{Pulse}}, \underline{b}_{\Delta\mathrm{Tx}}^{(qr)}\right) \quad 0\right], \end{aligned} \tag{N.27}$$

where we have used (N.16) in the last line. Thus $\mathbf{B}^H \mathbf{D}$ has the following form

$$\mathbf{B}^H \mathbf{D} = \left[\underline{x}_1 \quad \underline{0} \quad \underline{x}_2 \quad \underline{0} \quad \dots \quad \underline{x}_{N_{\mathrm{Targets}}} \quad \underline{0}\right], \tag{N.28}$$

where $\underline{x}_1, \dots, \underline{x}_{N_{\mathrm{Targets}}}$ are some vectors which are in general unequal $\underline{0}$. Multiplying from the left with a $N_{\mathrm{Targets}} \times N_{\mathrm{Targets}}$ matrix keeps this structure. Thus

$$\mathbf{C}^{(2)} = \left(\mathbf{D}^H \mathbf{B}\right)\left(\mathbf{B}^H \mathbf{B}\right)^{-1}\left(\mathbf{B}^H \mathbf{D}\right)$$

$$
\begin{aligned}
&= \begin{bmatrix} \underline{x}_1^H \\ \underline{0}^T \\ \vdots \\ \underline{x}_{N_{\text{Targets}}}^H \\ \underline{0}^T \end{bmatrix} \left(\mathbf{B}^H \mathbf{B}\right)^{-1} \begin{bmatrix} \underline{x}_1 & \underline{0} & \dots & \underline{x}_{N_{\text{Targets}}} & \underline{0} \end{bmatrix} \\
&= \begin{bmatrix} \underline{x}_1^H \\ \underline{0}^T \\ \vdots \\ \underline{x}_{N_{\text{Targets}}}^H \\ \underline{0}^T \end{bmatrix} \begin{bmatrix} \underline{y}_1 & \underline{0} & \dots & \underline{y}_{N_{\text{Targets}}} & \underline{0} \end{bmatrix} \\
&= \begin{bmatrix} \underline{x}_1^H \underline{y}_1 & 0 & \dots & \underline{x}_1^H \underline{y}_{N_{\text{Targets}}} & 0 \\ 0 & 0 & \dots & 0 & 0 \\ \vdots & \vdots & \ddots & \vdots & \vdots \\ \underline{x}_{N_{\text{Targets}}}^H \underline{y}_1 & 0 & \dots & \underline{x}_{N_{\text{Targets}}}^H \underline{y}_{N_{\text{Targets}}} & 0 \\ 0 & 0 & \dots & 0 & 0 \end{bmatrix},
\end{aligned} \tag{N.29}
$$

where $\underline{y}_1, \dots, \underline{y}_{N_{\text{Targets}}}$ are some vectors which are in general unequal $\underline{0}$. Hence the elements at the positions marked with $\times$ in (5.208) are 0. □

Bibliography

F. Athley. Threshold region performance of maximum likelihood direction of arrival estimators. *IEEE Transactions on Signal Processing*, 53(4):1359–1373, 2005. doi: 10.1109/TSP.2005.843717.

Chen Baixiao, Zhang Shouhong, Wang Yajun, and Wang Jun. Analysis and experimental results on sparse-array synthetic impulse and aperture radar. In *Proc. Radar CIE Int. Conf*, pages 76–80, 2001. doi: 10.1109/ICR.2001.984627.

I. Bekkerman and J. Tabrikian. Target Detection and Localization Using MIMO Radars and Sonars. *IEEE Transactions on Signal Processing*, 54(10):3873–3883, 2006. doi: 10.1109/TSP.2006.879267.

J. F. Böhme. *Stochastische Signale mit Übungen und einem MATLAB-Praktikum*. Teubner, 1998.

Johann F. Böhme. Source-Parameter Estimation by Approximate Maximum Likelihood and Nonlinear Regression. *IEEE Journal of Oceanic Engineering*, 10(3):206–212, Jul 1985. ISSN 0364-9059. doi: 10.1109/JOE.1985.1145098.

R. Boyer. Performance Bounds and Angular Resolution Limit for the Moving Colocated MIMO Radar. *IEEE Transactions on Signal Processing*, 59(4):1539–1552, 2011. doi: 10.1109/TSP.2010.2100387.

L. E. Brennan and L. S. Reed. Theory of Adaptive Radar. *IEEE Transactions on Aerospace and Electronic Systems*, AES-9(2):237–252, 1973.

I. N. Bronstein, K. A. Semendjajew, G. Musiol, and H. Mühlig. *Taschenbuch der Mathematik*. Harri Deutsch, 2008.

M. Bühren. *Simulation und Verarbeitung von Radarziellisten im Automobil*. PhD thesis, Universtität Stuttgart, 2008.

Chun-Yang Chen. *Signal processing algorithms for MIMO radar*. PhD thesis, California Institute of Technology, 2009. URL `http://thesis.library.caltech.edu/2521/`.

C.Y. Chong, F. Pascal, and M. Lesturgie. Estimation performance of coherent MIMO-STAP using Cramer-Rao bounds. In *Radar Conference (RADAR), 2011 IEEE*, pages 533 –537, 2011. doi: 10.1109/RADAR.2011.5960594.

M.P. Clark. On the resolvability of normally distributed vector parameter estimates. *IEEE Transactions on Signal Processing*, 43(12):2975–2981, 1995. ISSN 1053-587X. doi: 10.1109/78.476441.

Harald Cramer. *Mathematical methods of statistics*. Princeton Univ. Press, 1945.

A. J. den Dekker and A. van den Bos. Resolution: a survey. *J. Opt. Soc. Am. A*, 14:547–557, 1997. doi: http://dx.doi.org/10.1364/JOSAA.14.000547.

A. Dogandzic and A. Nehorai. Cramer-Rao bounds for estimating range, velocity, and direction with an active array. *IEEE Transactions on Signal Processing*, 49(6):1122–1137, 2001.

J. Dorey, G. Garnier, and G. Auvray. RIAS, synthetic impulse and antenna radar. In *International Conference on Radar*, 1989.

M.N. El Korso, R. Boyer, A. Renaux, and S. Marcos. A GLRT-based framework for the Multidimensional Statistical Resolution Limit. In *Statistical Signal Processing Workshop (SSP), 2011 IEEE*, pages 453–456, 2011. doi: 10.1109/SSP.2011.5967729.

R. Feger, S. Schuster, S. Scheiblhofer, and A. Stelzer. Sparse antenna array design and combined range and angle estimation for FMCW radar sensors. In *Radar Conference, 2008. RADAR '08. IEEE*, pages 1 –6, 2008. doi: 10.1109/RADAR.2008.4720809.

R. Feger, C. Wagner, S. Schuster, S. Scheiblhofer, H. Jager, and A. Stelzer. A 77-GHz FMCW MIMO Radar Based on an SiGe Single-Chip Transceiver. *IEEE Transactions on Microwave Theory and Techniques*, 57(5):1020–1035, 2009. doi: 10.1109/TMTT.2009.2017254.

E. Fishler, A. Haimovich, R. Blum, D. Chizhik, L. Cimini, and R. Valenzuela. MIMO radar: an idea whose time has come. In *Proc. IEEE Radar Conf*, pages 71–78, 2004. doi: 10.1109/NRC.2004.1316398.

Andrew S Fletcher and F Robey. Performance bounds for adaptive coherence of sparse array radar. In *Proceedings of the 12th Annual Workshop on Adaptive Sensor Array Processing*, 2003.

K.W. Forsythe and D.W. Bliss. Waveform Correlation and Optimization Issues for MIMO Radar. In *Conference Record of the Thirty-Ninth Asilomar Conference on Signals, Systems and Computers*, pages 1306 – 1310, 2005. doi: 10.1109/ACSSC.2005.1599974.

B. Friedlander. On the Relationship Between MIMO and SIMO Radars. *IEEE Transactions on Signal Processing*, 57(1):394–398, 2009. doi: 10.1109/TSP.2008.2007106.

B. Friedlander. Effects of Model Mismatch in MIMO Radar. *IEEE Transactions on Signal Processing*, 60(4):2071–2076, 2012. doi: 10.1109/TSP.2011.2179653.

D. R. Fuhrmann and G. San Antonio. Transmit beamforming for MIMO radar systems using partial signal correlation. In *Proc. Conf Signals, Systems and Computers Record of the Thirty-Eighth Asilomar Conf*, volume 1, pages 295–299, 2004. doi: 10.1109/ACSSC.2004.1399140.

D. R. Fuhrmann and G. San Antonio. Transmit beamforming for MIMO radar systems using signal cross-correlation. *IEEE Transactions on Aerospace and Electronic Systems*, 44(1):171–186, 2008. doi: 10.1109/TAES.2008.4516997.

J. Guetlein, J. Bertl, A. Kirschner, and J. Detlefsen. Switching scheme for a FMCW-MIMO radar on a moving platform. In *Radar Conference (EuRAD), 2012 9th European*, pages 91–94, 2012.

J. Guetlein, A. Kirschner, and J. Detlefsen. Motion compensation for a TDM FMCW MIMO radar system. In *Radar Conference (EuRAD), 2013 European*, pages 37–40, 2013a.

J. Guetlein, A. Kirschner, and J. Detlefsen. Calibration strategy for a TDM FMCW MIMO radar system. In *Microwaves, Communications, Antennas and Electronics Systems (COMCAS), 2013 IEEE International Conference on*, pages 1–5, Oct 2013b. doi: 10.1109/COMCAS.2013.6685266.

A. M. Haimovich, R. S. Blum, and L. J. Cimini. MIMO Radar with Widely Separated Antennas. *IEEE Signal Processing Magazine*, 25(1):116–129, 2008. doi: 10.1109/MSP.2008.4408448.

A. Hassanien and S. A. Vorobyov. Phased-MIMO Radar: A Tradeoff Between Phased-Array and MIMO Radars. *IEEE Transactions on Signal Processing*, 58(6):3137–3151, 2010a. doi: 10.1109/TSP.2010.2043976.

Aboulnasr Hassanien and Sergiy A. Vorobyov. Why the Phased MIMO-Radar Outperforms the Phased-Array and MIMO Radars. In *18th European Signal Processing Conference (EUSIPCO-2010)*, 2010b.

M. Jahn, R. Feger, C. Wagner, Ziqiang Tong, and A. Stelzer. A Four-Channel 94-GHz SiGe-Based Digital Beamforming FMCW Radar. *IEEE Transactions on Microwave Theory and Techniques*, 60(3):861–869, 2012. doi: 10.1109/TMTT.2011.2181187.

K-D. Kammeyer and K. Kroschel. *Digitale Signalverarbeitung*. Springer Verlag, 2012.

S. M. Kay. *Estimation Theory*, volume I of *Fundamentals of Statistical Signal Processing*. Prentice Hall PTR, Upper Saddle River, NJ, 1993.

M. Klemm, J. Leendertz, D. Gibbins, I.J. Craddock, A. Preece, and R. Benjamin. Towards contrast enhanced breast imaging using ultra-wideband microwave radar system. In *Radio and Wireless Symposium (RWS)*, pages 516 –519, jan. 2010. doi: 10.1109/RWS.2010.5434240.

H. Krim and M. Viberg. Two decades of array signal processing research: the parametric approach. *IEEE Signal Processing Magazine*, 13(4):67–94, 1996. doi: 10.1109/79.526899.

K.S. Kulpa, A Wojtkiewicz, M. Nalecz, and J. Misiurewicz. The simple method for analysis of nonlinear frequency distortions in fmcw radar. In *Microwaves, Radar and Wireless Communications. 2000. MIKON-2000. 13th International Conference on*, volume 1, 2000. doi: 10.1109/MIKON.2000.913915.

Moon-Sik Lee, V. Katkovnik, and Yong-Hoon Kim. System modeling and signal processing for a switch antenna array radar. *IEEE Transactions on Signal Processing*, 52(6):1513–1523, 2004. doi: 10.1109/TSP.2004.827204.

N. H. Lehmann, E. Fishler, A. M. Haimovich, R. S. Blum, D. Chizhik, L. J. Cimini, and R. A. Valenzuela. Evaluation of Transmit Diversity in MIMO-Radar Direction Finding. *IEEE Transactions on Signal Processing*, 55(5):2215–2225, 2007. doi: 10.1109/TSP.2007.893220.

Marc Lesturgie. Some relevant applications of MIMO to radar. In *International Radar Symposium*, 2011.

J. Li and P. Stoica. *MIMO Radar Signal Processing*. John Wiley & Sons, Inc., Hoboken, NJ, 2009.

Jian Li and P. Stoica. MIMO Radar with Colocated Antennas. *IEEE Signal Processing Magazine*, 24(5):106–114, 2007. doi: 10.1109/MSP.2007.904812.

Jian Li, Luzhou Xu, P. Stoica, K. W. Forsythe, and D. W. Bliss. Range Compression and Waveform Optimization for MIMO Radar: A Cramer-Rao Bound Based Study. *IEEE Transactions on Signal Processing*, 56(1):218–232, 2008. doi: 10.1109/TSP.2007.901653.

Z. Liu and A. Nehorai. Statistical Angular Resolution Limit for Point Sources. *IEEE Transactions on Signal Processing*, 55(11):5521–5527, 2007. doi: 10.1109/TSP.2007.898789.

U. Lübbert. *Target Position Estimation with a Continuous Wave Radar Network*. PhD thesis, Technische Universität Hamburg-Harburg, 2005.

A.-S. Luce, H. Molina, D. Muller, and V. Thirard. Experimental results on RIAS digital beamforming radar. In *Proc. Radar 92. Int. Conf*, pages 74–77, 1992.

T. McWhorter and L.L. Scharf. Cramer-Rao Bounds for Deterministic Modal Analysis. *IEEE Transactions on Signal Processing*, 41(5):1847–1866, May 1993. ISSN 1053-587X. doi: 10.1109/78.215304.

V. F. Mecca, D. Ramakrishnan, and J. L. Krolik. MIMO Radar Space-Time Adaptive Processing for Multipath Clutter Mitigation. In *Proc. Fourth IEEE Workshop Sensor Array and Multichannel Processing*, pages 249–253, 2006. doi: 10.1109/SAM.2006.1706131.

W. L. Melvin. A STAP overview. *IEEE Aerospace and Electronic Systems Magazine*, 19(1):19–35, 2004.

Openclipart. https://openclipart.org/, 2014.

S. Pasupathy and A.N. Venetsanopoulos. Optimum Active Array Processing Structure and Space-Time Factorability. *IEEE Transactions on Aerospace and Electronic Systems*, AES-10(6):770–778, 1974. ISSN 0018-9251. doi: 10.1109/TAES.1974.307883.

David Poole. *Linear Algebra: A Modern Introduction*. Brooks/Cole, Cengage Learning, 3. ed. edition, 2011. ISBN 978-0-538-73544-5.

K. Rambach and B. Yang. Colocated MIMO Radar: Cramer-Rao Bound and Optimal Time Division Multiplexing for DOA Estimation of Moving Targets. In *Proc. IEEE Int. Conf. Acoustics, Speech and Signal Processing (ICASSP)*, 2013. doi: 10.1109/ICASSP.2013.6638411.

K. Rambach and B. Yang. Direction of Arrival Estimation of Two Moving Targets Using a Time Division Multiplexed Colocated MIMO Radar. In *Proc. IEEE Radar Conference (Radarcon)*, 2014.

K. Rambach and B. Yang. Two-Dimensional TDM-MIMO Radar: Cramer-Rao Bound and Decoupling of the Direction of Arrivals from the Doppler Frequency of a Moving Target. In *to be published*, 2016a.

K. Rambach and B. Yang. MIMO Radar: Time Division Multiplexing vs. Code Division Multiplexing. In *to be published*, 2016b.

K. Rambach, M. Vogel, and B. Yang. Optimal Time Division Multiplexing Schemes for DOA Estimation of a Moving Target Using a Colocated MIMO Radar. In *Proc. IEEE International Symposium on Signal Processing and Information Technology (ISSPIT)*, 2014.

C. R. Rao. Information and the accuracy attainable in the estimation of statistical parameters. *Bulletin of the Calcutta Mathematical Society*, 37:81–91, 1945.

Eckhard Rebhan. *Theoretische Physik, Mechanik, Elektrodynamik, Relativitätstheorie, Kosmologie*. Spektrum Akademischer Verlag, Heidelberg, Berlin, 2001.

M. Reiher. *Optimierung von Sendesignalen zur Vermeidung von Scheinzielen für frequenzmodulierte Dauerstrich-Radarsysteme im Automobil*. PhD thesis, Universtität Stuttgart, 2012.

M. J. D. Rendas and J. M. F. Moura. Ambiguity in radar and sonar. *IEEE Transactions on Signal Processing*, 46(2):294–305, 1998. doi: 10.1109/78.655416.

F. C. Robey, S. Coutts, D. Weikle, J. C. McHarg, and K. Cuomo. MIMO radar theory and experimental results. In *Proc. Conf Signals, Systems and Computers Record of the Thirty-Eighth Asilomar Conf*, volume 1, pages 300–304, 2004. doi: 10.1109/ACSSC.2004.1399141.

G. San Antonio, D. R. Fuhrmann, and F. C. Robey. MIMO Radar Ambiguity Functions. *IEEE Journal of Selected Topics in Signal Processing*, 1(1):167–177, 2007. doi: 10.1109/JSTSP.2007.897058.

A. M. Sayeed and V. Raghavan. Maximizing MIMO Capacity in Sparse Multipath With Reconfigurable Antenna Arrays. *IEEE Journal of Selected Topics in Signal Processing*, 1(1):156–166, 2007. doi: 10.1109/JSTSP.2007.897057.

C.M. Schmid, R. Feger, C. Pfeffer, and A. Stelzer. Motion Compensation and Efficient Array Design for TDMA FMCW MIMO Radar Systems. In *Antennas and Propagation (EUCAP), 2012 6th European Conference on*, pages 1746–1750, March 2012. doi: 10.1109/EuCAP.2012.6206605.

M. Schoor. *Hochauflösende Winkelschätzung für automobile Radarsysteme*. PhD thesis, Universtität Stuttgart, 2010.

M. I. Skolnik. *Introduction to Radar Systems*. McGrawHill, 3. edition, 2001.

P. Stoica and A. Nehorai. MUSIC, maximum likelihood, and Cramer-Rao bound. *IEEE Transactions on Acoustics, Speech, and Signal Processing*, 37(5):720–741, 1989.

AG. Stove. Linear FMCW Radar Techniques. *Radar and Signal Processing, IEE Proceedings F*, 139(5), Oct 1992. ISSN 0956-375X.

Hongbo Sun, Frederic Brigui, and M. Lesturgie. Analysis and Comparison of MIMO Radar Waveforms. In *Internation Radar Conference*, 2014.

D. N. Tran, A. Renaux, R. Boyer, S. Marcos, and P. Larzabal. Weiss-Weinstein bound for MIMO radar with colocated linear arrays for SNR threshold prediction. *Signal Processing*, 92:1353–1358, 2012.

S. Uhlich. *Parameter Estimation with Additional Information*. PhD thesis, Universtität Stuttgart, 2012.

P. P. Vaidyanathan and P. Pal. MIMO radar, SIMO radar, and IFIR radar: a comparison. In *Proc. Conf Signals, Systems and Computers Record of the Forty-Third Asilomar Conf*, pages 160–167, 2009. doi: 10.1109/ACSSC.2009.5470139.

H. L. Van Trees. *Optimum Array Processing*, volume IV of *Detection, Estimation, and Modulation Theory*. John Wiley & Sons, Inc., New York, 2002.

Markus Vogel. Optimization of Direction of Arrival Estimation with a Time Division Multiplexed MIMO Radar. Master's thesis, University of Stuttgart, 2013.

J. Ward. Cramer-Rao bounds for target angle and Doppler estimation with space-time adaptive processing radar. In *Conference Record of the Twenty-Ninth Asilomar Conference on Signals, Systems and Computers*, volume 2, pages 1198 –1202, 1995. doi: 10.1109/ACSSC.1995.540889.

A. Weiss and E. Weinstein. A lower bound on the mean-square error in random parameter estimation (Corresp.). *IEEE Transactions on Information Theory*, 31(5):680–682, 1985. doi: 10.1109/TIT.1985.1057094.

Hermann Winner. *Handbuch Fahrerassistenzsysteme: Grundlagen, Komponenten und Systeme für aktive Sicherheit und Komfort*. Vieweg+Teubner Verlag / Springer Fachmedien Wiesbaden

GmbH, Wiesbaden, Wiesbaden, 2. edition, 2012. ISBN 978-3-8348-8619-4. doi: 10.1007/978-3-8348-8619-4.

M. Wintermantel. Radar System with Elevation Measuring Capability, 2010.

W. Wirtinger. Zur formalen Theorie der Funktionen von mehr komplexen Veränderlichen. *Mathematische Annalen*, 97(1):357–375, 1927. ISSN 0025-5831. doi: 10.1007/BF01447872.

Ming Xue, Duc Vu, Luzhou Xu, Jian Li, and P. Stoica. On MIMO radar transmission schemes for ground moving target indication. In *Proc. Conf Signals, Systems and Computers Record of the Forty-Third Asilomar Conf*, pages 1171–1175, 2009. doi: 10.1109/ACSSC.2009.5470010.

Ming Xue, W. Roberts, Jian Li, Xing Tan, and P. Stoica. MIMO radar sparse angle-Doppler imaging for ground moving target indication. In *Proc. IEEE Radar Conf*, pages 553–558, 2010. doi: 2010.5494560.

B. Yang. Statistical and adaptive signal processing. lecture notes, University of Stuttgart, 2011.

S. F. Yau and Y. Bresler. A compact Cramer-Rao bound expression for parametric estimation of superimposed signals. *IEEE Transactions on Signal Processing*, 40(5):1226–1230, 1992. doi: 10.1109/78.134484.

Alex Zwanetski and Hermann Rohling. Continuous wave mimo radar based on time division multiplexing. In *Radar Symposium (IRS), 2012 13th International*, pages 119–121. IEEE, 2012.